HD 6201.5
U58
B91

U. S. DEPARTMENT OF COMMERCE

BUREAU OF STANDARDS JOURNAL OF RESEARCH

Vol. 7 SEPTEMBER, 1931 No. 3

CONTENTS

RP. No.	TITLE AND AUTHOR	Page
348.	The resistance to wear of carbon steels. Samuel J. Rosenberg	419
349.	Permanence studies of current commercial book papers. John O. Burton	429
350.	Thermomagnetic investigation of tempering of quenched 0.75 per cent carbon steel. George A. Ellinger	441
351.	Hyperfine structures in the first spectra of krypton and xenon. C. J. Humphreys	453
352.	Accelerated aging test for paper. Royal H. Rasch	465
353.	Cryoscopic constant, heat of fusion, and heat capacity of camphor. Mikkel Frandsen	477
354.	The passage of gas through the walls of pyrometer protection tubes at high temperatures. Wm. F. Roeser	485
355.	An experimental study of several methods of representing photographic sensitivity. Raymond Davis and Gerald Kent Neeland	495
356.	Some experimental studies of the vibrations of quartz plates. R. B. Wright and D. M. Stuart	519
357.	Aqueous solutions of ethylene, glycol, glycerin, and sodium silicate as quenching media for steels. T. E. Hamill	555
358.	Optical rotation and atomic dimensions—halogeno-tetraacetyl derivatives of manose. Their configurational peculiarities. D. H. Brauns	573
359.	Soil-corrosion studies: Nonferrous metals and alloys, metallic coatings, and specially prepared ferrous pipes removed in 1930. K. H. Logan	585
360.	Isolation and determination of the cyclohexane in a midcontinent petroleum. Johannes H. Bruun and Mildred M. Hicks-Bruun	607

BUREAU OF STANDARDS JOURNAL OF RESEARCH

CONTENTS OF RECENT NUMBERS

March, 1931 (Vol. 6, No. 3)

RP282. Separation of normal octane from petroleum by distillation and crystallization. R. T. Leslie and Sylvester T. Schicktanz. Price 10 cents.
RP283. Further measurements of propeller fan characteristics. Paul S. Ballif and H. L. Dryden. Price 10 cents.
RP284. A precision cryostat with automatic temperature regulation. R. B. Scott and F. G. Brickwedde. Price 5 cents.
RP285. The paper-making properties of phormium tenax (New Zealand flax). Merle B. Shaw, George W. Bicking, and Martin J. O'Leary. Price 10 cents.
RP286. A method for the separation and gravimetric determination of osmium. Raleigh Gilchrist. Price 10 cents.
RP287. Application of the fluorating process to fructose. D. H. Brauns and Harriet L. Frush. Price 5 cents.
RP288. Moisture expansion of glazes and other ceramic finishes. H. G. Schurecht and G. R. Pole. Price 5 cents.
RP289. Extension of the standard visibility function to intervals of 1 millimicron by third-difference osculatory interpolation. Deane B. Judd. Price 5 cents.
RP290. Durability and strength of bond between mortar and brick. L. A. Palmer and J. V. Hall, jr. Price 10 cents.
RP291. Heat transfer through building walls. M. S. Van Dusen and J. L. Finck. Price 15 cents.

April, 1931 (Vol. 6, No. 4)

RP292. Variations caused in heating curves of glass by heat treatment. A. Q. Tool and C. G. Eichlin. Price 10 cents.
RP293. On the vibration of U bars. G. H. Keulegan. Price 10 cents.
RP294. Laundry "winter damage." John B. Wilkie. Price 10 cents.
RP295. The determination of the alpha cellulose content and copper number of paper. John O. Burton and Royal H. Rasch.
RP296. The structure of the arc spectrum of zirconium. C. C. Kiess and Harriet K. Kiess. Price 15 cents.
RP297. Radiation from metals bombarded by low-speed electrons. F. L. Mohler and C. Boeckner.
RP298. Pipe-line currents and soil resistivity as indicators of local corrosive soil areas. E. R. Shepard.
RP299. Two new crystalline difructose anhydrides from hydrolyzed inulin. Richard F. Jackson and Emma McDonald. Price 5 cents.
RP300. Measurement of fiber diameters by the diffraction method. H. J. McNicholas and H. J. Curtis. Price 10 cents.
RP301. Wind pressure on a model of a mill building. Hugh L. Dryden and George C. Hill. Price 10 cents.
RP302. Stabilization of boric acid buffers by aeration. Edna H. Fawcett and S. F. Acree. Price 5 cents.

May, 1931 (Vol. 6, No. 5)

RP303. Note on contraction coefficients of jets of gas. Edgar Buckingham. Price 5 cents.
RP304. The effect of small variations in pitch upon the inductance of a solenoid. Chester Snow. Price 5 cents.
RP305. Heat content values for aqueous solutions of the chloride, nitrates, and hydroxides of hydrogen, lithium, sodium, and potassium at 18° C. Frederick D. Rossini. Price 5 cents.
RP306. Accurate measurement of small electric charges by a null method. Lauriston S. Taylor. Price 10 cents.
RP307. Light sensitivity of rosin paper-sizing materials. Arthur E. Kimberly and J. F. G. Hicks. Price 5 cents.
RP308. Dimensional changes in the manufacture of electrotypes. N. Bekkedahl and W. Blum. Price 10 cents.
RP309. The heat of ionization of water. Frederick D. Rossini. Price 5 cents.
RP310. Factors affecting the strength of masonry hollow units. Douglas E. Parsons. Price 5 cents.
RP311. Determination of the benzene and the normal hexane content of a mid-continent petroleum. Johannes H. Bruun and Mildred M. Hicks-Bruun. Price 5 cents.
RP312. Calorimetric determinations of thermal properties of methyl alcohol, ethyl alcohol, and benzene. E. F. Fieck, D. C. Ginnings, and W. B. Holton. Price 5 cents.
RP313. Characteristics of airplane antennas for radio range-beacon reception. H. Diamond and G. L. Davies. Price 5 cents.

Research papers are available as separates for purchase from the Superintendent of Documents United States Government Printing Office, Washington, D. C.

U. S. DEPARTMENT OF COMMERCE
R. P. LAMONT, Secretary
BUREAU OF STANDARDS
GEORGE K. BURGESS, Director

BUREAU OF STANDARDS JOURNAL OF RESEARCH

September, 1931
Vol. 7, No. 3

UNITED STATES
GOVERNMENT PRINTING OFFICE
WASHINGTON : 1931

For sale by the Superintendent of Documents, Washington, D. C. - - Price $2.75 Per Year on Subscription

For a partial list of previous research papers appearing in BUREAU OF STANDARDS JOURNAL OF RESEARCH, see pages 2 and 3 of the cover.

DEPOSITED BY THE
UNITED STATES OF AMERICA

RP348

THE RESISTANCE TO WEAR OF CARBON STEELS

By Samuel J. Rosenberg

ABSTRACT

A study was made of the effect of heat treatment and carbon content upon the wear resistance of carbon steels as determined by the Amsler machine (combined rolling and sliding friction under heavy pressures). Annealed steels gave poor wear-resisting qualities unaffected by carbon content. Normalized steels showed less wear resistance in the low-carbon range than the annealed steels, but in the high-carbon range approached the relatively high wear resistance of the hardened steels. Hardened steels showed a very rapid increase in wear resistance with increased carbon content, this increase becoming relatively small after about 0.6 per cent carbon. Tempering a hardened steel resulted in a gradual lowering of the wear resistance.

The microstructures of the steels adjacent to the worn surfaces showed that this particular type of wear (combined rolling and sliding friction under heavy pressures) was generally accompanied by severe distortion of the structure. A martensitic-troostitic matrix was the most resistant to wear. Steels containing lamellar pearlite showed excellent wear resistance, while steels containing granular pearlite had poor resistance to wear. The presence of free ferrite, or of free cementite as spheroids, is detrimental to the wear resistance.

CONTENTS

	Page
I. Introduction	419
II. Method of test	419
III. Results of the tests	420
1. Film formation	420
2. Interpretation of test data	420
3. Effect of pressure between the test specimens	422
4. Materials tested	423
5. Effect of carbon content on the resistance to wear	423
6. Effect of tempering temperature on the resistance to wear	424
7. Examination of the abraded surfaces	425
IV. Discussion of results	426
V. Summary and conclusions	428
VI. Acknowledgments	428

I. INTRODUCTION

The resistance of carbon steels to abrasion by sand as determined by the Brinell machine has been reported in a previous paper.[1] As a continuation of this work, the present paper reports a study of the resistance of carbon steels to metal-to-metal wear against a hardened eutectoid carbon steel under combined sliding and rolling friction.

II. METHOD OF TEST

The apparatus used in this investigation for the evaluation of wear resistance was the Amsler machine. This machine has been described in detail in a previous paper.[2]

The test specimens used were in the form of small cylinders, 2 inches in diameter and 0.4 inch thick. The specimens were all

[1] Samuel J. Rosenberg, The Resistance of Steel to Abrasion by Sand, B. S. Jour. Research, 5 (RP 214); September, 1930; also Trans. Am. Soc. Steel Treat., 18, p. 1093; 1930.

[2] H. J. French, S. J. Rosenberg, W. LeC. Harbaugh, and H. C. Cross, Wear and Mechanical Properties of Railroad Bearing Bronzes at Different Temperatures. B. S. Jour. Research, 1 (RP 13); September, 1928.

finish ground to size. The finished surfaces were produced by wet grinding with a medium hard No. 46 wheel.

All steels were tested against an arbitrarily selected "standard" steel. This standard was a 0.81 per cent carbon steel normalized at 810° C. (1,490° F.), water quenched from 780° C. (1,435° F.), and tempered at 260° C. (500° F.). The Rockwell "C" scale hardness resulting from this treatment was just under 60. In all tests the standard specimen was mounted on the lower shaft of the machine, which was rotated at about 220 r. p. m. The test specimen was mounted on the upper shaft, its speed being about 200 r. p. m. In addition to the slip resulting from this difference in speed, the cam which is available on the Amsler machine for producing lateral motion of the upper specimen was used.

All tests were made in duplicate and a new standard specimen was used for each test specimen. Wear was measured by the losses in weight of both the specimens.

III. RESULTS OF THE TESTS

1. FILM FORMATION

The formation of surface films on specimens tested in the Amsler machine is a familiar phenomenon. In the case of the wear of steel against steel, this film appears to be an oxide of iron and to act as an abrasive. Fink [3] has shown that the partial or complete removal of this film causes a decided decrease in the rate of wear. He tested carbon steels in the Amsler machine under atmospheric conditions and found that a considerable amount of wear took place. When the same steels were inclosed in a gas-tight cell filled with nitrogen and tested under the same conditions of speed and pressure as before, no wear took place, the test surfaces being smooth and bright at the end of the test. These films are a natural result of the rolling and sliding abrasion of steel against steel under heavy pressures in the presence of air and the absence of lubrication. No attempt was made to remove films during the tests reported in this paper.

When two specimens of the same steel which have also been given the same heat treatment are tested in the Amsler machine, the upper specimen, which travels at the lower angular velocity, loses more weight than the lower specimen. The appearances of the films produced are quite different; the lower specimen has a much heavier film. The films produced on steels of like composition and treatment are shown in Figure 1. Since it is the lower specimen which forms the heavier film and the upper specimen which suffers the greater loss in weight, it was decided to mount the "standard" specimen on the lower shaft.

A possible explanation for the difference in losses of weight of two specimens treated alike lies in the fact that the lower specimen forms the heavier film. This film, which acts as an abrasive on the upper specimen, exerts a certain protective influence on the lower one.

2. INTERPRETATION OF TEST DATA

The weight loss of the upper (test) specimen was plotted against the revolutions of the lower (standard) specimen to show the relation of wear to slip. This may be conveniently expressed as weight lost per 10,000 revolutions, which was the ordinary duration of a test

[3] M. Fink, Wear Oxidation, a New Component of Wear, Trans. Am. Soc. Steel Treat., 18, p. 204 ;1930.

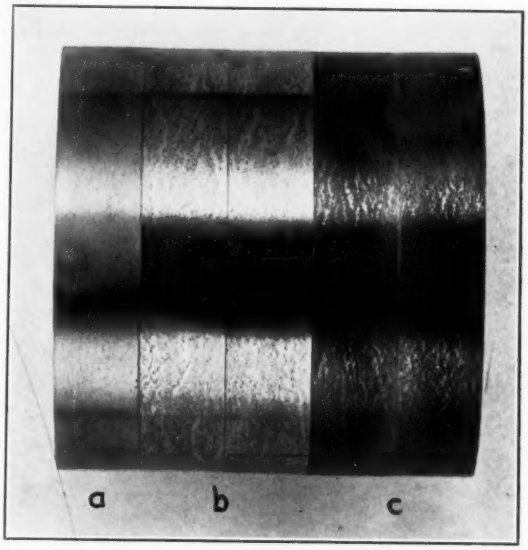

FIGURE 1.—*Appearance of specimens before and after test*

All specimens are 0.81 per cent carbon, water-quenched and tempered at 260° C. (500° F.). Test load was 60 kg. *a*, Original ground surface; *b*, appearance of upper specimen (light film); *c*, appearance of lower specimen (heavy film).

period. By plotting the weight loss against the work, as calculated from the integrating device on the Amsler machine, the wear per unit of work may be obtained.

Under similar conditions of test, the evaluation of wear by either method generally gives quite similar results. Results more truly

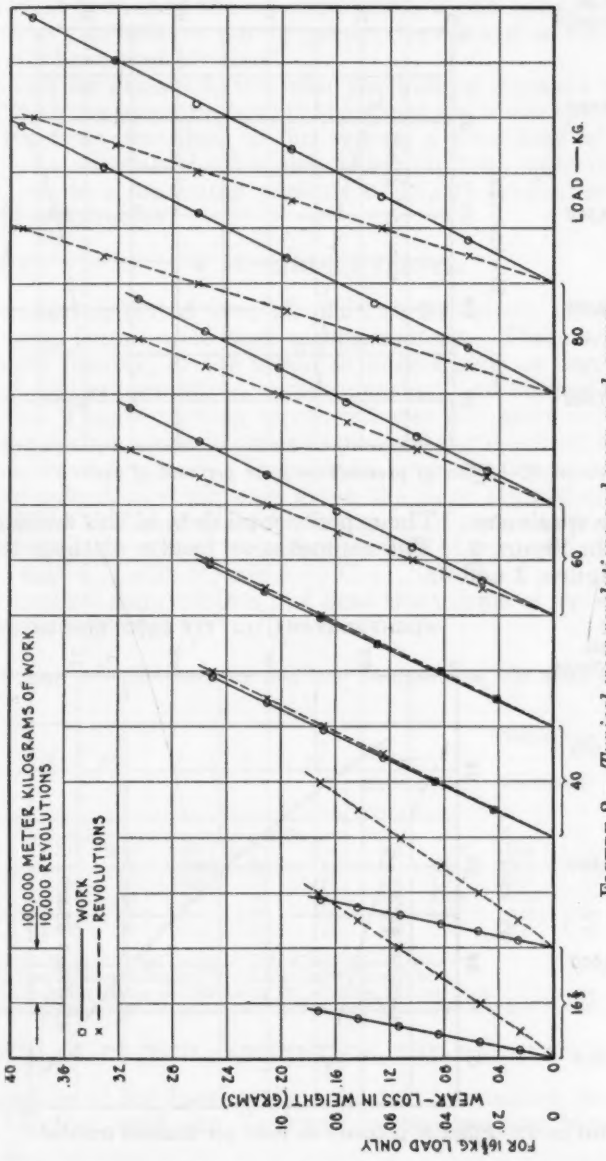

FIGURE 2.—*Typical wear-revolutions and wear-work curves*

The specimen tested was a "standard" specimen.

indicative of the materials are obtained, however, when the wear is correlated with the frictional work which caused it. For this reason, all comparisons of materials tested are based upon the wear per unit of work. Figure 2 illustrates wear-revolutions and wear-work curves.

3. EFFECT OF PRESSURE BETWEEN THE TEST SPECIMENS

A series of tests were made with two sets of "standard" specimens tested against each other to determine the effect of increasing pressure

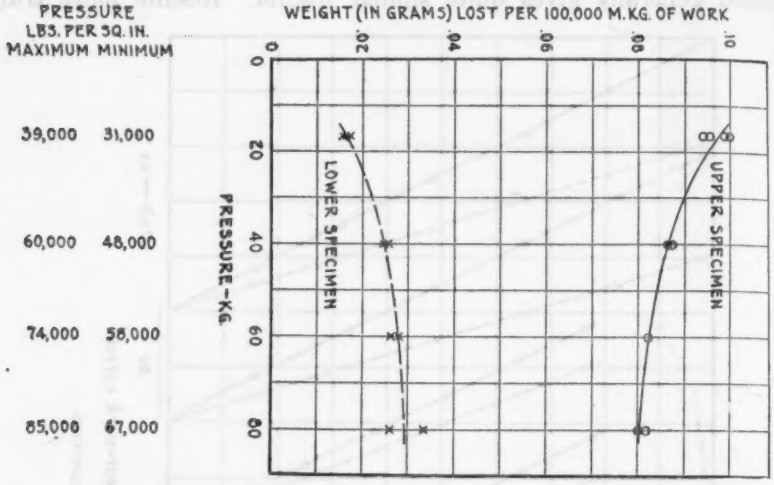

FIGURE 3.—*Effect of pressure on wear per unit of work*

between the specimens. The experimental data of this series of tests are shown in Figure 2. The comparative results of these tests are shown in Figures 3 and 4.

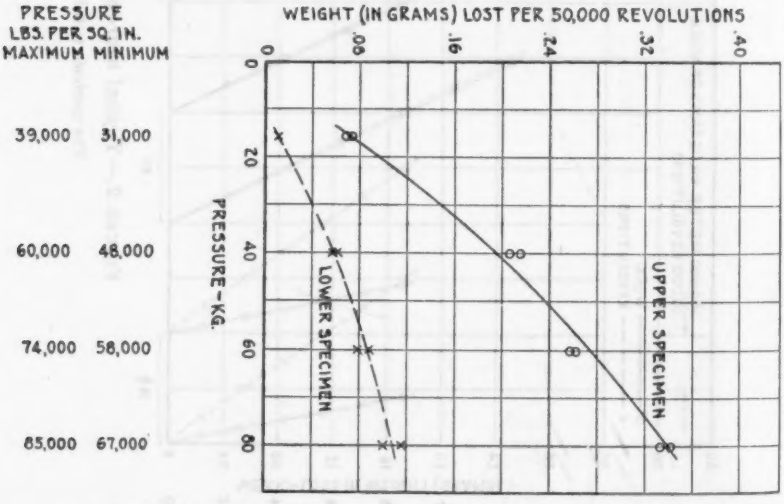

FIGURE 4.—*Effect of pressure on wear per distance traveled*

The wear per unit of work of the upper specimen decreased as the pressure increased, this decrease becoming less with increasing pressure. The lower specimen, on the other hand, showed an increased amount of wear per unit of work as the pressure increased. This

would seem to indicate that, were the pressure sufficiently great, the upper and lower specimens would both lose the same amount of weight. This, however, seems improbable because the curves show evidences of becoming asymptotic. Unfortunately, the frictional torque developed under a total load of 80 kg was so great that if a higher pressure had been used the counterweights would not have been sufficiently heavy to balance the torque developed, and no measure of the work could have been obtained.

As would be expected, the wear per unit of distance traveled increased with the pressure, both in the upper and lower specimens.

For the tests described in this report, a total load of 60 kg was chosen as a standard load under which all tests were made. This corresponds to a maximum pressure of 74,000 lbs./in.^{2} as calculated from Hertz' formulas.[4]

4. MATERIALS TESTED

The materials tested were all plain carbon steels, chosen so as to give a range from low to high carbon content. Three series of tests were made namely, of the steels as normalized, as normalized and annealed, and as normalized, water quenched, and tempered at 260° C. (500° F.). This tempering treatment was necessary in the case of the higher carbon steels in order to prevent any cracking which might otherwise have occurred. In order to keep the treatments uniform, all of the quenched steels were given the same tempering treatment.

In addition to these tests, a further series of tests was made upon the 0.81 per cent carbon steel to study the effect of tempering temperature between 260° C. (500° F.) and 600° C. (1,100° F.).

The chemical compositions and heat treatments of the steels tested are given in Table 1.

TABLE 1.—*Compositions and heat treatments of the steels tested*

Mark	C	Mn	P	S	Si	Temperature					
						Normalizing		Hardening		Annealing	
	Per cent	*Per cent*	*Per cent*	*Per cent*	*Per cent*	*°C.*	*°F.*	*°C.*	*°F.*	*°C.*	*°F.*
M33	0.12	0.44	0.020	0.021	0.25	960	1,760	930	1,705	910	1,670
M35	.34	.68	.024	.033	.22	890	1,635	860	1,580	840	1,545
M22	.58	.29	.014	.018	.27	825	1,515	795	1,465	775	1,425
EU	.81	.23	.024	.021	.28	810	1,490	770	1,420	755	1,390
M48	1.00	.29	.018	.016	.13	810	1,490	770	1,420	755	1,390
M52	1.26	.39	.024	.018	.28	925	1,695	770	1,420	755	1,390

Time of holding at normalizing and tempering temperatures, 1 hour.
Time of holding at annealing and hardening temperatures, one-half hour.
All hardening by water quenching, followed immediately by tempering at 260° C. (500° F.).

5. EFFECT OF CARBON CONTENT ON THE RESISTANCE TO WEAR

The results of the tests on the annealed, normalized, and hardened steels, together with the Rockwell hardnesses, are summarized in Figure 5.

The carbon content apparently had little effect upon the wear of annealed steels. Rather surprisingly, the wear of the low-carbon normalized steels was greater than that of the annealed steels of

[4] These formulas and methods of calculation are given in the reference noted in footnote 2.

similar carbon content, but with increasing carbon content the wear rate of the normalized steels decreased rapidly, approaching, in the high-carbon range, the relatively high wear resistance of the hardened steels. The wear of the hardened steels decreased rapidly and regularly with increasing carbon content in the lower ranges of carbon. In the higher ranges, however, increased carbon did not materially affect the wear resistance.

The microstructures of the annealed steels are shown in Figure 6, of the normalized steels in Figure 7, and of the hardened steels in Figure 8.

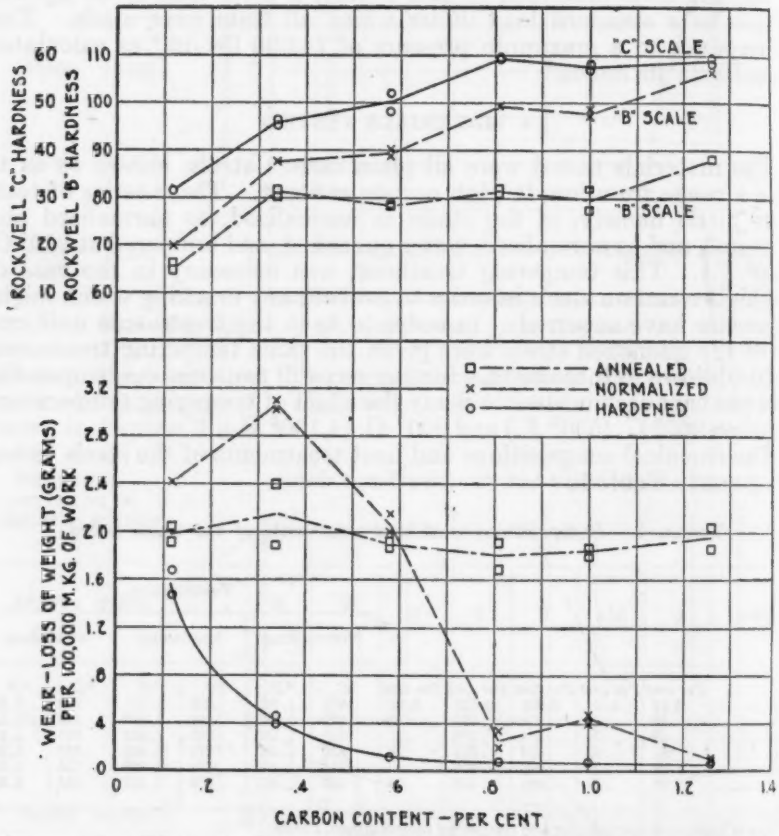

FIGURE 5.—*Effect of carbon content on the wear of cabon steels tested in the Amsler machine*

6. EFFECT OF TEMPERING TEMPERATURE ON THE RESISTANCE TO WEAR

The effect of tempering temperature on the resistance to wear of the 0.81 per cent carbon steel was studied. An attempt was made to test this steel as hardened and also as tempered at 150° C. (300° F.), but trouble was experienced due to cracking of the specimen. The results of the tests, together with the hardness determinations, are summarized graphically in Figure 9. These curves show that in-

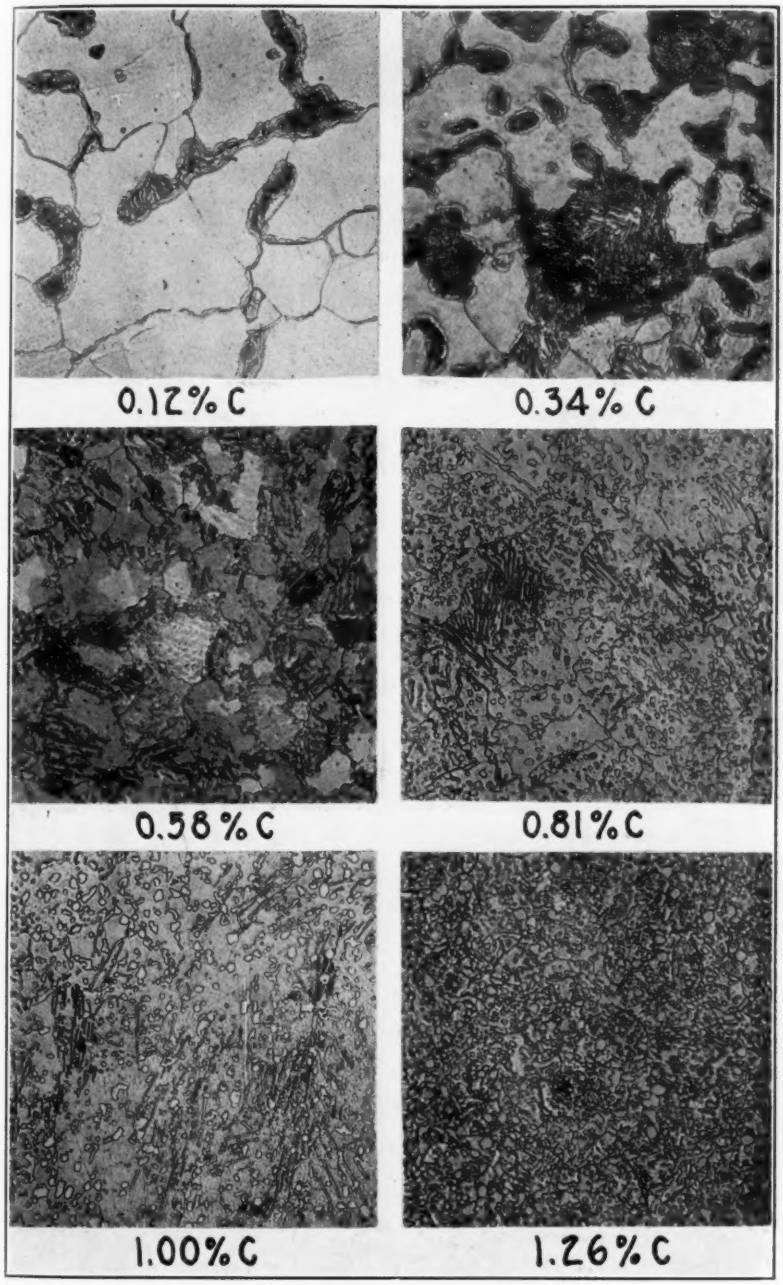

FIGURE 6.—*Microstructures of the annealed steels.* × *500*

Etched with 2 per cent nitric acid in alcohol.

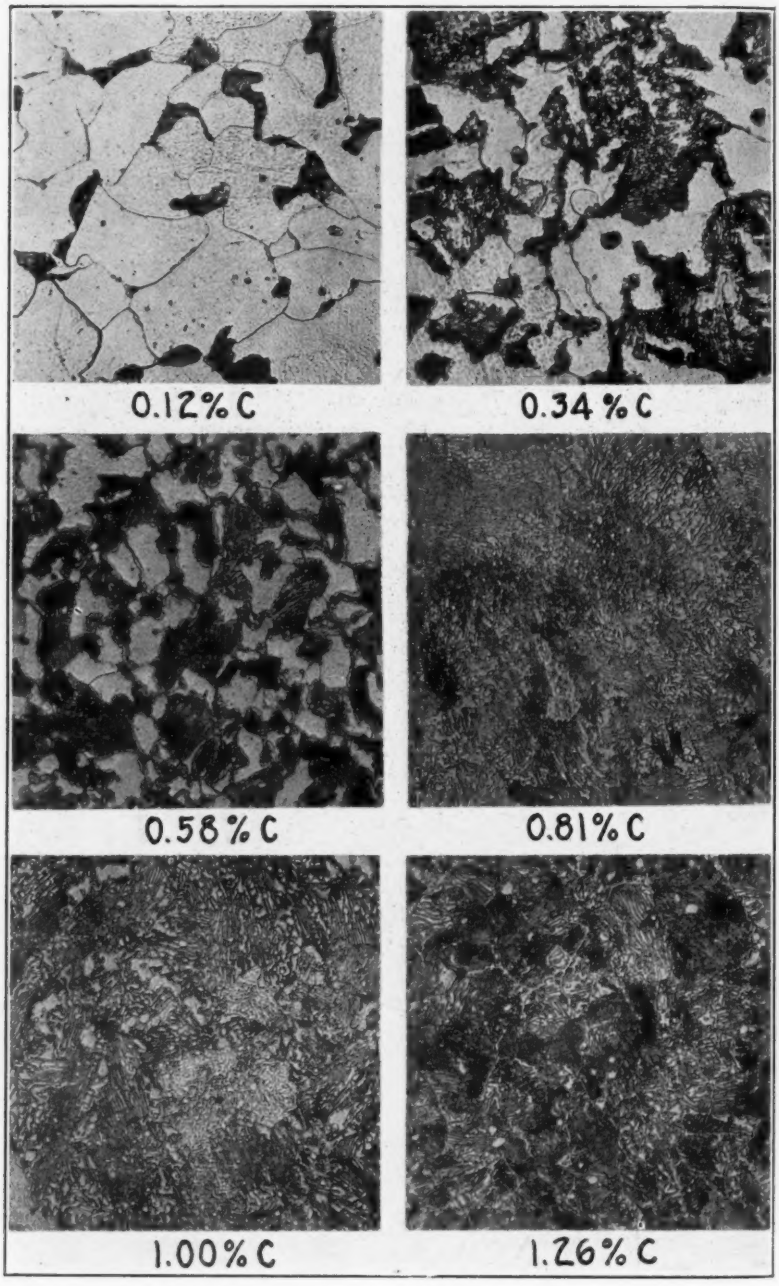

FIGURE 7.—*Microstructures of the normalized steels.* × *500*
Etched with 2 per cent nitric acid in alcohol.

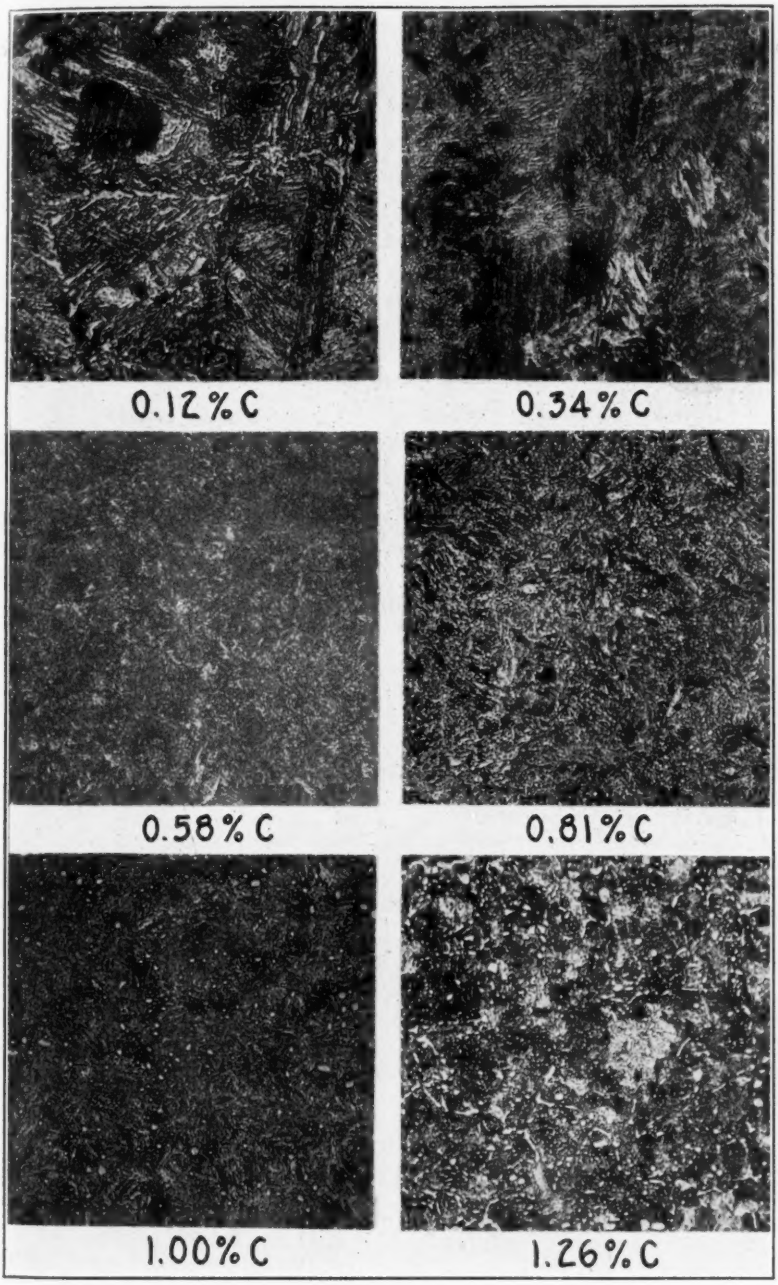

FIGURE 8.—*Microstructures of the hardened steels.* × *500*

Etched with 2 per cent nitric acid in alcohol.

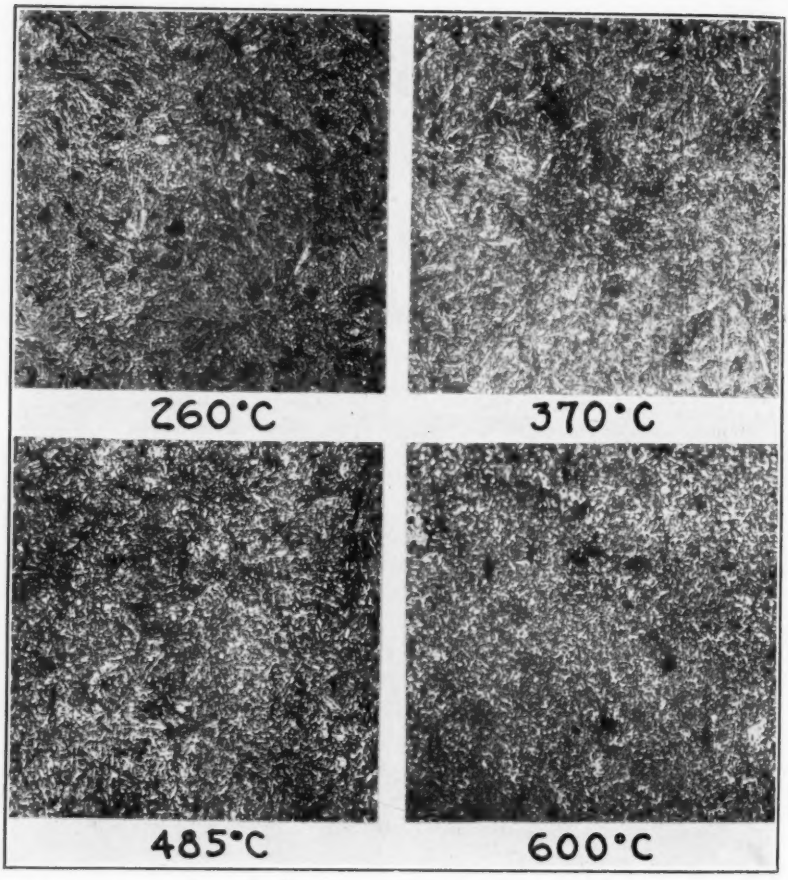

FIGURE 10.—*Microstructures of the tempered 0.81 per cent carbon steel.* × *500*
Etched with 2 per cent nitric acid in alcohol. Tempered at temperatures indicated.

crease in tempering temperature progressively lowered the resistance to wear of eutectoid carbon steel as determined in the Amsler machine. The microstructures of these steels are shown in Figure 10.

7. EXAMINATION OF THE ABRADED SURFACES

A study was made of the structures of the steels adjacent to the worn surfaces. The appearance of these structures in the steels representing the lowest and highest carbon contents are shown in Figure 11.

The low-carbon steel showed marked distortion of the grains near the surface after wear in all conditions of heat treatment. The gradation from distorted to normal structure can be seen in the micrographs. The micrographs of the high-carbon steel do not show any such gradation on the picture, but by comparing the structure near

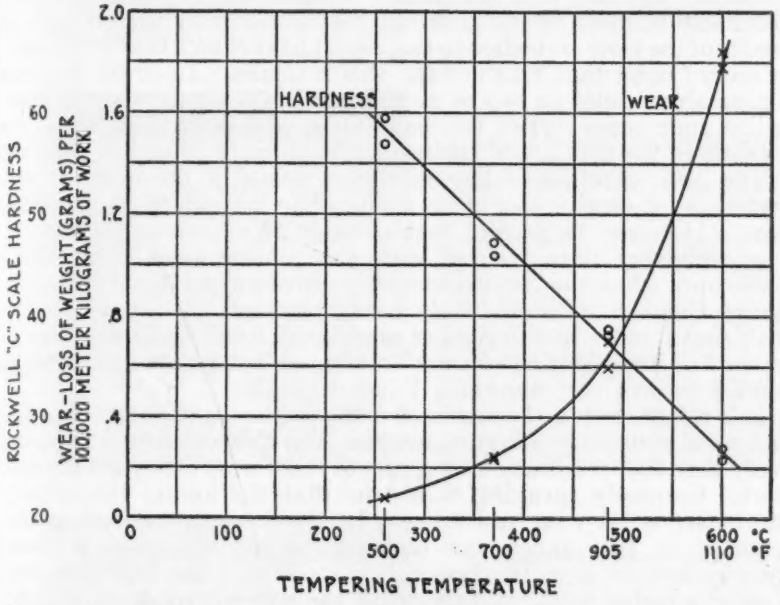

FIGURE 9.—*Effect of tempering temperature on the wear of an 0.81 per cent carbon steel*

the surface with the corresponding normal structure shown in Figures 6, 7, and 8 it can be seen that the entire layer of metal adjacent to the surface shown in the micrographs of the normalized and hardened steels was so severely distorted as to obliterate the base structure entirely. The structure of these two steels slightly below the worn surface could not be resolved under the microscope even when viewed at a magnification of 2,000 diameters. The structure of the annealed high-carbon steel slightly below the worn surface showed evidences of the carbide particles having been brought closer together, presumably by the distortion of the surface layers. Prolonged etching failed to reveal the ferrite boundaries adjacent to the surface. These boundaries were easily revealed at some distance below the surface.

Microscopic examination of the normalized 1.00 per cent carbon steel revealed some interesting and unusual features in the structure adjacent to the surface. At one point it was found that a distorted structure extended inward for some distance and, instead of merging gradually into the normal structure, was sharply separated from it by a wavy boundary. The appearance of this structure is shown in Figure 12 (*a*).

At other points adjacent to the surface, the same specimen showed no definite evidences of distortion of the structure at 500 magnifications. At 2,000 magnifications, however, a thin layer of severely distorted structure was found, as shown in Figure 12 (*b*). The normal structure at 2,000 magnifications is shown in Figure 12 (*c*).

IV. DISCUSSION OF RESULTS

Despite the fact that the Amsler wear testing machine has many peculiarities, most of which are at best imperfectly understood, the results of the tests embodied in this report have shown that it is possible to secure consistent results with this machine. In order to secure comparable results on two or more materials it is necessary to standardize upon some sort of test conditions, and then, if sufficient care is taken in the conduct of the tests, reliable data should be obtained.

The interpretation of test results in terms of the application of materials for service should be attended by considerable discrimination. Attempts to predict the behavior of metals in service from wear-resistance data secured with the Amsler machine should be made only when the service conditions involve combined rolling and sliding fraction under relatively heavy pressures of a type similar to that encountered in the Amsler machine. Results obtained by one method of investigation of wear usually can not be applied to service conditions involving wear of a different kind.

It is a fact that in the minds of many engineers the terms hardness and wear resistance are synonymous, and this opinion is evidenced every time the specification for a part to resist wear calls for a hardened steel. Generally speaking, it is true that the harder the material, the better is its wear resistance. In the case of the carbon steels reported in this paper, the high-carbon steels showed a greater wear resistance than the low-carbon steels and the hardened steels showed a higher wear resistance than the normalized steels, which, in turn, with the exception of the low-carbon range, showed a higher wear resistance than the annealed steels.

From a study of the data and the microstructures of the steels tested, it is evident that a martensitic, or rather a martensitic,troostitic structure is the most favorable for resisting wear of the type studied. Although both the annealed and the normalized steels in the high-carbon ranges are relatively soft as compared with the hardened steels, their resistance to wear varies widely. The normalized high-carbon steels show a resistance to wear almost as great as that of the hardened high-carbon steels, while the annealed high-carbon steels show a relatively poor resistance to wear. The structures of these normalized and annealed high-carbon steels vary markedly. They may be divided into two classes. The structures of the normalized steels are of lamellar pearlite, whereas those of the an-

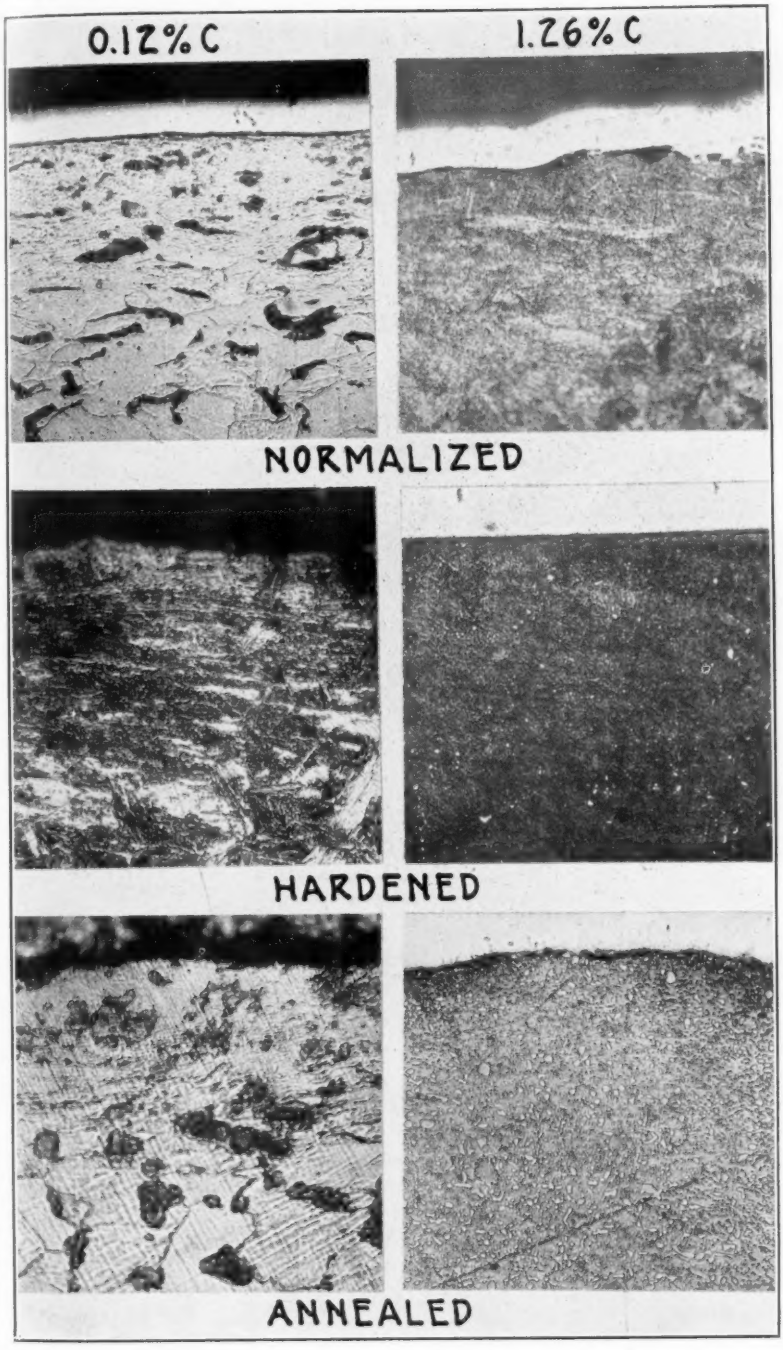

FIGURE 11.—*Micrographs of the structures adjacent to the worn surface of the low and high carbon steels tested.* × 500

Etched with 2 per cent nitric acid in alcohol.

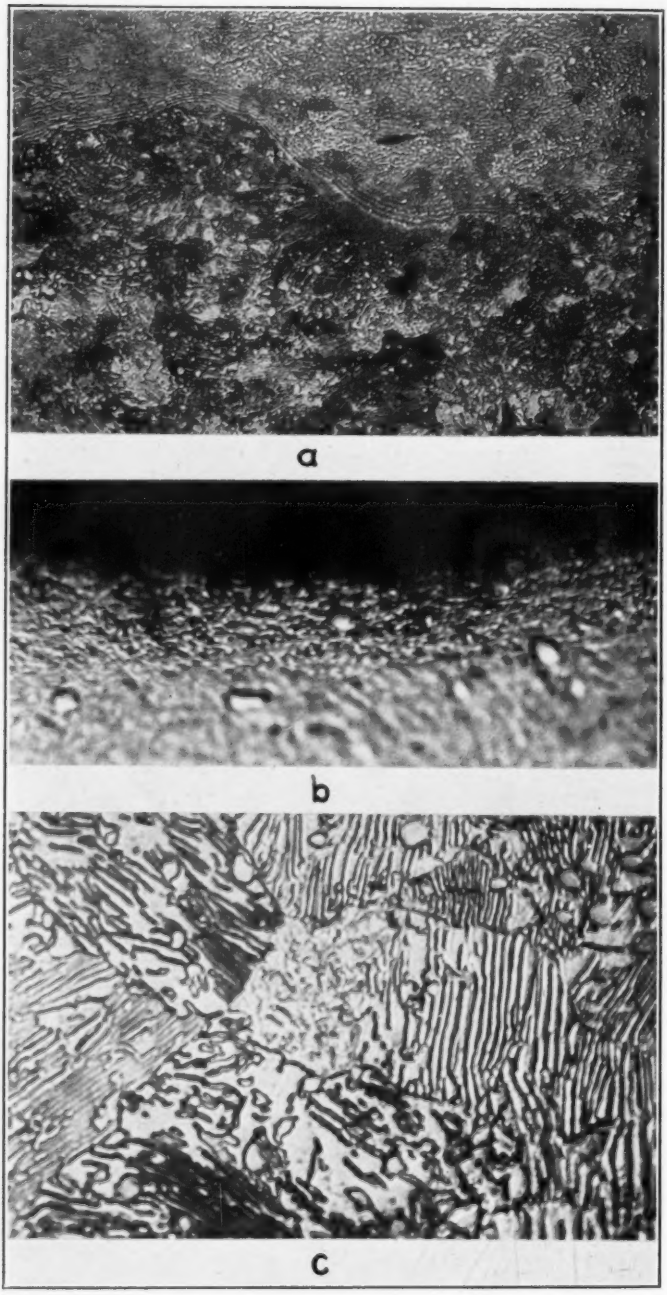

FIGURE 12.—*Some unusual features in the structure adjacent to the wearing edge of a normalized 1.00 per cent carbon steel*

Etched with 2 per cent nitric acid in alcohol. *a*, Micrograph showing a sharp line of demarcation between distorted and normal structure. × 500; *b*, micrograph showing a thin layer of severely distorted structure at the wearing surface. × 2,000; *c*, normal structure, × 2,000.

nealed steels are mostly spheroidized cementite and ferrite. This spheroidization was the result of the relatively slow cooling through the critical range undergone by the steels during the annealing treatment. From the curves shown in Figure 5, it would seem that lamellar pearlite is quite resistant to wear. This is in accordance with results reported by Lehman.[5] In making wear tests on cast iron he found that the main factor which governed the resistance to wear of cast iron was the percentage of pearlite.

Evidently the presence of either free ferrite or free cementite (as spheroids) is detrimental to the wear resistance of normalized carbon steels. That free ferrite is distinctly harmful is shown by the wear of the low-carbon steels, all of which exhibited low resistance to wear. The microstructures of these steels (fig. 7) show the normal amount of free ferrite.

In the high-carbon range, the 1.00 per cent carbon steel, as normalized, showed a somewhat greater loss of weight than either the 0.81 per cent or the 1.26 per cent carbon steel. (Fig. 5.) From the microstructures of these steels (fig. 7) it will be observed that the 1.00 per cent carbon steel shows relatively numerous patches of free cementite. The 1.26 per cent carbon steel, although containing, of course, more excess cementite than the 1.00 per cent carbon steel, has most of its excess cementite in the form of thin envelopes surrounding the pearlitic grains.

As previously mentioned, the normalized low-carbon steels showed slightly less resistance to wear than the same steels when annealed. An examination of the micrographs of these steels (figs. 6 and 7) revealed that the pearlite in the annealed steels was surrounded by cementitic envelopes. The normalized steels did not show this feature in their structures. These envelopes, being rather continuous and much stronger than the surrounding ferrite, are undoubtedly responsible for the wear resistance of the low-carbon annealed steels being greater than that of the same steels when normalized.

As would be expected, tempering a hardened steel resulted in a gradual lowering of its resistance to wear. It is interesting to note that the hardened 0.81 per cent carbon steel tempered at 600° C. (1,100° F.) showed practically the same resistance to wear as the same steel annealed. The microstructures of these two steels (figs. 6 and 10) seem, upon first glance, to be quite different, but a closer examination reveals that the tempered steel shows distinct evidence of spheroidization.

The microstructures of the steels adjacent to the worn surfaces show that the type of wear studied in this report was generally accompanied by severe distortion of the structure. This suggests a reason for the detrimental effect of spheroidal cementite. It would appear that cementite occurring as spheroids is easier to dislodge under severe rubbing action than cementite which occurs in lamellar pearlite or as relatively thin, continuous envelopes surrounding pearlitic grains in hypereutectoid steels.

[5] H. Lehman, Wear Tests on Cast Iron, Foundry Trade J., p. 36, January 13, 1927; p. 35, February 24, 1927.

V. SUMMARY AND CONCLUSIONS

The resistance to wear of a group of carbon steels was studied by means of the Amsler wear-testing machine in which the material is subjected to combined rolling and sliding friction under heavy pressures. Annealed carbon steels gave relatively poor wear-resisting qualities for all carbon contents. Normalized steels showed low wear resistance in the low-carbon range, but had greatly improved wear resistance in the high-carbon range. The hardened steels showed low wear-resistance in the lowest carbon ranges, but as the carbon content increased the wear resistance increased very rapidly until about 0.6 per cent carbon. Above this percentage the wear resistance increased very slowly. Tempering a hardened steel resulted in a gradual lowering of its wear resistance.

A martensitic-troostitic structure was the most favorable for resisting wear of the type studied. Properly normalized high-carbon steels, which showed a structure of lamellar pearlite, had almost as good wear resistance as the hardened steels. Annealed high-carbon steels, showing a structure predominately spheroidized cementite, had relatively poor resistance to wear. Apparently free ferrite or free cementite (as spheroids) are detrimental to the resistance to wear.

Wear of the type studied usually resulted in marked distortion of the structure of the steel adjacent to the worn surface.

VI. ACKNOWLEDGMENTS

The author desires to express his grateful appreciation to Houston Babb, junior scientific aid, for his conscientious assistance in many of the tests.

WASHINGTON, April 29, 1931.

PERMANENCE STUDIES OF CURRENT COMMERCIAL BOOK PAPERS

By John O. Burton

ABSTRACT

This is one of a series of articles dealing with permanence studies of current commercial writing and printing papers. A wide variety of current book papers was tested for purity and strength and the effects of an artificial aging treatment on these papers were studied. In general, these book papers do not have as high purity as has been found in writing papers made of the same kind and quality of fibrous materials, nor do they resist to as great an extent the effects of the heat test used as an artificial aging treatment. The lower permanence qualities of the book papers are probably caused by the emphasis placed on printing quality instead of permanence qualities during their manufacture. The content of acid materials of many of the papers is quite high. Data previously procured indicate that the acidity of a permanent paper should not exceed the equivalent of 0.1 per cent sulphuric anhydride. This is further substantiated by the data obtained in the present study. There is a good correlation between the acidity of the paper and the change in strength and purity caused by the accelerated aging treatment.

Using the test results obtained as a basis, the papers were classified as to their relative permanence qualities. According to this classification system only one of the 28 papers studied could qualify as a permanent paper, but several were only slightly deficient. There was no constant relation between the quality of the raw materials used and the permanence qualities of the papers as judged from the tests applied.

CONTENTS

	Page
I. Introduction	429
II. Description of papers studied	430
III. Description of test methods employed	431
1. Preparation of papers for testing	431
2. Physical tests	431
3. Chemical purity tests	432
4. Accelerated aging test	432
IV. Discussion of test data	432
1. Strength tests	432
2. Permanence tests	433
(*a*) Chemical purity tests	433
(*b*) Accelerated aging test	436
V. Classification of the papers relative to their permanence qualities	437
VI. Summary	439
VII. Conclusion	439

I. INTRODUCTION

The National Bureau of Standards, in cooperation with various interested governmental and private agencies, is studying problems connected with the permanence of papers used for records. A comprehensive program[1] was formulated, part of which involved the testing of commercial writing and book papers and the fibrous raw

[1] Scribner, B. W., Bureau of Standards Studies on the Deterioration of Paper, Pacific Pulp and Paper Industry, 4, No. 11, pp. 30-34; October, 1930.

materials used in their manufacture to determine as far as possible their probable permanence. A report of the results obtained in the study of the paper-making fibers and of a wide range of current commercial writing papers has been published.[2] A study of the permanence of representative commercial bond and ledger papers furnished by the United States Government Printing Office has been completed, and the results will be reported later. The present article contains the results of a study of current commercial book papers. The American Library Association and the National Association of Book Publishers both expressed their desire for this particular information. Thus, this article completes a rather thorough survey from a permanence standpoint of papers used for written and printed records that are obtainable on the market at the present time.

II. DESCRIPTION OF PAPERS STUDIED

An outline of the work planned was sent to several manufacturers of book papers with the request that they submit any papers which they considered suitable for the purpose. Some papers were also obtained from deliveries to the United States Government Printing Office. The papers received from these two sources are believed to be representative of current commercial book papers. Following is a list of the papers studied with the descriptions of the materials used in their preparation as furnished by the manufacturers. The numbers of the papers are those used throughout the article:

1. New cotton rags, 85 per cent, and new linen rags, 15 per cent; rosin sized.
2. Chemical wood fiber containing some highly purified wood fiber; rosin sized; clay filled.
3. Bleached cotton fiber, 75 per cent, and bleached sulphite pulp, 25 per cent; sized with 2 per cent rosin and alum.
4. Bleached sulphite pulp, 50 per cent, and unbleached sulphite pulp, 50 per cent; rosin sized; clay filled.
5. The same as paper No. 2, except that the highly purified wood fiber was replaced with an equal amount of cotton linters.
6. Rag fiber, 50 per cent, and sulphite pulp, 50 per cent; rosin sized; clay filled.
7. Rag fiber, 85 per cent, and sulphite pulp, 15 per cent; rosin sized; clay filled.
8. White, uncooked rags, 100 per cent; rosin sized.
9. Rag fiber, "twos and blues" grade, 55 per cent, and chemical wood fiber, 45 per cent; rosin sized; clay filled.
10. Rag fiber, "twos and blues" grade, 50 per cent, and chemical wood fiber, 50 per cent; rosin sized; clay filled.
11. Bleached chemical wood fiber, 100 per cent; rosin sized, clay filled.
12. Rag fiber, "twos and blues" grade, 100 per cent; rosin sized; clay filled.
13. Rag fiber, "No. 1 white" grade, 100 per cent; rosin sized; clay filled.
14. Rag fiber, "No. 2 white" grade, 100 per cent; rosin sized.
15. Rag fiber, "No. 2 white" grade, 100 per cent; rosin sized.

[2] Rasch, R. H., A Study of Purified Wood Fibers as a Paper-Making Material, B. S. Jour. Research, 3, pp. 469-506; September, 1929.

17. White linen and cotton rags, 100 per cent; rosin sized.

22. Rag fiber, 50 per cent, and bleached chemical wood fiber, 50 per cent; rosin sized; clay filled.

24. Bleached chemical wood fiber, 100 per cent; rosin sized; clay filled.

25. Rag fiber, 100 per cent; rosin sized; used for permanent editions of newspapers and periodicals.

28. Rag fiber, 50 per cent, and bleached chemical wood fiber, 50 per cent; rosin sized; clay filled.

31. Bleached chemical wood fiber, 100 per cent; double coated book paper.

32. Rag fiber, 50 per cent, and bleached chemical wood fiber, 50 per cent; double coated book paper.

37. New rags, 100 per cent; rosin sized.

38. "No. 1 white" grade of rags, 37.5 per cent, "thirds and blues" grade of rags, 37.5 per cent, and sulphite wood fiber, 25 per cent; rosin sized; clay filled.

40. Rag fiber, 50 per cent, bleached chemical wood fiber, 50 per cent; rosin sized; clay filled.

41. Rag fiber, 50per cent, and bleached chemical wood fiber, 50 per cent; double coated book paper.

45. New white and cream rags, 100 per cent; rosin sized. This paper was manufactured especially with a view to permanence.

46. Same as paper No. 45 but from a different delivery.

III. DESCRIPTION OF TEST METHODS EMPLOYED

1. PREPARATION OF PAPERS FOR TESTING

The samples for physical testing were conditioned and tested in a room maintained at a relative humidity of 65 per cent, ± 2 per cent, and at a temperature of 21° C., ±2° C. (70° F., ± 5° F.). These conditions are those specified by the paper testing committee of the technical Association of the Pulp and Paper Industry. The samples for the chemical purity tests were reduced to a uniform fibrous condition by means of mechanical disintegration. This method of preparation has been found necessary in order to insure complete reaction of the reagents with the fibers. A description of the grinder used and the reasons for this method of preparation have been given in full in previous publications.[3]

2. PHYSICAL TESTS

The determinations of thickness, weight, fiber composition, opacity, bursting strength, tearing strength, and tensile strength were made by the official testing methods of the Technical Association of the Pulp and Paper Industry.[4] The folding endurance was determined with a M. I. T. (Massachusetts Institute of Technology) type of tester, which is also described in Paper Testing Methods. This type of tester was used instead of the Schopper tester because it was necessary to use different tensions when testing different papers. Most of the book papers had insufficient strength to give a significant folding

[3] Burton, J. O., and Rasch, R. H., The Determination of the Alpha Cellulose Content and Copper Number of Paper, B. S. Jour. Research, **6**, pp. 603-619; April, 1931. See also footnote 2, p. 430.

[4] Paper Testing Methods, prepared by the Committee on Paper Testing of the Technical Association of the Pulp and Paper Industry, Lockwood Trade J. Co., New York; 1929.

endurance value when the Schopper machine available was used with the specified tension of 1 kg. A folding endurance of at least 100 double folds was desired on all of the papers. To obtain this value the tension on the folding strip would have to be less than 1 kg for most of the papers. On the other hand, for accuracy and to save time in testing, the maximum tension consistent with obtaining a significant folding endurance value should be used. Therefore, different tensions were required for testing different papers. The tension on the paper strip in the Schopper tester may be varied only to a slight extent without changing the spring, and each change of tension requires a painstaking recalibration, whereas the tension on the strip in the M. I. T. tester may be varied over a much wider range and recalibrated with ease. Therefore, the latter type of tester was used. However, even with this machine it was not always possible to obtain a folding endurance value of 100.

3. CHEMICAL PURITY TESTS

All of the chemical tests used have been described in the literature. The determinations of the amounts of rosin, ash, and casein were made by the official methods of the Technical Association of the Pulp and Paper Industry.[5] The alphacellulose method [6] was a modification of that of Jentgen, the copper-number method [6] was essentially that of Braidy, and the acidity method [7] was the one designed by Kohler and Hall.

4. ACCELERATED AGING TEST

A heat treatment at 100° C. (212° F.), for 72 hours was used to produce accelerated aging. The oven used for this purpose was equipped with a fan and duct for rapidly circulating the air. The temperature was controlled by means of a thermostat and relays to within ±1° C. (±2° F.). No attempt was made to purify the air nor to control its humidity. A detailed description and photograph of this oven were included in a previous publication.[8] The effects of this treatment were measured by the change in the strength of the papers and changes in their chemical purity.

IV. DISCUSSION OF TEST DATA

The test data are given in Table 1. Following is a discussion of them.

1. STRENGTH TESTS

It is difficult to compare the papers with one another as they vary widely in weight and finish. However, the strength of book papers is not such an important indication of quality as it is in the case of writing papers, since the latter are subjected to greater stresses. The folding endurance values obtained mean little in so far as the strengths of the papers are concerned, although they are significant in interpreting the effect of the aging treatment. This is because there is no common basis upon which the papers may be compared, since the

[5] See footnote 4.
[6] See footnote 3.
[7] S. Kohler, and G. Hall, Acidity in Paper, The Paper Ind., 7, No. 7; October, 1925.
[8] See footnote 2, p. 430.

tests were made at various tensions, and as far as is known there is no constant relation between the amount of tension and the folding value. The tearing strength and tensile strength are probably more indicative of the relative strengths of the papers. Some of the book papers compare very favorably with bond papers of the same weight in these two respects.

2. PERMANENCE TESTS

(a) CHEMICAL PURITY TESTS

The basic component of paper is cellulose, but several additional ingredients are added in the manufacturing process. For a permanent paper the cellulose composing the paper should have a high

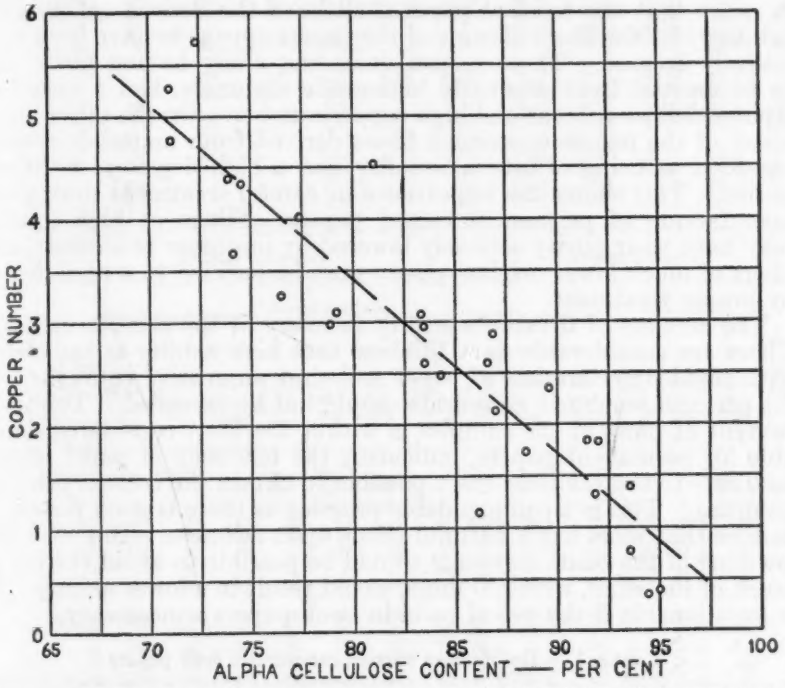

FIGURE 1.—*Relation between the copper number and the alpha-cellulose content of the book papers studied*

purity, and the amount of added ingredients, especially of those known to be harmful, should be a minimum. The copper number and the alpha-cellulose content are usually regarded as a measure of the purity of the cellulose. Papers of good quality are characterized by low copper numbers and high alpha-cellulose contents. Although there is no infallible rule relating these two purity tests, materials having a low copper number usually have a correspondingly high alpha-cellulose content. That this relation holds in general may be seen from Figure 1, where the copper numbers and alpha-cellulose contents of all the book papers studied are plotted with copper numbers as ordinates and alpha-cellulose contents as abscissas. There are nearly always two, and sometimes three, materials added

to book papers during the manufacturing process. These are rosin and alum for sizing and mineral filler for increasing the opacity and improving the printing quality. An excess of either of the first two is considered harmful. Excessive use of alum results in high acidity, which has a pronounced deteriorative effect upon paper. Nearly all mineral fillers used are chemically inert and are usually regarded as having no harmful effect upon the permanence of the paper.

The values obtained for the alpha-cellulose contents and the copper numbers (see Table 1) indicate a wide variation of purity among the different papers. In general, these book papers have a lower degree of purity than is found in writing papers made of the same quality of fibrous materials. This is probably due to the more severe cooking treatment given the fibers during book paper manufacture in order that the finished paper shall have the desired softness for printing; for the fibers of some of the papers appear to have been very severely treated. These papers, including many having fibers said to be derived from originally high-grade materials, had a very low alpha-cellulose content and high copper number. On the other hand, many of the papers containing fibers derived from materials usually regarded as being of inferior quality had a high degree of cellulosic purity. This shows the importance of careful treatment during the manufacture of permanent record papers. Fibers of high quality may have their purity seriously lowered by improper processing, and fibers of much lower original purity may be purified to a high degree by proper treatment.

The amount of titratable acidity in many of the samples is large. There are considerable data to show that high acidity is associated with rapid deterioration of paper and that an acidity equivalent to 0.1 per cent sulphuric anhydride should not be exceeded. The rosin content of most of the samples is within the limit considered desirable for permanent papers, indicating the tendency of paper manufacturers to use the least rosin possible to obtain the correct printing qualities. This is a commendable practice as there is good reason to believe that rosin has a harmful effect upon cellulose. But with the lowering of the rosin content it should be possible to avoid the use of much of the alum, which, if done, would result in a lower acidity. It is questionable if the use of rosin in book papers is necessary.

TABLE 1.— *Test data on current commercial book papers*

Sample No.	Fiber composition			Sizing		Ash	Weight, 500 sheets 24 by 40 inches	Thickness	Opacity	Bursting strength	
	Rag	Chemical wood, coniferous	Chemical wood, deciduous	Rosin	Casein					Before heating	After heating
	Per cent	*Per cent*	*Per cent*	*Per cent*	*Per cent*	*Per cent*	*Pounds*	*Inch*	*Per cent*	*Points*	*Points*
1	100			1.2		0.60	53.9	0.0037	83.0	34.6	30.0
2		50	50	0.5		14.67	54.1	.0040	92.9	14.9	14.5
3	75	15	10	1.6		1.61	38.5	.0030	79.4	15.2	14.0
4		100		1.4		16.43	35.9	.0021	86.1	8.8	7.8
5				0.7		15.53	54.0	.0041	93.0	11.7	11.2
6	50	50		1.1		14.26	62.3	.0052	93.4	19.3	19.0
7	90	10		1.0		12.35	62.2	.0066	94.0	11.8	12.1
8	100			1.3		.18	63.4	.0073	93.0	13.8	14.5
9	30	10	60	1.7		7.55	40.5	.0030	85.0	11.9	10.7
10	50	10	40	0.7		14.43	52.1	.0030	88.6	11.7	10.8

TABLE 1.—*Test data on current commercial book papers*—Continued

Sample No.	Fiber composition			Sizing		Ash	Weight, 500 sheets 24 by 40 inches	Thickness	Opacity	Bursting strength	
	Rag	Chemical wood, coniferous	Chemical wood, deciduous	Rosin	Casein					Before heating	After heating
	Per cent	*Per cent*	*Per cent*	*Per cent*	*Per cent*	*Per cent*	*Pounds*	*Inch*	*Per cent*	*Points*	*Points*
11		40	60	1.1		8.52	41.1	0.0031	84.4	14.6	10.4
12	100			1.3		7.97	53.1	.0038	85.2	17.8	16.3
13	100			1.7		11.12	66.0	.0066	93.4	11.0	9.5
14	100			2.4		3.91	41.8	.0041	84.8	10.0	9.5
15	95	5		1.7		6.06	57.3	.0032	90.0	15.3	13.8
17	100			1.4		1.33	88.8	.0118	94.9	33.6	33.3
22	50	30	20	2.5		5.50	43.5	.0035	87.1	13.1	9.5
24		40	60	0.9		9.68	46.5	.0026	83.1	13.0	10.8
25	100			1.0		.77	40.7	.0030	81.5	14.6	14.8
28	50	50		0.8		11.00	46.7	.0030	85.6	14.4	13.9
31		70	30	1.0	4.90	24.00	70.2	.0034	95.0	20.4	18.7
32	60	40		1.4	5.96	23.30	87.0	.0042	97.7	31.8	30.8
37	100			1.2		.64	45.1	.0071	96.2	25.7	26.2
38	75	25		1.4		12.68	41.9	.0027	86.7	13.6	12.5
40	50	50		2.0		9.87	40.0	.0031	86.6	10.8	12.3
41	60	35	5	1.5	5.78	24.86	89.3	.0042	97.0	28.4	27.9
45	100			1.7		.29	77.7	.0063		44.9	44.1
46	100			1.2		.20	76.7	.0060		52.3	51.5

Sample No.	Folding endurance							Tearing strength						
	Tension	Machine direction			Across machine direction			Average retention	Machine direction			Across machine direction			Average retention
		Before heating	After heating	Retention	Before heating	After heating	Retention		Before heating	After heating	Retention	Before heating	After heating	Retention	
	kg	*Double folds*	*Double folds*	*Per cent*	*Double folds*	*Double folds*	*Per cent*	*Per cent*	*g*	*g*	*Per cent*	*g*	*g*	*Per cent*	*Per cent*
1	1.0	159	75	47	98	62	63	55	100.4	66.4	66	104.0	68.4	66	66
2	.5	36	29	81	27	19	70	76	57.0	55.0	96	42.6	49.2	115	106
3	.5	142	81	57	39	32	82	70	42.8	43.6	102	37.8	33.4	88	95
4	.4	18	11	61	18	3	17	39	25.3	16.8	66	24.3	14.7	60	63
5	.4	23	16	70	18	14	78	74	37.6	36.4	97	36.8	32.6	89	93
6	.5	299	174	58	68	52	76	67	78.4	70.0	90	76.4	67.6	88	89
7	.3	57	41	72	27	21	78	75	46.4	46.4	100	42.0	39.8	95	98
8	.3	119	88	74	50	37	74	74	58.6	53.4	91	50.4	50.6	100	96
9	.5	16	10	63	16	10	63	63	33.2	26.0	78	30.4	27.2	89	84
10	.5	12	5	42	11	5	45	44	35.2	28.4	81	31.2	27.2	87	84
11	.5	53	3	6	32	4	13	10	36.6	18.4	50	29.2	14.8	50	50
12	.5	40	13	33	48	17	35	34	43.2	38.4	89	44.0	34.0	77	83
13	.3	21	7	33	18	7	39	36	54.4	45.0	83	47.4	45.0	95	89
14	.5	17	7	41	9	6	67	54	38.2	32.6	85	32.6	31.0	95	90
15	.5	41	17	41	23	15	65	53	49.0	37.6	77	38.9	31.8	82	80
17	.5	168	56	33	135	69	51	42	81.2	82.0	101	80.4	79.6	99	100
22	.5	118	9	8	35	8	23	16	38.8	35.2	91	31.0	34.8	112	102
24	.5	27	10	37	25	10	40	39	36.8	26.4	72	31.4	23.0	73	73
25	.5	299	316	106	138	100	72	89	58.4	62.4	107	60.0	57.8	96	102
28	.5	171	77	45	66	43	65	55	45.0	45.4	101	41.6	38.0	91	96
31	.5	21	18	86	34	28	82	84	36.0	32.2	89	36.4	30.6	84	87
32	.8	248	162	65	82	67	82	74	76.4	71.4	93	69.6	63.4	91	92
37	.5	177	158	89	74	87	118	104	98.0	97.2	99	99.2	99.2	100	100
38	.5	288	187	65	54	53	98	82	61.8	55.6	90	56.8	49.8	88	89
40	.5	54	30	56	12	12	100	78	38.0	37.2	98	33.6	37.6	112	105
41	.7	213	105	49	93	68	73	61	66.0	60.8	92	57.2	31.6	55	74
45	(1)	740	702	95	280	203	70	83	136.8	124.8	91	140.8	133.2	95	93
46	(1)	1,699	1,331	78	639	500	78	78	121.6	115.6	95	124.4	122.0	98	97

[1] The folding endurance of papers 45 and 46 was determined with the Schopper folding endurance machine.

TABLE 1.—*Test data on current commercial book papers*—Continued

Sample No.	Tensile strength							Alpha-cellulose content			Copper No.			Acidity	
	Machine direction			Across machine direction			Average retention	Before heating	After heating	Loss	Before heating	After heating	Increase	Sulphuric anhydride	Acid number
	Before heating	After heating	Retention	Before heating	After heating	Retention									
	kg	*kg*	*Per cent*	*kg*	*kg*	*Per cent*	*Per cent*	*Per cent*	*Per cent*	*Per cent*				*Per cent*	
1	6.90	6.71	97	4.18	3.95	95	96	86.56	82.36	4.20	2.56	3.09	0.53	0.096	24
2	3.92	3.89	99	2.17	2.11	97	98	76.53	76.26	.27	3.25	3.64	.39	.024	6
3	3.35	3.46	103	1.91	1.77	93	98	86.98	82.80	4.18	2.14	2.73	.59	.120	30
4	2.26	2.16	96	1.29	1.38	107	102	81.04	78.38	2.66	4.53	4.98	.45	.148	37
5	3.07	2.85	93	1.76	1.70	97	95	78.91	77.55	1.36	2.98	3.22	.24	.032	8
6	5.60	5.51	98	2.31	2.30	100	99	89.60	84.70	4.90	2.34	2.86	.52	.048	12
7	3.48	3.50	101	1.65	1.73	105	103	91.98	83.68	8.30	1.82	2.39	.57	.020	5
8	3.93	4.10	104	2.04	2.18	107	106	93.54	85.99	7.55	1.41	1.90	.49	.040	10
9	3.08	2.90	94	1.86	1.79	96	95	74.09	68.75	5.34	3.69	4.29	.60	.232	58
10	3.16	2.93	93	1.78	1.72	97	95	70.95	63.93	7.02	5.33	5.70	.37	.188	47
11	3.78	3.62	96	1.83	1.61	88	92	71.08	58.61	12.47	4.75	5.56	.80	.240	60
12	4.20	3.86	92	2.56	2.37	93	93	73.90	69.53	4.37	4.40	4.88	.48	.180	45
13	3.19	2.84	89	1.96	1.83	93	91	72.23	66.87	5.36	5.75	6.15	.40	.152	38
14	2.64	2.51	95	1.26	1.28	102	99	83.49	77.63	5.86	2.61	3.17	.56	.184	46
15	4.02	3.82	95	2.19	2.08	95	95	77.37	71.16	6.21	4.03	4.32	.29	.208	52
17	6.93	6.82	98	4.92	5.05	103	101	88.45	84.02	4.43	1.72	2.19	.47	.152	38
22	3.31	2.69	81	1.56	1.39	89	85	83.31	67.68	15.63	3.07	4.17	1.10	.196	49
24	3.70	3.50	95	1.90	1.90	100	98	74.43	68.42	6.01	4.35	4.84	.49	.196	49
25	3.10	3.20	103	1.80	1.90	106	105	91.92	91.06	.86	1.32	1.46	.14	.080	20
28	4.00	3.80	95	2.00	2.00	100	98	83.40	81.37	2.03	2.95	3.28	.33	.092	23
31	5.15	4.82	94	3.14	2.85	91	93	79.23	76.56	2.67	3.10	3.18	.08	------	------
32	7.20	6.93	96	3.77	3.66	97	97	86.09	85.82	.27	1.13	1.77	.64	------	------
37	6.10	6.30	103	3.70	3.70	100	102	93.36	92.16	1.20	.77	1.02	.25	.060	15
38	3.30	3.20	97	1.60	1.50	94	96	91.51	90.21	1.30	1.85	2.37	.51	.048	12
40	3.50	3.70	106	1.60	1.70	106	106	86.92	85.23	1.69	2.87	3.34	.47	.068	17
41	7.30	7.20	99	3.80	3.80	100	100	84.20	82.10	2.10	2.48	2.95	.47	------	------
45	9.27	9.22	99	5.30	5.47	103	101	95.00	92.49	2.51	.40	.93	.53	.028	7
46	10.02	9.93	99	6.22	6.33	102	101	94.40	92.38	2.02	.35	.64	.29	.015	4

[1] The acid number is the number of ml of 0.01 *N* NaOH required to neutralize the three successive hot water extracts of 10 g of ground paper.

(b) ACCELERATED AGING TEST

The effect of the accelerated aging treatment, heating for 72 hours at 100° C. (212° F.), is shown by the change in strength of the papers and changes in their chemical purity. In an investigation such as this where a number of kinds of papers from a variety of sources is being studied there are too many variables to obtain very definite relationships among the properties determined. However, several general relationships may be observed.

A high content of acid materials is accompanied by a correspondingly large decrease in alpha-cellulose content. It is noticeable that all of the papers appear to fall into two groups. One of these groups contains papers which lose less than 2 per cent alpha cellulose during the heat treatment, and the other group contains papers which lose more than 4 per cent. The papers in the first group have an acidity less than 0.1 per cent sulphuric anhydride, and those in the second group have an acidity greater than 0.1 per cent sulphuric anhydride. Papers 6, 7, and 8 are exceptions to this classification. These three papers were made by the same manufacturer and according to his

description were made from good materials. They had low acidities, but the decrease of alpha-cellulose content of all three was high. This large decrease in alpha-cellulose content during the heat treatment may have been caused by a too severe treatment of the stock during manufacture.

The increase of the copper number by the heat treatment was not particularly significant. There is a very general relationship in that the best papers, judged from the other tests, increased very little in copper number. Other than this there appeared to be no constant relation between increase in copper number and the other tests.

The loss of strength caused by the heat treatment is best measured by the change in folding endurance. The other strength factors are but slightly changed by this treatment and the more sensitive folding endurance test is the best criterion of loss in strength. There was a general relationship between the chemical purity tests and the retention of folding strength after the accelerated aging treatment. Papers which retained the most strength decreased the least in alpha-cellulose content. There was again the occurrence of two distinct groups of papers. Those which decreased less than 2 per cent in alpha-cellulose content retained more than 70 per cent of their folding strength. Those which decreased more than 4 per cent in alpha-cellulose content retained less than 70 per cent of their folding strength. Samples 6, 7, and 8 are again exceptions to this grouping.

V. CLASSIFICATION OF THE PAPERS RELATIVE TO THEIR PERMANENCE QUALITIES

A system of classification of printing and writing papers relative to their permanence qualities has been suggested by the National Bureau of Standards.[9] This classification is based upon the purity and strength of the finished paper. The values given are derived from the results of the extensive investigations of this bureau during the past four years on the permanence of paper. In these investigations tests similar to the ones described here have been made on a large number and variety of papers, and it is believed that papers fulfilling the requirements of the various groups will have the relative degree of permanence indicated.

In this system of classification all papers are divided into four classes. The first class contains those papers which may be expected to have maximum longevity. A book paper fulfiling the requirements of this class would be particularly suitable for bound volumes of records having permanent value. The second class contains papers of high purity. Papers used for semipermanent records and in fine editions of rare and costly books should fulfill the requirements of this class. The third class is composed of papers which, while not having as high a degree of purity as those in the first two classes, have a fair degree of purity. Such papers could be used where moderate longevity is desired, such as in reference periodicals. Papers in the fourth class are those suitable for current use only. Table 2 illustrates in detail how such a system of classification might be applied to book papers. Of the book papers studied in the present investiga-

[9] B. W. Scribner, Permanence Standards for Printing and Writing Papers, Trans. A. S. M. E., 52, No. 19, P. I. 52-55; May-August, 1930. Also, Paper Mill, 53, p. 13; June 21, 1930.

tion No. 37 is the only one that fulfills completely the requirements of Class I. Some of the other papers fulfill the requirements of this class except in one or two respects. Nos. 25, 32, 38, 45, and 46 fall in Class II; Nos. 1, 2, 3, 5, 6, 7, 8, 17, 28, 31, 40, and 41, in Class III; and the remainder in Class IV.

TABLE 2.—*Classification of book papers*

Class I. PAPERS OF MAXIMUM PURITY FOR PERMANENT RECORDS

Stock: Free from unbleached or ground wood fibers. Alpha cellulose content not less than 90 per cent. Copper number not more than 1.0.
Acidity: pH value not less than 4.5 and acid number less than 25.
Rosin: Not more than 1.0 per cent.
Stability: When heated for 72 hours at 100° C. the alpha-cellulose content shall decrease not more than 1.5 per cent, the folding endurance shall decrease not more than 25 per cent, and the copper number shall increase not more than 0.5.
Weight, strength, and opacity:

Weight: (25 by 40, 500)—pounds	35	40	50	60	70
Weight: (25 by 38, 500)—pounds	33.3	38.0	47.5	57.0	66.5
Folding endurance: Average each direction, not less than double folds	75	100	125	160	200
Bursting strength: Average not less than—points	20	25	30	35	40
Thickness: Average—inch	0.0035	0.0040	0.0050	0.0060	0.0060
Tensile breaking strength: Average not less than kg per 15 mm width—					
Machine direction	4.0	5.0	6.0	7.0	8.0
Across machine direction	2.0	2.5	3.0	3.5	4.0
Opacity: Contrast ratio not less than—per cent	84	86	89	90	90

Color, finish, formation, cleanliness, and printing quality: Shall be in accordance with sample.
Testing methods: The testing methods shall be those approved by the Technical Association of the Pulp and Paper Industry. The physical specifications are for a relative humidity of 65 per cent and a temperature of 70° F., which are the testing conditions approved by this association.

Class II. PAPERS OF HIGH PURITY FOR SEMIPERMANENT RECORDS

Stock: Free from unbleached or ground wood fibers. Alpha-cellulose content not less than 80 per cent. Copper number not more than 2.0.
Acidity: pH value not less than 4.5 and acid number less than 25.
Rosin: Not more than 1.5 per cent.
Weight, strength, and opacity:

Weight: (25 by 40, 500)—pounds	35	40	50	60	70
Weight: (25 by 38, 500)—pounds	33.3	38.0	47.5	57.0	66.5
Folding endurance: Average each direction, not less than double folds	30	40	60	80	100
Bursting strength: Average not less than—points	12	14	18	22	26
Thickness: Average—inch	0.0030	0.0035	0.0045	0.0050	0.0050
Tensile breaking strength: Average not less than kg per 15 mm width—					
Machine direction	3.0	3.0	4.0	5.0	6.0
Across machine direction	1.5	1.5	2.0	2.5	3.0
Opacity: Contrast ratio not less than—per cent	84	86	89	90	90

Color, finish, formation, cleanliness, and printing quality: Shall be in accordance with sample.
Testing methods: The testing methods shall be those approved by the Technical Association of the Pulp and Paper Industry. The physical specifications are for a relative humidity of 65 per cent and a temperature of 70° F., which are the testing conditions approved by this association.

Class III. PAPERS OF FAIR PURITY FOR RECORDS REQUIRING MODERATE LONGEVITY

Stock: Free from unbleached or ground wood fibers. Alpha-cellulose content not less than 70 per cent. Copper number not more than 3.5.
Acidity: pH value not less than 4.5 and acid number less than 25.
Rosin: Not more than 2.0 per cent.
Weight, strength, and opacity:

Weight: (25 by 40,500)—pounds	35	40	50	60	70
Weight: (25 by 38,500)—pounds	33.3	38.0	47.5	57.0	66.5
Folding endurance: Average each direction not less than—double folds	15	20	30	40	50
Bursting strength: Average not less than—points	11	12	15	19	22
Thickness: Average—inch	0.0025	0.0030	0.0033	0.0040	0.0050
Tensile breaking strength: Average not less than kg. per 15 mm. width—					
Machine direction	3.0	3.0	3.5	3.5	4.0
Across machine direction	1.5	1.5	2.0	2.0	2.5
Opacity: Contrast ratio not less than—per cent	84	86	89	90	90

Color, finish, formation, cleanliness, and printing quality: Shall be in accordance with sample.
Testing methods: The testing methods shall be those approved by the Technical Association of the Pulp and Paper Industry. The physical specifications are for a relative humidity of 65 per cent and a temperature of 70° F., which are the testing conditions approved by this association.

TABLE 2.—*Classification of book papers*—Continued

Class IV. PAPERS FOR TEMPORARY USE

Stock, acidity, and rosin: No requirements.					
Weight, strength, and opacity:					
Weight: (25 by 40,500)—pounds	35	40	50	60	70
Weight: (25 by 38,500)—pounds	33.3	38.0	47.5	57.0	66.5
Bursting strength: Average not less than—points	9	10	12	14	15
Thickness: Average—inch	0.0025	0.0030	0.0033	0.0040	0.0050
Tensile breaking strength: Average not less than kg. per 15 mm. width—					
Machine direction	3.0	3.0	3.5	3.5	4.0
Across machine direction	1.5	1.5	2.0	2.0	2.0
Opacity: Contrast ratio not less than—per cent	84	86	89	90	90
Color, finish, formation, cleanliness, and printing quality: Shall be in accordance with sample.					
Testing methods: The testing methods shall be those approved by the Technical Association of the Pulp and Paper Industry. The physical specifications are for a relative humidity of 65 per cent and a temperature of 70° F., which are the testing conditions approved by this association.					

VI. SUMMARY

1. In general, the book papers studied have a lower degree of purity and are affected to a greater extent by the heat test than writing papers made of the same kind and quality of fibrous materials.

2. The rosin content of most of the papers does not appear to be excessive, but the high acidity of many of them indicates an excessive use of alum, a practice which is very detrimental to the permanence of the papers.

3. The accelerated aging test shows that the change in purity, as measured by the change in alpha-cellulose content, is closely related to the loss of strength, as measured by the change in folding endurance, and that both of these factors are closely related to the acidity of the paper.

4. In general, the stability of these papers, as determined by the heat test, was dependent primarily on their chemical purity and had little relation to the source of the paper fiber or to its initial quality.

5. The system of classification suggested distributes the papers among the various classes in about the ratio to be expected of commercial papers selected in the manner herein described.

VII. CONCLUSION

The data produced in this study indicate that book papers, as they are commercially available at the present time, do not have, in general, as high permanence qualities as have been found in writing papers. This is probably largely true because in book papers printing quality appears, in general, to have been given more consideration than permanence, possibly because the purchaser of book papers is usually not so directly concerned with the preservation of printed records as is the purchaser of paper for written records. However, the fact that one of the papers may be classed as a paper of maximum permanence shows that it is possible to obtain permanence qualities in book papers comparable to those which can be obtained in writing papers, and at the same time preserve the printing qualities. A decided trend toward realization of this and of the need for more consideration of permanence qualities by book-paper makers and users is evident. The increasing cooperation in this respect between manufacturer, printer, and librarian will, no doubt, assist materially in making more certain that the paper in publications containing valuable records will have the desired longevity.

WASHINGTON, June 16, 1931.

THERMOMAGNETIC INVESTIGATION OF TEMPERING OF QUENCHED 0.75 PER CENT CARBON STEEL

By George A. Ellinger

ABSTRACT

Previous investigators have shown that martensite and retained austenite are present as constituents of quenched carbon steels. A study of the decomposition of these constituents in water quenched 0.75 per cent carbon steel has been made by means of thermomagnetic analysis. An astatic magnetometer was used to show changes in magnetization of specimens at various temperatures and these magnetization changes have been interpreted in the light of constitutional changes in the steel. Immediately upon the application of heat, an increase in magnetization took place, which is believed to represent stress release, caused by the precipitation of carbon from the supersaturated solid solution of carbon in alpha iron. The degree of tempering is believed to be dependent upon temperature and time, the first stage being completed at 200° C. in about six and one-half hours. The precipitated carbon is believed to combine with iron in the range between 200° and 300° C. to form iron carbide. This combination is progressive with time, being completed at 300° C. in about one hour. From 300° to 700° C. no further magnetic changes were noted upon holding at constant temperatures, consequently no further constitutional changes were believed to take place in this range, but the carbide apparently coagulated to form larger and larger particles. An increase in magnetization at about 235° C. was believed to indicate the decomposition of austenite, the decomposition being completed in about 45 minutes at that temperature.

CONTENTS

		Page
I.	Introduction	441
II.	Previous investigations	442
III.	General considerations	443
IV.	Method and material	444
	1. Apparatus	444
	2. Specimens and treatment	444
V.	Observations and results	445
VI.	Summary	450
VII.	Acknowledgment	451

I. INTRODUCTION

The decomposition or tempering of martensite is of great importance to the metallurgist interested in the heat treatment of steel. Various methods of observation have been used in studying this phenomenon, such as microscopic analysis, X-ray analysis, dilatometric measurements, thermal analysis, electrical resistance measurements, and thermomagnetic analysis. The first five methods are well known and need no explanation.

Thermomagnetic analysis reveals, in terms of changes in magnetic properties upon heating or cooling, certain constitutional transformations which are difficult to follow by means of most of the other methods. It was thought, therefore, that it might be possible to obtain by this method a fairly complete picture of the decomposition of martensite, taking place upon the tempering of quenched steels.

The condition of the carbon in the quenched state and that occurring as the tempering process proceeds is of considerable importance, and is not definitely known. Any light that can be thrown on this question, therefore, should aid materially in the solution of this problem. It has been very well established by several investigators that cementite undergoes a magnetic transformation, similar to the A_2 transformation in iron, at a temperature of approximately 215° C. This transformation, known as the A_0 transformation, is clearly shown by curves obtained by thermomagnetic analysis and, therefore, serves as a valuable criterion in the interpretation of results. It is of utmost importance to distinguish clearly between variations in magnetization which are due to actual structural changes and those which may be of purely magnetic origin.

This paper is a report on one phase of a more comprehensive study of quenched and tempered steels by means of thermomagnetic analysis with the cooperation of R. L. Sanford, chief of the magnetic measurements section of the National Bureau of Standards.

II. PREVIOUS INVESTIGATION

Honda[1] has concluded that cementite is in solid solution in quenched steels and that upon gradual rise of tempering temperature to 400° C., the carbide is precipitated.

Ishiwara[2] investigated the tempering of 0.94 per cent carbon steel and found an increase in magnetization at 130° C., which he attributed to the tempering of martensite to troostite.

Saito[3] investigated quenched and tempered steels and concluded that upon tempering a quenched steel at 300° C., cementite was first set free, but owing to the extremely fine particle size, it decomposed rapidly into iron and carbon, which subsequently recombined to form cementite.

Heyn and Bauer[4] determined the solubility in acids, of steels treated in various ways. Quenched steel, tempered at 400° C., was the most soluble, the rate of solubility decreasing in either direction, toward martensite on one side and pearlite on the other. Troostitic specimens left no residue of carbide, but a residue of carbon containing little or no iron. The authors suggested that some substance which they called "X" separated from martensite upon tempering up to 400° C. This substance differed greatly from cementite in its reactions with hydrochloric and sulphuric acids.

Maurer[5] investigated the magnetic properties of various steels and found results similar to those of Heyn and Bauer.

Dearden and Benedicks[6] investigated various annealed and quenched steels by means of thermomagnetic analysis. They found a slight increase in magnetization, for annealed steels, at about 130° C. and a point of decreased magnetization, at 210° C. Steels

[1] Kotaro Honda, On the Magnetic Investigation of the States of Cementite in Annealed and Quenched Carbon Steels, Sci. Repts., Tohoku Imperial Univ., Sendai, **6**, p. 149; 1917.

[2] Torajiro Ishiwara, On the Magnetic Analysis of Carbides Found in Different Kinds of Steel, Sci. Repts., Tohoku Imperial Univ., Sendai, **6**, p. 285; 1917.

[3] Seizo Saito, On the State of Carbon Steels, Quenched and Tempered, Sci. Repts., Tohoki Imperial Univ., Sendai, **9**, p. 281; 1920.

[4] E. Heyn and O. Bauer, Influence of the Treatment on the Solubility of Steels in Sulphuric Acid, J. Iron and Steel Inst., **79**, p. 109; 1909.

[5] E. Maurer, Recherches sur la trempe et le revenu du fer et de l'Acier, Revue de Metallurgie, **5**, p. 711; 1908.

[6] W. H. Dearden and C. Benedicks, Magnetic Changes in Iron and Steel Below 400° C., J. Iron and Steel Inst. **113**, p. 393; 1926.

quenched from 910° C. showed weak changes in magnetization at 120° and 260° C.

Duell [7] investigated the magnetic properties of carbon steels by means of a ballistic galvanometer method. Upon heating quenched specimens to high temperature, he found a discontinuous drop in magnetism at 300° C., explaining this as "possibly being due to the formation of iron carbide, the carbon of which was finely divided throughout the mass." Duell found no evidence which would indicate the formation of troostite from austenite, and concluded that austenite tempers at a "lower temperature and is probably not a very abrupt change." In this investigation a rather low magnetizing force of the order of 7.6 gilberts per centimeter was used.

Enlund [8] made electrical resistance measurements on eight carbon steels, and found that martensite started to temper to troostite at 100° C. and that the tranformation was most marked at 110° C., while austenite tempered at about 260° C. to troostite.

Results reported recently by Sefing [9] on the energy evolved during solution of quenched and tempered steel, obtained by means of an adiabatic calorimeter are in accord with the results of the present investigation. The maximum evolution of heat was obtained with specimens tempered at 150° C. and a second maximum was obtained with specimens previously tempered at 350° C.

III. GENERAL CONSIDERATIONS

As pointed out in the introduction, it is of great importance, in the interpretation of the results of thermomagnetic analysis, to distinguish clearly between changes due to constitutional transformations and those due to normal magnetic origin.

The normal magnetization curve consists of three more or less distinct stages. In the first stage, there is a considerable degree of magnetic stability, but the magnitudes to be measured are small and the curve is quite sentitive to the effects of previous magnetic history.

In the second stage, the curve is relatively steep and represents a region of magnetic instability. In this region many effects, such as strain, temperature, etc., have their maximum influence on the magnetization. It is difficult, therefore, to interpret data obtained in the second stage of magnetization with any degree of certainty. This point is often overlooked in researches in the field of magnetic analysis.

The third stage of magnetization represents the region of greatest magnetic stability in which differentiation between the effects of various influences can be made more easily. It is generally preferable to work in the third stage of magnetization.

For the type of steel under investigation it is generally necessary to apply a magnetizing force of at least 100 gilberts per centimeter to bring the material into the third stage. In the present investigation, the value of the applied magnetizing force was always 277 gilberts per centimeter. For the dimensional ratio of the specimens

[7] Clifford C. Duell, Magnetic Investigations of Carbon Steel, Transactions, Am. Soc. Steel Treating, 15, p. 630; 1929.
[8] B. D. Enlund, On the Structure of Quenched Carbon Steels, J. Iron and Steel Inst., 111, p 305; 1925.
[9] Frederick G. Sefing, Thermodynamics of a Heat Treated Steel, Bull. Michigan Eng. Expt. Station, East Lansing, Mich., 6, No. 7; May 1931.

used, the demagnetizing factor was of such a value that the effective magnetizing force was never less than 150 gilberts per centimeter.

The inflection in the magnetization-temperature curve in the neighborhood of 200° C. has been the subject of study by various investigators, notably by Honda and his associates,[10] [11] and is generally agreed to be due to the magnetic transformation of cementite, Fe_3C. The temperature at which this change is complete on heating and begins on cooling has been established by Honda, as 215° C. The A_0 transformation in pearlitic steels, increases in intensity as the carbon content increases. The minimum carbon content, at which the transformation will be found is not definitely known. However, from unpublished records of the magnetic measurements section of the National Bureau of Standards it has been found that annealed steel containing 0.14 per cent carbon shows a very definite A_0 transformation, the intensity of which is approximately 3 per cent.

It is conceivable that when cementite is present as one of the constituents of steel there might be conditions, such as the form and distribution of the carbide, or strain effects, etc., which would modify the transformation temperature just as other transformation points are altered by various alloying elements. There is some evidence in the results here reported that this is the case.

IV. METHOD AND MATERIAL

1. APPARATUS

The magnetometer method of thermomagnetic analysis was adopted as being the most suitable for the present investigation. By this method, changes in magnetization at a constant value of applied magnetizing force can be continuously observed as the heating or cooling progresses. The degree of magnetization is indicated by the deflection of an astatic magnetometer, so adjusted as to be practically free from the influence of outside magnetic disturbances. The apparatus used was a slightly modified form of that previously described by Sanford.[12]

2. SPECIMENS AND TREATMENT

The material studied was a basic open-hearth steel of the following composition:

	Per cent		Per cent
Carbon	0. 75	Silicon	0. 12
Manganese	. 52	Chromium	. 08
Phosphorus	. 018	Nickel	. 05
Sulphur	. 033	Copper	. 06

The specimens were 10 cm in length and 6 mm in diameter having a length to diameter ratio of 16.7, so that the self-demagnetizing effect of the specimens was not excessive. The specimens were normalized after machining to relieve any residual strains which may have been present.

[10] Kotaro Honda and Hiromu Takagi, On the Magnetic Transformation of Cementite, Sci. Repts., Tohoku Imperial Univ., Sendai, **4**, p. 161; 1915.

[11] Kotaro Honda and Takejiro Murakami, On the Thermomagnetic Properties of the Carbides Found in Steel, Sci. Rpts., Tohoku Imperial Univ., Sendai, **6**, p. 23; 1917.

[12] R. L. Sanford, Apparatus for Thermomagnetic Analysis, B. S. Jour. Research, **2** (RP50), p. 659; 1929.

The normalized specimens were packed in carburizing boxes containing fine silica sand and charcoal and heated to 825° C. in an automatically controlled electric muffle furnace. After holding at temperature for 30 minutes, certain specimens were hardened by quenching in a large volume of water at approximately 20° C. Other specimens were allowed to cool in the furnace.

Quenched specimens were placed in the apparatus immediately and normal magnetization-temperature curves taken, using a heating and cooling rate of approximately 2° C. per minute. From these curves, temperatures were selected at which to temper other freshly quenched specimens. These specimens were then placed in the apparatus, heated to the various selected temperatures, and held until it was certain that all magnetic changes had been completed. The specimens were then cooled slowly to room temperature, observations being made during both heating and cooling.

V. OBSERVATIONS AND RESULTS

Magnetization-temperature curves for electrolytic iron and for annealed and quenched 0.75 per cent carbon steel are shown in Figure 1. Magnetization is plotted in per cent, 100 per cent representing the magnetization at room temperature at the start of a run.

Electrolytic iron showed no A_0 transformation, the magnetization remaining constant over the range of temperatures investigated.

The annealed steel showed a very definite pearlitic A_0 transformation ending at about 215° C. on heating and commencing at the same temperature on cooling. There was some hysteresis, probably thermal, as is indicated by the difference in percentage magnetization between the heating and cooling curves at 400° C. This steel was heated above the critical range and cooled, only those portions of the curves being shown which lay between 0° and 400° C., this being the range of temperatures in which the primary interest of the investigation lay. It was found that between 400° and 700° C. no magnetization change with time took place upon holding at various temperatures in this range.

The magnetization-temperature curves, as determined on a specimen freshly quenched in cold water from 825° C. are also shown in Figure 1. There is a small increase in magnetization up to approximately 125° C., after which the increase is more rapid as heating progresses. At approximately 250° C. another increase in rate takes place, the curve reaching a maximum at about 290° C., after which the magnetization rapidly decreases to 400° C. Upon cooling, the A_0 transformation, which is entirely lacking on the heating curve, appears. As in the case of the annealed steel, this specimen was heated above the critical range and cooled, but only those parts of the curves between 0° and 400° C. are shown.

The lack of an A_0 transformation could be due to three things—the masking effect of stress release, the presence of carbide in sufficiently finely divided particles so that the transformation might be suppressed, or to the absence of carbide. In order to determine which of these might have been responsible in this case, several investigations were made.

Highly stressed steel shows no A_0 transformation. This is very well shown in cold-drawn steel wire. Martensite, as is well known,

is in a very highly stressed condition and could mask the $A°$ transformation, even if carbide were present.

In order to determine whether the absence of the A_0 transformation was due to the masking effect of stress release, a freshly quenched specimen was heated to 200° C. and held until all change in magnetization was complete. The specimen was then cooled with the results shown in curve 1, Figure 2. Curve 1, Figure 3, shows the change

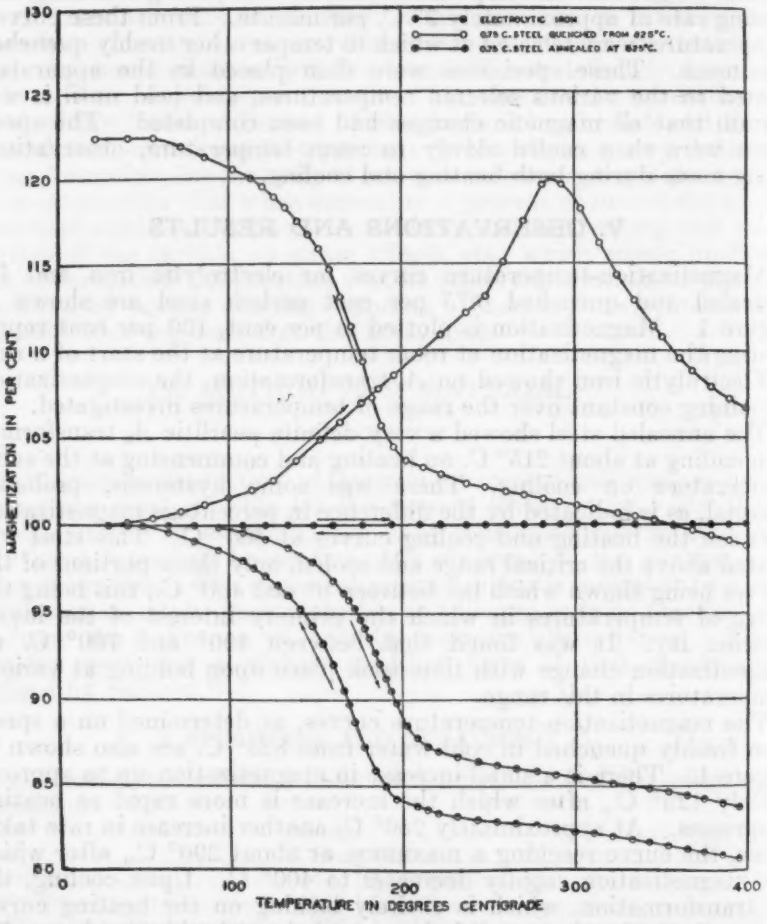

FIGURE 1.—*Magnetization-temperature curves for annealed electrolytic iron, annealed steel, and quenched steel containing 0.75 per cent carbon*

of magnetization with time at constant temperature and represents the portion *a–b* as indicated on curve 1 of Figure 2. Heating and cooling are indicated on the curves by directional arrows.

At 200° C. the magnetization gradually increased for six and one-half hours, after which no further change took place at that temperature. There was no change in magnetization upon cooling to room temperature, the curve being a straight line. Upon reheating, after cooling to room temperature, the magnetization remained con-

stant until a temperature of 235° C. was reached, shown in curve 2, Figure 2. This indicates that no A_0 transformation had taken place,

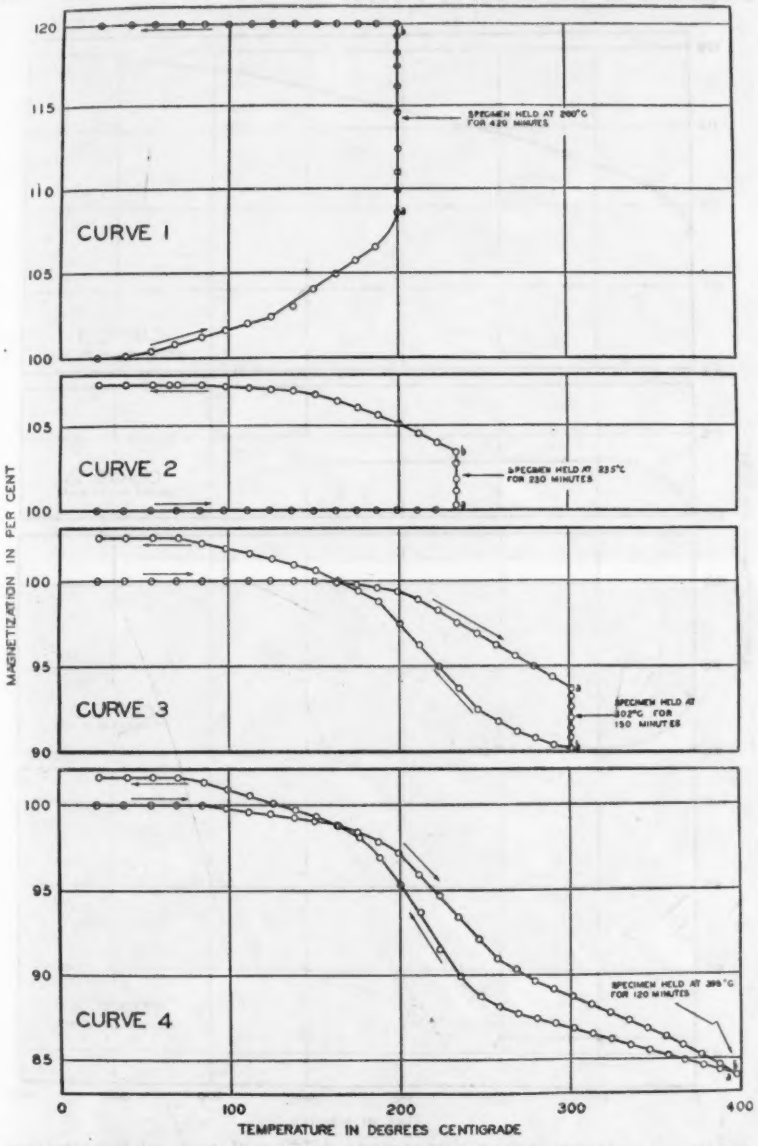

FIGURE 2.—*Magnetization change with temperature in heating a quenched 0.75 per cent carbon steel to various temperatures*

The portion a-b of each curve represents the change at the tempering temperature. Heating and cooling curves are indicated by directional arrows

and that the increase in magnetization shown upon the first heating of the quenched steel to 200° C. was probably due to the release of stresses and did not mask an A_0 transformation.

To determine whether or not the presence of carbide in very finely dispersed particles would fail to show an A_0 transformation, a detailed investigation of the effect of carbide size was made. The results

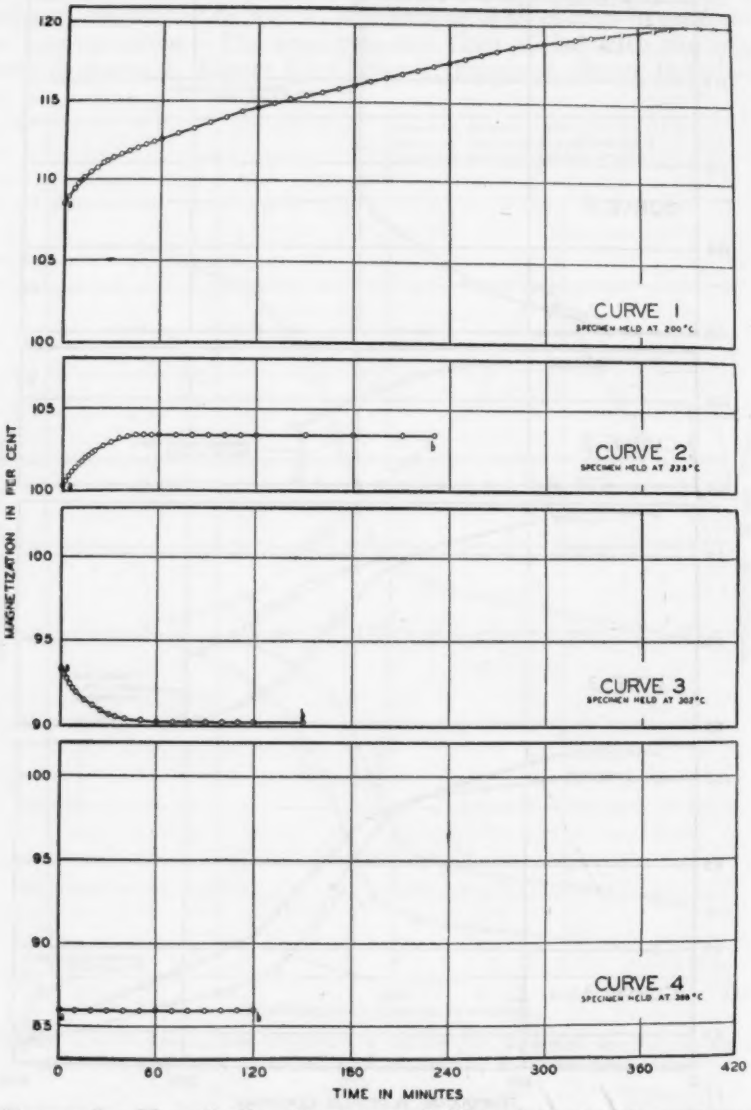

FIGURE 3.—*Magnetization change upon holding at constant temperatures*

These curves represent the portion *a-b* of the corresponding curves shown in Figure 2

have been reported in another publication.[13] It was found that the intensity of the transformation increased as the particle size decreased. Specimens in which the carbides were so fine as to be barely resolvable

[13] R. L. Sanford and G. A. Ellinger, Thermomagnetic Analysis and the A_0 Transformation in 0.75 C steel. Paper presented before the Am. Soc. Testing Materials, June 1931.

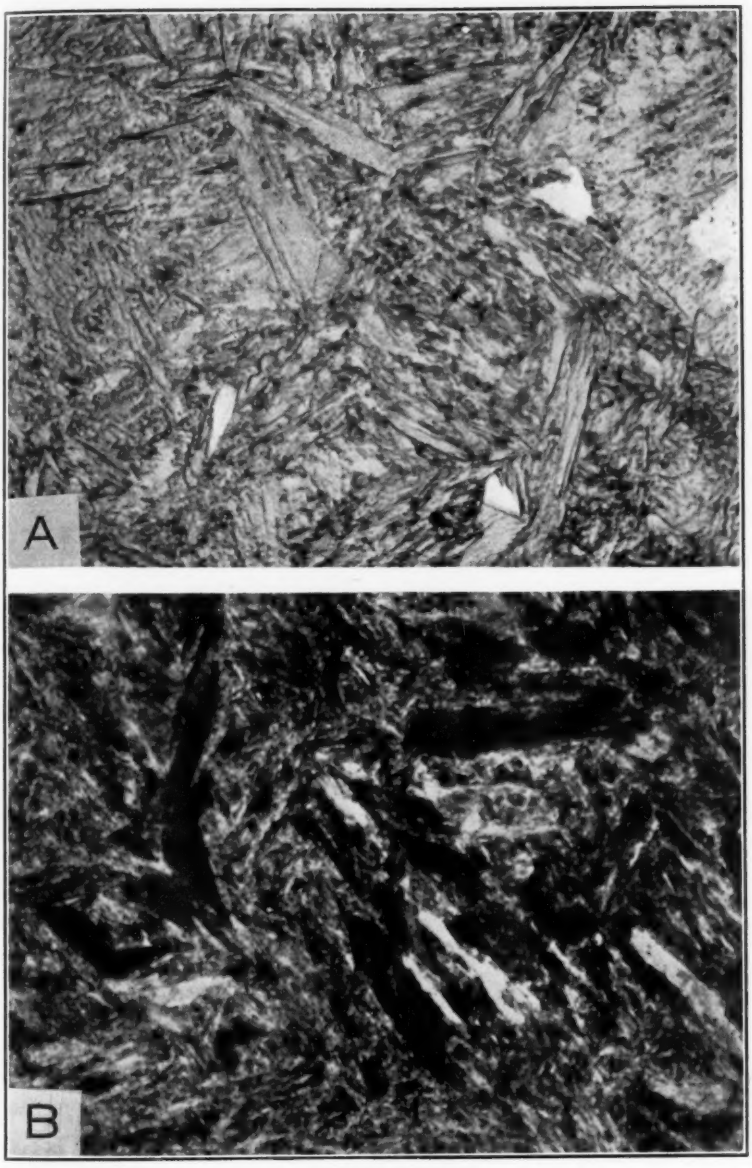

FIGURE 4

A, Structure of freshly quenched specimen, × 2,000; *B*, structure of same specimen tempered at 200° C. for 7 hours, × 2,000.

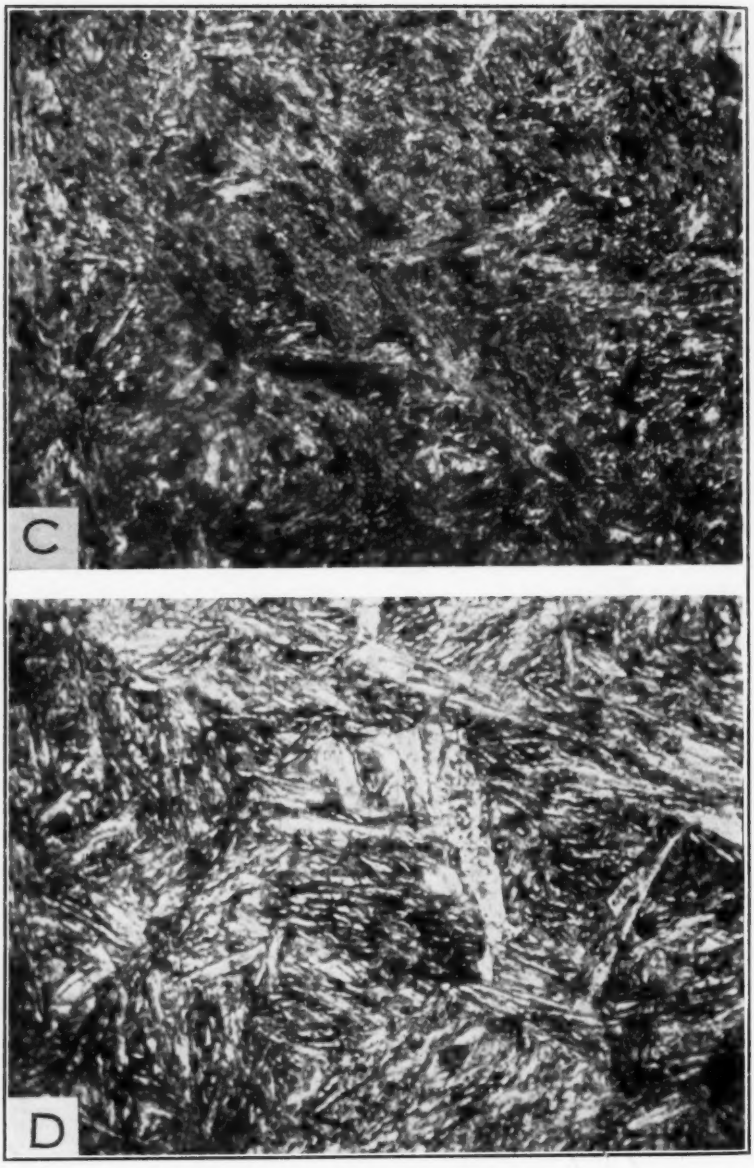

FIGURE 5

C, Structure of same specimen tempered at 235° C. for nearly four hours. × 2,000; *D*, structure of same specimen tempered at 302° C. for two and one-half hours. × 2,000.

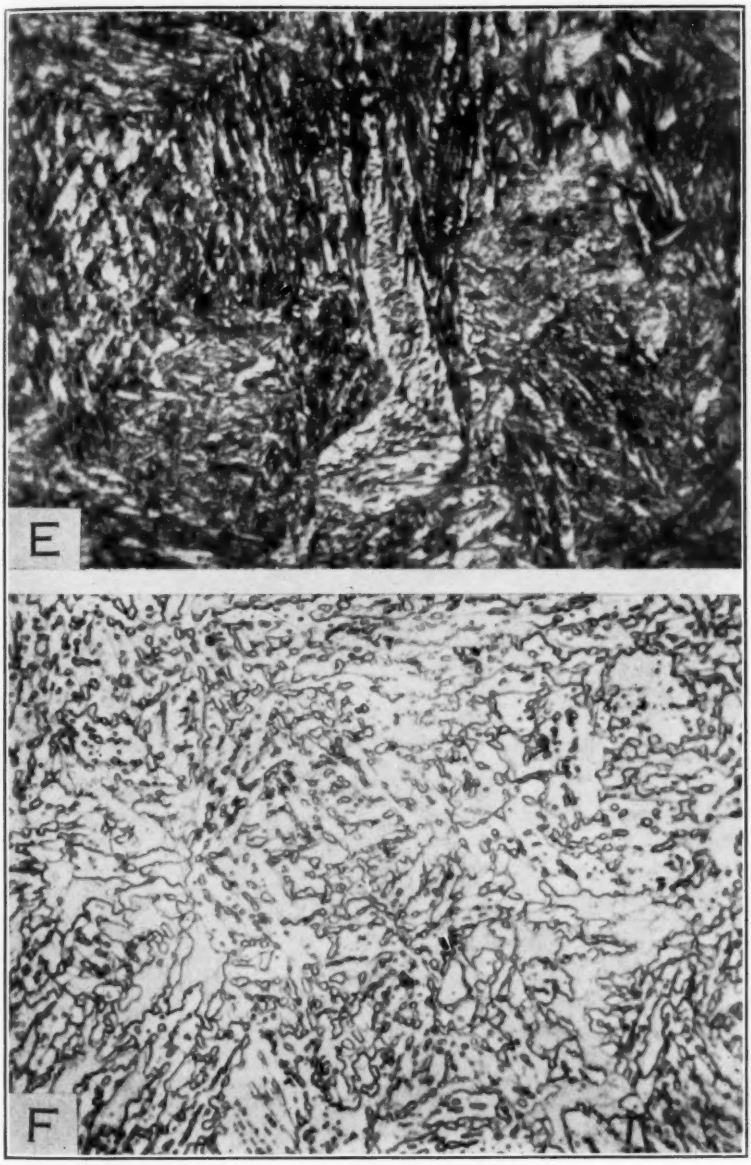

FIGURE 6

E, Structure of same specimen tempered at 400° C. for two hours. × 2,000; *F*, structure of same specimen tempered at 700° C. for one hour. × 2,000.

under the microscope, had an A_0 transformation, the intensity of which was about half of that of pearlite, whereas specimens containing cementite, spheroidized for various lengths of time, showed a decrease in intensity with growth of particle size.

As a result of these investigations, it is believed that the lack of an A_0 transformation is due to the absence of carbide in the first stages of the tempering of martensite.

Most metallurgists are agreed that martensite is a supersaturated solid solution of carbon in alpha iron. Jeffries,[14] discussing the formation of martensite, said:

> The transformation in carbon steel is from a solid solution of carbon in gamma iron to a solid solution of carbon in alpha iron. Only one new crystalline phase is formed, the carbide formation being prevented because the time-temperature conditions do not permit of substantial diffusion of carbon.

Heindlhofer and Bain [15] considered the carbon to be atomically dispersed and the martensite grains to be greatly stressed by their formation. If freshly quenched martensite is considered to contain no carbide and to be in a highly stressed condition, it seems reasonable to attribute the first magnetic change upon heating to 200° C. to the release of stress, at least in part. At 200° C. the change, as already noted, requires over six hours for completion. Investigation of tempering at 125° C. indicates that the same type of change takes place, but that a much greater length of time is required for completion.

Photomicrographs of the material as freshly quenched and after the treatment at 200° C. (shown in *A* and *B*, fig. 4), give a clear visual indication that the structure has been altered considerably by the treatment. The original white martensite needles are colored after tempering. The Rockwell hardness also has decreased from C 64 to C 56. Cooling curve 1 and heating curve 2 of Figure 2 indicate that whatever change has taken place in the material, at this stage, has been completed.

Upon reheating to 235° C. an increase in magnetization took place, which was completed in about 45 minutes. After this the magnetization remained constant for over three hours. This is shown in curve 2 of Figures 2 and 3.

The increase in magnetization indicates that some constituent, previously not contributing to the magnetization, has now become ferromagnetic. Enlund [16] has stated that austenite tempers at 260° C. The obvious conclusion is that the retained austenite decomposed at this point, the gamma iron being transformed into the magnetic alpha iron.

Upon cooling to room temperature a slight gradual increase in magnetization was noted. This is presumably the appearance of a carbide transformation.

The miscrostructure of the specimen at this stage, shown in *C* (fig. 5), indicated that some change had taken place. The structure was fine, being beyond the stage of clear resolution. Some traces of the needles of tempered martensite were still visible. The structure was not that of ordinary troostite as it etched at a somewhat slower

[14] Zay Jeffries, A Contribution to the Theory of Hardening and the Constitution of Steel, Trans., Am. Soc. Steel Treating, 13, p. 369, 1928.
[15] K. Heindlhofer and E. C. Bain, A study of the grain structure of martensite, Transactions, American Society for Steel Treating 18, p. 70, 1930.
[16] See footnote 8, p. 443.

rate and had a lighter color than that characteristic of the troostitic range of structures. The hardness was Rockwell C 54, nearly as hard as after treatment at 200° C.

The specimen was then slowly reheated to approximately 300° C. This is shown graphically in curve 3, Figure 2. A gradual decrease in magnetization took place upon heating, followed by another decrease upon holding at constant temperature. This latter decrease was complete in about one hour, no further change being noted upon holding for one and one-half hours. The rapid decrease at this stage indicated that a change was taking place within the material, which was effectively decreasing the magnetization of some of the iron.

Upon cooling from 302° C., the A_0 transformation was very pronounced as shown in curve 3 of Figure 2. The temperature at which the A_0 transformation appeared to begin on cooling was approximately 240° C., instead of 215° C., as observed for this point in the pearlitic structure of the annealed specimen shown in Figure 1. This confirms the results of the previous investigation [17] on the influence of carbide particle size, which showed that the A_0 transformation comes at higher temperatures, the smaller the particle size.

The structure, shown in *D* (fig. 5) was quite different from that of the preceding specimen. The etching rate was somewhat more rapid and the particles were beginning to resolve. The hardness, Rockwell C 49, was somewhat lower than that of the specimen after the 235° C. treatment.

When the specimen was heated to 400° C., the A_0 transformation was found, but no change in magnetization occurred upon holding at this temperature for two hours, as shown in curve 4 of Figures 2 and 3. Apparently there was no further constitutional change between 300° C. and the A_1 transformation, as no magnetic change with time was observed even upon holding the temperature at 700° C. for one hour.

The microstructure of the specimen held at 400° C., shown in *E* (fig. 6) was not greatly different from that of the specimen held at 300° C. The structure was somewhat coarser and the particle size had increased slightly. The Rockwell hardness had decreased to C 40.

The structure of the specimen held at 700° C. (shown in *F*, fig. 6) was that of partially spheroidized cementite and the hardness was Rockwell C 12.

All constituents which were stable in the tempering range had been formed at or slightly below 300° C., any further heating or holding at constant temperatures have apparently no effect in the formation of new constituents. Coagulation of carbide particles took place in the range from 300° to 700° C. and gave a continuous series of structures ranging from troostite to speroidized cementite.

VI. SUMMARY

Properly applied and interpreted, thermomagnetic analysis is capable of revealing constitutional changes in steel which are difficult or impossible to detect by other methods of investigation. This method has been utilized in an investigation of the transformations associated with the tempering of a freshly quenched 0.75 per cent

[17] See footnote 13, p. 448.

carbon steel, and the following phenomena were observed to occur during the process:

1. A pronounced increase in magnetization took place immediately upon the application of heat. After reaching and holding constant at a temperature of 200° C. this increase continued for approximately six and one-half hours.

2. Another increase in magnetization was noted at about 235° C. in a specimen previously treated at 200° C.

3. A decrease in magnetization took place upon holding at a temperature of 300° C.

4. No change in magnetization with time upon holding at constant temperatures in the range 400° to 700° C. was noted.

The explanations of Jeffries, Archer, Sykes, Bain, and others that martensite is a supersaturated solid solution or pseudo solid solution of atomically dispersed carbon in alpha iron, existing only because the conditions of its formation are such as to prevent carbon precipitation is generally accepted as an established fact. That martensite is in a highly stressed condition has also been demonstrated by the X-ray investigations of Heindlhofer, Bain, and others.

With this in mind, the following hypothetical explanation of the tempering of martensite is suggested and is believed to fit the observed phenomena.

The first stage of tempering freshly quenched martensite below 200° C. resulted in an increase in magnetization which was apparently due to stress release. After this change was completed, no A_0 or carbide transformation was found. It is conceivable that, during this stage of tempering, the carbon was being precipitated from the solid solution and remained in dispersed form throughout the ferrite. The absence of an A_0 transformation may be considered to indicate that no carbide had been formed in quantities sufficient to be detected by the magnetic method used.

At approximately 235° C., the austenite which had been retained during quenching decomposed and in the range, 200° to 300° C., carbide formation was progressing. After a period of approximately one hour at the latter temperature the formation of carbide was completed. It is possible that this reaction may be completed at a lower temperature, however, over longer periods of time. At higher temperatures, under the critical range, however, no further magnetization changes with time took place, a fact which suggests that no further constitutional changes occur in steel under these conditions.

VII. ACKNOWLEDGMENT

Grateful acknowledgment is made to R. L. Sanford, chief of the magnetic measurements section, for the use of the thermomagnetic apparatus and for his kind assistance in the interpretation of results.

Washington, June 10, 1931.

HYPERFINE STRUCTURES IN THE FIRST SPECTRA OF KRYPTON AND XENON

By C. J. Humphreys

ABSTRACT

The stronger arc lines of krypton and xenon have been examined for hyperfine structures. Methods of observation include the use of a Hilger Fabry-Perot interferometer having quartz plates of 6 cm aperture, a number of fixed étalons, and two quartz Lummer-Gehrcke plates. The relative advantages of these two types of interferometers are considered. The results obtained by different methods show very satisfactory agreement. Structures of the following lines have been measured: Krypton, 5,570.2890, 7,685.2472, 8,059.5053, 8,104.3660, 8,281.042, and 8,508.8736 A; xenon, 4,193.5296, 4,500.9772, 4,734.1524, 8,231.6348, 8,409.190, and 8,819.412 A.

The observed complex lines in the two spectra are not spectroscopically analogous. No definite numerical regularities in the spacing of components, such as have been reported in the case of neon, have been observed. Five of the six complex xenon lines are due to combinations with the low $^2P_2$ level. The regularities in the fine structures of neon are discussed. The satellites of neon lines are supposed to be due to Ne isotope 22. Krypton and xenon are reported to have 6 and 9 isotopes, respectively, and the fine structure might be expected to be more complicated.

The relative abundance of isotopes of odd atomic weight in krypton and xenon leads to the consideration of the possibility that the satellites sufficiently separated for observation may be due to the nuclear moment of these odd isotopes, in accordance with a suggestion advanced by Schüler to explain the hyperfine structures in mercury. It is hoped that, by operating the sources at low temperatures, and using still higher resolving power, additional structures may be observed.

CONTENTS

		Page
I.	Introduction	453
II.	Experimental procedure	454
III.	Reduction of observations	458
IV.	Discussion of results	459

I. INTRODUCTION

The examination of the hyperfine structures in the spectra of krypton and xenon has been undertaken in connection with the complete investigation of these spectra. The progress of this investigation which had its origin in the suggestion that some line from the krypton spectrum might be more suitable as a primary standard of wave length than the red line of cadimum, has been reported in earlier papers. The description and classification of the first spectra of krypton and xenon are contained in two papers by Meggers, de Bruin, and Humphreys.[1] Interference measurements of the wave lengths of the more intense lines have been published by Humphreys.[2] The examination of the interference patterns, made in connection with the precise measurement of wave lengths by aid of Fabry-Perot fixed

[1] Meggers, de Bruin, Humphreys, B. S. Jour. Research, **3**, pp. 129 and 731; 1929.
[2] Humphreys, B. S. Jour. Research, **5**, p. 1041; 1930.

étalon interferometers, clearly indicated that certain of the lines of xenon were complex. The resolving power employed was not sufficient, however, for a satisfactory measurement of the patterns. The use of apparatus of higher resolving power has now permitted the measurement not only of the xenon fine structure patterns, but also those of a number of krypton lines. This note is to be regarded as preliminary, however, to the report of a more extended investigation. Hyperfine structures have been actually observed for only a relatively small number of Kr and Xe lines. If, as is generally supposed, the complexity in spectral lines of these gases is due to isotopes, satellites should be expected in the case of all lines intense enough to show them. No structural similarities have been observed between spectroscopically analogous lines in the two spectra. Thus the lines of krypton, arising from the same term combinations as the complex lines of xenon, are apparently free of structure, and vice versa. These facts lead to the belief that possibly other lines of both spectra are complex but still unresolved. When the investigation is resumed it is planned to use still higher resolving power and to operate the light sources at lower temperatures to improve the sharpness of the lines.

II. EXPERIMENTAL PROCEDURE

The apparatus and the experimental arrangement used in this investigation were essentially as described in the report on the interference measurements.[3] At the beginning of the experiments it was expected to immerse the tubes used as sources of radiation in liquid air, in the hope of sharpening the lines by reducing the Doppler motions of the radiating atoms. This procedure had been successful in the case of experiments with neon.[4] With this idea in mind pyrex tubes were designed with the capillary portion shaped to permit of end-on emission of radiation when immersed in an unsilvered Dewar flask. Attempts to use such xenon-filled tubes in this manner were not successful, however, because the discharge could not maintain a sufficiently high temperature to prevent condensation or freezing of the gas. Tubes of this design proved to be useful, however, in connection with observations made with Lummer-Gehrcke plates in which case end-on illumination is the most economical method of using the available radiation. For the examination of the krypton spectrum a tube obtained from Robert Götze in Leipzig was used. This tube, designed especially for end-on use, had a very fine capillary and emitted a much stronger radiation than any other tubes available. The use of the end-on tube caused certain of the krypton lines to appear reversed. The reversals could be eliminated and thus distinguished from genuine fine structures by repeating the observations with a side-on exposure.

A Hilger interferometer, having crystal quartz plates of 60 mm available aperture, and permitting variable separation of the plates up to 100 mm was used in connection with the glass E_2 spectrograph in making some of the first exposures. Among a large number only two satisfactory spectrograms were thus obtained. The apparatus was not sufficiently stable to maintain the adjustment of the plates during an exposure time of from two to five hours necessary with the

[3] Humphreys, B. S. Jour. Research, **5**, p. 1041; 1930.
[4] E. Thomas and E. J. Evans, Phil. Mag., **10**, p. 128; 1930.

relatively faint sources of radiation available. It was, therefore, found advisable to resort to the fixed étalon method for the examination of those lines suited to observation with a Fabry-Perot interferometer. A pair of glass plates of 40 mm diameter were resilvered, by the cathode sputtering process, with as heavy a coat as could be used consistent with a reasonable exposure time. These plates were used with 15 or 20 mm separators for observing the hyperfine structures of infra-red xenon lines. Observations of a portion of the xenon spectrum were also repeated using a set of étalons which were constructed to accommodate the large quartz plates.

The observations on the xenon lines were repeated with Lummer-Gehrcke plates. This method disclosed some additional complex lines and additional satellites in the structures already known. It also revealed the complex lines of krypton which had not been found by aid of Fabry-Perot interferometers, a result which is to be accounted for by the fact that the complex infra-red lines are of moderate intensity and in most cases lie close to very strong lines. With the heavy silvering on the interferometer plates requisite for high resolving power, it is doubtful if the satellites of these lines could be recorded with reasonable exposures, using Fabry-Perot étalons. It was found necessary in the examination of the krypton lines, 5,570 and 5,870 A, to use the Lummer-Gehrcke plates in connection with the Anderson grating in order that the spectral dispersion might be sufficient to permit a distinction to be drawn between genuine satellites and faint lines lying close to the strong lines. Observations in the infra-red region were also repeated using the grating as the dispersing instrument.

Two quartz Lummer-Gehrcke plates were available, the respective lengths and thicknesses being 130 by 4.24 mm and 190 by 6.24 mm. The attached prisms were of the form designed by Twyman to permit the incident light to enter parallel to the plate faces and allow the sources to be mounted in a line along the axis of the spectrograph.[5] The Lummer-Gehrcke plates were mounted on the supporting stand used with the étalon mountings with the same arrangement of optical parts, only slight adjustments being necessary when substituting one form of interferometer for the other. The arrangement, which has been described in the previous publication,[6] makes use of two lenses, one to transform the radiation incident upon the interferometer into a beam of parallel rays, and the other an achromatic lens, in this case of 50 cm focal length, to project the fringe system upon the slit of the spectrograph. The Lummer-Gehrcke plates were mounted with the surfaces in the horizontal position so that the system of approximately straight horizontal fringes was at right angles to the slit. Although the mounting permitted the utilization of the interference systems from both the upper and lower surfaces of the plate, only one set of fringes was used at a time.[7] Since the Lummer-Gehrcke plates were of quartz which is doubly refracting it was necessary to pass the

[5] This condition is not realized in the strictest sense, especially if an end-on tube, which effectively reduces the incident light to a narrow pencil, is used. If a fixed direction of emergence from the Lummer-Gehrcke plate, parallel to the optic axis of the spectrograph, is maintained, the direction of incidence will depend upon the wave length, because if the varation of the index of refraction of the plate material with wave variation in direction of incidence is small it must be taken into account in selecting a particular spectral region for study.

[6] Humphreys, B. S. Jour. Research, 5, p. 1041; 1930.

[7] The number of fringes which can be photographed obviously depends upon the magnification of the projected interference system in relation to the length of the slit, which is governed by the focal length of the projecting lens.

incident radiation through a nicol prism in order to eliminate one of the two interference systems which would be formed if the light were not polarized.

A further advantage in the use of polarized light, which is realized also with plates of isotropic material, is increased resolving power, provided the proper orientation of the plane of polarization is chosen. It has been pointed out that the maximum resolving power is obtained with the Lummer-Gehrcke plate if the intensities of successive interfering beams emergent from the surface are equal. While complete realization of this ideal condition is not possible, it is known that the least diminution in intensity of successive beams occurs when the ratio of reflected to transmitted light at the inner surface is a maximum, a condition which is realized for a given angle of incidence if the light is polarized so that the direction of vibration or electric vector is parallel to the plate surface and at right angles to the direction of propagation of the radiation. In practice, quartz Lummer-Gehrcke plates are cut with the optic axis parallel to the surface or nearly so and at right angles to the greatest dimension of the plate. Consequently, incident radiation polarized in the most advantageous direction, has its direction of vibration parallel to the optic axis and is transmitted as the extraordinary radiation. The requisite orientation of a nicol prism of the usual type is to place it so that the short diagonal of the rhomb-shaped end face is parallel to the plate surface.

The relative advantages of the different forms of interference apparatus used may be considered briefly. In the examination of any complex spectral line it is desirable that the spacing of the components in any one order of the interference pattern be as large as possible without overlapping of successive orders. Since the realization of this condition depends entirely upon the choice of the proper retardation, the Fabry-Perot interferometer with variable separation of plates would seem to be the ideal instrument. The difficulties we have encountered because of the lack of stability have been mentioned, and it seems doubtful if the instrument, at least as now designed, can be used with faint sources where good adjustments must be maintained for several hours. The fixed étalon mounting is remarkably stable, and not affected by slight mechanical disturbances. We have found that the condition of parallelism between the plates has in many instances been maintained for a number of days without adjustment. The simplicity of design and relative ease of construction of the étalons and mountings renders this type of apparatus available for general laboratory use. The Lummer-Gehrcke plate, having its surfaces ground parallel, requires no adjustment to make it ready for use other than to place it in the correct position with respect to the other parts of the apparatus. The range of usefulness of a given plate is, however, restricted to the study of those structures for which the retardation corresponds to a satisfactory dispersion of the components. A single Lummer-Gehrcke plate is essentially equivalent to a pair of Fabry-Perot plates used with one fixed étalon. It is obvious that if a series of étalons is available a suitable retardation may be chosen for any wave length in the accessible region or for a pattern of any separation within the limits which can be set for examination by interferometer methods,. The resolving power may

also be altered at will by changing the retardation or the reflecting power.

Under the best conditions of illumination the Lummer-Gehrcke plate yields a more intense interference pattern than the Fabry-Perot interferometer. This is mainly due to the loss of light in the latter, due to reflection and absorption at the silver surfaces. For a given retardation the practical resolving power of a Lummer-Gehrcke plate is superior to that of a Fabry-Perot étalon interferometer unless the reflecting power is exceedingly high. This is especially true in the violet and ultra-violet regions where the reflecting power of metallic films begins to fall off.

The Lummer-Gehrcke plate is reported to be extremely sensitive to temperature variation. Hansen[8] has calculated that a change of 5° C. is sufficient to cause a shift of a given fringe into the position of the adjacent fringe. The Fabry-Perot étalon is affected in a number of ways due to changes of temperature or pressure. The index of refraction of air may change, and the variation in the length of the invar separators is not entirely negligible. We have used both instruments in a basement laboratory in which the temperature was fairly steady but not controlled. No difficulty has been experienced provided the temperature variations did not exceed 0.1° to 0.2° C.

The reduction of observations obtained by aid of an étalon is much less laborious than those obtained with a Lummer-Gehrcke plate, because of the simple relationship $\lambda p = 2e$, which exists in the former case between wave length, retardation, and plate separation. This formula is not only easy to apply, but permits extremely accurate comparisons of wave length. The corresponding formula for the Lummer-Gehrcke plate involves the index of refraction of the plate material which must usually be interpolated or extrapolated for the wave length being observed. It can be used successfully only for the determination of the separation of satellites.

In any case the method chosen should be suited to the particular structure under observation. The xenon line 4,501 A for which the fine structure pattern has a total width of 0.06 A, is most satisfactorily observed with an étalon of 10 mm thickness, but both of the Lummer-Gehrcke plates available have yielded excellent results in the study of this structure. On the other hand, the pattern of four strong components of 8,231 A, having a separation of 0.085 A has been clearly resolved only with étalons ranging from 15 to 25 mm in thickness.[9] In general, the Fabry-Perot étalon method is recommended for the study of structures in the visible and infra-red regions where the width of the pattern is 0.1 A or less. A Lummer-Gehrcke plate of the conventional size is best adapted to the study of wide patterns in the visible and infra-red regions and if of transparent material to general use in the ultra-violet. Wherever possible, the observation of a structure by both methods is desirable.

---

[8] Hansen, Zeits. for wiss. Phot., **23**, p. 17; 1925.

[9] The change in wave length, $\Delta\lambda$, corresponding to the displacement in the interference pattern between one maximum and the corresponding maximum in the adjacent order, varies directly as the square of the wave length for either type of interferometer, and inversely as the retardation. The ratio of the separation of a satellite from a line to this displacement of adjacent orders should be large for most satisfactory observation up to the point of actual overlapping. The ratio can be increased for a given wave length only by increasing the retardation. The practical limitations on the thickness of Lummer-Gehrcke plates sets a lower limit on the closeness of patterns which may be thus observed, which increases rapidly as we go to longer wave lengths.

III. REDUCTION OF OBSERVATIONS

The computation of the wave lengths of the satellites in the observed patterns was carried out in the case of observations made with étalons according to the method described in the paper [10] in which interference measurements in these spectra were discussed. The values of the xenon wave lengths reported in the earlier paper were used as standards. The method requires the precise determination of the separation, e, of the plates and the retardation, p, expressed as the number of wave lengths in a path equal to $2e$.

These quantities then permit the solution of the equation

$$\lambda = \frac{2e}{p}$$

The corresponding equation applying to the Lummer-Gehrcke plate is

$$\lambda = \frac{2e}{p}\sqrt{\mu^2 - \cos^2 E}$$

in which μ is the index of refraction and E is the angle between the emergent beam and the plate surface. The retardation, p, is not capable of direct determination. We calculate instead the quantity $\Delta\lambda$ which is the increment in wave length corresponding to the displacement between adjacent fringes, that is $\Delta\lambda$ is evaluated when $p=1$. It may be shown that

$$\Delta\lambda = \frac{\lambda^2\sqrt{\mu^2 - \cos^2 E}}{2e\left(\mu^2 - \cos^2 E - \lambda\mu\frac{\partial\mu}{\partial\lambda}\right)}$$

This reduces to

$$\Delta\lambda = \frac{\lambda^2\sqrt{\mu^2 - 1}}{e\left(\mu^2 - 1 - \lambda\mu\frac{\partial\mu}{\partial\lambda}\right)}$$

when the interference pattern corresponding to nearly grazing emergence is used. The separation of any satellite from the main component of a pattern is given by

$$\delta\lambda = f \cdot \Delta\lambda$$

where f is determined from the measurements of the observed interference pattern. For the precise evaluation of f, it is necessary to observe the complete interference pattern formed by the radiation emerging from both plate surfaces. If the respective distances between fringes of the same order on opposite sides of the central dark portion of the pattern are given by D_1, D_2, D_3, etc., and if D_{s_1}, D_{s_2}, D_{s_3}, are the corresponding differences between the fringes due to a given satellite

$$f = \frac{D_1^2 - D_{s_1}^2}{D_2^2 - D_1^2} = \frac{D_2^2 - D_{s_2}^2}{D_3^2 - D_2^2}, \text{ etc.}$$

The detailed treatment of the theory of the Lummer-Gehrcke plate has been given by several writers, among whom Hansen [11] and

[10] Humphreys, B. S. Jour. Research, 5, p. 1041; 1930.
[11] Gehrcke, Handbuch der physik. Optik, 2, p. 199.

Simeon [12] may be mentioned. The second article referred to contains an excellent bibliography. In the present investigation, only half of the interference pattern was observed. A linear interpolation method was used to determine the values of f, which, while not strictly rigorous, is in the present instance as good as the measurements justify. The method which is due to MacNair [13] may be understood from a study of the figure.

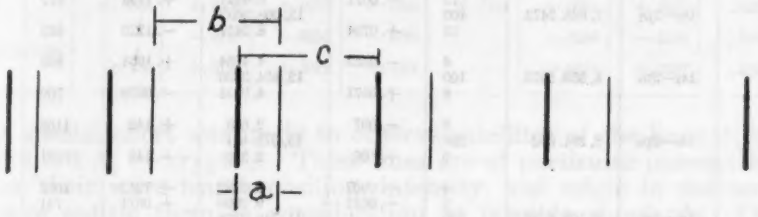

The values of f are computed by aid of the formula,

$$f = \frac{a}{\frac{b+c}{2}}$$

The calculation is repeated for successive orders in a given fringe system and should give essentially constant values of f.

IV. DISCUSSION OF RESULTS

The results of the investigation are summarized in Tables 1 and 2. In addition to the average values of $\delta\lambda$, the values of $\delta\nu$, and of $\frac{\delta\nu}{\nu}$ have been assembled in the hope of finding possible regularities. The relative intensities of the satellites are estimated by taking for the main components the values of the intensities of the respective lines to which they belong as given in the published descriptions of the first spectra of krypton [14] and xenon.[15] The hyperfine structures of a number of the xenon lines have been analyzed by both of the two methods described. A satisfactory check has been obtained, especially in the case of those lines in the visible spectrum for which the satellite separations were suitable for observation with a Lummer-Gehrcke plate. Table 3 gives a comparison of the observations made on the lines 4,501 and 4,734 A. It is to be noted, however, that in all cases except one the probable error of the arithmetical mean of individual observations made by a single method is less than the corresponding difference between the mean result obtained by the two methods. The exceptional case, that of the satellite on the short wave length side of 4,734, is to be regarded as accidental, because, of all the satellites measured, this was the least well resolved. We believe that this comparison is significant in any consideration of the accuracy of measurement of fine structures by a single type of interferometer.

[12] Simeon, J. Sci. Inst. **1**, p. 296; 1924.
[13] MacNair, Phil. Mag., **2**, p. 613; 1926.
[14] Meggers, deBruin, Humphreys, B. S. Jour. Research. (In press.)
[15] Meggers, deBruin, Humphreys, B. S. Jour. Research, **3**, p. 129; 1929.

TABLE 1.—*Krypton hyperfine structures*

Combination	λ, air	Intensity	δλ Lummer-Gehrcke plates	ν, vacuum	δν	$\frac{\delta\nu}{\nu}\times10^9$
		50	−0.0333	7.5263	+0.1073	598
$1s_5-2p_3$	5,570.2890	2,000		17,947.4190		
		15	−.0671	8.4817	+.1135	872
$1s_3-2p_1$	7,685.2472	400		13,008.3682		
		12	+.0724	8.2457	−.1225	942
		6	−.0653	4.4034	+.1004	809
$1s_3-2p_4$	8,059.5053	100		12,404.3030		
		8	+.0571	4.2151	−.0879	709
		8	−.007	2.603	+.142	1168
$1s_3-2p_2$	8,281.042	200		12,072.461		
		6	+.100	2.316	−.145	1201
		4	−.0907	9.3380	+.1252	1066
		1	−.0631	9.2999	+.0871	741
$1s_5-2p_4$	8,508.8736	200		11,749.2128		
		6	+.0820	9.0996	−.1132	964

TABLE 2.—*Xenon hyperfine structures*

Combination	λ, air	Intensity	δλ Fabry-Perot etalons	δλ Lummer-Gehrcke plates	δλ final value	ν, vacuum	δν cm^{-1}	$\frac{\delta\nu}{\nu}\times10^9$
		3		−0.016	−0.016	9.658	+0.091	382
$1s_5-4s$	4,193.5296	30				23,839.567		
		3		+.018	+.018	9.465	−.102	428
		12	−0.0238	−.0234	−.0236	1.3041	+.1164	524
$1s_5-2p_2$	4,500.9772	100				22,211.1877		
		6	+.0197	+.0191	+0194	1.0920	−.0957	431
		5	+.0368	+.0356	+.0362	1.0091	−.1786	804
		5	−.0248	−.0248	−.0248	7.328	+.111	525
$1s_4-2p_3$	4,734.1524	100				21,117.217		
		15	+.0182	+.0197	+.0190	7.133	−.084	398
		2		−.085	−.085	5.046	+.125	1,029
		40	−.0371	−.042	−.0371	4.9756	+.0547	450
$1s_5-2p_6$	8,231.6348	300				12,144.9209		
		5	+.0288		+.0288	4.8784	−.0425	350
		15	+.0478	+.046	+.0478	4.8504	−.0705	580
		3		+.093	+.093	4.783	−.138	1,136
		6	−.0437	−.041	−.0437	8.5506	+.0618	520
$1s_5-2p_7$	8,409.190	60				11,888.4888		
		3	+.043	+.042	+.043	8.428	−.061	513
		40	−.0330		−.0330	5.5577	+.0424	374
$1s_5-2p_8$	8,819.412	200				11,335.5153		
		5	+.0223		+.0223	5.4866	−.0287	253
		12	+.0436		+.0436	5.4593	−.0560	494

TABLE 3.—*Comparison of observations by two methods*

FABRY-PEROT ÉTALONS

λ, air	Individual values of δλ				δλ mean	Probable error	Differences between mean values by two methods
4,500.9772	−0.0239	−0.0233	−0.0239	−0.0240	−0.0238	0.0001	0.0004
	+.0202	+.0209	+.0193	+.0185	+.0197	.0004	.0006
	+.0368	+.0379	+.0366	+.0358	+.0368	.0003	.0012
4,734.1524			−.0257	−.0239	−.0248	.0006	.0000
	+.0168	+.0177	+.0196	+.0185	+.0182	.0004	.0015

TABLE 3.—*Comparison of observations by two methods*—Continued

LUMMER-GEHRCKE PLATES

λ, air	Individual values of δλ						δλ mean	Probable error
4,500.9772	−0.0231	−0.0229	−0.0238	−0.0236	−0.0233	−0.0236	−0.0234	0.0001
	+.0195	+.0182	+.0194	+.0190	+.0196	+.0189	+.0191	.0001
	+.0338	+.0350	+.0370	+.0358	+.0357	+.0361	+.0356	.0006
4,734.1524		−.0240	−.0254	−.0245		−.0254	−.0248	.0002
	+.176	+.0198	+.0219	+.0207		+.0184	+.0197	.0005

A special effort was made to observe satellites of the lines, 5,570 and 5,870 A, of krypton. These lines are of particular interest because their wave length position, intensity, and origin in the term scheme entitle them to consideration as possible standards. One faint satellite has been observed for 5,570 A. It can not be said with certainty whether 5,870 A is complex, the evidence from different spectrograms being somewhat contradictory. The investigation also revealed the presence of a companion to the krypton lines, 8,104 A, and has permitted the precise determination of its wave length. The significance of this line is discussed in the second paper on the first spectrum of krypton by Meggers, deBruin, and Humphreys.[16]

Attention should be directed to a number of earlier investigations of selected portions of the spectra of krypton and xenon, made with interferometers for the purpose of finding hyperfine structures. Gehrcke and Janicki,[17] using Lummer-Gehrcke plates, examined 16 krypton lines (4,273 to 5,870 A) and 42 xenon lines (4,078 to 6,768 A), including all the stronger visible lines. They report all the krypton lines sharp, especially 5,570 and 5,870 A.

Of the xenon lines examined two were found to be complex, 4,501 and 4,734 A. The analysis of the patterns by Gehrcke and Janicki is as follows:

λ	δλ	Intensity
4,734.30	−0.0254	1/10
	+0.0176	1/3
4,501.13	−0.043	1/20
	−0.0225	1/3
	+0.0306	1/5

We are unable to agree with this analysis of 4,501 A as to position and intensity of the three satellites. In view of the agreement

[16] Meggers, deBruin, Humphreys, B. S. Jour. Research. (In press.)
[17] Gehrcke and Janicki, Ann. der Physik, 81, p. 314; 1926.

between our results, obtained with Fabry-Perot étalons and Lummer-Gehrcke plates, we feel certain that the results of Gehrcke and Janicki for 4,501 A are in error.

Other investigations are confined to the examination of the yellow and green lines of krypton. Perard [18] studied the lines 5,570 and 5,870 A, with a Michelson interferometer, and reported that each has two close satellites. Weber,[19] at the Reichsanstalt, examined three krypton lines 5,570, 5,649, and 5,870 A, and proposed the yellow-green line 5,649 as a primary standard. A more recent report from the Reichsanstalt [20] states that the line 5,649 is sharp, but that 5,570 has five satellites, and 5,870 two very close faint satellites.

The hyperfine structures in the rare gases are supposed to be due to isotopes. Investigations of the Ne lines by Hansen,[21] by Nagaoka and Mishima,[22] and by Thomas and Evans [23] indicate that all the lines due to *sp* combinations have a single satellite on the short wave length side of from $\frac{1}{10}$ to $\frac{1}{4}$ the intensity of the main component. This is to be expected in the case of an element having two isotopes. There is some recent evidence for a Ne isotope of atomic weight 21, but the amount is so small that any observed hyperfine structures would be expected to arise from Ne 20 and Ne 22 only. Although they have not been able to predict the exact satellite separations on theoretical grounds, Thomas and Evans have shown that the ratio $\frac{\delta\nu}{\nu}$ has a constant value for combinations with each of the low *s* levels. In the present investigation no definite regularities have been found either in the values of $\delta\nu$ or $\frac{\delta\nu}{\nu}$. It may be seen also that only a relatively small number of the *sp* combinations show structures. In the krypton spectrum most of the complex lines are combinations with s_2, or in the present standard notation $^1P_1$, whereas in the case of xenon, five of the six observed complex lines involve s_5; that is, $^3P_2$ combinations. No definite analogies can be traced. It is likely that the xenon lines involving s_5 all have a close pattern of one satellite on the short wave length side and two on the long with possibly others farther removed as shown by 8,231 A. The outer satellites of 8,819 A are shown, but too faint for measurement on some of the plates. The resolution of the patterns of 4,193 and 8,409 A is imperfect.

Since krypton and xenon are reported to have 6 and 9 isotopes, respectively, the hyperfine structures would be expected to be more complicated than those in neon. We would expect all lines due to *sp* combinations to be complex. A possible interpretation of the hyperfine structures in mercury has recently been suggested by Schüler [24] according to which the nuclear moment of the isotopes of odd atomic weight may be responsible for the resolved structures, whereas the structures due to the even isotopes are too narrow to permit the resolution of the heavy central component. In support of this he gives the relative proportions of the isotopes and notes that those of odd atomic weight comprise about 30 per cent of the total mass,

[18] Perard, Comp. Rend., 176, p. 1060; 1923.
[19] Weber, Physik. Zeit., 29, p. 233; 1928.
[20] Bureau of Standards Yearbook for 1930, p. 33.
[21] Hansen, Nature, 119, p. 239; 1927.
[22] Nagoka and Mishima, Imp. Acad., Tokyo Proc., 5, p. 200; 1929
[23] Thomas and Evans, Phil. Mag., 10, p. 128; 1930.
[24] Schüler, Naturwissenschaften, 43, p. 895; 1930.

and further that the sum of the intensities of the satellites is between 25 and 32 per cent of the total intensity of a given pattern. These considerations can scarcely apply to neon because the scarcity of isotope 21 has been mentioned, but they may apply to krypton in which isotope 83 is fourth in order of abundance, and with still greater force to xenon in which isotopes 129 and 131 are first and third, respectively.

The imperfect resolution of some of the patterns and the strong probability that an additional number, if not all, of the strong lines are complex makes it advisable to continue the investigation, with the conditions of emission controlled so as to increase the sharpness of the lines and with still higher resolving power.

WASHINGTON, June 10, 1931.

ACCELERATED AGING TEST FOR PAPER

By Royal H. Rasch[1]

ABSTRACT

A series of Government bond and ledger papers was studied with reference to certain properties that appear to be related to permanence. These papers, purchased on specification, were assumed to be representative of the different commercial grades.

A thorough study was made of the physical and chemical properties of the papers as well as of their behavior when exposed to various accelerated aging tests.

The results indicate the feasibility of classifying papers by means of suitable chemical, strength, and accelerated aging tests. The chemical tests include tests for fiber purity and noncellulosic impurities, such as acid and rosin, used in sizing. The fiber purity, which is indicated by the alpha cellulose content and copper number, was found to bear an important relation to the stability of the papers. The accelerated aging test, which consists in exposing the papers to a temperature of 100° C. for 72 hours, and then determining the effect produced on the chemical and physical properties, appears to arrange the papers in about the same order of stability that would be expected on natural aging. A comparison of the results of the above-mentioned aging treatment with results obtained by using more nearly normal conditions (60° C. for 860 hours, and sunlight exposures) shows that they all classified the papers in the same order of stability. These two findings are evidence that the more drastic treatment, which is desirable in respect to convenience and rapidity, gives results in line with more normal aging effects.

CONTENTS

	Page
I. Introduction	466
II. Description of samples studied	466
III. Test methods employed	466
1. Official methods of the Technical Association of the Pulp and Paper Industry	466
2. Tentative chemical testing methods	467
(*a*) Acidity	467
(1) Kohler-Hall method	467
(2) Acidity of fiber suspension	467
(*b*) Copper number	468
(1) Preparation of solutions	468
(2) Procedure	468
(*c*) Alpha cellulose content	469
3. Accelerated aging tests	469
(*a*) Oven tests	469
(*b*) Sunlight exposures	469
IV. Results	469
1. Strength tests	469
2. Permanence tests	469
(*a*) Chemical purity tests	469
(1) Copper number	469
(2) Alpha cellulose content	470
(3) Acidity	470
(4) Rosin	471
3. Accelerated aging tests	471
(*a*) Oven treatment at 100° C. for 72 hours	471
(*b*) Special oven treatments involving variations of temperature and duration of treatments	473
(*c*) Sunlight exposures	474
4. Classification of papers	474
V. Summary	475

[1] Research associate of the Brown Co., Berlin, N. H.

I. INTRODUCTION

In previous work, which involved the comparative study of highly purified wood fiber papers with other common commercial types of papers, it was indicated that the source of the fibers composing a paper did not necessarily determine certain qualities which have an important bearing on its serviceability, and that accurate evaluations of the quality of paper could be made only on the basis of pertinent performance and purity tests.[1]

While the samples employed in the previous tests were probably typical high-grade products of the manufacturers from whom they were obtained, there was some question as to how well this series of papers represented the different commercial grades. It was decided, therefore, that the testing of papers purchased on definite quality specifications would be of value. A series of samples was obtained for study, consisting of 11 bond and ledger papers representative of deliveries on contracts to the Government Printing Office.

The Government, which is a large user of paper of all kinds, purchases paper on a competitive-bid basis, and awards contracts to the lowest bidders. Papers furnished by contractors must conform to certain minimum requirements which are stated in the proposal. These requirements include specifications of source of fiber, strength, and, in the case of the higher grade papers, purity requirements, such as content of rosin and acid; because it is now generally recognized that even the highest-grade paper-making fibers may be ruined at various steps in the paper-making process. While there has been an increasing use of paper-testing methods to aid in the selection of papers for various purposes, few attempts have been made to grade papers on the basis of fiber quality or purity. The following data, and those previously obtained, show, however, that such a basis of classification is feasible.

II. DESCRIPTION OF SAMPLES STUDIED

The samples studied were 11 in number. The bond papers consisted of four grades, classified as 100 per cent sulphite fiber, 30 per cent rag, 50 per cent rag, and 100 per cent rag. The ledger papers, in addition to these grades, included a 75 per cent rag paper. Three different 100 per cent rag ledger papers were tested. All of the papers, with the exception of the 100 per cent sulphite fiber papers, which were beater sized only, were surface sized with starch or glue.

III. TEST METHODS EMPLOYED

1. OFFICIAL METHODS OF THE TECHNICAL ASSOCIATION OF THE PULP AND PAPER INDUSTRY[2]

All the strength tests, as well as tests for sizing quality, ash, resin, glue, and starch, were made according to the official T. A. P. P. I. methods.

---

[1] Rasch, R. H., A Study of Purified Wood Fibers as a Paper-Making Material, B. S. Jour. Research 3 (RP107), p. 469; September 6, 1929. Price 15 cents. Superintendent of Documents, Washington, D. C.

[2] Copies of the Official Paper-Testing Methods of the Technical Association of the Pulp and Paper Industry may be obtained from the secretary at 18 East Forty-first Street, New York, N. Y.

2. TENTATIVE CHEMICAL TESTING METHODS

(a) ACIDITY

(1) *Kohler-Hall method.*[4]—Two methods for the determination of acidity were employed—the Kohler-Hall method, and a method first proposed by Dr. J. E. Minor, of the Rag Content Manufacturers Association, in which a fiber suspension is swept free of CO_2 and titrated directly. Each method appears to have certain inherent advantages. In the method described by Kohler and Hall 5 g of the ground paper is extracted with 250 ml portions of hot water. The authors express the result as the "total acidity number," which is defined as the number of milliliters of 0.01 normal sodium hydroxide required to make the first three extracts of 10 g of oven-dry fiber neutral to phenolphthalein indicator. For convenience and uniformity, however, results in this paper are expressed as per cent SO_3. In the case of surface-sized papers we have the acidity of the basic paper (internal acidity), and the acidity due to the alum present in the glue or starch surface sizing (external acidity). As stated by Kohler and Hall, the former is harmful from the standpoint of permanence, and the latter is relatively without effect.[5] The important feature of the Kohler-Hall method is that it includes a method for estimating the internal acidity. This is obtained indirectly by determining the external acidity and subtracting it from the total acidity. Kohler and Hall show that a single short extraction of pieces of the unground paper will bring practically all the acid contained in the surface sizing into solution without dissolving any significant amount of the internal acid. The procedure for the determination of the external acidity consists in boiling 10 g of paper, in the form of one-half-inch squares, for two minutes in 250 ml of water. The extract is decanted, cooled, and titrated with 0.01 normal sodium hydroxide solution.

(2) *Acidity of fiber suspension.*—The method for determining the acidity of a fiber suspension appears to offer an advantage over the Kohler-Hall method in that it determines the total titratable acidity present in the fiber, whereas the latter determines what is apparently a variable fraction of the total acidity. The procedure used follows: Weigh out about 1 g of air-dry, ground paper in a small beaker. Heat to boiling 150 ml of distilled water, and moisten the fibers with a little of the hot water. With the aid of a stirring rod and the remainder of the water, transfer the fibers to an Erlenmeyer flask. Heat to boiling and boil for one minute, then set aside until cooled to room temperature. After cooling, bubble a stream of carbon dioxide-free air through the suspension for 15 minutes in order to remove any dissolved carbon dioxide, then titrate with 0.01 normal sodium hydroxide solution, using phenolphthalein indicator. Continue to bubble a slow stream of air through the suspension during the titration. The end point is taken as a pink color which pervades the liquid for one minute. In making the titration the tip of the burette containing the sodium hydroxide solution is inserted through the stopper of the test flask. In order to aid in the distribution of air bubbles, a glass rod reaching to the bottom of the flask is secured to the stopper.

[4] S. Kohler, and G. Hall, Acidity in Paper, Paper Ind., 7, pp. 1-5; October, 1925.
[5] See footnote 4.

Total acidity, as per cent SO_3, may be calculated by the following formula.

$$\text{Acidity} = \frac{4 \times (ml\ \text{NaOH} - ml\ \text{NaOH for blank}) \times N}{W}$$

where N is the normality of the sodium hydroxide solution, and W is the oven-dry weight in grams of the sample.

(b) COPPER NUMBER

The method employed was essentially that of Schwalbe-Braidy, as described by Clibbens and Geake.[6] The procedure as given by them was followed with a few slight modifications to make it more adaptable for the testing of papers. The changes applied to the original Braidy modification were: (1) Reduction of the sample to a finely ground condition, (2) the use of a 1.5 g sample instead of a 2.5 g sample, (3) the use of the phosphomolybdic acid solution instead of ferric ammonium sulphate in the determination of cuprous oxide. The modified procedure as used at the bureau follows.

(1) *Preparation of solutions.*—Copper sulphate solution: Dissolve 100 g $CuSO_4.5H_2O$ in distilled water, and make up to 1 liter.

Sodium carbonate—sodium bicarbonate solution: Dissolve 50 g $NaHCO_3$ and 350 g $Na_2CO_3.10H_2O$ in distilled water, and make up to 1 liter.

Phosphomolybdic acid solution: Dissolve 100 g of sodium molybdate ($Na_2MoO_4.2H_2O$) and 75 ml of phosphoric acid (83 per cent) in a solution containing 275 ml of concentrated sulphuric acid and 1,750 ml of water.

Sodium carbonate solution: Make up a solution containing approximately 5 per cent Na_2CO_3.

Potassium permanganate solution: Make up a solution having a normality of 0.05.

(2) *Procedure.*—Immediately before use add 5.0 ml of the copper sulphate solution to 95 ml of the sodium carbonate-sodium bicarbonate solution. Bring the mixture to a boil, and pour over 1.5 g of the finely ground sample in a 125-ml Erlenmeyer flask. Stir well with a glass rod in order to distribute the fibers and to remove air bubbles. Fit the flask with a Bunsen valve and submerge completely in a steam bath at atmospheric pressure. Occasionally fibers tend to float to the surface, therefore the flask should be shaken from time to time in order to redistribute them. Remove the flask from the steam bath at the end of three hours. Filter on a filter paper in a Büchner funnel, using suction. Wash with 100 ml of 5 per cent sodium carbonate solution, and then with 250 ml of hot water. Transfer fiber and filter paper to a small beaker, add 25 ml of the molybdate solution, and macerate well with a flattened glass rod. Transfer to a Büchner funnel again and wash thoroughly with cold water until the blue molybdenum color is removed from the fibers. Titrate the filtrate with 0.05 normal potassium permanganate to a faint pink.

The copper number is defined as the number of grams of copper in the cuprous oxide reduced from the cupric hydroxide solution by 100 g of the sample. It may be calculated from the following formula.

$$\text{Copper number} = \frac{6.357 \times ml\ KMnO_4 \times N}{W}$$

[6] Text. Inst., Trans., *15*, pp. 27-38; 1924.

TABLE 1.—*Data*

Sample No.	Lot No.	Fiber composition		Kind of sizing used	Aging test		Physical tests [1]																
		Rag	Chemical wood		Temperature	Duration	Weight 500 sheets 25 by 40 inches	Thickness	Bursting strength	Ratio bursting strength to weight	Folding endurance			Folding endurance in per cent of initial			Folding endurance at 50 per cent relative humidity.			Tensile strength			
											Machine direction	Across machine direction	Average	Machine direction	Across machine direction	Average	Machine direction	Across machine direction	Average	Machine direction	Across machine direction	Average	
		Per cent	*Per cent*		*°C.*	*Hours*	*Pounds*	*Inch*	*Points* [2]	*Per cent*	*Double folds*	*Double folds*	*Double folds*	*Per cent*	*Per cent*	*Per cent*	*Double folds*	*Double folds*	*Double folds*	*kg*	*kg*	*kg*	
A-O	102	0	100	Engine sizing	(3)		53.1	0.0040	29.2	55	484	191	338				212	201	207	7.0	3.9	5.5	
A-H72					100	72	52.9	.0039	19.7	37	8.4	7.3	5.4	1	4	3				5.7	3.2	4.5	
B-O	110	30	70	Engine and tub sizing.	(3)		42.6	.0030	29.6	69	630	239	435				588	381	485	7.5	3.9	5.7	
B-H72					100	72	44.1		26.6	60	149	104	127	24	44	34				7.3	3.6	5.5	
C-O	121	50	50	do	(3)		43.1	.0031	30.9	72	726	321	524				585	405	495	7.5	4.1	5.8	
C-H72					100	72	43.9		30.4	69	346	154	250	48	48	48				7.4	4.1	5.8	
D-O	128	100	0	do	(3)		58.1	.0048	63.0	108	4,039	2,870	3,455				2,859	2,375	2,617	11.3	7.3	9.3	
D-H72					100	72	58.0		58.4	101	2,154	1,462	1,808	53	51	52				10.3	6.7	8.5	
E-O	151	0	100	Engine sizing	(3)		92.7	.0064	43.1	47	1,629	220	925				693	123	408	10.7	5.1	7.9	
E-H72					100	72	92.4	.0064	27.8	30	1.0	1.6	1.3	0	1	1				8.7	4.7	6.7	
F-O	154	40	60	Engine and tub sizing.	(3)		78.3	.0055	45.3	58	867	272	570				487	333	410	9.6	5.7	7.7	
F-H72					100	72	77.8	.0056	39.5	51	177	84	131	20	31	26				9.1	5.2	7.2	
G-O	161	55	45	do	(3)		85.6	.0055	57.6	67	951	361	656				635	311	473	13.3	6.8	10.1	
G-H72					100	72	85.1		50.9	60	126	94	110	13	26	20				12.3	6.4	9.4	
H-O	169	85	15	do	(3)		88.4	.0061	61.9	70	4,576	705	2,641				3,179	862	2,021	13.1	7.4	10.3	
H-H72					100	72	88.3		61.6	70	1,809	532	1,171	40	76	58				12.8	7.0	9.9	
I-O	176	100	0	do	(3)		68.5	.0047	77.9	114	3,344	2,663	3,004				2,055	1,439	1,747	13.6	8.3	11.0	
I-H72					100	72	68.5		71.4	104	2,692	2,199	2,446	80	83	82				13.0	7.9	10.5	
J-O	178	100	0	do	(3)		88.1	.0064	75.5	86	3,876	2,112	2,994				3,123	1,302	2,213	14.2	8.8	11.5	
J-H72					100	72	88.3		73.0	83	2,506	993	1,750	65	47	56				13.7	8.3	11.0	
K-O	177	100	0	do	(3)		78.3	.0052	71.1	91	6,426	4,384	5,405				4,035	3,375	3,705	14.5	7.6	11.1	
K-H72					100	72	77.8		69.0	89	5,269	3,329	4,299	82	76	79				14.6	7.6	11.1	

[1] Physical tests made at 65 per cent relative humidity except as noted.

[2] Acidity expressed as per cent SO_3.

[3] Internal acidity equals total acidity minus external acid

Data on bond and ledger papers

	Elongation			Elongation in per cent of initial			Tearing strength			Tearing strength in per cent of initial			Degree of sizing		Sizing materials present			Ash	Acidity [3]				Alpha cellulose content [4]	Decrease in alpha cellulose in per cent of initial	Alpha-cellulose content corrected for sizing materials present [4]	Copper number	Increase in copper number
																			Acidity Kohler-Hall method			Acidity of fiber suspension					
	Machine direction	Across machine direction	Average	Machine direction	Across machine direction	Average	Machine direction	Across machine direction	Average	Machine direction	Across machine direction	Average	Indicator (21° C.)	Curl (21°C.)	Resin	Glue	Starch		Total	External	Internal [5]						
	Per cent	*Per cent*	*Per cent*	*Per cent*	*Per cent*	*Per cent*	*g*	*g*	*g*	*Per cent*	*Per cent*	*Per cent*	*Seconds*	*Seconds*	*Per cent*	*Per cent*	*Per cent*	*Per cent*	*Per cent*	*Per cent*	*Per cent*	*Per cent*	*Per cent*	*Per cent*	*Per cent*	*Per cent*	
.5	2.8	6.8	4.8				57.0	51.0	54.0				20.6	23.4	0.9	0	Trace.	0.77	0.126			0.185	78.3		79.0	3.51	
.5	1.4	3.9	2.7	50	57	54	23.4	20.8	22.1	41	41	41											72.1	7.9		4.43	0.92
.7	2.6	6.7	4.7				39.8	39.8	39.8				9.6	15.4	1.0	0	5.42	1.00	.104	0.019	0.085	.223	77.5		83.0	2.50	
.5	2.4	5.5	4.0	92	82	87	35.5	34.0	34.8	89	85	87											75.3	2.9		3.01	.51
.8	2.7	7.0	4.9				45.0	45.0	45.0				10.1	15.0	1.7	2.56		1.15	.110			.208	77.6		81.0	2.50	
.8	2.5	5.4	4.0	93	77	85	38.8	38.8	38.8	86	86	86											74.7	3.8		2.87	.37
.3	5.2	7.6	6.4				104.0	96.0	100.0				14.3	23.3	1.3	7.34	Trace.	.69	.188	.087	.101	.204	85.4		93.5	0.99	
.5	4.6	7.0	5.8	88	92	90	90.0	86.0	88.0	87	90	89											84.1	1.5		1.46	.47
.2	2.5	5.0	3.8				144.0	130.8	137.4				33.9	51.1	1.0	0	0	.60	.144			.202	79.0		80.0	3.83	
.7	1.4	3.0	2.2	56	60	58	54.2	49.4	51.8	38	38	38											72.4	8.3		4.49	.66
.7	3.4	6.4	4.9				112.4	99.6	106.0				24.1	34.1	2.1	0	2.49	.69	.098	.012	.086	.185	78.7		82.5	2.47	
.2	3.0	4.9	4.0	88	77	83	86.0	76.8	81.4	77	77	77											74.5	5.4		3.15	.68
.1	3.4	7.4	5.4				123.6	111.6	117.6				28.7	41.4	1.7	2.05	Trace.	.68	.108	.032	.076	.188	76.9		80.0	2.35	
.4	2.9	6.0	4.5	85	81	83	100.4	86.4	93.4	81	78	80											73.7	4.2		2.87	.52
.3	4.3	7.4	5.9				160.8	147.6	154.2				24.2	37.9	1.8	1.94	1.23	.68	.066	.010	.056	.103	83.5		88.0	1.61	
.9	3.9	7.2	5.6	91	97	94	140.8	124.8	132.8	88	85	87											80.7	3.4		1.78	.17
.0	4.8	8.4	6.6				128.8	112.4	120.6				16.0	24.0	1.4	7.05	Trace.	.75	.142	.039	.104	.147	82.8		90.5	1.80	
.5	4.1	7.8	6.0	85	93	89	106.4	108.4	107.4	83	96	90											81.9	1.0		2.05	.25
.5	4.2	8.5	6.4				179.2	169.2	174.2				20.1	28.4	1.6	4.05	2.51	.62	.140	.058	.082	.171	87.8		95.5	0.96	
.0	4.1	7.9	6.0	98	96	97	169.2	140.0	154.6	94	83	89											86.8	1.1		1.32	.36
.1	3.9	8.7	6.3				178.4	164.0	171.2				18.1	31.2	0.8	3.62	Trace.	.96	.152	.031	.121	.163	90.1		94.5	1.01	
.1	4.0	7.9	6.0	103	91	97	163.6	146.0	154.8	92	89	91											89.3	0.9		1.09	.08

Chemical tests

acidity.

[4] Not corrected for sizing materials present.

[5] Values to nearest 0.5 per cent.

[6] Approximately pounds per square inch.

[7] Control sample.

where N is the normality of the potassium permanganate solution and W is the oven-dry weight of the sample.

The amount of copper in the cuprous oxide reduced from the reagent alone under the conditions of the method should be determined and applied as a correction to the copper number.

(c) ALPHA-CELLULOSE CONTENT

Alpha cellulose determinations were made according to the procedure outlined in a previous publication.[7]

3. ACCELERATED AGING TESTS

(a) OVEN TESTS

In order to obtain information on relative stability, all the paper samples included in this study were subjected to a heat treatment at 100° C. for 72 hours in a special air-circulating oven, described in a previous publication.[7] The stability is estimated by a consideration of the effect of this treatment on the strength properties of the paper, as well as on the alpha cellulose content and copper number.

A criticism commonly directed at the above-mentioned method of estimating the permanence of papers is that it subjects papers to exaggerated conditions which never obtain under natural aging. Therefore a few supplementary experiments were made in which papers were subjected to a temperature of 60° C. for various lengths of time, in order to determine whether a much less drastic treatment of this type would classify papers in the same order of stability as the oven treatment at higher temperature. Other experiments were made in which papers were subjected to temperatures of 90° and 120° C., respectively.

(b) SUNLIGHT EXPOSURES

In order to compare the effects of sunlight and oven heat treatments, a few of the papers were exposed, side by side, to the direct rays of the sun for 100 sun-hours on each surface.

IV. RESULTS

1. STRENGTH TESTS

Results of strength tests are given in Table 1. Except in one case all these tests were made at 65 per cent relative humidity, the folding endurance being determined at 50 per cent relative humidity as well. In general, no great differences in original strength are noted among papers ranging from 0 to 50 per cent in rag fiber content. The 100 per cent rag bonds and ledgers are, however, markedly higher in strength than the other papers, reflecting, undoubtedly, the superior quality of fibers in these papers, relative to that of the other papers included in this study.

2. PERMANENCE TESTS

(a) CHEMICAL PURITY TESTS

(1) *Copper number.*—The copper number appears to be the most convenient and best single method for estimating the purity of the

[7] See footnote 2, p. 466.

basic fibers in papers. The relation between the different grades of papers and their copper numbers is quite straightforward in this series. Thus, the two all-sulphite fiber papers, the lowest grade included in this series, have the highest copper numbers, while the highest grade papers, the 100 per cent rag papers, have the lowest copper numbers. Intermediate grades correspond with copper numbers of intermediate value.

(2) *Alpha-cellulose content.*—The alpha-cellulose contents of the papers when corrected for sizing materials present classify the samples in approximately the same order of chemical purity as the copper numbers do. As will be seen in Figure 1, there is a distinct tendency for high copper numbers to be associated with low alpha cellulose contents, and vice versa. It is important that corrections for sizing

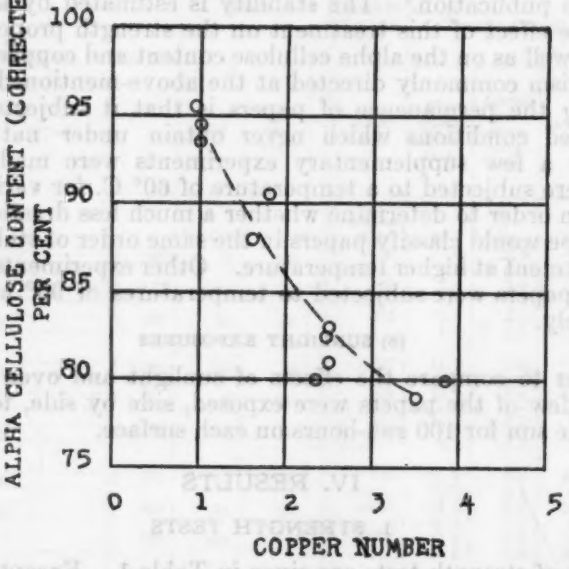

FIGURE 1.—*Relation between alpha-cellulose content and copper number*

materials present in the paper be applied to the alpha cellulose values before conclusions are drawn regarding the purity of the fibers. In this paper corrected alpha cellulose values are reported only to the nearest one-half per cent, to allow for cumulative errors, which are unavoidably introduced when applying corrections for sizing materials.

(3) *Acidity.*—The relation between the acidity of a fiber suspension, and the "total acidity" by the Kohler-Hall extraction method is apparently not a constant one for different papers. The ratio of the results by the former method to results by the latter method varies with different papers anywhere from 1 to 2. Acidities of the all-sulphite fiber papers, as determined by the Kohler-Hall method, are noticeably higher than the internal acidities of the rag content, surfaced-sized papers, as is to be expected.

(4) *Rosin.*—It is noteworthy that the rosin contents of the papers, particularly the two 100 per cent sulphite fiber papers, are relatively low, revealing a laudable tendency among paper manufacturers to reduce the amount of rosin used to just that required for adequate sizing.

3. ACCELERATED AGING TESTS

(a) OVEN TREATMENT AT 100° C. FOR 72 HOURS

In Table 1 the effects of the heat treatment at 100° C. on the strength and chemical properties of the papers are shown. If we

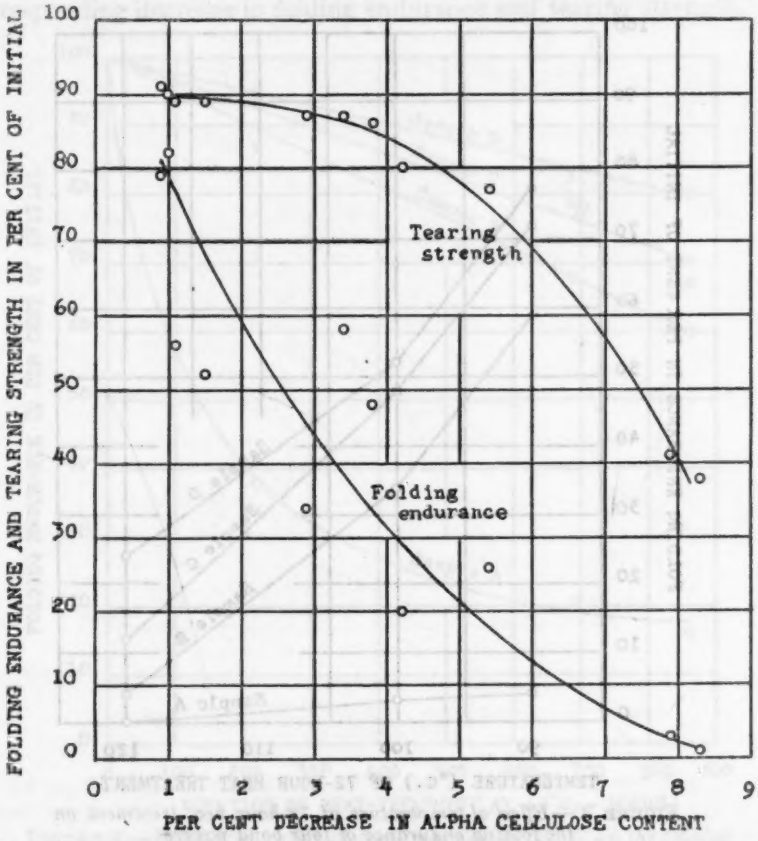

FIGURE 2.—*Relation between effects produced by heating on the strength and alpha-cellulose content*

assume that the papers represented in the highest grade are the most permanent, that those in the lowest grade are the least permanent, and that the intermediate grades occupy an intermediate position in regard to permanency, it is evident from the test data that the heat treatment rates the papers of this series in the same order as normal aging would. The assumptions made above are in accord with the purposes for which the Government paper specifications were designed, and with the general consensus of present opinion regarding factors which influence permanence. Thus, it is well

known that paper carefully prepared from new white rags has lasted for centuries. Specifications for Government papers require that those intended for permanent uses shall be made of "100 per cent new rags, white, cream, or unbleached." This and the other requirements for strength, acidity, and sizing make it probable that this grade of paper is, for all practical purposes, permanent. The lowest grade of Government bond and ledger paper is made from chemical wood pulp prepared by the usual sulphite process. While numerous examples are available of sulphite papers which have resisted deterioration a score or more of years, and while their lasting qualities are

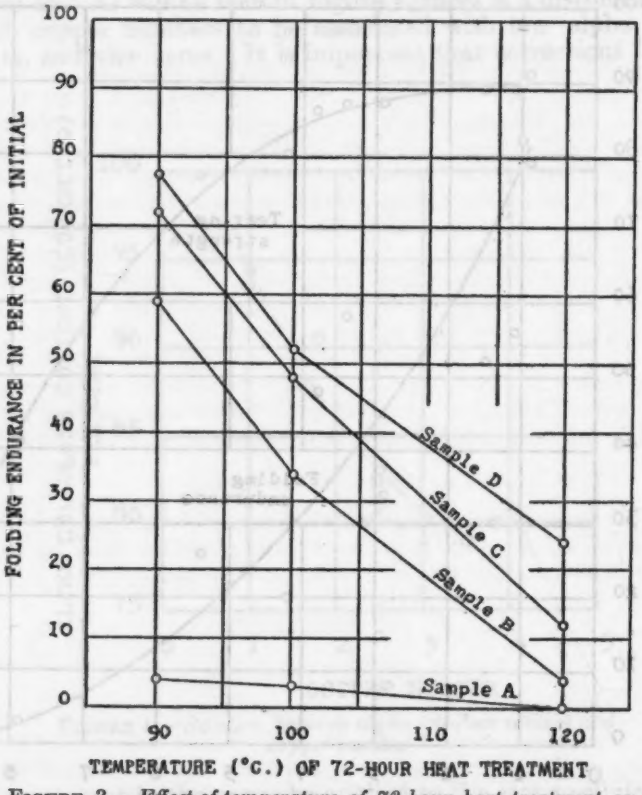

FIGURE 3.—*Effect of temperature of 72-hour heat treatment on the folding endurance of four bond papers*

frequently underestimated, it is safe to say that the ordinary types of such papers stand lower on a relative scale of permanency than those made from purer grades of paper-making fibers.

The test results show that the stability of the papers toward the heat test is related to their chemical purity. Samples A and E were found to be composed of fibers having the highest copper numbers, and the lowest alpha cellulose content, pointing to a lower degree of purity relative to the other papers in the series. Samples D, H, I, J, and K, on the other hand, had the lowest copper numbers and the highest alpha cellulose values. On comparing the effects produced on the papers by heating them for 72 hours at 100° C., it will be noted

that A and E retain but 3 and 1 per cent of their initial folding endurances, respectively, while D, H, I, J, and K retain 52, 58, 82, 56, and 79 per cent, respectively. In the case of the tearing strengths the retentions of these papers are, respectively, 41 and 38, on the one hand, and 89, 87, 90, 89, and 91, on the other. The decreases in alpha cellulose content for the same papers are, in order, 7.9 and 8.3, as against 1.5, 3.4, 1.0, 1.1, and 0.9. The data show that the heat treatment produces a definite alteration in the chemical as well as the physical properties of the cellulose fibers. Figure 2 shows the relation between the decrease in alpha cellulose content and the corresponding decrease in folding endurance and tearing strength.

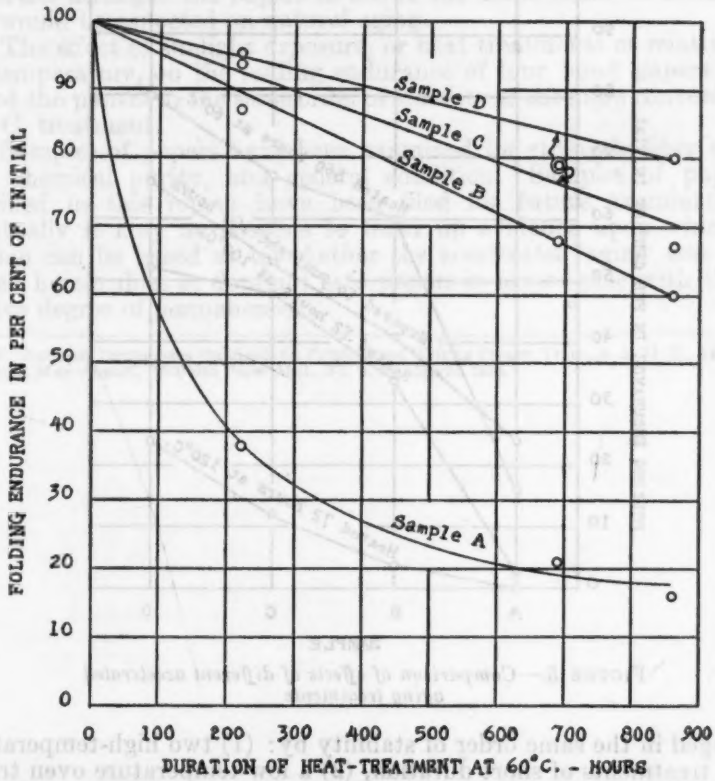

FIGURE 4.—*Effect of duration of heat treatment at 60° C. on the folding endurance of four bond papers*

(b) SPECIAL OVEN TREATMENTS INVOLVING VARIATIONS OF TEMPERATURE AND DURATIONS OF TREATMENTS

Treatments for 72 hours at 90° C. and 120° C. as well as at 100°C. were made on the four bond papers. The effect of the treatments on the folding endurance is shown graphically in Figure 3.

Next, treatments of the same papers at the comparatively low temperature of 60° C. were carried out for 240, 692, and 860 hours, respectively. Exposures for such long durations were necessary in order to obtain noticeable effects. Treatments at this temperature are much less drastic than at 100° C., and yet the papers rate in the same order of stability. The results are shown graphically in Figure 4.

(c) SUNLIGHT EXPOSURES

Another stability test tried consisted in the exposure of these papers to the action of the sun's rays. Here, too, the effects on folding endurance rate the papers in the same order of stability as the heat tests do.

In Figure 5 a comparison of the effects of the various treatments on the folding endurances of the four papers is shown graphically. The fact of significance shown in Figure 5 is that the four papers, probably covering a fairly wide range of permanence qualities, are

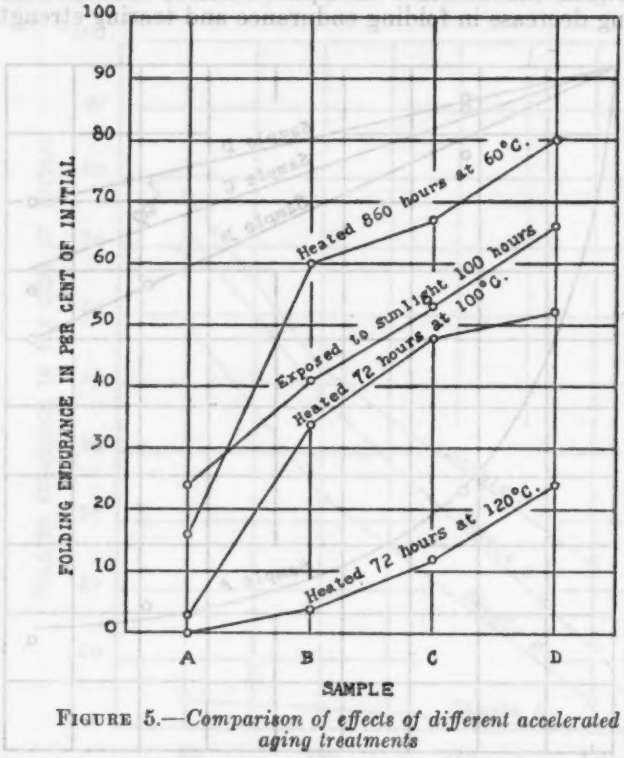

FIGURE 5.—*Comparison of effects of different accelerated aging treatments*

arranged in the same order of stability by: (1) two high-temperature oven treatments of short duration, (2) a low-temperature oven treatment of long duration, and (3) an exposure to direct sunlight.

4. CLASSIFICATION OF PAPERS

From a consideration of these results, and the others previously reported, then, it appears that the various chemical and physical tests mentioned agree in their order of classification of the various papers with respect to their deterioration under the test conditions, when the folding endurance, tearing strength and alpha cellulose tests are used as an index of this deterioration. Furthermore, this order is substantially the same as that of the life expectancy of the papers in so far as this can be inferred from the information available. On this assumption two of the attributes of a permanent paper appear

to be low copper number and high alpha cellulose content. The heat test seems to be a promising means of estimating the probable relative life of a paper. Recently a system of classification of printing and writing papers has been suggested, in which performance tests and purity tests alone are the determining factors in grouping papers according to their aging properties.[8]

V. SUMMARY

1. An accelerated aging test, which determines the effect of a 72-hour heat treatment at 100° C. on various physical and chemical properties arranged the papers in about the same order of stability that would be expected on natural aging.

2. The effect of sunlight exposure, or heat treatments of relatively low temperature, on the folding endurance of four bond papers arranged the papers in the same order of stability as the more convenient 100° C. treatment.

3. Samples of papers have been examined for strength, fiber content, chemical purity, and general condition. Samples of papers described in this report have been filed for future examination. Eventually it may be possible to build up evidence upon which a decision can be based as to whether the accelerated aging test described herein does or does not rate papers in accordance with their relative degree of permanence.

[8] B. W. Scribner, Permanence Standards for Printing and Writing Papers, Trans. A. S. M. E., **52**, No. 19, PI-52-5; May-August, 1930; also Paper Mill., **53**, p. 13; June 21, 1930.

RP353

CRYOSCOPIC CONSTANT, HEAT OF FUSION, AND HEAT CAPACITY OF CAMPHOR

By Mikkel Frandsen

ABSTRACT

In order to determine the cryoscopic constant of camphor the latent heat of fusion of this substance was measured calorimetrically. Values for the heat capacities of solid and liquid camphor were obtained at the same time. The determinations were made on synthetic camphor, the freezing point of which was found to be 178.43° C. Two samples of this material and one of pure silver, serving as a reference substance, were sealed in evacuated, thin-walled glass tubes, and successively heated to constant, well-defined temperatures in a narrow glass tube surrounded by the vapors of various liquids, boiling in the range from 20° to 212° C. In each case the heat content of the sample was measured by transferring it to a silvered Dewar tube, containing about 300 g of water. From a plot of the heat content against the temperature the following results were obtained:

The latent heat of fusion at 178.4° C., $l_p = 10.74 \pm 0.40$, $cal_{15}\ g^{-1}$, or, $L_p = 1{,}630 \pm 60$, $cal_{15}\ mole^{-1}$. The cryoscopic constant, $k_p = 37.7 \pm 1.4$° C. $mole^{-1}$ kg. The heat capacity of crystalline camphor in the range from 20 to 178.4° C., $c_{(solid)} = (0.4208 + 0.000215\ t) \pm 0.0035$, $cal_{15}\ g^{-1}°C.^{-1}$, or, $C_{(solid)} = (64.0 + 0.033\ t) \pm 0.5$, $cal_{15}\ mole^{-1}°C.^{-1}$ The heat capacity of liquid camphor in the range from 178.4° to 210° C., $c_{(liquid)} = 0.571 \pm 0.045$, $cal_{15}\ g^{-1}C^{-1}$., or, $C_{(liquid)} = 87 \pm 7\ cal_{15}$ $mole^{-1}°C.^{-1}$.

CONTENTS

		Page
I.	Introduction	477
II.	Material	478
III.	Calorimetric apparatus and procedure	479
IV.	Experimental results	480
	1. Data and discussion	480
	2. Latent heat of fusion	481
	3. The cryoscopic constant	481
	4. Heat capacities	482
V.	Conclusions	482
VI.	Acknowledgment	483

I. INTRODUCTION

Camphor is often used as a solvent in determinations of molecular weights by the freezing-point method. Unfortunately, however, there seems to be some difference of opinion in regard to the value of the cryoscopic constant for this substance. From a large number of determinations Jouniaux [1] has obtained the average value 49.5, and Efremov's [2] determinations lead to an average of 48.7. Rast,[3] on the other hand, gives the value as 39.7, which also was used by Smith and Young,[4] while Houben [5] and Carlsohn [6] used the value 40.0.

[1] Jouniaux, Compt. rend., **154**, p. 1592; 1912. Bull. soc. chim., **11**, pp. 722, 993; 1912.
[2] Efremov, Tables Annuelles Internationales de Constants et Donnés Numériques, **5**, p. 853; 1922.
[3] Rast, Ber., **55**, pp. 1051, 3727; 1922.
[4] Smith and Young, J. Biol. Chem., **75**, p. 289; 1927.
[5] Houben, J. prakt. Chem., **105**, p. 27; 1922.
[6] Carlsohn, Ber., **60**, p. 473; 1927.

Since the true cryoscopic constant of a substance is completely defined by its melting point and latent heat of fusion, a determination of these two properties should lead to a clarification of the situation with respect to this constant for camphor. The equipment required for these measurements being at hand in connection with another investigation, advantage was taken of the possession of a small sample of pure synthetic camphor to carry out a few determinations. Incidentally, approximate values for the heat capacities of solid and liquid camphor, respectively, were also obtained.

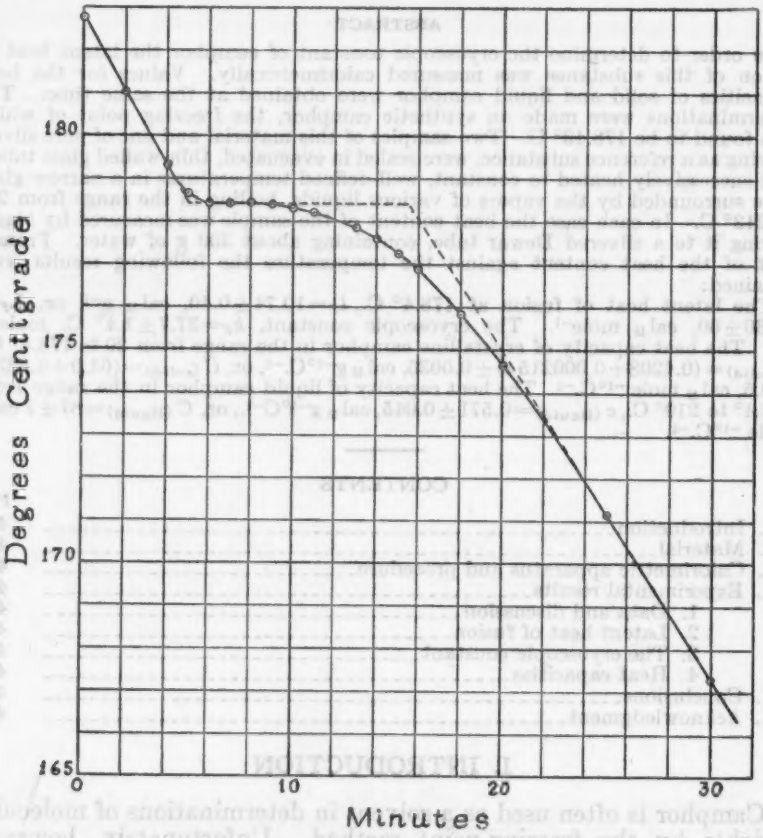

FIGURE 1.—*Cooling curve of camphor*

II. MATERIAL

The material on which the determinations were made was synthetic camphor, which had been purified by several recrystallizations from ethyl alcohol.[7]

The freezing point of this material was determined in a small silvered Dewar tube, using the procedure described by Washburn.[8]

A cooling curve obtained as an average of four single curves is shown in Figure 1. From this curve the freezing point is found to be

[7] This material was supplied by Dr. C. L. Reese, of the DuPont Co.
[8] Washburn, Ind. Eng. Chem., 16, p. 275; 1924.

178.43 ± 0.04° C. A comparison with the determinations made by Komppa [9] and Haller,[10] namely, 178° to 178.5° C. and 178.8° C., respectively, leads to the conclusion that the material was sufficiently pure. It may not have been absolutely pure, however, since an equilibrium cooling curve should have the shape indicated by the dotted lines in Figure 1. Possibly complete equilibrium was not attained toward the end of the crystallization owing to the thermometer becoming covered with solid camphor.

III. CALORIMETRIC APPARATUS AND PROCEDURE

In this investigation the calorimetric method of mixtures was employed in a manner substantially that described by Andrews, Lynn, and Johnston.[11]

The calorimeter consisted of a silvered Dewar tube, 5.1×25.4 cm, surrounded by appropriate insulating material, and charged with about 300 grams of water. The heat capacity of the calorimeter was accurately determined by electrical calibration and the procedure was standardized against metallic silver as in the experiments of Andrews, Lynn, and Johnston.

The true temperature rise in the calorimeter was found by the graphic method described by Dickinson.[12]

On account of the low thermal conductivity of solid camphor it was found necessary, first, to leave the samples in the high-temperature bath for at least four hours; second, to use an after-period of 30 minutes; and third, to remove the sample of camphor from the calorimeter before observing the final rate of temperature change.

Corrections were applied for the heat given up to the calorimeter by the suspending wire and glass containing-tube, and for the vaporization of a small amount of camphor at the higher temperatures. corrected quantity of heat given up by the sample, divided by the mass of camphor, is the quantity of heat required to raise the temperature of 1 g of camphor from the final temperature of the calorimeter to the initial temperature of the sample. This is equal, within the limit of experimental error, to the heat content of 1 g of camphor at its initial temperature and under any constant low pressure, if the heat content at the final temperature of the calorimeter is taken as zero. The final temperature of the calorimeter was not the same in all experiments, although it was always close to 20° C. To make the results comparable, the values of heat content were all reduced to the basis of heat content = 0 at 20° C., using the value 0.425 calories per gram for the heat capacity of camphor at room temperature, a value which results from this investigation.

[9] Komppa, Ber., **41**, p. 4473; 1908.
[10] Haller, Compt. rend., **105**, p. 68; 1887.
[11] Andrews, Lynn, and Johnston, J. Am. Chem. Soc., **48**, p. 1274; 1926.
[12] Dickinson, B. S. Bull., **11**, p. 251; 1915.

IV. EXPERIMENTAL RESULTS

1. DATA AND DISCUSSION

The experimental results are shown in Table 1.

The heat contents in Table 1 have been plotted against the temperature as shown in Figure 2. From this figure it is seen that the

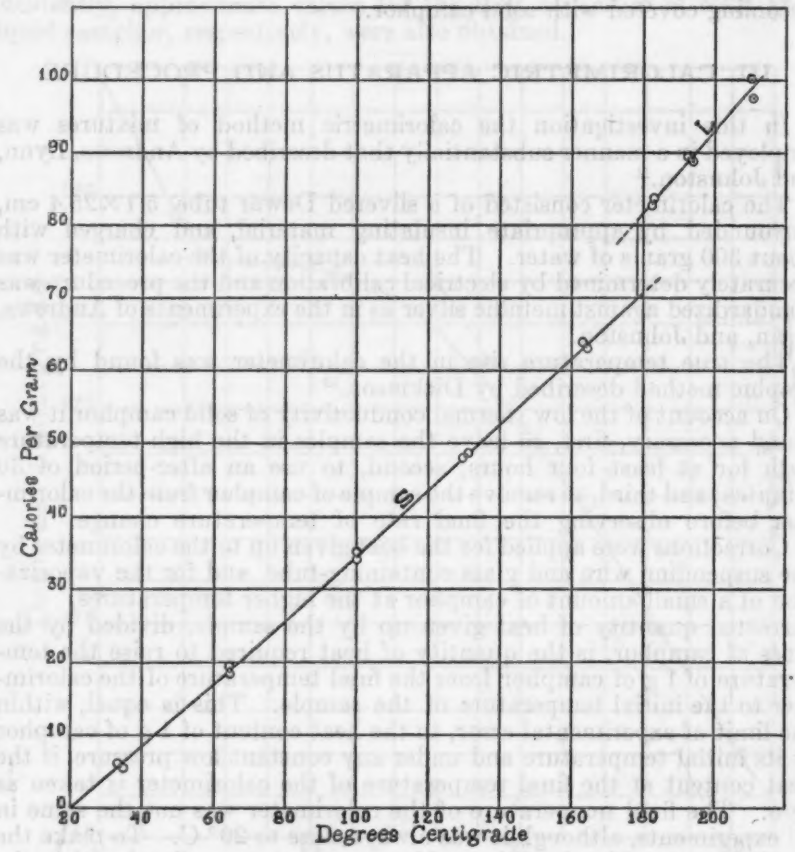

FIGURE 2.—*Heat content of camphor as a function of temperature*

The ordinate shows the heat content at the temperatures given on the abscissa less the heat content at 20° C. Curve *S* refers to solidified camphor. Curve *L* results from determinations above the melting point.

duplicate determinations on solidified camphor are in good agreement. The fact that the curve for this material when extrapolated passes through the point (0, 20) indicates that the results are not vitiated by the most probable types of systematic errors.

TABLE 1.—*Heat content of synthetic camphor at various temperatures*

Run No.	Vapor bath	Temperature	H_t-H_{20}	State of camphor	Run No.	Vapor bath	Temperature	H_t-H_{20}	State of camphor
		° C.	Cal./g				° C.	Cal./g	
1	Ethyl ether	33.8	5.83	Solidified melt.	11	Aniline	182.5	82.97	Liquid.
2	do	34.1	5.71		12	do	182.7	83.44	
3	Methyl alcohol	64.4	19.31		13	Dimethyl-aniline	192.6	89.42	
4	do	64.5	18.64		14	do	193.9	88.98	
5	Water	100.1	34.87		15	Nitro-benzene	210.1	100.17	
6	do	100.1	34.59		16	do	210.5	97.56	
7	Chloro-benzene	130.6	48.50						
8	do	130.2	48.30						
9	Butyl butyrate	163.6	63.61						
10	do	164.1	63.30						

The duplicate determinations on liquid camphor at 193° and 210° C. do not agree so well, probably on account of incipient decomposition of the camphor caused by prolonged heating at those temperatures.

For two reasons it is important to find out whether complete crystallization of the fused camphor took place when the sample was plunged into water at room temperature. If so (1) the slope of the curve for solidified camphor represents the heat capacity of solid, crystalline camphor; and (2) the difference in the ordinates of the two heat content curves at the melting point represents the latent heat of fusion of the same substance. A crystallographic examination of a sample of camphor which had been quenched from the liquid state on a microscope slide showed no detectable amount of vitreous material. Crystallization in the calorimeter may, therefore, be assumed to have been complete.

2. LATENT HEAT OF FUSION

From Figure 2 the latent heat of fusion, determined as the difference in heat content of liquid and crystalline camphor at the freezing point, is found to be

$$\left.\begin{aligned} l_f &= 10.74 \pm 0.40, \text{ cal.}_{15} \text{ per gram} \\ \text{or} \quad L_f &= 1630 \pm 60, \text{ cal.}_{15} \text{ per mole} \end{aligned}\right\} \text{at } 178.4° \text{ C.}^{13}$$

3. THE CRYOSCOPIC CONSTANT

The cryoscopic constant, k_f, of a substance is defined as the limiting value for infinite dilution of the freezing point lowering, Δt_F, produced per mole of solute in 1,000 g of the substance, or

$$k_f = \lim_{N_1 = 0} \left(\frac{\Delta t_f}{N_1} \right)$$

where N_1 is the concentration of the solute in moles per 1,000 g of solvent. The cryoscopic constant may be calculated from the formula

$$k_f = \frac{1.987\ T^2_f}{1{,}000\ l_f} \text{ ° C. mole}^{-1} \text{ kg}$$

[13] Attempts to calculate the heat of fusion, by means of the Thomson-Kirchhoff relation, from the vapor pressure curves of the two phases in the neighborhood of the freezing point were unsuccessful, owing to lack of accuracy in the available data, the two curves apparently intersecting at 160° instead of 178° C.

in which T_r is the melting point of the solvent in °K. and l_r its latent heat of fusion in $cal._{15}$ per gram.

Substituting the values for camphor

$$T_r = 178.4 + 273.1$$

and

$$l_r = 10.74 \pm 0.40$$

gives

$$k_r = 37.7 \pm 1.4, \text{ ° C. mole}^{-1} \text{ kg}$$

for the cryoscopic constant of camphor.

4. HEAT CAPACITIES

For the curve in Figure 2 showing the heat content of solidified camphor, the following equation has been derived:

$$H_t = (-8.459 + 0.4208\ t + 0.0001076\ t^2) \pm 0.25, \text{ cal.}_{15}\ g^{-1}$$

By differentiation of this equation the heat capacity of solid camphor is found to be

$$c_{\text{(solid)}} = \frac{dH}{dt} = (0.4208 + 0.000215\ t) \pm 0.0035, \text{ cal.}_{15}\ g^{-1°}\ C.^{-1}$$

or

$$C_{\text{(solid)}} = (64.0 + 0.033\ t) \pm 0.5, \text{ cal.}_{15}\ \text{mole}^{-1°}\ C.^{-1}$$

These three equations apply to solid camphor, in the range from 20° to 178.4° C.

Similarly the slope of the upper curve in Figure 2 gives for the heat capacity of liquid camphor

$$c_{\text{(liquid)}} = 0.571 \pm 0.045, \text{ cal.}_{15}\ g^{-1°}\ C.^{-1}$$

or

$$C_{\text{(liquid)}} = 87 \pm 7, \text{ cal.}_{15}\ \text{mole}^{-1°}\ C.^{-1}$$

in the range from 178.4 to 210° C.

Strictly speaking, these heat capacities are the heat capacities of the solid and liquid camphor, respectively, under an external pressure at all times equal to the vapor pressure. They do not differ appreciably, however, from the heat capacities at a constant pressure of 1 atmosphere.

V. CONCLUSIONS

From calorimetric measurements the following thermal data for pure synthetic camphor were obtained:

The latent heat of fusion at 178.4° C.

$$l_r = 10.74 \pm 0.40, \text{ cal.}_{15}\ g^{-1}$$

or

$$L_r = 1630 \pm 60, \text{ cal.}_{15}\ \text{mole}^{-1}$$

The cryoscopic constant,

$$k_r = 37.7 \pm 1.4° \text{ C. mole}^{-1} \text{ kg}$$

The heat capacity of solid, crystalline camphor

$$c_{(\text{solid})} = (0.4208 + 0.000215\,t) \pm 0.0035,\ \text{cal.}_{15}\ \text{g}^{-1^\circ}\ \text{C.}^{-1}$$

or

$$C_{(\text{solid})} = (64.0 + 0.033\,t) \pm 0.5,\ \text{cal.}_{15}\ \text{mole}^{-1^\circ}\ \text{C.}^{-1}$$

in the range from 20° to 178.4° C.

Similarly, for liquid camphor,

$$c_{(\text{liquid})} = 0.571 \pm 0.045,\ \text{cal.}_{15}\ \text{g}^{-1^\circ}\ \text{C.}^{-1}$$

or

$$C_{(\text{liquid})} = 87 \pm 7,\ \text{cal.}_{15}\ \text{mole}^{-1^\circ}\ \text{C.}^{-1}$$

in the range from 178.4° to 210° C.

The freezing point, obtained from the cooling curve, was found to be 178.43° ± 0.04° C.

VI. ACKNOWLEDGMENT

The author is greatly indebted to E. W. Washburn, of this bureau, under whose direction this work was done.

WASHINGTON, June 2, 1931.

RP354

THE PASSAGE OF GAS THROUGH THE WALLS OF PYROMETER PROTECTION TUBES AT HIGH TEMPERATURE

By Wm. F. Roeser

ABSTRACT

After a brief discussion of the contamination of thermocouples resulting from the use of tubes which are not gas tight, the results of the measurements of the rate of passage of air through 36 tubes of refractory porcelain (11 different classes), 2 of fused silica, 1 of pyrex glass, 2 of alundum, and 15 of metal are given for various temperatures which the tubes would withstand without noticeable deformation. Methods of testing are described and a very breif discussion given of the processes by which air may pass through the tube walls. The results also indicate the degree of vacuum obtainable in porcelain tubes at 1,400° C.

CONTENTS

		Page
I.	Introduction	485
II.	Apparatus and methods	486
III.	Results	488
IV.	Discussion of results	491
V.	Summary	494
IV.	Bibliography	494

I. INTRODUCTION

The wires of platinum to platinum rhodium thermocouples, as received from the manufacturers, are among the purest materials used in industrial plants and technical laboratories at the present time. Since the electromotive force generated by a thermocouple is very sensitive to changes in composition of its elements, the protection of the wires from contaminating gases and vapors is of prime importance. Base metal couples are usually protected by metal tubes and rare metal couples by tubes made of refractory porcelain or fused silica. In some cases, however, rare metal couples are portected by both porcelain and metal tubes.

In general, exposure to a reducing atmosphere is the most severe condition which is encountered. Little difficulty is encountered when thermocouples are used only in oxidizing or neutral atmospheres. Any reducing gas within the protection tube of a rare-metal couple will generally produce contamination, particularly since the tube or insulators usually contain silica. The silica is reduced to silicon which is readily absorbed by platinum and its alloys. This not only changes the thermoelectric properties of the couples, but also impairs their mechanical properties.

At least one of the elements of a base-metal couple is usually an alloy and if the couple is exposed alternately to oxidizing and reducing atmospheres its thermoelectric properties are subject to great changes due to preferential oxidation and reduction of the components of the alloy wires, in addition to the contamination by

silicon from the insulators. Gas-tight pyrometer protection tubes are, therefore, desirable in order to prevent any reducing gas from getting inside the protection tube. The most direct method of testing the effectiveness of tubes might be to observe changes in couples protected by various tubes exposed to reducing atmospheres under controlled conditions. This procedure would be tedious and expensive. Another method is to test the tubes for gas tightness when exposed to controlled reducing atmospheres. Since safe equipment was not available for making these tests, it was decided to test the tubes for gas tightness in air and, if possible, correlate the results with the very meager data vailable on the changes in the properties of couples when placed in the same type of tubes and exposed to reducing atmospheres. It may be taken as a general rule, having but few exceptions, that the air tightness of a tube is a good indication of its tightness with respect to deleterious furnace gases. This would certainly be true for leakage through cracks, pores, and small openings generally. Probably it would not be true for any process of transfer involving solution or chemical reaction which might take place.

There are very few data available on the rate of flow of air through the refractory materials widely used at high temperatures. One of these materials is the highly refractory procelain which is sometimes called sillimanite or mullite. The nickel-chromium alloys which probably corrode less than any of the other base metal alloys at high temperatures form another class of materials on which very few data are available.

An investigation was undertaken at the National Bureau of Standards to determine the rate of flow of air through the walls of various pyrometer protection tubes at high temperatures. The method used to determine air leakage through the various types of tubes furnishes, in addition, an indication of the degree of vacuum obtainable in them at high temperatures by the use of ordinary laboratory types of mercury vapor pumps. Several other materials similar in composition and characteristics to those previously mentioned have been included in this investigation. Most of the tubes were supplied by the leading manufacturers of pyrometers and pyrometer protection tubes. Their cooperation and interest in this project is greatly appreciated.

II. APPARATUS AND METHODS

The method of test consists in evacuating the tubes and measuring the rates of rise in pressure after the pump is shut off. A diagram of the apparatus is shown in Figure 1. The tubes being tested were placed in a horizontal cylindrical furnace and sealed to the pyrex glass vacuum system with De Khotinsky cement. The vacuum system consisted of a McLeod gage, a reservoir having a capacity of 2,320 cm^3, and a mercury cutoff for sealing the system from the mercury vapor pump. The total volume of the system, depending somewhat upon the size of the tube being tested, was approximately 2,500 cc. The tubes were immersed in the furnace to a depth of 35 cm.

A furnace wound with an alloy ribbon of 80 per cent platinum, 20 per cent rhodium was used in heating the porcelain and silica tubes. A platinum to platinum rhodium thermocouple placed with

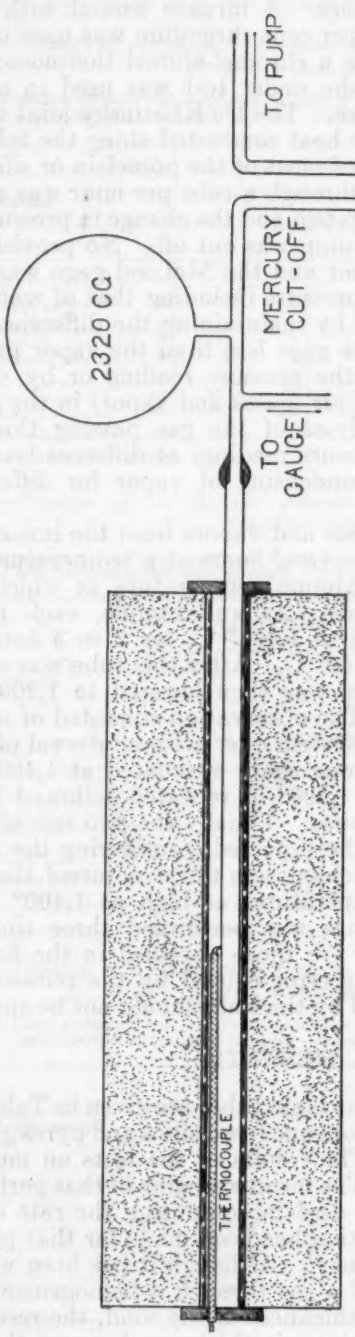

FIGURE 1.—*Diagram of apparatus used in testing pyrometer protection tubes*

its junction near the center of the furnace was used in measuring and controlling the temperature. A furnace wound with an alloy wire of 80 per cent nickel, 20 per cent chromium was used in heating the metal tubes. In this case a chromel-alumel thermocouple with its junction welded to the tube under test was used in measuring and controlling the temperature. The De Khotinsky joint was water cooled to prevent softening by heat conducted along the tube. This was not necessary in the case of most of the porcelain or silica tubes.

The amount of air passing through a tube per hour was computed from the total volume of the system and the change in pressure during the known period when the pump was cut off. No provisions were made for removing water vapor and the McLeod gage was so operated as to measure the total pressure including that of water vapor. This was accomplished either by maintaining the difference in level of the mercury columns of the gage less than the vapor pressure of water at the time of taking the pressure reading or by measuring the volume of the compressed air (gases and vapor) in the gage at a series of pressures. No analyses of the gas passing through the tubes were made, but the pressure readings at different levels in the McLeod gage revealed no condensing of vapor for differences in mercury levels up to 60 mm.

In order to drive off the gases and vapors from the inner surfaces, the tubes were evacuated for several hours at a temperature at least 100° C. higher than the maximum temperature at which leakage observations were to be made. As an example, each refractory porcelain tube was evacuated at 1,400° C. for 2 to 3 hours before taking the observations at 1,300° C. After this tube was evacuated at 1,300° C., the temperature was then lowered to 1,200° C. and another observation taken. The observation consisted of measuring the change in pressure in the system over a time interval of approximately 16 hours. The tube was again evacuated at 1,400° C. and the observation at 1,300° and 1,200° C. repeated, followed by observations at the lower temperatures. Usually the two sets of observations agreed as well as could be expected, considering the nature of the test and the possibility of changes in the structureof the material on continued heating at temperatures as high as 1,400° C. In a few cases the above procedure was performed three times. The values reported in this paper are those obtained in the final set of observations during which the error caused by the release of gases and vapors originally adsorbed by the walls should not be appreciable.

III. RESULTS

The results of the tests on porcelain tubes are given in Tables 1, 2, 3, and 4. The results of tests on opaque fused silica and pyrex glass tubes are also given in Table 4. The results of the tests on metal tubes are given in Tables 5 and 6. The mean wall area of that portion of the tube in the furnace has been used in computing the rate of flow of gas per unit area. No correction has been made for that part of the tube protruding from the furnace. Although it has been well established that the rate of flow of a gas through a homogeneous solid is inversely proportional to the thickness of the solid, the results given here have not been reduced to unit thickness because there is no assurance that this would be justified in the case of such nonhomo-

geneous specimens as glazed porcelain or plated metal tubes. The thickness of each tube is given in the tables.

TABLE 1.—*Passage of air through American-made refractory porcelain tubes (unglazed), manufacturer A*

[Amount of air passing through wall, expressed in units of 10^{-6} cm³/hr.-cm² reduced to room temperature and standard atmospheric pressure. Pressure difference one atmosphere]

Temperature	No. 1	No. 2	No. 3	No. 4	No. 5	No. 6	No. 7	No. 8	No. 9
	3-mm wall						3.5-mm wall		1-mm wall
°C.									
25	0	[1] 2	0	[1] 8	2	[1] 610	0	1	0
400	0	[1] 6	0	1	Tube broken during test	[1] 620	0	1	0
600	0	[1] 12	0	1		[1] 640	0	2	0
800	0	0	0	2		[1] 600	2	3	0
1,000	1	5	10	31	62	25	12	15	3
1,200	18	170	74	150	150	62	98	72	25
1,300	95	590	260	410	310	210	280	300	15

[1] Tube cracked while cooling down.

TABLE 2.—*Passage of air through American-made refractory porcelain tubes, manufacturer B*

[Amount of air passing through wall, expressed in units of 10^{-6} cm³/hr.-cm² reduced to room temperature and standard atmospheric pressure. Pressure difference one atmosphere]

Temperature	Unglazed tubes				Glazed tubes				
	No. 1	No. 2	No. 3	No. 4	No. 1	No. 2	No. 3	No. 4	No. 5
	3-mm wall		2-mm wall		3-mm wall		2-mm wall		1-mm wall
°C.									
25	0	0	0	2	0	2	0	0	0
400	0	0	0	4	0	2	0	0	0
600	0	0	0	8	0	2	0	0	0
800	5	0	0	19	4	2	0	2	0
1,000	35	1	20	46	21	5	3	21	0
1,200	110	27	150	330	83	38	61	66	7
1,300	180	49	410	740	290	210	320	150	26

TABLE 3.—*Passage of air through American-made refractory porcelain tubes (unglazed), manufacturer C*

[Amount of air passing through wall, expressed in units of 10^{-6} cm³/hr.-cm² reduced to room temperature and standard atmospheric pressure. Pressure difference one atmosphere]

Temperature	No. 1	No. 2	No. 3	No. 4	No. 5	No. 1	No. 2	No. 3
	3-mm wall					2.5-mm wall		1-mm wall
°C.								
25	150,000	0	0	3	0	[1] 8	0	0
400	76,000	0	0	3	0	([1])	0	0
600	58,000	4	1	2	0	([1])	0	0
800	53,000	25	8	9	2	11	0	0
1,000	53,000	41	55	25	19	170	10	5
1,200	53,000	190	230	310	200	570	47	24
1,300	53,000	720	330	1,100	820	1,000	380	420

[1] Tube cracked while cooling down.

TABLE 4.—*Passage of air through miscellaneous tubes*

[Amount of air passing through wall, expressed in units of 10^{-6} cm³/hr.-cm² reduced to room temperature and standard atmospheric pressure. Pressure difference one atmosphere]

Temperature	Unglazed porcelain	Glazed porcelain					Fused silica		Pyrex glass
	Manufacturer D[1]	Manufacturer E[2]		Manufacturer F[3]	Manufacturer G[1]				
		No. 1	No. 2		No. 1	No. 2	No. 1	No. 2	
	2-mm wall	4-mm wall		1.5-mm wall	2-mm wall		1-mm wall		1-mm wall
° C.									
25		0		0	25,000	3,800	3	0	0
400				0		1,500	3	0	0
500									0
600	31		2	0		850	4	0	
800			7	6		690	28	0	
1,000	34	53	22	49	2,000	560	36	10	
1,200			67			560	120	140	
1,300	(3)	(4)	[4] 210	(5)	(3)		(3)		

[1] These tubes are not being manufactured at present.
[2] These tubes were manufactured in Germany. The tube headed by manufacturer F was purchased previous to 1914.
[3] Tubes collapsed at 1,400° C.
[4] Glaze stuck to furnace wall and opened holes in tubes.
[5] Soft glaze.

All of the following tubes leaked too rapidly for measurement in the vacuum system. The leakage was observed by subjecting the tubes to air pressure and immersing them in water.

1. Two unglazed porcelain tubes with 1-mm walls and one glazed porcelain tube with a 3-mm wall obtained from manufacturer D. Incidentally these tubes are no longer being manufactured.
2. Two unglazed tubes with 3-mm walls obtained from an American, manufacturer H.
3. Two alundum tubes with 2.5-mm walls.

TABLE 5.—*Passage of air through nickel-chromium tubes (cast)*

[Amount of air passing through wall, expressed in units of 10^{-6} cm³/hr.-cm² reduced to room temperature and standard atmospheric pressure. Pressure difference one atmosphere]

Temperature	Manufacturer J			Manufacturer K		
	No. 1	No. 2	No. 3	No. 1	No. 2	No. 3
	5-mm wall	4-mm wall	5-mm wall	6-mm wall		
° C.						
25	1,200	1	1		1	1
400	1,200	37	30		11	15
600	1,200	62	110		45	30
800	1,400	330	330	170	110	67
1,000	6,300	3,300	1,700	1,500	770	6,000

NOTE.—Samples of these tubes collapsed at 1,200° C.

TABLE 6.—*Passage of air through miscellaneous metal tubes*

[Amount of air passing through wall, expressed in units of 10^{-6} cm³/hr.-cm² reduced to room temperature and standard atmospheric pressure. Pressure difference, 1 atmosphere]

Temperature (°C.)	Ni-Mn (cast), 6-mm wall	Ni-Fe (cast), 4.5-mm wall	Cr-Fe (drilled from solid stock), 6-mm wall	Cr-Fe (rolled and welded), 2-mm wall	Cr-Steel (drilled from solid stock), 5-mm wall	Extra heavy seamless steel, 6-mm wall	Cr-plated seamless steel, 3-mm wall	Calorized wrought iron, 3.5-mm wall	Ni-Cr [1] welded to iron, 5-mm wall
25	110,000	13,000	3	5,500	4	2,000	12	8	230,000
400	55,000	12,000	36	1,800	9	2,400	37	11	170,000
600	37,000	10,000	750	1,700	37	3,200	490	52	150,000
800	33,000	9,100	3,600	2,500	99	54,000	11,000	130	130,000
1,000	55,000	12,000	58,000	21,000	3,700	760,000	37,000	210	180,000

[1] This tube leaked through pinholes in the Ni-Cr. Another tube was tested, but leaked through pinhole in the weld.

Measurements show that if the pressure of the system was 0.001 mm of Hg with the pump operating steadily then the leakage of gas into the system was approximately 0.12 cm³/hr. (reduced to room temperature and atmospheric pressure). Since the mean area of a tube in the furnace was approximately 150 cm², this corresponds to a leak of about 800×10^{-6} cm³/hr.-cm². The pressure in the system with the pump operating was less than 0.001 mm of Hg for most of the refractory porcelain tubes at 1,300° C.

For those tubes which leaked less than 400×10^{-6} cm³/hr.-cm² at 1,300° C., the pressure in the system with the pump operating steadily and the tube at 1,400° C. was usually less than 0.001 mm of Hg. A few measurements made on some of the tubes indicated that the leak was approximately twice as much at 1,400° as at 1,300° C.

IV. DISCUSSION OF RESULTS

A study of the data reveals that tubes which leak less than 500×10^{-6} cm³/hr.-cm² at 1,300° C. for a pressure difference of 1 atmosphere, may be obtained from several sources. Experience with such tubes in a reducing atmosphere indicates that they are sufficiently gas tight for use as primary pyrometer protection tubes. Experience also indicates that the use of tubes which leak badly may result in contamination of thermocouples, especially under adverse conditions. In the absence of a contaminating atmosphere, gas tightness may be of little importance. It seems reasonable to require tubes which do not leak more than about 500×10^{-6} cm³/hr.-cm² at 1,300° C. since, in general, the American-made refractory porcelain tubes which were gas tight at room temperature meet this requirement.

Research workers desiring to maintain an evacuated space at high temperatures may be guided in their requirements by the degree of vacuum desired and by the limitations of the materials as indicated by measurements. As the tubes tested in this investigation were presumably not selected, it is entirely possible that better performance would be obtained with selected tubes.

Theoretical analysis of the passage of air through solids at high temperatures is extremely difficult because of our lack of knowledge of the structure of solids. The structure of porcelain is indeed complex and indefinite. In general, porcelain may be regarded as a translucent body composed essentially of mullite ($3Al_2O_3 \cdot 2SiO_2$)

crystals in a glass matrix and often containing undissolved quartz and clay. Little is known regarding the properties of the glass matrix. The relative amounts of mullite, glass, quartz, and clay will depend upon a great many factors, such as the composition of raw materials, amount and kind of flux used, firing temperature, etc.

The physical processes by which air may pass through such solids may be divided into three general classes, namely, (1) viscous flow through pinholes (holes which are large in diameter compared to the mean free path of the gas molecules), (2) molecular flow through very fine capillaries or interstices, and (3) diffusion of dissolved gases through the solid.

If a tube leaks through one or more pinholes (defined as above), the volume of gas flowing through the holes, according to the kinetic theory is inversely proportional to the viscosity (assuming constant dimensions of the holes). Since the viscosity of a gas increases with temperature, the flow through such holes should decrease as the temperature increases. Some of the tubes studied in this investigation leaked through pinholes, and it was found in some cases that the quantity of gas leaking into the tubes decreased as the temperature increased up to some point (approximately 800° C.) at which other factors began to play an important part. Calculations show that the mass (or volume reduced to standard conditions) of gas flowing through pinholes should be approximately five times as much at room temperature as at 500° C. However, if the tube has several pinholes in it and some of these holes are in that part of the tube protruding from the furnace, the relation between the leakage and temperature becomes more complicated. Tubes which leak in this way are of no particular interest in this investigation, since such large leaks can be found easily and the tubes discarded.

Tubes may be tested for large pinholes by applying air pressure to the tubes and immersing them in water. The presence of pinholes is indicated by bubbles. It is very important that the air pressure be applied to the tubes before immersion. Tubes on which bubbles formed when tested in this way failed to yield bubbles when immersed before the application of the air pressure. The pressure used with these tubes was evidently not sufficient to force the adsorbed water from the holes or pores. Leaks as small as 10 cm^3/hr., due probably to two or three pin holes,were detected by applying air pressure of 15 lbs./$in.^2$ and then immersing in water, but in other cases of leaks of this magnitude, due probably to a very large number of smaller holes, could not be detected in this manner.

If a tube leaks, through very fine capillaries or interstices (which are small in comparison with the mean free path of the gas molecules) then according to the kinetic theory, the volume of a gas passing through the tube by this means, should be directly proportional to the square root of the absolute temperature. In this case, calculations show that the mass (or volume reduced to standard conditions) of gas passing through the tube wall should be approximately 1.6 times as much at room temperature as at 500° C. In the case of a few tubes, there is no doubt that these processes were the governing ones for temperatures up to 800° or 1,000° C., but at higher temperatures all the experimental data indicate an increase in the rate of flow of air with temperature.

In the two processes just discussed it is assumed that the dimensions of the holes are constant. Changes in the dimensions of the

holes by thermal expansion of the material would normally be expected to cause relatively small changes in the rate of flow.

Since both of these processes would be expected to give a relationship between leakage and temperature very different from that observed, it is interesting to consider the third process suggested at the beginning of this discussion, the diffusion of dissolved gases through the solid. From what little we know of such processes, their rapidity appears to bear some such relationship to temperature as is needed to explain the observed phenomenon.

We might expect solution and diffusion to take place at about the same rate in different tubes of the same general composition and to find much more rapid diffusion through a thin walled tube than a thick walled one. This may be true only if the tubes have received approximately the same mechanical and thermal treatments during manufacture. If we compare tubes 7, 8, and 9 of manufacturer A, which so far as we know are made of essentially the same materials, and all of which show about the same relative relationship between temperature and the rate at which gas appeared in the tubes, we find that the 3.5-mm tubes showed about six times the apparent permeability of the 1 mm tube instead of a third or a fourth of the permeability as might have been expected. There is no assurance, however, that the thin and thick walled tubes had received the same mechanical and thermal treatments. In fact, microscopic examination showed differences in the structure of the material in these two types of tubes and it is therefore possible that the large difference in the rates of apparent diffusion may be due to some differences associated with the body structures.

Similarly, the permeability of three nickel-chromium tubes of the same wall thickness from manufacturer K, all of which showed similar increases in apparent permeability with increasing temperature varied from 770 to $6{,}000 \times 10^{-6}$ cm^3/hr.-cm.^{2} at 1,000° C. Such results with materials of similar, if not identical chemical composition, are possibly caused by differences in constitution dependent on variations in mechanical and thermal treatments.

It is, of course, possible that the gas collected in the case of the tubes which showed these very high temperature coefficients did not come through the tubes at all, but was originally adsorbed on the walls or in the pores of the material or came from the decomposition of some constituent of the complex solid. Time did not permit the verification of any one of these several possible hypotheses as to the origin and method of transmission of the gas collected.

Either the driving off of adsorved gases of the decomposition of dissolved carbides, oxides, sulphides, etc., might be expected to have some such relationship to temperature as was observed. The fact that repeated long evacuation at high temperatures did not, within the limit of measurement, decrease the rate at which gas was collected, may be taken as evidence indicative that the gas came from outside the tube.

If porcelain and silica tubes are free from holes they may be used as protection tubes for platinum couples in a reducing atmosphere for a considerable time without detrimental contamination of the couple. The reducing gas will reduce the silica at the outer surface of the tube leaving a coating of silicon which is of no consequence until the action has proceeded far enough into the tube to reach pores communicating with the interior. In the case of a very porous

porcelain body glazed on the outside, the period of effectiveness of the protection may be comparatively short in an extremely reducing atmosphere.

V. SUMMARY

The results of the measurements of the rate of passage of air through 36 tubes of refractory porcelain, both glazed and unglazed, (11 different classes) 2 of fused silica, 1 of pyrex glass, 2 of alundum, and 15 of metal are given for various temperatures which the tubes would withstand without noticeable deformation. The tests indicate that the very refractory porcelain tubes (often referred to as sillimanite or mullite) are decidedly superior to the older porcelain tubes, both in refractoriness and gas tightness.

The results indicate that tubes of calorized wrought iron are more gas tight than those of other metals at the higher temperatures. Nickel-chromium tubes, in general, were more gas tight than those of other alloys.

The tests also showed that it was possible to maintain pressures of less than 0.001 mm of Hg in a refractory porcelain tube at 1,400° C. by the use of an ordinary laboratory type mercury vapor pump.

Methods of testing are described and a very brief discussion given of the processes by which air may pass through the tube walls.

No attempt has been made to correlate the data reported in this paper with data obtained by other observers, since measurements have not been made under similar conditions. Most of the data reported have been on the passage of gases through glass, silica, and metals. No data have been found on the passage of air through solids or on the passages of gases through porcelain.

VI. BIBLIOGRAPHY

A selected bibliography is given here for those interested in this subject:

(Richardson and Ditto, Diffusion of Neon through Hot Quartz, Phil. Mag., **22,** p. 704; November, 1911.

Charpy and Bonnerot, Permeability of Iron to Hydrogen, Comptes Rendus, 154, p. 592; Feburary, 1912.

A. Holt, Diffusion of Hydrogen through Palladium, Roy. Soc. Proc., **91,** p. 148; February, 1915.

E. C. Mayer, Leakage of Gases through Quartz Tubes, Phys. Rev., **6,** p. 283; October, 1915.

Edwards and Pickering, Permeability of Rubber to Gases, B. S. Bull. **16,** p. 327; 1920.

E. Cardoso, Diffusion of Hydrogen, Helium, and Neon Through Heated Glass, Accad. Lincei. Atti., **31,** 1, p. 28; 1922.

Schmidt and Lucke, Diffusion of Hydrogen through Iron and Platinum, Zeits. f. Physik, **8,** 3, p. 152; 1922.

Johnson and Burt, Passage of Hydrogen through Quartz Glass, J. Opt. Soc. Amr. **6,** p. 734; 1922.

Deming and Hendricks, The Diffusion of Hydrogen through Metals, J., Am. Chem. Soc., **45,** p. 2857; 1923.

V. Lombard, Permeability of Iron and Platinum to Hydrogen Gas, Compt. Rend., **184,** p. 1557; 1927.

V. Lombard, Permeability of Nickel to Hydrogen Gas. Effect of Thickness of Metal, Compt. Rend., **184,** p. 1327; 1927.

Borelius and Lindblom, Diffusion of Hydrogen through Iron., Ann. d. Physik., **82,** 4, p. 201; 1927.

G. Borelius, Solubility and Diffusion of Hydrogen in Metals, Ann. d. Physik, **83,** 4, p. 121; 1927.

W. E. Deming, Diffusion of Hydrogen through Iron, Phil. Mag., **5,** p. 1081; 1928.

WASHINGTON, May 20, 1931.

RP 354

AN EXPERIMENTAL STUDY OF SEVERAL METHODS OF REPRESENTING PHOTOGRAPHIC SENSITIVITY

By Raymond Davis and Gerald Kent Neeland

ABSTRACT

The relation between photographic sensitivity and the amount of development has been studied using as indices of sensitivity three modifications of Hurter and Driffield's method of measuring plate speeds. The results are generally in accord with those of Bullock, who investigated the relation of threshold speed to development time. An optimum time of development is indicated which varies with the type of emulsion considered.

The study brought out the differences between the three indices considered and led to the conclusion that no single value is adequate to represent the sensitivity of a given emulsion. It is more satisfactory to represent the sensitivity of an emulsion in terms of a curve plotted between a sensitivity index and development time.

CONTENTS

	Page
I. Introduction	495
II. Methods of measuring sensitivity	496
III. Experimental results	498
IV. Discussion of results	509
1. Characteristics of the three methods	509
2. Method of expressing relative sensitivity	514
3. Summary	517

I. INTRODUCTION

Several ways of measuring the sensitivity of photographic emulsions have been proposed from time to time. At first sensitivity or "speed" was taken as inversely proportional to the exposure required to produce (on development) a just perceptible image. This has been called threshold speed. The difficulty in specifying accurately a "just perceptible" density discouraged the use of the method, although modifications are still employed to some extent.

In 1890 Hurter and Driffield began their series of papers describing a new system of representing characteristics of photographic plates. The basis of this system was a "characteristic curve" representing density as a function of log exposure. The exposure value of the intersection of an extension of the straight line portion of this curve with the base line was called the "inertia" of the plate. The "speed" of the plate was taken as proportional to the reciprocal of the inertia.

They found that (in the absence of soluble bromides) these plate speeds were constant for a given plate regardless of the time of development. In other words, extensions of the straight line portions of the characteristic curves met at a point on the exposure axis. In the work at this laboratory during the past 20 years an emulsion has rarely been found giving a family of curves such that extensions of the straight line portions met at a point on the exposure axis.

Neitz,[1] in 1920, after an extended study, found that the extensions of the straight line portions of characteristic curves, plotted on a basis of total densities (instead of the total density minus fog density basis used by Hurter and Driffield), for several times of development, intersected at a point. The location of this point was on or below the axis, depending on the plate and developer used.

More recently, others have been unable to find a common intersection point for extensions of the straight line portions of a family of characteristic curves either when plotted on a total density or a total density minus fog density basis. This discrepancy between the results of Hurter and Driffield and those of later workers is thought to be due to changes in the methods of manufacturing emulsions.

Bullock [2] investigated the relation between threshold speed (using a Chapman Jones plate tester) and development time. He obtained curves indicating an optimum time of development.

The present paper gives the results of an experimental investigation of the characteristics of several types of emulsions undertaken to determine the relative merits of three modifications of Hurter and Driffield's method of expressing sensitivity and to observe the influence of the amount of development on sensitivity.

II. METHODS OF MEASURING SENSITIVITY

As previously stated, Hurter and Driffield [3] took as a measure of sensitivity a quantity proportional to the reciprocal of the inertia i. Inertia was defined as the exposure value of the intersection of an extension of the straight line portion of the characteristic curve with the base line. They considered density to be the difference between the total density of the deposit and that density due to glass, gelatin, and fog (here termed fog density). This is equivalent to plotting total density against log exposure and taking inertia as the exposure value of the intersection of an extension of the straight line portion of the characteristic curve with a horizontal line representing the fog density on an unexposed portion of the same sample.

For an emulsion having a straight line characteristic over the exposure range under consideration this is a very satisfactory method of expressing sensitivity because it is possible to calculate the density for any exposure within this range from the following relation:

$$D = \gamma (\log E - \log i)$$

where

D = total density minus fog density;
γ = slope of straight line portion;
E = exposure;

and

i = inertia.

Unfortunately, emulsions in present use give characteristic curves which seldom possess a central straight portion. It is necessary, therefore, to adopt some other method in these cases.

---

[1] A. H. Neitz, The Theory of Development, Monographs on the Theory of Photography No. 2 from the Research Laboratory of the Eastman Kodak Co.

[2] E. R. Bullock, On Variations in Threshold Speed According to the Developer and Conditions of Development, I and II, Comm. No. 268, Abridged Scientific Publications, Research Laboratory, Eastman Kodak Co., p. 144; 1926.

[3] F. Hurter and V. C. Driffield, The Hurter and Driffield System, The Hurter and Driffield Memorial Volume, p. 300.

The three different methods of deriving a sensitivity index from the characteristic curve which were considered in the present study are illustrated in Figure 1.

The first method substitutes for the extension of the straight-line portion the tangent to the curve at the point of maximum gradient (G (max.)). The intersection of this tangent with a horizontal line representing the fog density is designated as ι (iota). The sensitivity index on this basis is $10/\iota$ as shown in the third column of Tables 2 to 6, inclusive. It should be pointed out that the density for a given exposure value can be calculated from either ι or i only over the straight portion of the characteristic curve.

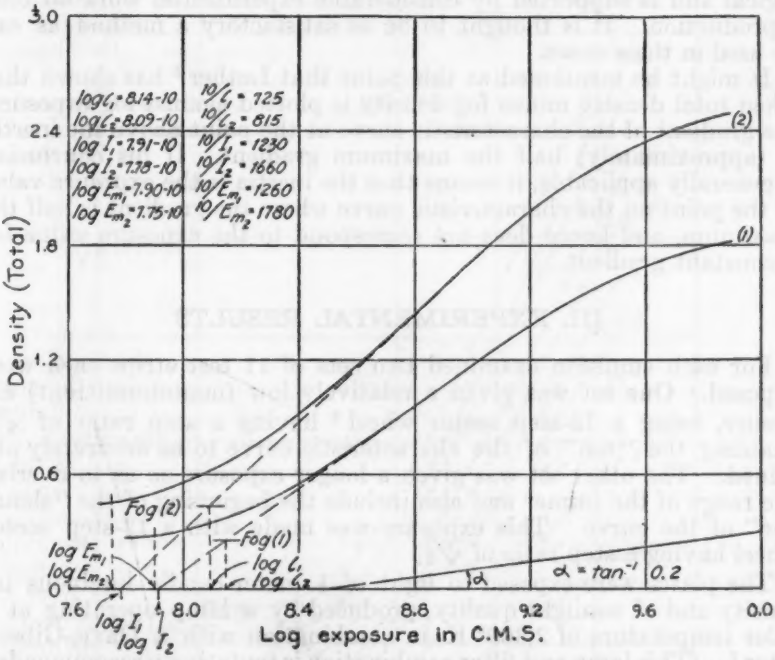

FIGURE 1.—*Illustrating the methods of obtaining the three indices of sensitivity from each of two characteristic curves*

A method of deriving an index of sensitivity from the characteristic curve which has been frequently used is similar to H. & D.'s, except, that sensitivity is taken as proportional to the exposure value of the point of intersection of an extension of the straight line portion of the characteristic curve with the zero density axis, on a total density log exposure diagram. This point is sometimes erroneously called the inertia. In the second method used in the present work a quantity, I, is defined as the exposure value of the intersection of the tangent to the characteristic curve at the point of maximum gradient with the zero density line. The sensitivity index on this basis is $10/I$.

It should be noted that ι will be equal to i; and I will be equal to this erroneous inertia when the characteristic curve has a central straight portion.

The third method of gaging sensitivity studied here is that of Jones and Russell,[4] who take speed as proportional to the reciprocal of a quantity E_m which is defined as the exposure corresponding to the point in the "toe" region of the characteristic curve where the gradient is 0.20.

When the characteristic curves are not straight for an appreciable length, or especially when one is dealing with a range of exposures which more than covers the straight line portion (which often occurs in practical photography), the expression of sensitivity in terms of inertia is obviously unsatisfactory. These cases demand some other method. The system proposed by Jones and Russell seems logical and is supported by considerable experimental work on tone reproduction. It is thought to be as satisfactory a method as can be used in these cases.

It might be mentioned at this point that Luther[5] has shown that when total density minus fog density is plotted against log exposure, the gradient of the characteristic curve at the point above the inertia is (approximately) half the maximum gradient. If his conclusion is generally applicable, it means that the inertia is the exposure value of the point on the characteristic curve where the gradient is half the maximum, and hence does not correspond to the exposure value for a constant gradient.

III. EXPERIMENTAL RESULTS

For each emulsion examined two sets of 11 test strips each were exposed. One set was given a relatively low (nonintermittent) exposure, using a 13-step sector wheel[6] having a step ratio of $\sqrt{2}$, enabling the "toe" of the characteristic curve to be accurately obtained. The other set was given a longer exposure so as to overlap the range of the former and also include the beginning of the "shoulder" of the curve. This exposure was made with a 13-step sector wheel having a step ratio of $\sqrt[3]{4}$.

The plates were exposed to light of 1 meter-candle luminous intensity and of sunlight quality, produced by a lamp operating at a color temperature of 2,360° K. in combination with a Davis-Gibson filter.[7] (This lamp and filter combination is tentatively recommended as standard by the Seventh International Congress of Photography for use in the sensitometry of negative materials.)

In accordance with customary practice in sensitometric work at this laboratory, the plates were backed, previous to exposure, with a black shellac mixture in order to prevent halation.

The 11 exposed test strips were placed together in a single tray of developer at 20° C. The strips were removed one at a time at intervals giving development times from 1 to 22 minutes. This more than covered the usual range of development times. Agitation of the developer was secured by brushing the plates with a camels-

[4] L. A. Jones and M. E. Russell, The Expression of Plate Speed in Terms of Minimum Useful Gradient, Proc. Seventh Intern. Cong. Photography, p. 130.

[5] R. Luther, The Under-exposure Period of the Characteristic Curve, Trans. Far. Soc., 19, p. 340; 1923.

[6] For details of the sensitometer used, see, Raymond Davis, A Nonintermittent Sensitometer, B. S. Sci. Papers, No. 511.

[7] Raymond Davis and K. S. Gibson, Filters for the Reproduction of Sunlight and Daylight and the Determination of Color Temperature, B. S. Miscellaneous Publication No. 114.

hair brush. A. B. C. pyro developer was used according to the following formula:

(A)	Water	cc	1,000
	Potassium metabisulphite	g	12
	Pyro	do	60
(B)	Water	cc	1,000
	Sodium sulphite (anhydrous)	g	90
(C)	Water	cc	1,000
	Sodium carbonate (anhydrous)	g	75

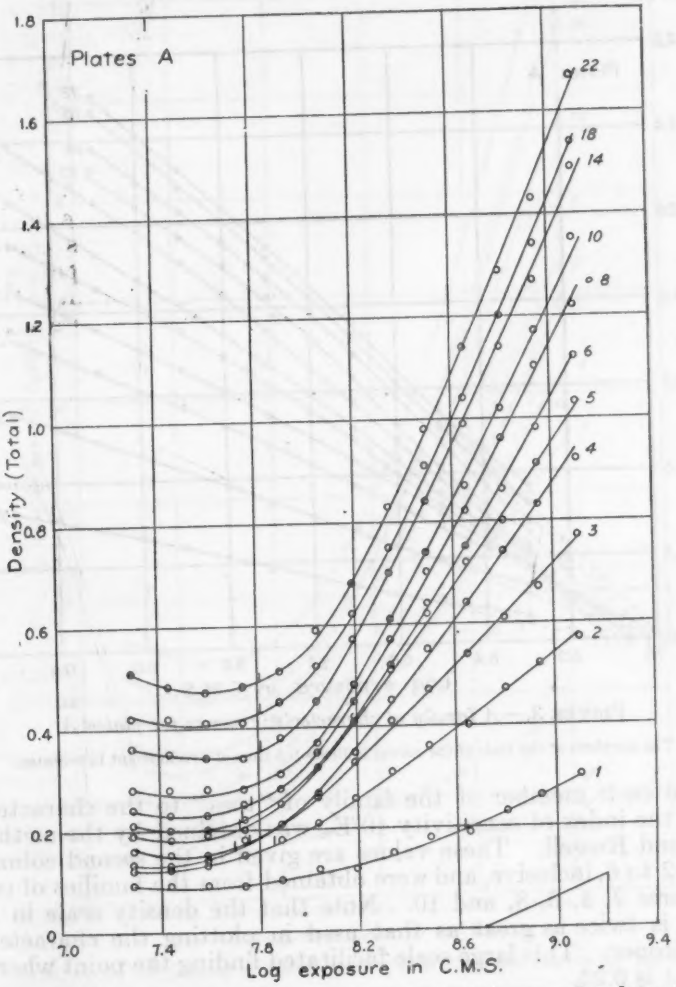

FIGURE 2.—*A family of "toes" to the characteristic curves for plates A*

The numbers at the ends of the curves indicate the time of development in minutes.

To develop, 1 part each of A, B, and C was mixed with 7 parts of water.

Throughout the paper, values of total density are given as read on a Martens polarization photometer [8] with diffuse illumination. For densities over 1.5 a supplementary density was employed, as is usual, in order to minimize the effect of stray light in the instrument.

Families of characteristic curves obtained for each of the five plates A, B, C, D, and E are given in Figures 3, 5, 7, 9, and 11, respectively. The values of $10/\iota$ and $10/I$ obtained from the corresponding curves are given in the third and fourth columns of Tables 2 to 6, inclusive.

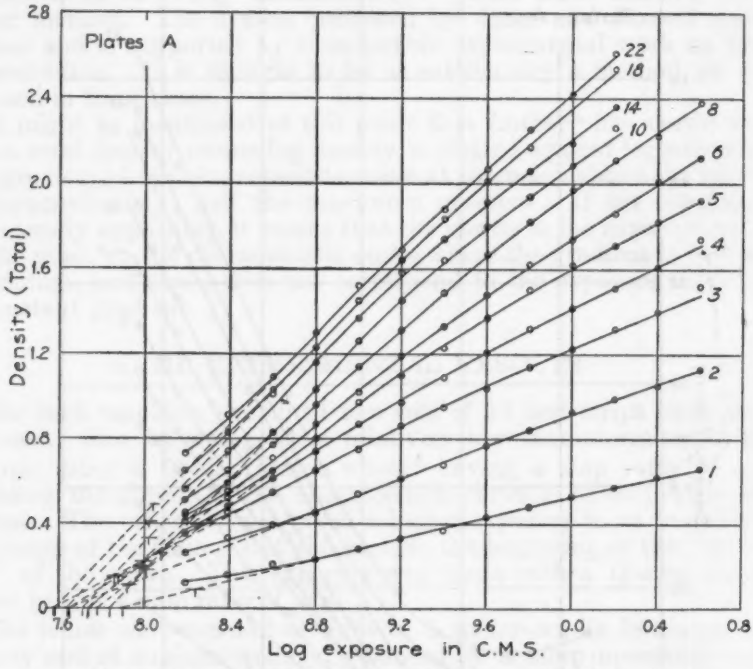

FIGURE 3.—*A family of characteristic curves for plates A*

The numbers at the ends of the curves indicate the time of development in minutes.

From each member of the family of "toes" to the characteristic curves the index of sensitivity $10/E_m$ was obtained by the method of Jones and Russell. These values are given in the second column of Tables 2 to 6, inclusive, and were obtained from the families of curves in Figures 2, 4, 6, 8, and 10. Note that the density scale in these figures is twice as great as that used in plotting the characteristic curve proper. This large scale facilitated finding the point where the gradient is 0.20.

It should be pointed out in connection with the characteristic curves (and the "toes"), that the data were plotted as obtained without smoothing. In all cases curves were drawn through the points without anticipating straight line portions. In one or two cases noted in the tables, defective or irregularly developed test strips were en-

[8] Raymond Davis and F. M. Walters, jr., Sensitometry of Photographic Emulsions and a Survey of the Characteristics of Plates and Films of American Manufacture, B. S. Sci. Papers No. 439, p. 22.

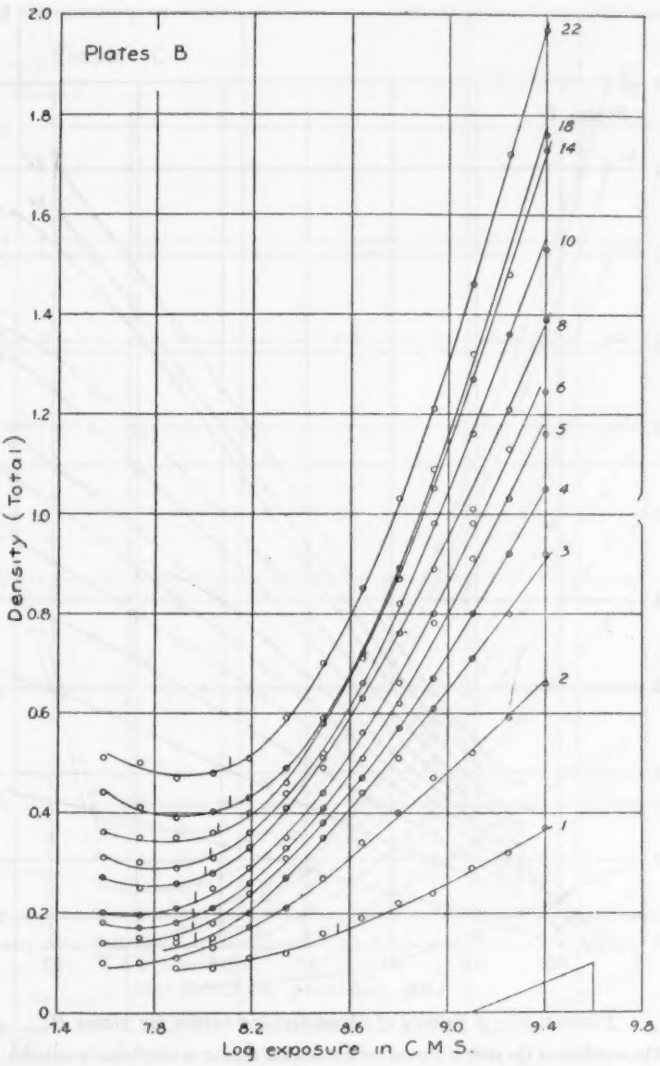

FIGURE 4.—*A family of "toes" to the characteristic curves for plates B*

The numbers at the ends of the curves indicate the time of development in minutes.

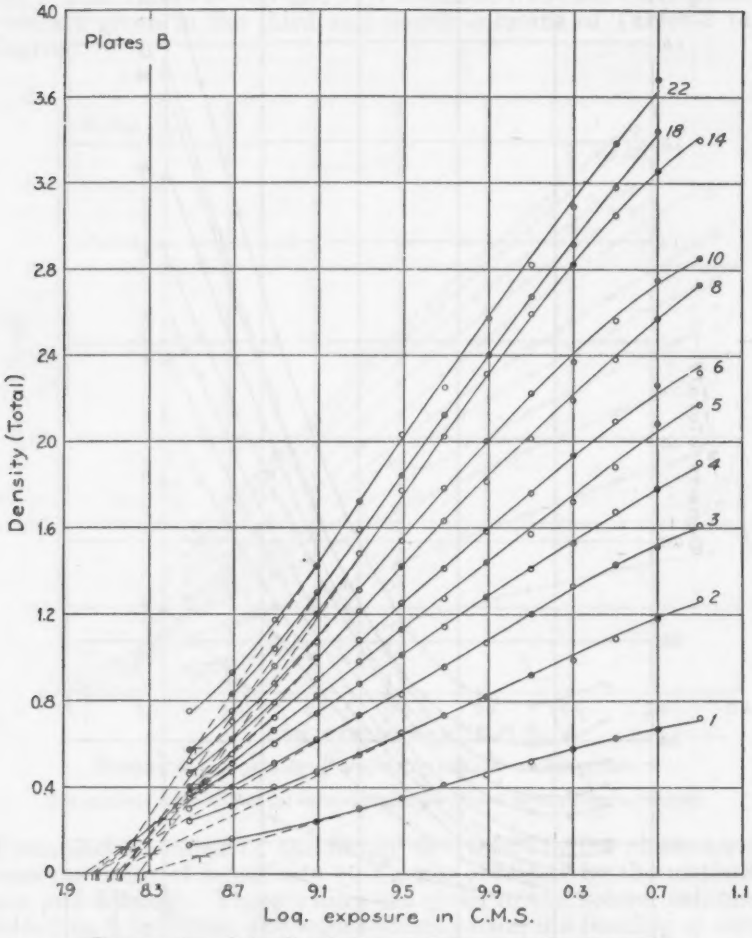

FIGURE 5.—*A family of characteristic curves for plates B*

The numbers at the ends of the curves indicate the time of development in minutes.

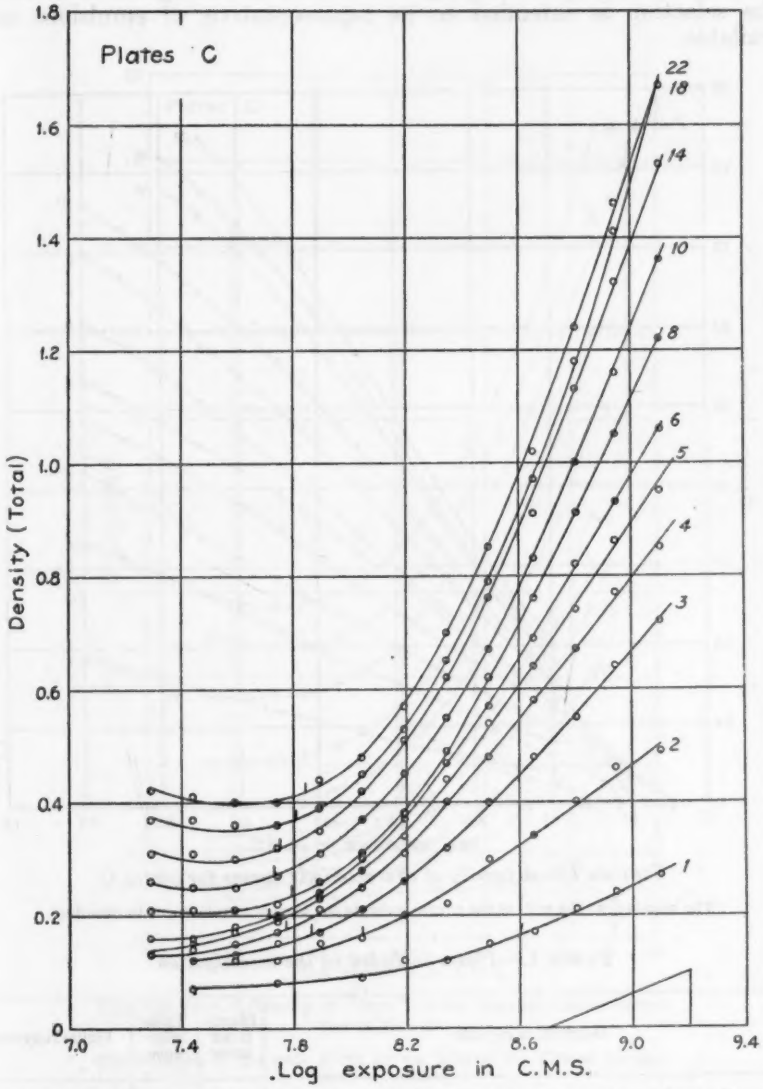

FIGURE 6.—*A family of "toes" to the characteristic curves for plates C*

The numbers at the ends of the curves indicate the time of development in minutes.

countered. However, these cases do not influence the corresponding sensitivity, development time curves appreciably.

In Table 1 are listed the plates included in this study, the types of emulsions, and the identifying letters used in the figures and tables. The selection is intended to be representative of emulsions now available.

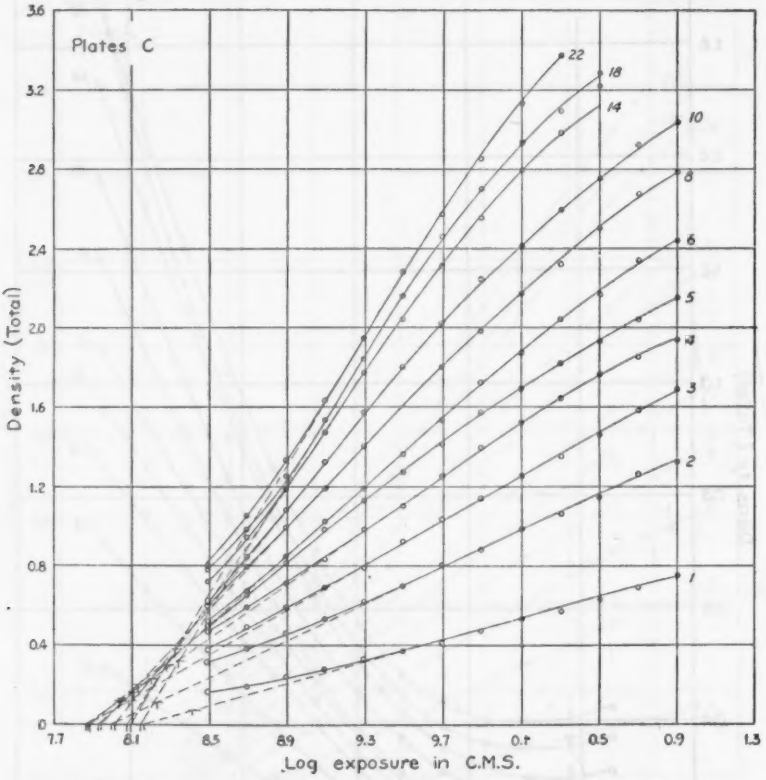

FIGURE 7.—*A family of characteristic curves for plates C*

The numbers at the ends of the curves indicate the time of development in minutes.

TABLE 1.—*Plates included in the investigation*

Description of plate	Identifying letter	Table reference	Figure reference
American "speed" orthochromatic	A	2	2, 3, 12, 17.
American "medium speed" ordinary	B	3, 7	4, 5, 13, 17, 18, 19.
German "speed" orthochromatic	C	4	6, 7, 14, 17.
English "speed" panchromatic	D	5	8, 9, 15, 17.
American "process" ordinary	E	6	10, 11, 16.

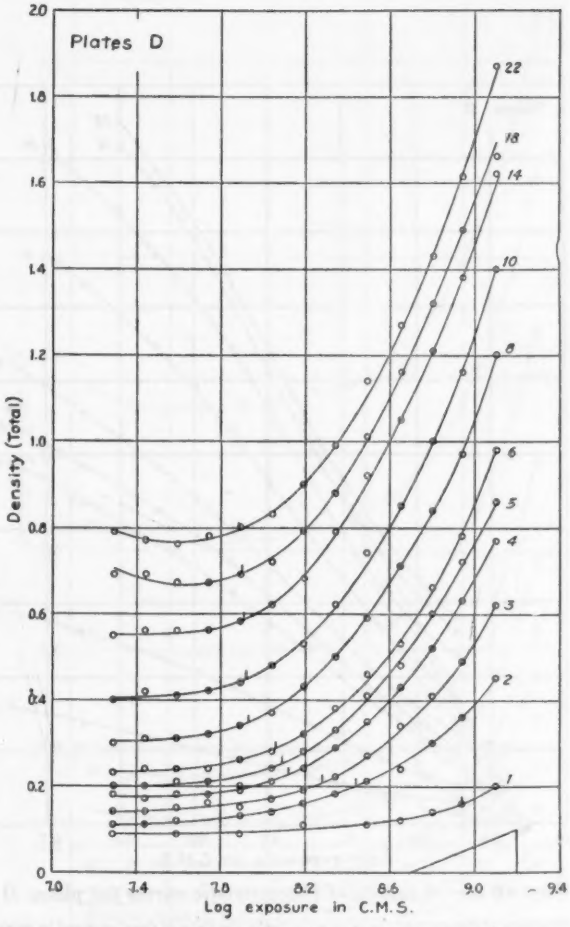

FIGURE 8.—*A family of "toes" to the characteristic curves for plates D*

The numbers at the ends of the curves indicate the time of development in minutes.

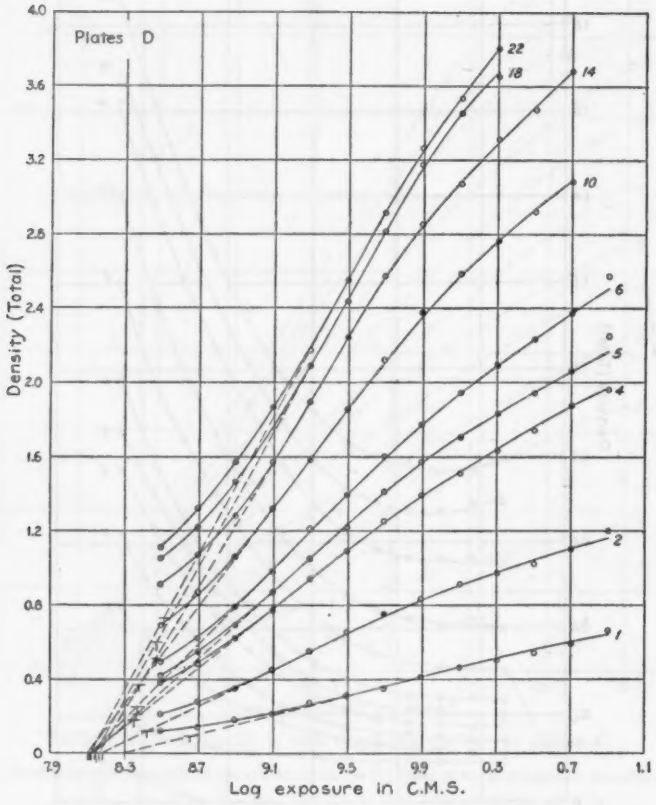

FIGURE 9.—*A family of characteristic curves for plates D*

The numbers at the ends of the curves indicate the time of development in minutes.

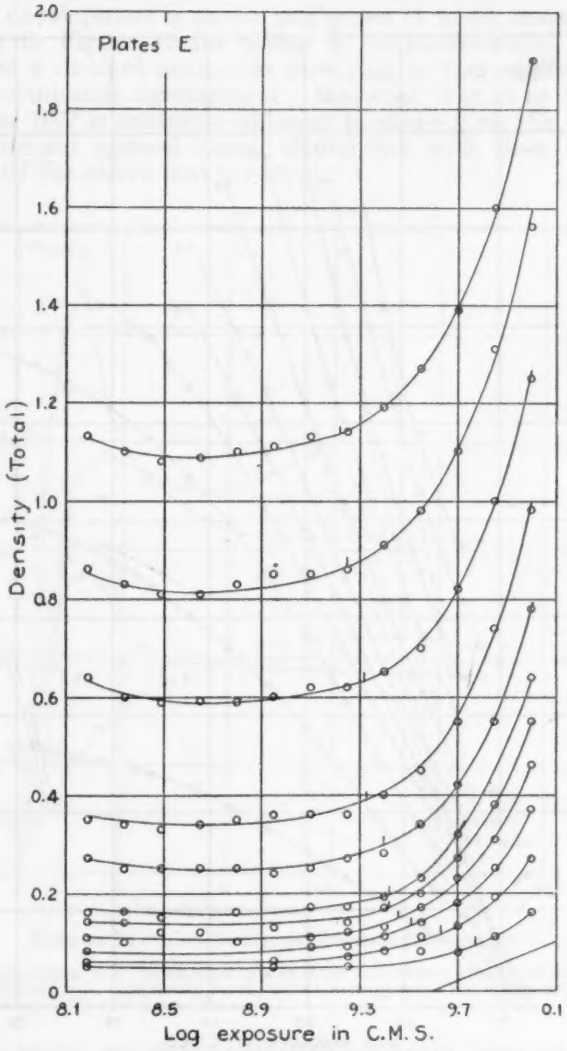

FIGURE 10.—*A family of "toes" to the characteristic curves for plates E*

The numbers at the ends of the curves indicate the time of development in minutes.

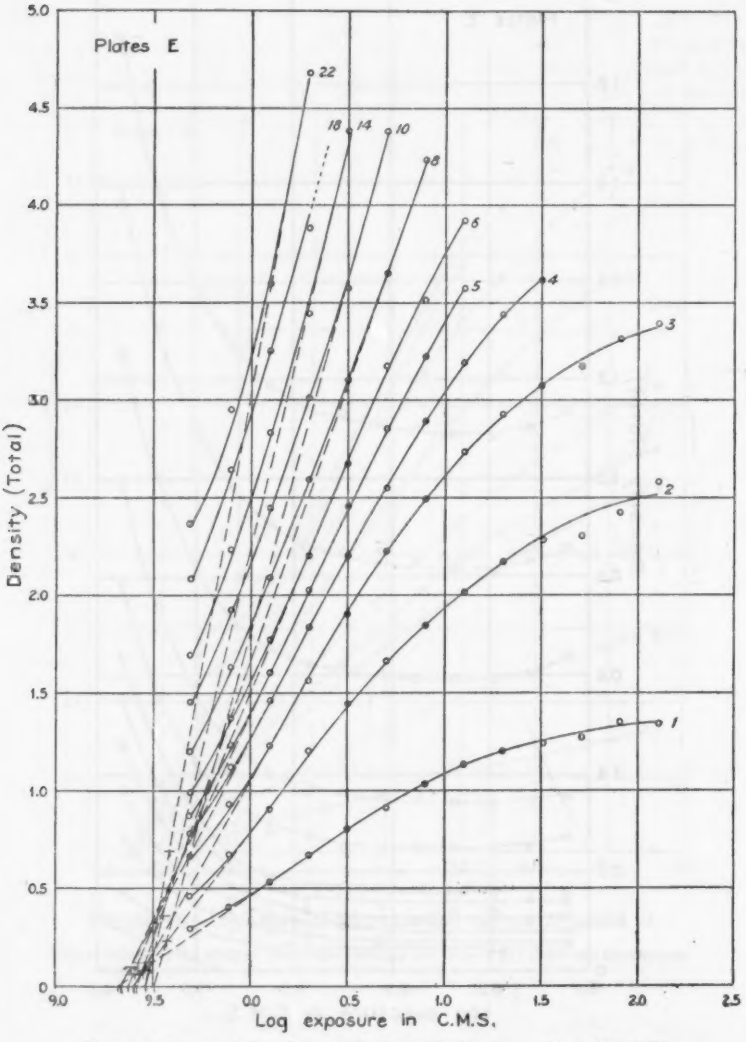

FIGURE 11.—*A family of characteristic curves for plates E*

The numbers at the ends of the curves indicate the time of development in minutes.

IV. DISCUSSION OF RESULTS

1. CHARACTERISTICS OF THE THREE METHODS

How the sensitivity as measured by the three methods varies with the time of development is shown in Figures 12 to 16, respectively.

Referring to Figure 12 for plates A (orthochromatic), all three indices show a distinct maximum occurring in the neighborhood of three to four minutes development. However, it is to be noted that the curve for $10/I$ is distinctly different in shape from the other two, showing a second upward trend. Note that with these plates the curve for $10/I$ lies above that for $10/E_m$.

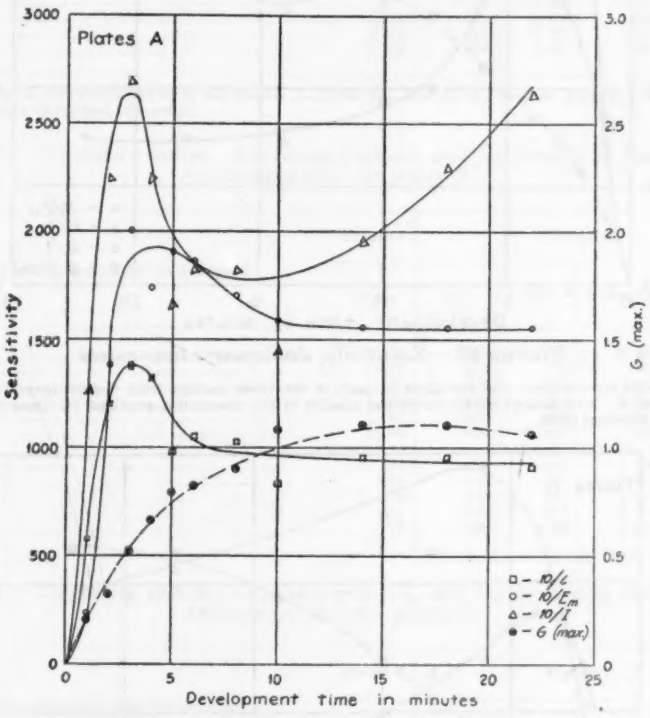

FIGURE 12.—*Sensitivity, development time curves*

The solid curves show the variation in each of the three indices with development time for plates A. The dashed curve shows the change in the maximum gradient (G (max.)) with development time.

In Figure 13 for plates B (ordinary) we again have all indices a maximum at about three to four minutes development. As before, the curve for $10/I$ is different in shape from the other two.

In Figure 14, plates C (orthochromatic), similar results were obtained. The curve for $10/I$ is less different from the other two, but the beginning of a second upward trend is indicated at about 18 minutes development.

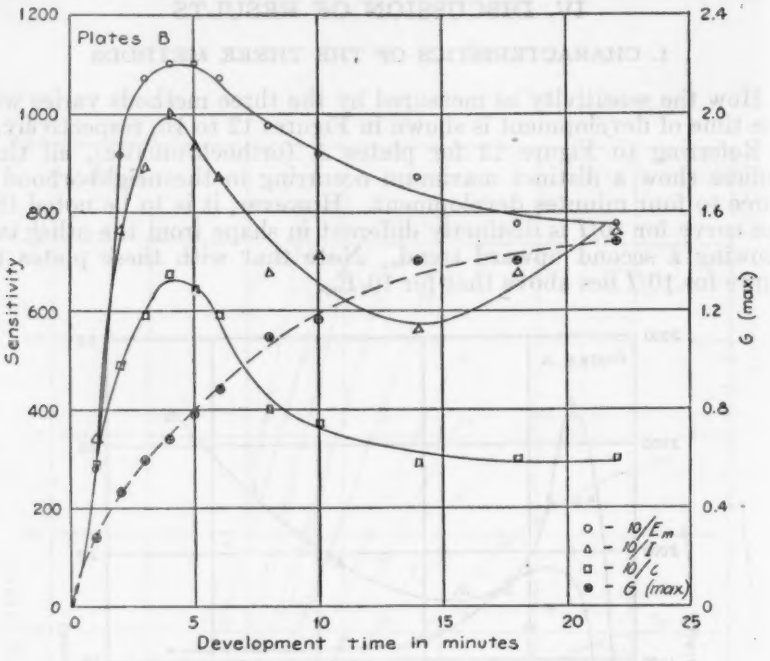

FIGURE 13.—*Sensitivity, development time curves*

The solid curves show the variation in each of the three indices with development time for plates B. The dashed curve shows the change in the maximum gradient (G (max.)) with development time.

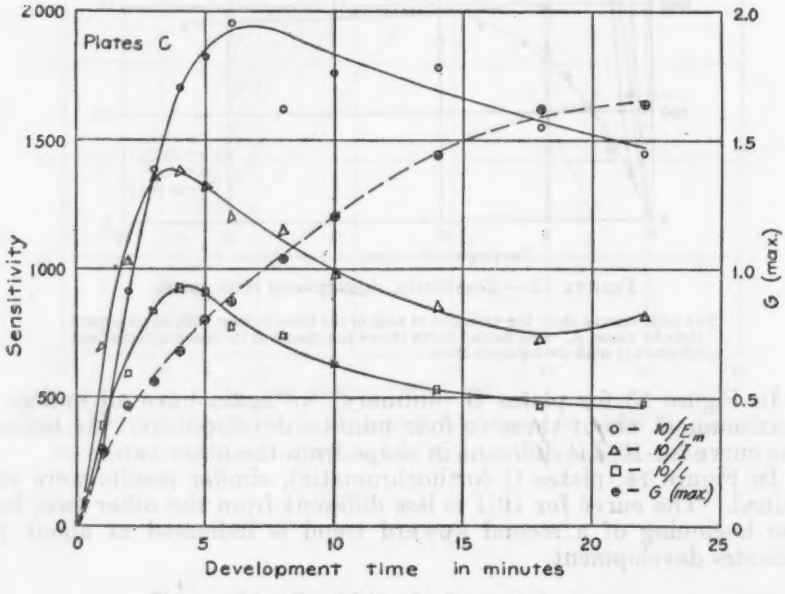

FIGURE 14.—*Sensitivity, development time curves*

The solid curves show the variation in each of the three indices with development time for plates C. The dashed curve shows the change in the maximum gradient (G (max.)) with development time.

TABLE 2.—*Sensitivity indices, maximum gradient, and fog density as functions of development time for plates A*

Development time (in minutes)	Figure 2	Figure 3			
	$10/E_m$	$10/\iota$	$10/I$	G (max.)	Fog density [1]
1	235	575	1,260	0.20	0.09
2	1,380	1,200	2,240	.32	.11
3	2,000	1,380	2,690	.52	.15
4	1,740	1,320	2,240	.66	.15
5	1,900	[2] 980	[3] 1,660	[3] .79	[3] .18
6	1,860	1,050	1,820	.82	.20
8	1,700	1,025	1,820	.90	.22
10	1,585	[2] 830	[3] 1,445	[3] 1.08	[3] .26
14	1,550	955	1,950	1.10	.33
18	1,550	955	2,290	1.10	.41
22	1,550	910	2,630	1.06	.49

[1] Throughout this paper the term fog density includes that density due to glass, gelatin, and fog.
[2] Irregularly developed test strips.

TABLE 3.—*Sensitivity indices, maximum gradient, and fog density as functions of development time for plates B*

Development time (in minutes)	Figure 4	Figure 5			
	$10/E_m$	$10/\iota$	$10/I$	G (max.)	Fog density
1	280	290	240	0.28	0.08
2	930	490	760	.46	.09
3	1,070	590	890	.59	.11
4	1,095	675	1,000	.68	.12
5	1,095	645	935	.78	.12
6	1,070	590	870	.88	.15
8	975	400	675	1.09	.25
10	935	370	710	1.16	.32
14	870	290	560	1.41	.41
18	775	300	675	1.40	.48
22	775	300	760	1.48	.58

TABLE 4.—*Sensitivity indices, maximum gradient, and fog density as functions of development time for plates C*

Development time (in minutes)	Figure 6	Figure 7			
	$10/E_m$	$10/\iota$	$10/I$	G (max.)	Fog density
1	250	390	690	0.28	0.07
2	910	590	1,025	.46	.11
3	1,380	830	1,350	.56	.12
4	1,700	930	1,380	.68	.12
5	1,820	910	1,320	.80	.13
6	1,950	775	1,200	.87	.16
8	1,620	740	1,150	1.04	.20
10	1,860	630	980	1.20	.23
14	1,780	525	850	1.44	.30
18	1,550	460	725	1.62	.32
22	1,445	480	815	1.64	.38

TABLE 5.—*Sensitivity indices, maximum gradient, and fog density as functions of development time for plates D*

Development time (in minutes)	Figure 8	Figure 9			
	$10/E_m$	$10/i$	$10/I$	G (max.)	Fog density
1	115	225	500	0.26	0.09
2	365	380	660	.49	.12
3	525	[1]	[1]	[1]	[1]
4	760	450	760	.80	.18
5	815	440	725	.90	.21
6	870	425	760	1.02	.25
8	1,175	[1]	[1]	[1]	[1]
10	1,200	425	795	1.34	.37
14	1,230	345	690	1.68	.51
18	1,260	340	725	1.80	.60
22	1,320	310	760	1.84	.73

[1] Defective test strips.

TABLE 6.—*Sensitivity indices, maximum gradient, and fog density as functions of development time for plates E*

Development time (in minutes)	Figure 10	Figure 11			
	$10/E_m$	$10/i$	$10/I$	G (max.)	Fog density
1	17	39	48	0.89	0.06
2	23	36	40	1.32	.07
3	31	36	40	1.76	.08
4	35	42	46	1.91	.09
5	38	41	46	2.12	.10
6	38	38	42	2.40	.12
8	40	35	38	2.84	.12
10	47	27	31	3.66	.25
14	48	28	35	4.14	.36
18	56	[1]	[1]	[1]	.64
22	60	27	35	5.60	.69

[1] Characteristic curve incomplete.

TABLE 7.—*Variation of the sensitivity, development time curve with the value taken as the minimum useful gradient*

[The data was obtained from the curves for plates B in fig. 4]

Development time (in minutes)	Values of $10/E_m$ at the gradients indicated			
	0.10	0.20	0.25	0.30
1	725	280	110	[1]
2	1,585	930	645	515
3	[1]	1,070	870	775
4	1,585	1,095	935	815
5	1,445	1,095	910	830
6	1,515	1,070	935	815
8	1,260	975	870	795
10	1,200	935	850	760
14	1,095	870	775	710
18	975	775	710	660
22	975	775	710	660

[1] Characteristic curve incomplete at this point.

In Figure 15, plates D (panchromatic), the curves for both $10/\iota$ and $10/I$ indicate an early maximum which is not shown by the curve for $10/E_m$. The second upward trend of the $10/I$ curve begins at about 14 minutes development.

In Figure 16, plates E (process), the curves for both $10/\iota$ and $10/I$ again indicate an early maximum sensitivity. Note that the G (max.) curve here does not flatten out as it does with the other plates. As with plate D the curve for $10/E_m$ indicates maximum sensitivity at a time of development in excess of 22 minutes. (Bullock [9] found the threshold speed for a lantern plate to be a maximum at about 40 minutes development, using another developer.)

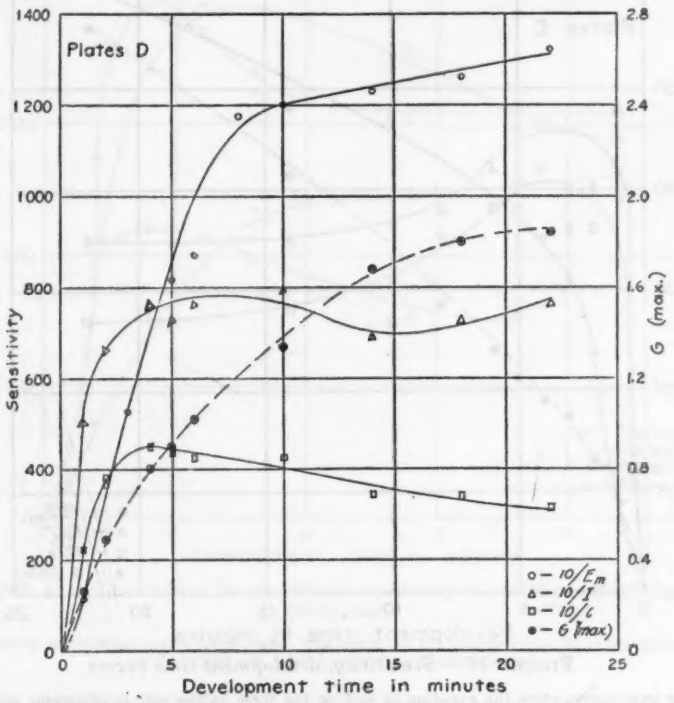

FIGURE 15.—*Sensitivity, development time curves*

The solid curves show the variation in each of the three indices with development time for plates D. The dashed curve shows the change in the maximum gradient (G (max.)) with development time.

With the exception of the panchromatic and process plates it may be said [10] that sensitivity increases rapidly to a maximum and then decreases more or less rapidly with further development.

Figures 12 to 16, inclusive, show that the second upward trend in the $10/I$ curve usually occurs at about the point where the rate of increase of maximum gradient falls off.[11] That is, after this point is

[9] See footnote 2, p. 496.

[10] Other emulsions were tested besides those included in this paper. The results were entirely analagous to those here presented.

[11] On all except the process plate, the rate of growth of fog was practically constant over this range of development times.

reached the maximum gradient line tends to shift parallel to itself, resulting in an increase in the values of $10/I$. That this rise does not necessarily signify an actual increase in sensitivity may be seen from the "hypothetical" case discussed in a note[12] by the authors. In this "hypothetical" case we have two identical characteristic curves, one raised above the other. The straight line portions are, of course, parallel and intersect the zero density line of a total density, log exposure diagram so that the upper curve gives the higher value of $10/I$. It is obvious that the two emulsions represented by these curves should be considered equally sensitive, since if two negatives were made

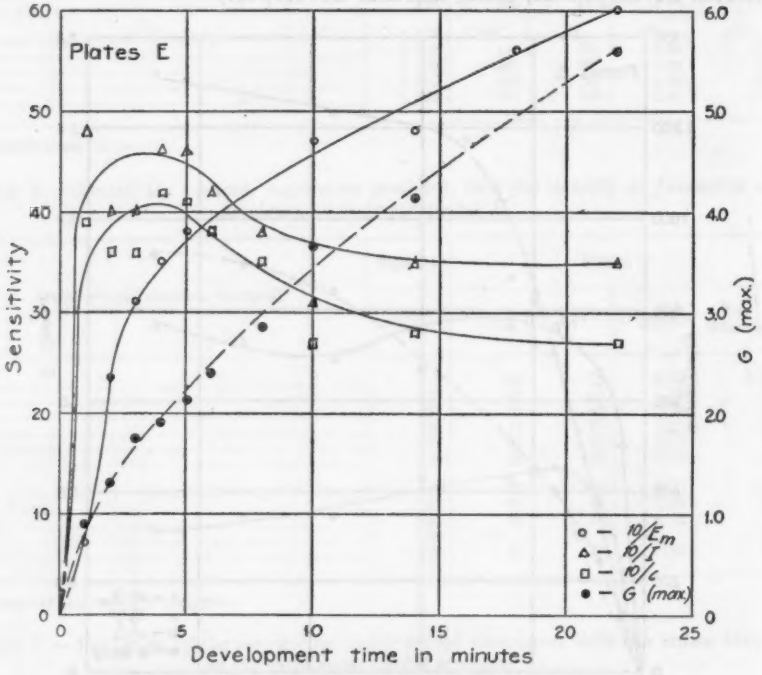

FIGURE 16.—*Sensitivity, development time curves*

The solid curves show the variation in each of the three indices with development time for plates E. The dashed curve shows the change in the maximum gradient (G (max.)) with development time.

under the same conditions, one on each emulsion, they would yield (by proper adjustment of the printing exposure) identical positives. The experimental curves strikingly illustrate this objection to the use of $10/I$.

2. METHOD OF EXPRESSING RELATIVE SENSITIVITY

In Figure 17 the sensitivity, development time curves, are plotted for plates A, B, C, and D, the index of sensitivity used being $10/E_m$. From this figure the superiority of a sensitivity, development time curve as compared with a single quantity is obvious. The sensitivity

[12] Raymond Davis and G. K. Neeland, A Note on the "Speed" of Photographic Emulsions, J. Opt. Soc. Am., July, 1931.

of an emulsion having a comparatively flat (sensitivity, development time) curve can be satisfactorily represented by a single value, while an emulsion having a curve with a pronounced maximum obviously can not. The procedure of some workers of giving indices for three times of development is sufficient in certain cases, provided the times of development are properly chosen. However, an adequate presentation of the difference in sensitivity between emulsions seems to call for their sensitivity, development time curves.

The shape of the curves for emulsions other than the panchromatic or process types shows that where the utmost sensitivity of the plate is

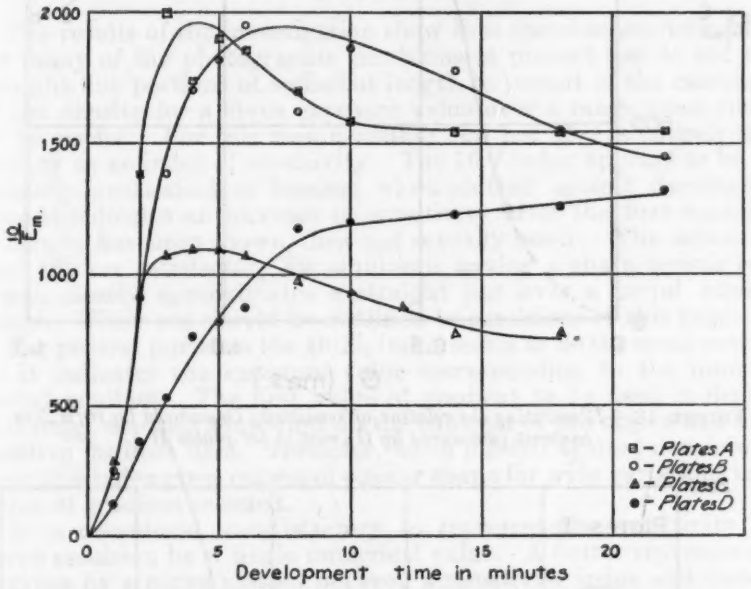

FIGURE 17.—*Illustrating the manner of expressing the relative sensitivity of emulsions*

All curves are plotted to the same scale. The curve for the process plate (E) is not included as its sensitivity is too low to show to advantage.

required, development should not be carried very far. This is important where it is desired to record very feeble sources.

The relation of sensitivity to contrast is illustrated in Figure 18 where the sensitivity index $10/E_m$ for Plate B is plotted against maximum gradient. Since Neitz[13] and others have shown that contrast first increases to a maximum and then decreases with continued development, it will be seen that a sensitivity, maximum gradient curve will be hook shaped if the development is carried sufficiently far (and no correction is made for fog by one of the formulas[14] for that purpose). In order to avoid such an inconvenient form of expression, sensitivity indices were plotted against time of development, and a curve giving the relation of maximum gradient to development time has been included in Figures 12 to 16, inclusive.

[13] See footnote 1, p. 496.

[14] A family of characteristic curves "corrected" for fog by one of these formulas shows contrast increasing to a maximum and then remaining constant with further development.

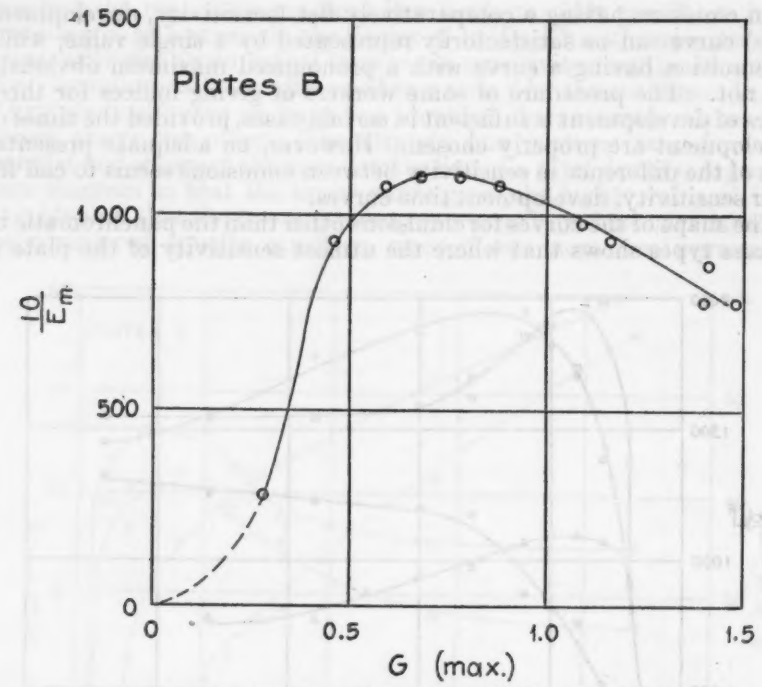

FIGURE 18.—*Illustrating the relation of sensitivity (measured by $10/E_m$) to contrast (measured by G (max.)) for plates B*

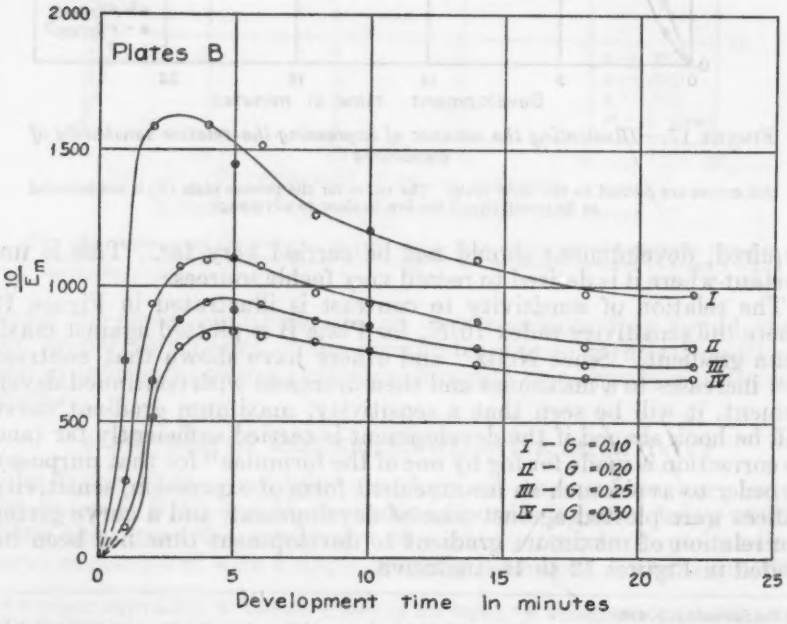

FIGURE 19.—*A family of sensitivity, Development time curves ($10/E_m$) for plates B showing the effect of change in the value taken as the minimum useful gradient*

The most satisfactory value of gradient to be used in deriving the $10/E_m$ index depends to some extent upon the contrast in the object and the contrast of the positive medium used. The effect of variation in the value of gradient chosen upon the sensitivity, development time curve is given in Table 7 for Plates B and illustrated by the family of curves in Figure 19. The curves all show a maximum whose prominence decreases as the value taken as the minimum useful gradient is increased. The development time corresponding to maximum sensitivity increases slightly, but the shape of the curve remains essentially the same.

3. SUMMARY

The results of the investigation show that the characteristic curves for many of the photographic emulsions in present use do not have straight line portions of sufficient length to permit of the calculation of the density for a given exposure value over a range great enough to be useful. For this reason neither $10/\iota$ nor $10/I$ is entirely satisfactory as an index of sensitivity. The $10/I$ index appears to be particularly unsatisfactory because when plotted against development time it indicates an increase in sensitivity after the first maximum which, it has been shown, does not actually occur. The indices $10/\iota$ and $10/i$ are satisfactory for emulsions having a characteristic curve which closely approximates a straight line over a useful exposure range. Their use should be confined to emulsions of this type.

For general purposes the $10/E_m$ index seems to be the most practical as it indicates the exposure value corresponding to the minimum useful gradient. The best value of gradient to be used in deriving this index depends somewhat on the contrast of the object and of the positive medium used. However, when plotted against development time this index gives curves of similar shape for wide variations in the value of gradient selected.

It is considered unsatisfactory to represent the sensitivity of a given emulsion by a single numerical value. A better representation is given by a curve plotted between a sensitivity index and development time. For work not requiring the greatest accuracy, however, values of the index for at least three development times may be satisfactory provided the development times are properly chosen.

WASHINGTON, June 13, 1931.

SOME EXPERIMENTAL STUDIES OF THE VIBRATIONS OF QUARTZ PLATES

By R. B. Wright and D. M. Stuart

ABSTRACT

Numerous modes of vibration of 0 and 30 degree cut circular and rectangular crystalline quartz plates were studied experimentally. Various methods were employed in studying these modes which are piezo-electrically excited. The behavior of lycopodium powder applied to the vibrating faces proved to be the most fruitful source of information. A number of photographs of the patterns thus formed are produced and described. Although of limited utility two mechanical devices also were employed in these studies.

The direction of maximum radial displacement was determined for the two active lower frequency modes of 0° circular plates. It was found that these directions are nearly parallel to directions of critical values of Young's modulus. Facts were disclosed concerning specially oriented rectangular plates and rods. Experimental values of Young's modulus based on vibration frequencies of the latter were found to agree closely with corresponding values computed from a known theoretically derived expression. Rough experimental verification of the direction of one of the critical values of Young's modulus was obtained.

Equations are derived for the modulus of rigidity and Poisson's ratio for crystalline quartz as functions of orientation, and graphs of these two functions as well as of Young's modulus are given.

Methods are indicated, which may prove advantageous, of rigidly mounting quartz plates.

CONTENTS

	Page
I. Introduction	520
II. Experiments of a general nature	520
1. Studies of glow-discharge patterns	520
2. Studies of powder patterns formed on the surface of plates	523
(*a*) Zero-degree circular plates	524
(*b*) Zero-degree square plates	527
(*c*) Thirty-degree circular plates	528
(*d*) Thirty-degree square plates	529
(*e*) Comments concerning surface power patterns	530
3. Studies of powder patterns formed by air currents emanating from the periphery of plates	530
(*a*) Zero-degree circular plates	530
(*b*) Zero-degree square plates	531
(*c*) Thirty-degree circular plates	531
(*d*) Thirty-degree square plates	531
(*e*) Specially oriented 0 and 30 degree cut rectangular plates and rods	532
(*f*) Comments concerning air current patterns	534
III. Experiments of a more specific nature	536
1. Study of the air currents emanating from the periphery of circular 0° plates	536
2. Studies of the displacement of the periphery of circular plates by means of a probing mechanism	539
(*a*) First mode of a 0° circular plate	539
(*b*) Second mode of a 0° circular plate	541
(*c*) The mode of a 36.03 by 4.805 mm 0° circular plate responding at 136 kc	541
(*d*) Comments concerning results of probing studies	542
IV. Comment and conclusion	542
V. Supplementary Note	544
VI. Appendix I. The development of Poisson's ratio and the modulus of rigidity for crystalline quartz	545
VII. Appendix II. The evaluation of Young's modulus	551

I. INTRODUCTION

That branch of the theory of elasticity dealing with the vibrations of isotropic solid bodies may be said to be still in its infancy, even though it covers to-day quite an extensive field of endeavor. With few exceptions the theory in its present state of development allows the handling of only the simpler cases in an approximate manner. The manifest limitations appear to be principally of a mathematical nature. This situation becomes painfully evident as a definite impediment in the specialized study of piezo electrically excited oscillations of quartz plates such as are utilized in the art of radiocommunication. A second and formidable impediment is found in the fact that quartz, like other crystalline substances, is not isotropic. A third factor tending to impede progress in the study lies in the fact that owing to the necessary precision in present-day frequency requirements, inexact solutions can not be expected to yield a large degree of satisfaction. Moreover, solutions of an approximate nature, in common with any simple exact solutions that may be found by considering special cases, may be expected to give little more than a glimpse at the manifold infinity of possible modes of response.

The various experimental studies of the modes of vibration of quartz plates described in this paper were undertaken in an attempt to gain information which it was hoped would prove helpful in the theoretical study of the problem, as well as useful in practice.

II. EXPERIMENTS OF A GENERAL NATURE

1. STUDIES OF GLOW-DISCHARGE PATTERNS

The method employed in studying the piezo-electrically excited oscillations of cylinders cut from crystals of quartz, which was described in a paper by Hund and Wright,[1] was tried on circular and square plates of quartz. Briefly, this method consists in the observation of the various patterns created by the resonance radiation of the gas molecules, usually termed glow discharge, accompanying the piezo-electrically excited oscillations or vibrations of the quartz bodies in an atmosphere of helium under a pressure of a few millimeters of mercury. The vacuum tube oscillator circuit used to sustain the quartz plate in vibration in this second application of the method is shown in Figure 1. As did the one previously used, it incorporates sufficient regeneration to afford independent oscillation. The quartz plate to be studied is placed on a plane metallic surface which serves as one electrode. As the upper electrode, a fine wire mesh or screen is used. This upper electrode is not distinguishable in the photographs of the phenomenon appearing at the surface of the quartz plate, because of the fineness of the wire and owing to the fact that it was supported somewhat above the face of the quartz plate on which the camera was focused.

Photographs of some of the various patterns observed are shown in Figure 2. As indicated, the quartz plates appearing in these 12 photographs are of the 0° or Curie cut variety; that is, were so oriented in the process of cutting that the faces of the plate lie perpendicular

[1] August Hund and R. B. Wright, New Piezo Oscillations With Quartz Cylinders Cut Along the Optical Axis. B. S. Jour. Research, 4, pp. 383-394, 1930; or Proc. I.R.E., 18, pp. 741-761; 1930.

to an electric axis. In the case of the square plates, a major face (one of the faces largest in area) was in turn so oriented in its plane that two of its edges lie perpendicular to the optic axis, requiring, of course, that the remaining two edges of this face lie perpendicular to the mechanixal axis. (A more detailed treatment of the subject of orientation is involved in the accompanying appendixes).

It is common knowledge that the frequencies at which a given quartz plate will vibrate with appreciable amplitude in a vacuum tube circuit incorporating external regeneration are very numerous indeed. In 1923 Pierce [2] published a so-called spectrum of response frequencies. He pointed out that at the majority of these numerous modes the plate responded with small amplitude, and that of the few at which the plate responded with relatively large amplitude in a regenerative circuit of this nature, one could be identified with each of the very limited number which he found would respond in his single tube piezo oscillator. He distinguished between the action of the

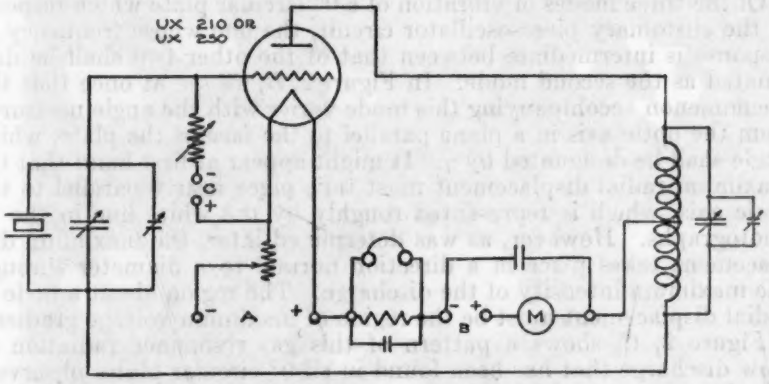

FIGURE 1.—*Type of vacuum tube circuit used in the various experimental studies*

two types of circuits on a quartz plate by describing the effect of the former type as resonating and that of the latter as oscillating. This is a good distinction to be made when possible. However, in many cases no sharp distinction can be drawn. This is particularly true in the case of the highly regenerative circuit (fig.1), used in the studies to be described here. A large number of the modes studied could be sustained indefinitely, although unstably so, in this circuit.

It has been known for some time that a 0° circular quartz plate may be caused to execute sustained free vibrations at three different frequencies [3] when placed in that type of piezo-oscillator circuit in common use, in which the piezo-electric element is connected either between the grid and the filament, or the grid and plate of a vacuum tube, and in which a condenser in parallel with an inductor is employed in the anode branch.[4] The ratio of the two lower of these frequencies of response is roughly $1/\sqrt{2}$. Furthermore, it has been recognized

[2] G. W. Pierce, Piezoelectric Crystal Resonators and Crystal Oscillators Applied to the Precision Calibration of Wave Meters. Proc. A. A. A. S., **59**, pp. 81–106; 1923.

[3] A. Hund, Uses and Possibilities of Piezo-Electric Oscillators, Proc. I. R. E., **14**, pp. 447–469; 1926.

[4] The particular type referred to here is described more fully in the paper by A. Hund referred to in footnote 3.

for a number of years that the direction (in a plane parallel to a face, and with respect to some crystallographic axis, for example, the principal or optic axis) in which the maximum radial displacement takes place differs for the two lower of these three modes of response of circular plates.[5] In Figure 2, *A*, is shown the phenomenon that appears when a 0° circular plate is caused to oscillate in the described regenerative circuit and electrode system, at that one of these three modes which responds at the lowest frequency. This mode, for the sake of brevity, shall be designated as the first mode.

The phenomenon appearing agrees in pattern or configuration with observations made by Namba and Matsumura,[6] and also by Meissner.[7] No favored direction of displacement is indicated, unfortunately. The phenomenon appears as a concentric circular discharge of rough definition. (The periphery of the lower electrode which, because of its smaller size, may be indistinctly seen through the quartz plate, should not be confused with the circular discharge pattern which occupies less than half the area of the face of the quartz plate.)

Of the three modes of vibration of a 0° circular plate which respond in the customary piezo-oscillator circuit, the one whose frequency of response is intermediate between that of the other two shall be designated as the second mode. In Figure 2, *B*, we see at once that the phenomenon accompanying this mode varies with the angle measured from the optic axis in a plane parallel to the face of the plate, which angle shall be designated by γ. It might appear at first hand that the maximum radial displacement must take place nearly parallel to the optic axis, which is represented roughly by the white line in the 12 photographs. However, as was determined later, the maximum displacement takes place in a direction normal to a diameter through the maximum intensity of the discharge. The region about a node of radial displacement must be the region of maximum voltage gradient.

Figure 2, *C*, shows a pattern of this gas resonance radiation or glow discharge that has been found in all 0° circular plates observed. The frequency at which this pattern appears for the particular plate, is 241 kc. In Figure 2, *D*, *E*, and *G* are shown patterns which are of frequent occurrence. A peculiarity of these patterns is that it is difficult to cause two or more of these curious figures to appear simultaneously on the face of a plate, even though a complete pattern may consist of several. The explanation of this is not evident. The pattern shown in Figure 2, *F*, appears consistently, and is to be found on plates of various sizes. It emphasizes the difficulty of interpreting these phenomena.

The third and highest in frequency of the three modes of 0° circular plate which respond in the customary piezo-oscillator circuit will be termed for brevity the third mode. This mode is often called the thickness mode. The pattern accompanying oscillation at this mode is given in Figure 2, *H*. Here is indicated the breaking up of the face of the plate into "nodes" and "antinodes." This breaking up of the face of a plate in oscillation at the third mode was roughly indicated in Crossley's experiments on rectangular plates.[8] In studies

[5] See A. Meissner, Untersuchungen am Quarz, Phys. ZS., **28**, pp. 621–625; 1927.
[6] S. Namba and S. Matsumura, General Properties of Piezo-Electric Quartz and the Value of a Quartz Oscillator as a Frequency Standard, Researches of the Electrotechnical Laboratory No. 248; April, 1929.
[7] A. Meissner, Strukturbestimmung durch akustische Eigenschwingungen, ZS. f. Phys., **65**, pp. 145–157; 1930.
[8] A. Crossley, Modes of Vibration in Piezo-Electric Crystals, Proc. I. R. E., **16**, pp. 416–423; 1928.

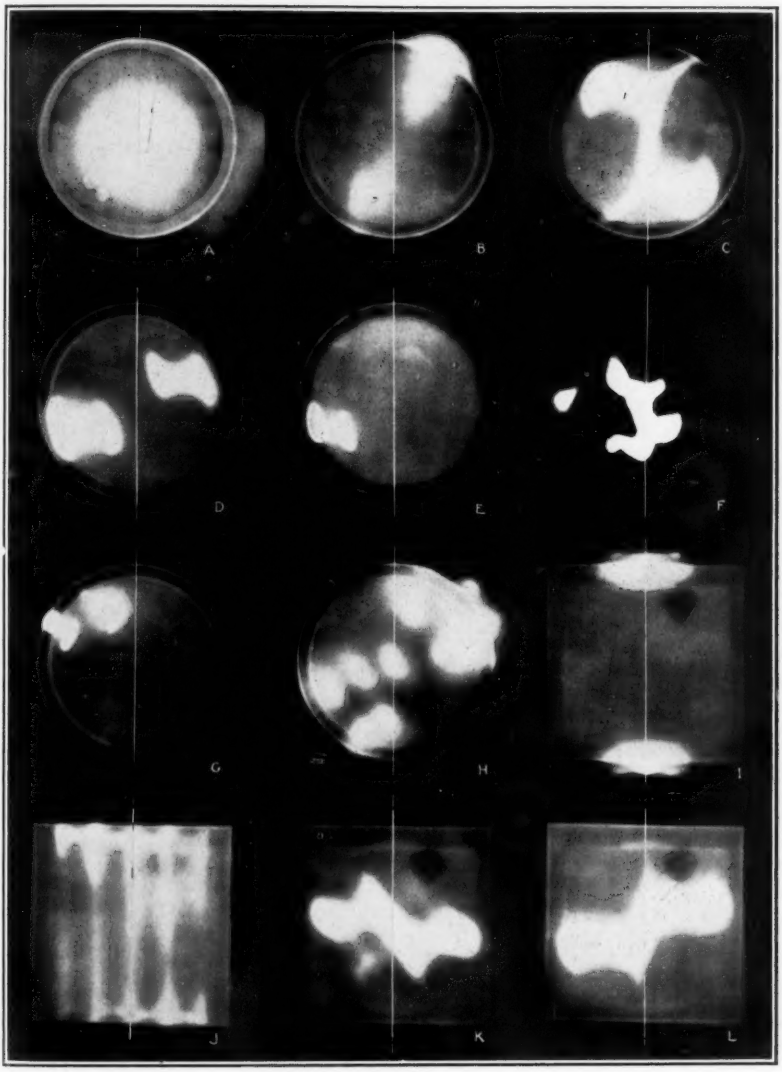

FIGURE 2.—*Zero-degree plates*

Circular plate; diameter 36.03 mm, thickness 4.805 mm; square plate; ∥ optic axis 35.98 mm; ⊥ optic axis 36.02 mm, thickness 4.810 mm.

A, 75.3 kilocycles.
B, 106 kilocycles.
C, 241 kilocycles.
D, 292 kilocycles.
E, 397 kilocycles.
F, 431 kilocycles.
G, 552 kilocycles.
H, 599 kilocycles.
I, 80.4 kilocycles.
J, 177 kilocycles.
K, 210 kilocycles.
L, 255 kilocycles.

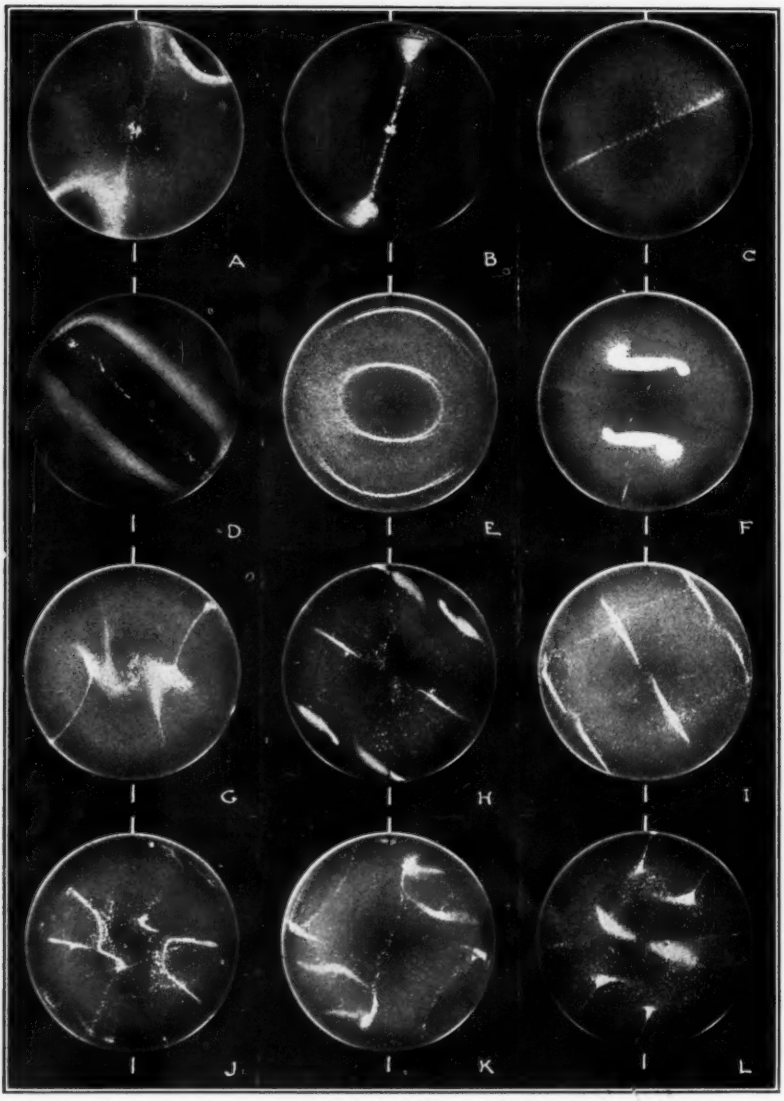

FIGURE 3.—*Zero-degree plate*

Diameter 36.03 mm, thickness 4.805 mm (excepting *A*, for which dimensions are, diameter 36.16 mm; thickness 4.815 mm).

A, 74.9 kilocycles.
B, 75.3 kilocycles.
C, 93.5 kilocycles.
D, 106 kilocycles.
E, 125 kilocycles.
F, 135 kilocycles.
G, 146 kilocycles.
H, 169 kilocycles.
I, 170 kilocycles.
J, 234 kilocycles.
K, 236 kilocycles.
L, 251 kilocycles.

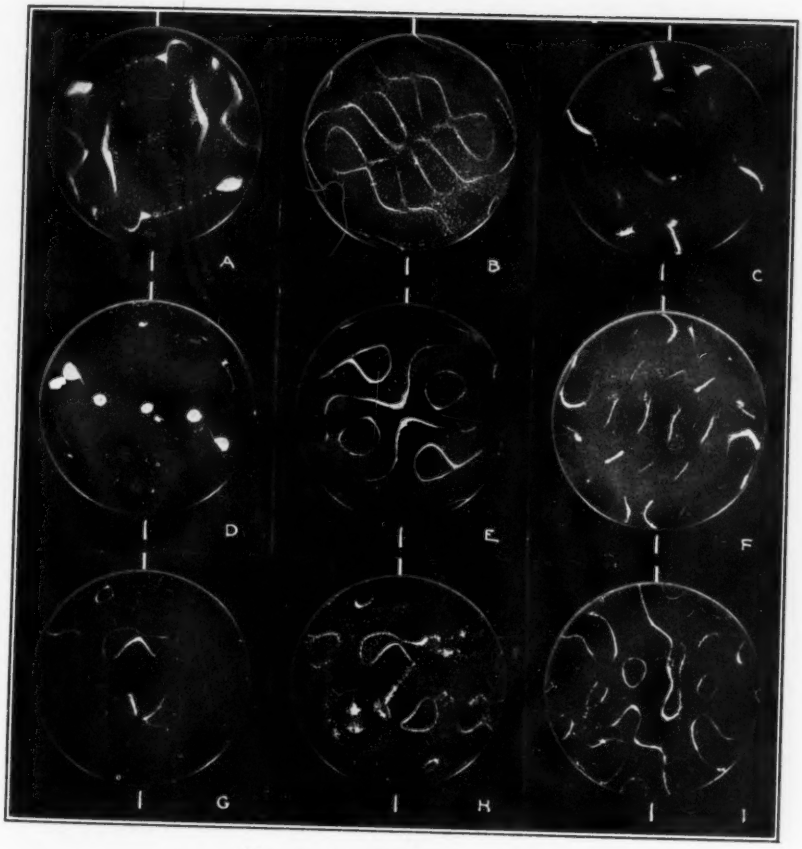

FIGURE 4.—*Zero-degree plate*

Diameter 36.03 mm; thickness 4.805 mm.

A, 258 kilocycles.
B, 360 kilocycles.
C, 389 kilocycles.
D, 397 kilocycles.
E, 400 kilocycles.
F, 494 kilocycles.
G, 597 kilocycles.
H, 597 kilocycles.
I, 599 kilocycles.

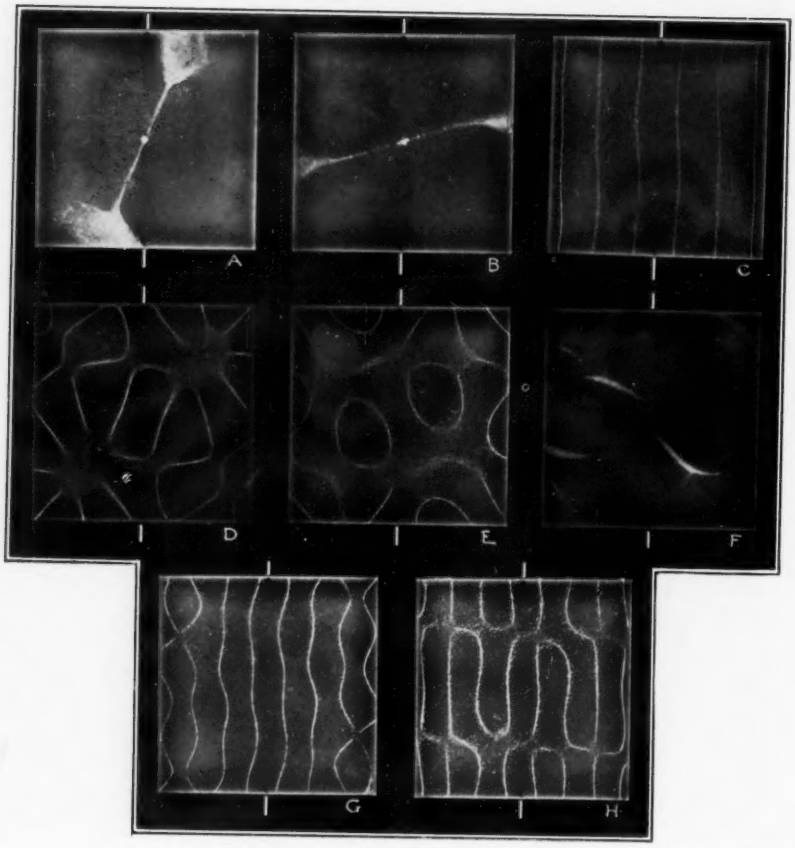

FIGURE 5.—*Zero-degree plate*

∥ Optic axis 35.98 mm. ⊥ Optic axis 36.02 mm. Thickness 4.810 mm.

A, 66.8 kilocycles.
B, 83.6 kilocycles.
C, 177 kilocycles.
D, 202 kilocycles.
E, 204 kilocycles.
F, 210 kilocycles.
G, 270 kilocycles.
H, 288 kilocycles.

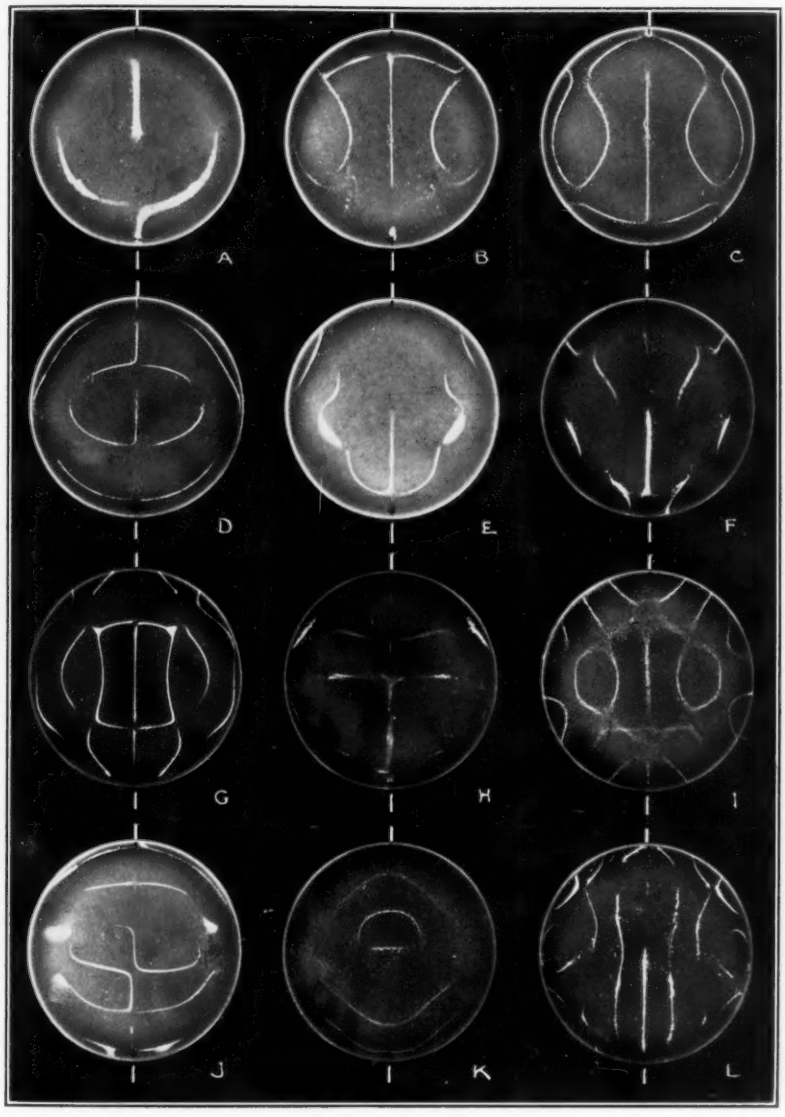

FIGURE 6.—*Thirty-degree plate*

Diameter 36.04 mm; thickness 4.810 mm.

A, 91.2 kilocycles.
B, 145 kilocycles.
C, 146 kilocycles.
D, 161 kilocycles.
E, 181 kilocycles.
F, 192 kilocycles.
G, 246 kilocycles.
H, 250 kilocycles.
I, 253 kilocycles.
J, 261 kilocycles.
K, 289 kilocycles.
L, 298 kilocycles.

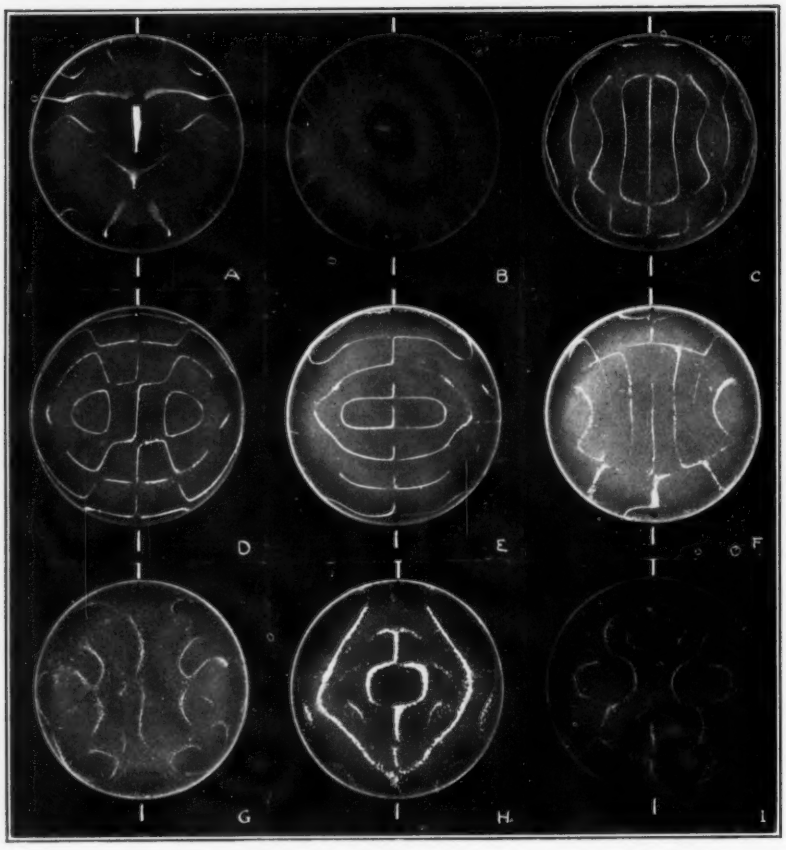

FIGURE 7.—*Thirty-degree plate*

Diameter 36.04 mm; thickness 4.810 m.m.

A, 314 kilocycles.
B, 323 kilocycles.
C, 333 kilocycles.
D, 346 kilocycles.
E, 370 kilocycles.
F, 402 kilocycles.
G, 406 kilocycles.
H, 408 kilocycles.
I, 415 kilocycles.

FIGURE 8.—*Thirty-degree plate*

36.15 by 36.15 by 4.819 mm.

A, 74.0 kilocycles.
B, 132 kilocycles.
C, 161 kilocycles.
D, 208 kilocycles.
E, 221 kilocycles.
F, 277 kilocycles.
G, 284 kilocycles.

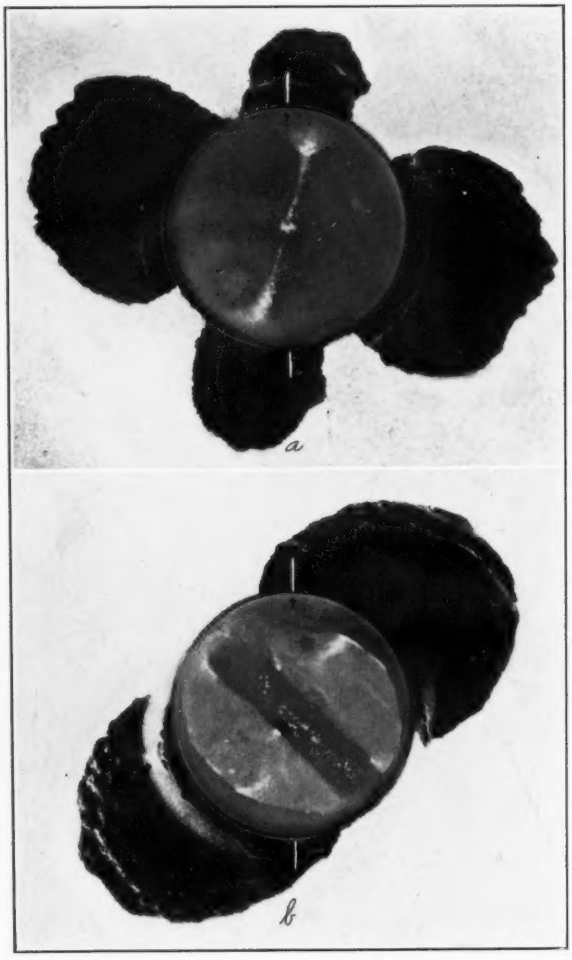

FIGURE 9.—*Zero-degree plate*

Diameter 36.03 mm; thickness 4.805 mm. *A*, 75.3 kilocycles; *B*, 106 kilocycles.

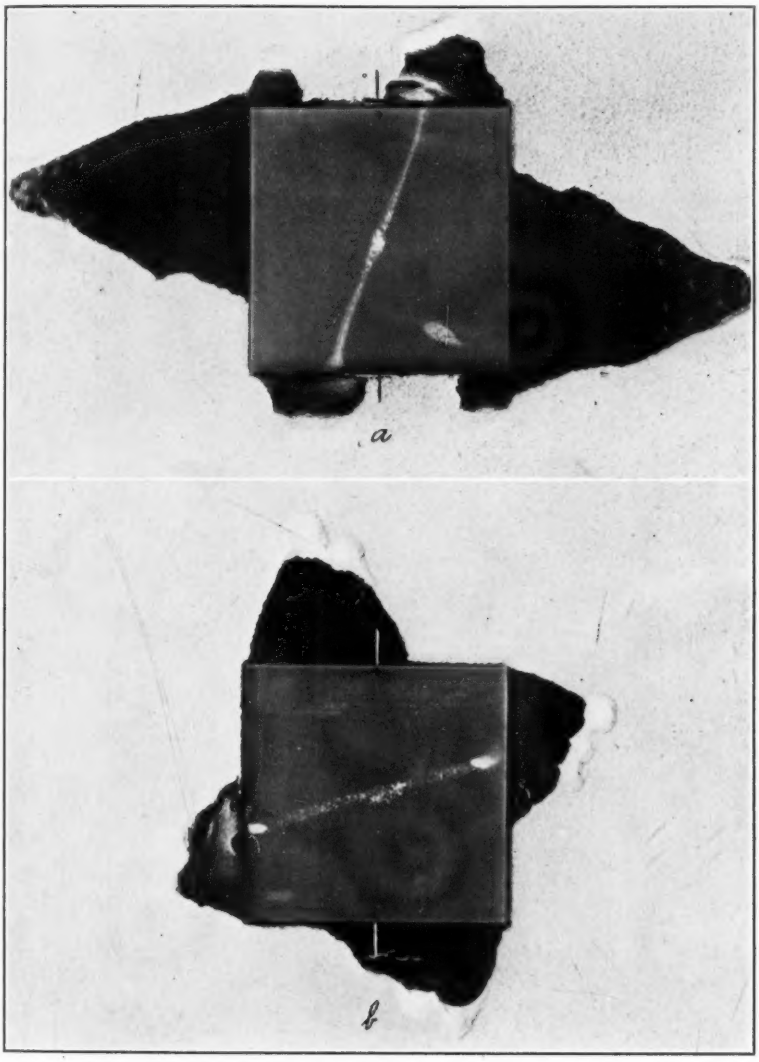

FIGURE 10.—*Zero-degree plate*

$\parallel$ optic axis 35.98 mm; $\perp$ optic axis 36.02 mm; thickness 4.810 mm. *A*, 66.8 kilocycles; *B*, 83.6 kilocycles.

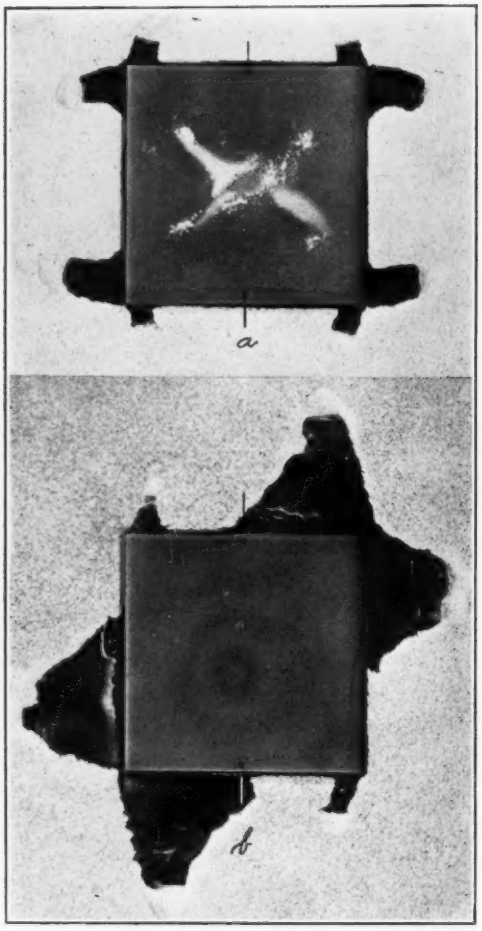

FIGURE 11.—*Zero-degree plate*

∥ optic axis 35.98 mm; ⊥ optic axis 36.02 mm; thickness 4.810 mm. *A*, 80.4 kilocycles; *B*, 90.0 kilocycles

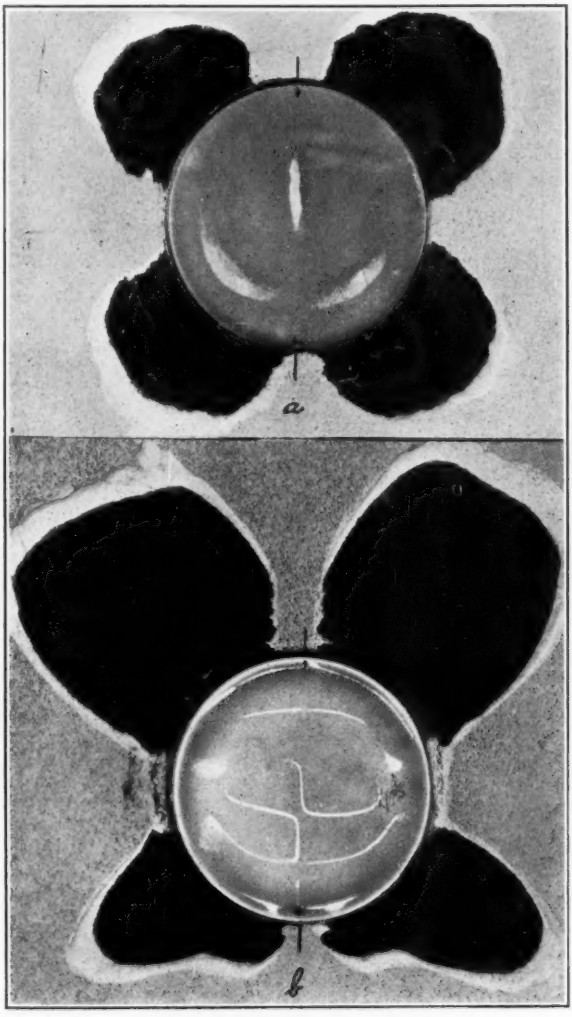

FIGURE 12.—*Thirty-degree plate*

Diameter 36.04 mm; thickness 4.810 mm. *A*, 91.2 kilocycles; *B*, 261 kilocycles.

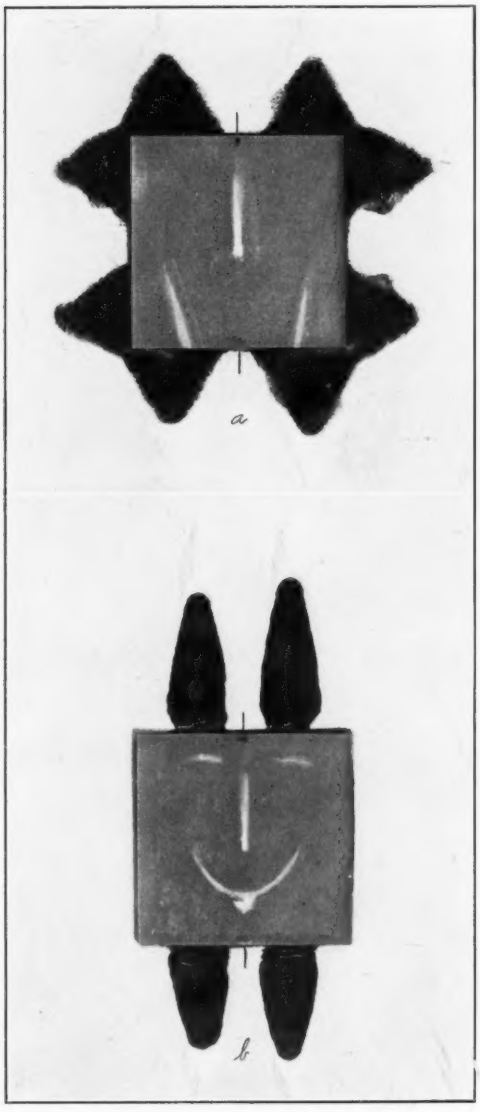

FIGURE 13.—*Thirty-degree plate*

36.15 by 36.15 by 4.810 mm. *A*, 74.0 kilocycles; *B*, 161 kilocycles.

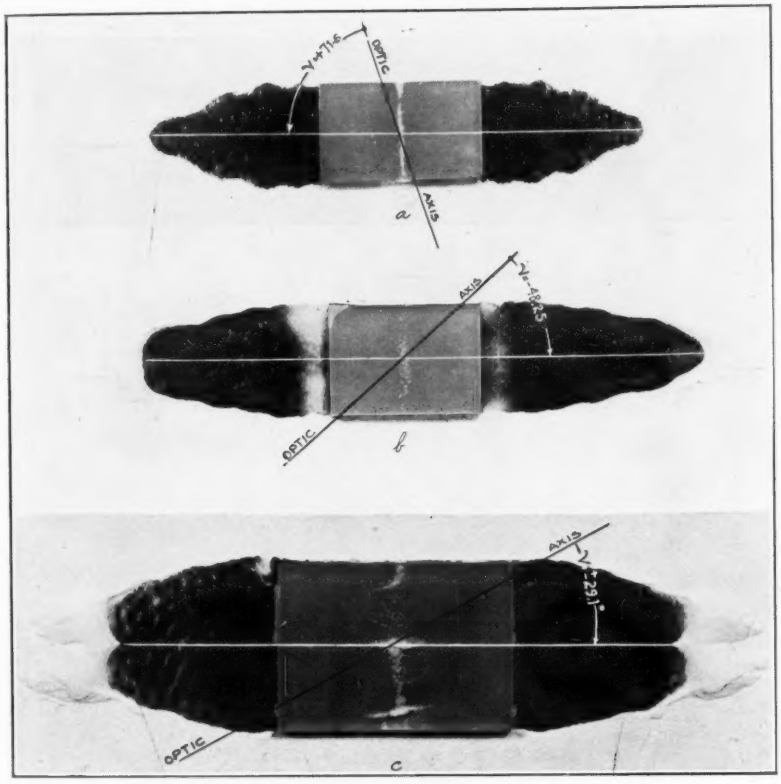

FIGURE 14.—*Specially oriented 0° and 30°*

a, 0° plate rotated −18.4° (γ=+71.6°); 30.985 mm (γ=−18.4°); 18.27 mm; thickness 4.81 mm; 82.4 kilocycles. *b*, 0° plate rotated +41.75° (γ=−48.25°); 28.920 mm (γ=+41.75°); 20.62 mm; thickness 4.84 mm; 120.9 kilocycles. *c*, 30° plate rotated ±60.88° (γ=±29.12°); 45.165 mm (γ=±60.88°); 31.28 mm; thickness 4.84 mm; 69.7 kilocycles.

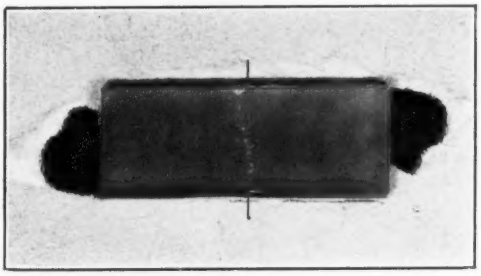

FIGURE 15.—*Zero-degree plate of customary orientation*

carried on by means of polarized light by Osterberg,[9] it is proved beyond doubt that the faces of rectangular plates break up in this manner. Evidence of this nature, which is added to in other studies treated below, is entirely contrary to a statement made, with diagrammatic illustration, by Namba and Matsumura,[10] to the effect that the faces are distorted as a whole in this mode of vibration.

Only four photographs of interest were obtained of this gas resonance radiation phenomenon when produced by the vibration of square plates. All four are of a 0° plate. In Figure 2, *I*, is shown the only low-frequency pattern obtained before this manner of investigation was concluded. As will be recognized later, this pattern is only indirectly indicative of the type of displacement experienced by the plate. In Figure 2, *J*, is shown an interesting pattern, representing what may appear to be a three wave length distribution of a flexural vibration [11] with waves propagated in a direction perpendicular to both the optic and electric axes, or along the mechanical axis. Figure 2, *K* and *L*, picture patterns which were observed with a great number of 0° rectangular plates. These patterns, it will be noticed, resemble the one in Figure 2 *C*.

It is possible, but rather improbable, that a thorough-going study of this type of phenomenon might prove profitable. But in its present development this medium of study is much too uncertain.[12] In an effort to obtain more definite information concerning the modes of vibration of quartz plates, a study was made of patterns formed by lycopodium powder sprinkled on the vibrating faces.

2. STUDIES OF POWDER PATTERNS FORMED ON THE SURFACE OF PLATES

In this work the same type of oscillator circuit and electrodes were used. The plates studied were both 0° and 30° cuts, square and round. The orientation of these plates is known to be quite accurate in the majority of cases; with certain exceptions they are well within a degree of the stated orientation, probably in most cases within 10 minutes of arc. Purposesly, the first exception is shown in Figure 3, *A*. The only other exception of importance is the 0° square plate. Twinning and inclusions were avoided insofar as it was possible.

---

[9] H. Osterberg, An Interferometer Method of Observing the Vibrations of an Oscillating Quartz Plate, Proc. N. A. S., **15**, pp. 892–896; 1929.

[10] See footnote 6, p. 522.

[11] Using the equation $f=\frac{\pi b v}{4\sqrt{3}l^2}\left(\frac{ml}{\pi}\right)^2$, which is of a similar type to that used by J. R. Harrison (Piezo-Electric Resonance and Oscillatory Phenomena with Flexural Vibrations in Quartz Plates, Proc. I. R. E., **15**, pp. 1040–1054; 1927), and to that used by S. Jimbo, except for a typographical error (An International Comparison of Frequencies by Means of a Luminous Quartz Resonator, Proc. I. R. E., **18**, pp. 1930–1934; 1930); where l and b are the greater and lesser actively concerned dimensions of the rod, v is the velocity of propagation, and $\left(\frac{ml}{\pi}\right)$ is the quantity, using Lamb's notation (H. Lamb, Dynamical Theory of Sound), which is equal to $(2S-1/2)+2\alpha_s/\pi$ for the symmetrical case and $(2S+1/2)-2\beta_s/\pi$ for the asymmetrical case, S being an integral number representing the order of the mode, α_s being neglible for $S\geq 3$, and β_s negligible for $S\geq 2$; and putting $S=3$, for symmetrical case

$$f=\frac{\overline{5.5}^2\pi b v}{4\sqrt{3}\,l^2}$$

For $v=5.4\times 10^5$, $l=3.6$, and $b=0.48$; $f=274$ kc. This is not in good agreement with the observed value of 177 kc, but the discrepancy should not necessarily be considered sufficiently grave to preclude the possibility of the flexural type of vibration.

[12] For further evidence of the unsatisfactory nature of this method of study, see the plates in the publications by A. M. Skellett, Modes of Vibration of a Round Plate Cut from a Quartz Crystal, J. Opt. Soc. Am. & Rev. Sci. Inst., **20**, pp. 293–302; 1930; and A Visual Method for Studying Modes of Vibration of Quartz Plates, J. Opt. Soc. Am. & Rev. Sci. Inst., **17**, pp. 308–317; 1928; and see sketches of phenomenon of this nature, appearing in that publication referred to in footnote 6, p. 522, by Namba and Matsumura.

In Figures 3 to 8 the optic axis is represented quite accurately by the white ruled-in line. One end of the diameter, or in the case of the square plates the line passing through the center of the face parallel to the optic axis, is marked in these photographs by a short black line near the edge of the plate; and the other end by a cross, so that it may be distinguished. When visible in the photographs, these marks may be used as more accurate reference.

(a) ZERO-DEGREE CIRCULAR PLATES

The orientation of the 0° circular plate is known to be very accurate. It was cut from optically left rotating quartz,[13] and is always shown in the photographs with the face uppermost, which becomes positively charged upon application of a normal tensile stress.

As indicated above, the pattern in Figure 3, *A*, is shown to illustrate the effect of a small inaccuracy of orientation. The actual orientation of this plate was not verified by measurement. However, experience seems to indicate that had the plate been accurately oriented the pattern would have been that shown in Figure 3, *B*. This fact illustrates well the critical nature of patterns formed by lycopodium on the surface of plates whose vibration involves areal dilatation. The difference in frequency of vibration of the two plates shown is due principally to the difference in diameter, rather than to the "pattern" of displacement. This mode is the first mode of a 0° circular plate in a field parallel to the electric axis. At this mode the displacement is, neglecting second order effects, limited to planes parallel to the face of the plate. Careful study of the motion of the periphery of the two plates under discussion would no doubt show that the two vibrate in a very similar manner, despite the fact that the patterns on their faces differ considerably.

Very little resemblance is to be seen between the surface powder pattern (fig. 3, *B*) and the glow discharge pattern (fig. 2, *A*) for the same mode. The latter, it will be seen, is a poor indication of the nature of the displacements. The powder pattern, on the contrary, is quite informative. The corresponding line to be found on the reverse face forms in a direction parallel to the one shown. Measurement of a series of these patterns indicates that this line is inclined 17° 30′ (± 1°) from the optic axis. Reference to Figure 23, Appendix II, will show that if this angle is taken in the negative sense, the line is closely perpendicular to the direction of the minimum of Young's modulus for the 0° plane. The plate shown in Figures 3, *B*, to 4, *I*, is of optically left rotating quartz, and its upper face, upon which the patterns are formed in all cases, is the one that becomes negatively charged upon application of a normal tensile stress. This, as explained in more detail in Appendix II, requires that the angle between the optic axis and this line be negative in sense in order to correspond to conventions upon which the given curves of Young's modulus are based. Thus the "nodal" line is closely perpendicular to the direction of the minimum of Young's modulus.

However, this line is not a nodal line in the strict sense of the word. The powder forming it runs outward, spreading before reaching the periphery of the plate. Thus it appears that the line marks a node of

[13] As viewed when looking toward the light source.

only those displacements in the plane of the face which are normal to the line. The reason for the outward motion of the powder will be made apparent in the description of patterns formed by air currents set up by the oscillation of the plate.

In Figure 3, *C*, is shown a very similar pattern. As in the preceding case, the line on the lower face is found to lie in a direction parallel to the one on the upper face. Here, however, the line is inclined approximately 67° from the optic axis, in a negative sense as before. Young's modulus for the 0° plane will be seen to pass through a maximum at $\gamma = +10° 50'$. Although the correspondence between this and the normal to the line in the pattern is not close, relation between the two will be shown to be quite probable. This mode is one of relatively weak response.

Coming now to Figure 3, *D*, a pattern of somewhat different nature is shown. Judging from the formation of the dust pattern in this case, this line is strictly a nodal line; there is no apparent movement of the powder forming it. During formation the powder moves perpendicularly away from it toward the periphery. The powder stops on reaching a midway region where it assumes a dancing motion. The line in this case is found to be between $-43°$ and $-44°$ from the optic axis. This direction is quite closely perpendicular to the direction of maximum Young's modulus, $\gamma = -48° 15'$. The mode accompanied by this pattern is the second mode of vibration of 0° circular plates. It is the same as that accompanied by the discharge pattern seen in Figure 2, *B*. The optic axis was not very accurately determined in this latter case, as will be evident from a comparison of the two photographs. It is quite certain, however, that the diameter through the center of the discharge corresponds to the nodal line formed by the lycopodium for this mode. Either the plate in the former case was of optically right rotating quartz or its upper face is the one which would become positively charged upon application of a normal tensile stress. These deductions may be made, knowing, as in both the above cases, that the line forming on the reverse face takes a direction parallel to the line on the upper face.

At 125 kc the interesting pattern shown in Figure 3, *E*, appears. The amplitude with which the plate responds at this mode is very small. This mode may be one of flexural vibration. It appears to have maximum displacement in the direction of the optic axis. With some plates, of practically the same dimensions, this pattern develops into complete rings.

Figure 3, *F*, shows the pattern accompanying a mode at which this plate responds with fairly large amplitude at 136 kc. At both ends of the two figures composing this pattern the powder revolves rapidly. It is interesting to note that these figures are roughly perpendicular to the optic axis. A symmetrical pattern for this mode is found only in a few plates.

In Figure 3, *G*, appears the pattern observed at 146 kc. In this the powder takes on a revolving motion at the center. With some plates this pattern is altered to resemble closely that shown in Figure 6, *C*, which is produced on a 30° plate at a frequency less than a kilocycle different from that of the former. It is quite probable that the plates on which the pattern is altered would be found to be inaccurately oriented with respect to the electric axis.

The principal difference between patterns shown in Figures 3, *H* and *I*, lies in the angle of inclination. Both modes of vibration are fairly strong. The one responding at 169 kc was found the more vigorous.

The pattern shown in Figure 3, *J*, accompanies a stronger oscillation than those accompanied by patterns in Figure 3, *H* and *I*. The strength of this oscillation is about the same as the 136 kc mode, the pattern for which is shown in Figure 3, *F*.

The mode whose pattern is shown in Figure 3, *K*, is, perhaps, a little stronger than that accompanied by the pattern in Figure 3, *F*, while that whose pattern is shown in Figure 3, *L*, is a little weaker. The pattern shown in Figure 4, *A*, is again stronger, being nearly equivalent in response to the modes accompanied by patterns shown in Figures 3, *F*, *J*, *K*.

The mode represented by the pattern in Figure 4, *B*, on the other hand, is quite weak. The rest of the modes whose patterns are shown, however, are stronger.

Both modes represented by patterns in Figure 4, *C* and *D*, are about equivalent in strength to those whose patterns are shown in Figures 3, *F*, *J*, *K*, and 4, *A*. The larger spots in Figure 4, *D*, are regions in which the powder revolves rapidly.

The figure for the 400 kc mode shown in Figure 4, *E*, is quite representative. Whereas some of the patterns found above 146 kc for the particular plate used are not always to be found with all plates, this figure nearly always occurs.

In Figure 4, *G* and *H*, are to be seen two patterns of the same mode of vibration. This mode is the third mode of 0° circular plates. The displacement is principally in the direction of the thickness, which makes it difficult to obtain any sort of a powder pattern. A strong current of air is given off the face of the plate causing the powder to be blown away. An unmistakable symmetry of form will be noticed in this pattern. Moreover, this pattern constitutes very good evidence of the breaking up of the surface, mentioned above, during this oscillation. It has been noticed that the pattern accompanying this oscillation is quite critical with respect to dimensional ratio and accuracy of orientation.

The pattern in Figure 4, *I*, accompanies quite a vigorous vibration. In it is seen some tendency toward symmetry. The fact that the pattern is not entirely symmetrical may have bearing on the fact that this oscillation is weaker than the one appearing at a slightly lower frequency.

It was found that the four lower modes shown (fig. 3, *B*, *C*, *D*, *E*, and *F*) remain relatively unchanged in manner of response through a wide range of the ratio of the diameter to the thickness.

For many modes, particularly those occurring at frequencies about midway between the lowest and highest frequencies concerned here, straight lines formed on the periphery of the plate, parallel to the axis of physical or geometric symmetry of the plate, different modes involving different numbers and spacing thereof. In some of the patterns of more eleaborate design these lines on the periphery of the plate curve around in an attempt to complete the pattern, instead of being straight and parallel.

(b) ZERO-DEGREE SQUARE PLATES

As already mentioned, the orientation of the 0° square plate used in these studies is not very accurately known. It is probably within 2° of the proper orientation. It is of optically right rotating quartz, and that face which becomes negatively charged upon application of a normal tensile stress is always uppermost in the photographs. Thus the orientation with respect to the observer, of the elastic characteristics of this plate is similar to that of the circular plate.

The first pattern is of considerable interest, a "nodal" line within less than 5° of the direction taken by a similar line in the case of the circular plate. Not only does the line in Figure 5, *A*, correspond closely in direction to that in Figure 3, *B*, but it also resembles the latter in manner of formation; the powder forming the line moves outward, finally spreading as it did on the circular plate.

A second correspondence is found between the pattern in Figure 5, *B*, and that for the circular plate shown in Figure 3, *C*. In this case the angle γ is about $+73°$ for the square and about $+67°$ for the circular plate. It will be noticed that in the case of the square plate the frequencies of the two modes are about as nearly inversely proportional to the square roots of Young's modulus in directions perpendicular to the corresponding "nodal" lines as they are in the case of the circular plate. This relation which appears to be a coincidence is explained, no doubt, by the fact that the intercepted perdendicular bisectors of the "nodal" lines in the two cases for the square plate are about of equal length. This fact should be by no means difficult to accept considering that the "nodal" line which forms on the circular plate at the lower frequency is inclined to the optic axis by an angle which is about equal to that with which the "nodal" line accompanying the higher frequency mode is inclined to the normal to the optic axis. Although dependent upon the former and latter facts, and therefore again an apparent coincidence, it should be interesting to note that the ratio of the lower frequency of the circular plate (fig. 3, *B*) to that of the square plate (fig. 5, *A*); that is, $\frac{75.3}{66.8}=1.13$, is practically equal to the corresponding ratio of the higher frequencies, $\frac{93.5}{83.6}=1.12$.

When this series of patterns was photographed no presentable pattern could be obtained for that mode of response of the square plate corresponding to the mode of a circular plate whose pattern is shown in Figure 3, *D*. However, such a mode exists; the frequency at which it responds is 90 kc. Description of this mode will be reserved for a succeeding section, as will be the discussion of an additional pattern not obtained during the photographing of this series, which may be found in Figure 11, *A*.

Figure 5, *C*, shows the powder pattern corresponding to the gas resonance radiation pattern in Figure 2, *J*. Judging from the distance of the two outer lines from the edges of the plate the lines marked by the powder are probably nodal in nature, indicating that lines marked by the glow discharge in Figure 2, *J*, are of an antinodal nature.

At 202 kc is found the pattern shown in Figure 5, *D*, and at 204 kc the less elaborate pattern in Figure 5, *E*. The plate responds quite

feebly at this latter mode of vibration. In Figure 5, *F*, is shown the peculiar but symmetrical pattern found at 210 kc. At this frequency the plate vibrates relatively strongly.

In Figure 5, *G* and *H*, are to be seen patterns which appear as though they might accompany flexural vibrations. These modes do not respond very strongly.

Just as in the case of the circular plate, straight lines were found to form on the edges perpendicular to the faces of the square plate varying in number and disposal with the modes which they accompany, while for some modes curved lines formed on the edges in a manner tending to complete the pattern forming on the face.

(c) THIRTY-DEGREE CIRCULAR PLATES

The 30° plate shown in this series of photographs was cut from optically left rotating quartz. It is in all cases shown in such a position that the edge to the left is the one that would become positively charged upon application of a tensile stress along the electric axis. Its orientation is known to be very accurate. The white ruled-in line as before represents the optic axis. The plate itself is marked in the same manner as were both the square and round 0° plates, with a short line and a cross representing the optic axis.

It is common knowledge that the strongest mode of vibration of 30° plates responds at a frequency about two-thirds that at which is found the strongest response of 0° plates of the same dimensions. The type of vibration occurring at the frequency of strongest vibration of 30° plates is as pointed out by Cady,[14] essentially of a shearing nature. When a 30° plate is caused to oscillate at this frequency in the usual type of vacuum tube circuit, beat notes may usually be heard in phones placed in the circuit, indicating that several modes of vibration are being sustained simultaneously.

Comparable with the lower modes of strong response found for 0° circular plates, there is found for 30° plates the mode whose pattern is to be seen in Figure 6, *A*. A certain amount of importance is to be attached to this mode of vibration, for it may be executed by circular plates of practically any orientation. The frequency at which the mode responds differs for the different orientations, but the pattern formed remains quite unchanged. It was even found to be executed by a plate cut accurately perpendicular to the optic axis. The pattern on the reverse face, as would be expected, is the duplicate of the one shown, with an orientation that may be described as that taken by the latter upon rotation through 180° about the electric axis.

Although the patterns shown in Figure 6, *B* and *C*, are quite similar, and occur at very nearly the same frequency, they appear to belong to different clases or series. The patterns shown in Figures 6, *G*, and 7, *F*, appear related to that shown in Figure 6, *B*. The modes accompanied by these three patterns are all quite strong in response, the strength increasing with frequency. The one of highest frequency is one of the most vigorous modes of the plate. The mode accompanied by the pattern in Figure 7, *C*, appears to belong to the same series as that whose pattern is shown in Figure 6, *C*. These two modes are quite weak. The mode whose pattern is seen in

[14] W. G. Cady, A Shear Mode of Crystal Vibration (abstract), Phys. Rev., **29**, p. 617; 1927.

Figure 6, *E*, is strong, and its pattern appears to be a higher development of that in Figure 6, *A*, accompanying the mode already described, which is also of strong response. Moreover, the frequency of the mode whose pattern is shown in Figure 6, *E*, is very nearly double that whose mode is shown in Figure 6, *A*. Correspondingly, patterns in Figures 6, *J*, and 7, *E*, appear as developments of that in Figure 6, *D*, and that in Figure 7, *A*, as a development of that in Figure 6, *H*, the modes accompanied by the latter two patterns being quite strong.

At the modes accompanied by patterns shown in Figure 6, *L* and *F*, the plate responds quite readily while at those whose patterns are shown in Figure 6, *I* and *K*, the response is weak as it is at the mode whose pattern is shown in Figure 7, *B*.

When the particular 30° plate used in these experiments is caused to oscillate in the customary piezo-oscillator circuit, it responds simultaneously at all three modes whose patterns are shown in Figure 7, *F*, *G*, and *H*. In plates of approximately the same dimensions, the mode whose pattern is shown in Figure 7, *I*, is found to be sustained simultaneously with the other three in the ordinary circuit.

(d) THIRTY-DEGREE SQUARE PLATE

The particular plate used in obtaining the series of photographs of patterns formed on the face of 30° square plates during vibration, was cut from optically right rotating quartz. In all cases the plate is shown in a position such that the edge that becomes positively charged upon application of a normal tensile stress is to the right.

As might be expected from the behavior of 0° square and round plates at the lower frequencies, there is found for the lowest mode of vibration of a 30° square plate a pattern resembling that accompanying the lowest mode of a 30° circular plate. Resemblance between patterns in Figures 8, *A*, and 6, *A*, is undeniable.

In Figure 8, *B*, is shown a pattern very similar to that shown in Figure 5, *C*. Both appear as though they may be formed by a flexural type of vibration.[18]

At 161 kc. was found the pattern shown in Figure 8, *C*. Similarity between this pattern and the one for the 30° circular plate shown in Figure 6, *D*, is quite evident. Incidently it will be noted that the frequencies are the same. The square plate oscillates quite strongly at this frequency.

At 208 kc appeared the pattern in Figure 8, *D*. This pattern is similar to some extent to the one referred to above and shown in Figure 5, *C*, except that the "nodal" lines are roughly perpendicular to the optic axis. That the two are of similar nature despite the fact that the lines are fairly straight in one case and not in the other is indicated by the fact that the frequencies of the two are quite closely proportional to the half power of Young's modulus for the two directions.

In Figure 8, *E*, is the pattern produced by a similar type of vibration of higher order. At this and the mode previously discussed the plate responds quite readily in the circuit used.

[18] This would correspond to the second order asymmetric case, for which $S=2$, making $(\frac{ml}{\pi})=4.5$ in the equation given in footnote 11, p. 523. Using this, $f=183$ kc, which is much higher than the observed frequency of 132 kc.

At 284 kc the square plate responded quite vigorously with the pattern shown in Figure 8, *G*. The pattern in Figure 8, *F*, accompanied also a strong response.

Lines on the edges of both circular and square 30° plates were found to accompany most patterns of intermediate modes. These lines resemble those for the 0° plates, with the difference that in this latter case the straight lines perpendicular to the faces appeared to predominate, whereas in the case of the 30° plates the curved ones which tend to complete the facial patterns, were found more frequently.

(c) COMMENTS CONCERNING SURFACE POWDER PATTERNS

In Figure 23, Appendix II, is shown reflected symmetry of the elastic modulus in the XZ-plane with respect to both the optic and electric axes. On the other hand, the elastic modulus in the YZ-plane shows only an axis of symmetry, the covering operation being rotation through 180°. This might lead one to expect twofold symmetry of patterns on 30° plates, and merely an axis of symmetry in the case of patterns on 0° plates. In fact, in the case of 0° plates, the axis of symmetry is found present with hardly an exception. However, in the case of 30° plates, only reflected symmetry with respect to the optic axis is found. The fact that the patterns show no symmetry with respect to the electric axis may be attributed to the lack of reflected symmetry of Young's modulus in the YZ-plane.

Thus, it is seen that while the patterns may be very difficult of interpretation, and must be analyzed with the utmost caution, they nevertheless appear to involve nothing in discord with the well established elastic structure of quartz. And this is indicative, to some extent at least, that electric forces play only a minor part in the formation of these patterns. It is possible that the critical nature of some may be caused by the action of electric forces, but there is no apparent reason for such an effect.

Patterns of this nature are obtainable in number without end. Those reproduced and described here constitute only a small part.

3. STUDIES OF POWDER PATTERNS FORMED BY AIR CURRENTS EMANATING FROM THE PERIPHERY OF PLATES

(a) ZERO-DEGREE CIRCULAR PLATES

As is well illustrated by experiments carried on by Meissner,[16] plates when driven with sufficient amplitude create quite strong disturbances in the surrounding air. The air currents set up in this manner may be employed as a means of studying the vibrations of plates. These currents, when the plate is excited at its lower frequency modes of vibration, emanate from its periphery. If the plane of the lower electrode is extended for some distance beyond the periphery and a layer of lycopodium is sprinkled on this extended surface, the air currents will cause some of the powder to be displaced. In Figure 9*A*, may be seen the effect on lycopodium sprinkled around a zero-degree circular plate when it is caused to vibrate at 75.3 kc. At this excitation frequency, it will be recalled, is found the first mode of vibration of this 0° plate. It will be recognized by its surface powder pattern,

[16] A. Meissner, Piezo-Electric Crystals at Radio Frequencies, Proc. I. R. E., 15, pp. 281-296; 1927; or ZS. f. Techn. Phys., 7, pp. 585-592; 1926.

which is the same as that shown in Figure 3, *B*. The reason for the outward motion of the powder forming the "nodal" line is now apparent. In the general direction of the line is seen the maximum of a secondary antinodal region of areal displacement.

In Figure 9, *B*, is shown the air current pattern formed at the second mode of a 0° plate, illustrating the difference between the two modes of vibration. It is seen that the line in this case must be quite strictly a nodal line.

Meissner [17] shows photographs of this nature. His, however, appear to be the results of the two modes superposed.

(b) ZERO-DEGREE SQUARE PLATES

The patterns shown in Figure 5, *A* and *B*, for 0° square plates, are shown again in Figure 10, *A* and *B*, in company with the corresponding air current pattern. Comparison of Figures 9, *A* and 10, *A*, show that the modes of vibration involved are quite similar.

In Figure 11, *B*, appears the air current pattern for the mode corresponding to the second mode of 0° circular plates. No presentable surface powder pattern could be obtained for this mode as was stated above. The air current pattern, in itself, however, is quite convincing evidence of the correspondence.

The air current and surface patterns for the mode whose ionization pattern is shown in Figure 2, *I*, are presented in Figure 11, *A*. Comparison of the two shows little similarity. The gas resonance radiation apparently marks a nodal region in this case, while in others it is found to mark antinodal regions.

(c) THIRTY-DEGREE CIRCULAR PLATES

The air current pattern for the mode of vibration shown in Figure 6, *A*, together with the surface pattern, is to be seen in Figure 12, *A*. In company with the air current pattern the surface pattern takes on a more rational appearance. As previously explained, the pattern on the reverse face when seen through the plate would tend to complete the symmetry. It might be pointed out here that Young's modulus for the plane of a 30° plate shows a maximum at $\gamma = \pm 29° 6'$. Whether the maximum radial displacement takes place at these angles as might be expected from observations of the behavior of 0° circular plates, or at $\gamma = \pm 45°$ as one might be led to expect by the air current pattern shown, is not clear; it will probably be found somewhere between.

A somewhat better idea of the type of displacement involved in modes of the apparent series (figs. 6, *D* and *J*, and 7, *E*), may be gained from Figure 12, *B*. As in the case of surface patterns on 30° plates, rotation of the plate about the electric axis through 180° would result in the same pattern. But rotation of the plate by the same amount about either the optic or mechanical axes would cause an apparent rotation of the air current pattern through an equal angle about the electric axis.

(d) THIRTY-DEGREE SQUARE PLATES

Fundamental similarity is again shown between modes of vibration in square and circular plates of quartz, by a comparison of Figure 13, *A*, with Figure 12, *A*. Of course, patterns caused by air currents are

[17] A. Meissner, Untersuchung über Pyro- und Piezo-Elektrizität. Die Naturwissenschaften, 17, pp. 25-31; 1929; and in the publication of his, referred to in footnote 5, p. 522.

not always to be interpreted directly. But particles in the corners of the square plate are apparently displaced principally along a diagonal, for this mode of vibration.

The air current pattern for the mode whose surface pattern was first shown in Figure 8, *C*, is given in Figure 13, *B*. It shows that the displacement is principally in the direction of the optic axis.

Air current patterns for the different cuts and shapes may be obtained in large numbers. Only a few are shown and discussed here.

(c) SPECIALLY ORIENTED 0° AND 30° CUT RECTANGULAR PLATES AND RODS

As previously indicated, results of these studies show that the directions of maximum displacement in several of the low frequency modes of 0° circular plates are to be found nearly parallel to the direction of some one of the critical values of Young's modulus, and to have similar tendencies in low-frequency modes of 0° rectangular plates. Acting upon this information, four rectangular plates were cut, three 0° and one 30°, each with length parallel to one of these critical directions.[18] Two of the 0° plates and the one 30° plate are shown in Figure 14, together with the pattern of the mode found for each in which the displacements are principally parallel to the lengths as indicated both by the fact that the "nodal" lines form perpendicular to the lengths and by the nature of the accompanying air current patterns. The remaining 0° plate, which was cut with length parallel to the critical direction of Young's modulus in the 0° plane to be found at $\gamma = +10° 50'$, could not be caused to vibrate with sufficient amplitude to produce an air current pattern. However, a similar simple mode of vibration was found for this plate, as evidenced by the nodal line perpendicular to its length.

In Figure 15 is shown a 0° rectangular plate of the conventional orientation, in company with the pattern caused by vibration at the one of its modes having principal displacements most nearly parallel to its length. The "nodal" line forms, as shown, in a direction inclined to the edges. The displacements experienced by this plate are thus seen to be of a more complex nature than those depicted in Figure 14.

Referring again to Figure 14, if the frequency in any one of the three cases shown were squared and multiplied by the square of twice the greatest dimension of the corresponding plate and by 2.654, the density in grams per cubic centimeter, there would result, as shown below, a value which corresponds very closely to the value of Young's modulus for the direction parallel to this greatest dimension. The same is true of the 0° plate which was so oriented in cutting that its greatest dimension is parallel to the direction, $\gamma = +10° 50'$, for which no air current pattern is shown. This plate is 32.71 by 22.70 by 4.81 mm, and its frequency of response at that mode involving a "nodal" line perpendicular to its greatest dimension, is 95.4 kc. The operations indicated above for these four cases give, in kilomegabaryes (10^9 dynes per cm^2) 692, 1,035, and 1,298 for the specially oriented 0° plates, and 1,051 for the specially oriented 30° plate. The corresponding values of Young's modulus are, as given in Appendix II, respectively, 691, 1,014, 1,285, and 1,045, in the same units. The

[18] A patent was taken out by the Telefunken Co. (Patent No. 294174) for orientations of quartz plates, presumably 0°, such that edges would be parallel and perpendicular to the directions γ=48° and 70°, as reported in the Wireless World, May 29, 1929.

former values, it will be noticed, are in each case slightly larger, but all are within 3 per cent.

In order to determine how closely the length and frequency of rods cut in these various critical directions would agree with the computed values of Young's modulus (which, of course, are based on measurements of certain elastic constants, as explained in Appendix II), rods of square cross section were cut from each of these plates in such a manner as to leave the length and thickness dimension undisturbed. The frequencies of these rods were found to be 82.7, 95.2, 119.7, and 69.6 kc. With the given lengths results are obtained which agree with the theoretical critical values of Young's modulus given above within less than 2 per cent. These results are to be found entered in Table 1, column 5. In column 6 appear corresponding values which have been approximately corrected for lateral effects. The arbitrary correction factor used, the nature of which is explained at the bottom of the table, reduces to that proposed by Chree [19] when σ_1 is placed equal to σ_2; in fact, this is about the only justification that may be advanced for its use, except that it would result in a little closer approximation, in all probability, than would the one proposed by Chree into which some average value of σ is substituted.[20] The corresponding computed values of Young's modulus are to be found in column 7. In column 8 are given the per cent deviation between values in columns 6 and 7.

It is interesting to note in this respect that the length and frequency of three of the longer 0° rods used by Cady give values agreeing no closer than from 5 to 14 per cent, when corrected for lateral effects, with the computed value of Young's modulus in the direction of their length, namely, 770 kilomegabaryes. One [21] of these was 12.02 by 2.16 by 1.08 mm with a frequency of 235.9 kc. A second,[22] whose frequency was 91.66 kc, measured 30.3 by 2.64 by 1.23 mm. The third,[22] resonating at 89.87 kc, measured 30.7 by 4 by 1.4 mm. These all have one lateral dimension about 10 to 12 per cent of the length, while the other lateral dimension is much less. Operations similar to those above give the results, respectively, 880, 819, and 808 kilomegabaryes. The ratios of the greater of the two lateral dimensions to the length dimension are approximately 18, 9, and 13 per cent, respectively.

Measurements of the maximum radial displacement for the first mode of a 0° circular plate gave a result 1° 50′ greater than the predicted angle of the minimum value of Young's modulus. This indicates a possibility of a discrepancy between actual and predicted direction of this minimum. In order to verify the angle at which the actual minimum occurs, three 0° rods were cut, all of the same length, with such orientations that their lengths are parallel, respectively, to the three directions, $\gamma = +67.31°, +71.56°, +73.74°$. The fundamental frequencies at which these rods respond proved to be, respectively, 79.117, 79.007, and 79.242 kc. The first of these frequencies is 0.30 per cent and the third 0.14 per cent higher than the second. Assuming for each the same correction for lateral inertia

[19] C. Chree, On Longitudinal Vibrations, Quart. J. Math., **23**, pp. 317–342; 1889.

[20] It might be well to explain here that although a correction factor of this nature can not be considered adequate or appropriate for rods whose lateral dimensions are as proportionately great as some given in the table, its use should nevertheless place the values given in column 5 on a more compatible basis.

[21] W. G. Cady, An International Comparison of Radio Wave-Length Standards by Means of Piezo-Electric Resonators, Proc. I. R. E., **12**, pp. 805–816; 1924.

[22] W. G. Cady, Piezo-Electric Standards of High Frequency, J. Opt. Soc. Am. & Rev. Sci. Inst., **10**, pp. 475–489; 1925.

effects, and using the computed values of Young's modulus, the frequency of the first rod would be 0.26 per cent and the frequency of the third 0.07 per cent greater than that of the second. From this we may conclude that the predicted and actual angles of the minimum of Young's modulus agree within a degree. The dimensions of the three rods, which are all quite accurately oriented in the 0° plane (probably ±0.1°) are given in Table 1.

Concerning the frequencies of these rods, it will be seen that the values given in columns 6 and 7 opposite the one whose length is oriented parallel to the direction $\gamma = +71.56°$ differ by 0.97 per cent. This is in close agreement with the corresponding variation for the first rod given in the table, considering the (measured) direction along which the first rod is oriented.

Another rod was cut from a 30° rectangular plate of the usual orientation. The results for this rod are shown in Table 1, for $\gamma = \pm 90°$. Inasmuch as Young's modulus passes through a minimum at this angle in the 30° plane it was hoped that its value might thus be verified for the equatorial plane. Unfortunately the discrepancy turned out to be one of the largest.

It will be noted that with one exception all the "high frequency values" of Young's modulus are greater than the computed values. It appears quite possible that this excess, which is made more evident when lateral inertia effects are taken into account, may be in part a manifestation of elastic hysteresis. Experimenters studying mechanically excited vibrations of isotropic rods have uncovered such a discrepancy. However, the variations are all less than 2 per cent and three are within 1 per cent.

TABLE 1

Cut	γ in degrees (assumed)	Size			Frequency	$4\rho l^2 f^2 \times 10^{-9}$	$4\rho l^2 f^2 \times k^2 \times 10^{-9}$	$E \times 10^{-9}$ (theoretical)	Departure	γ in degrees (measured)
		Thickness	Breadth	Length						
1	2	3			4	5	6	7	8	9
		mm	mm	mm	kc				*Per cent*	
0°----------	+71.60	4.81	18.27	30.985	82.4	692.00	707	691	----------	+71.95
		4.805	4.80	30.985	82.7	697.00	699	691	+1.16	+71.95
0°----------	+10.83	4.81	22.70	32.716	95.4	1,035.00	1,037	1,014	----------	+10.68
		4.803	4.802	32.716	95.2	1,030.00	1,032	1,014	+1.78	+10.68
0°----------	−48.25	4.84	20.62	28.92	120.9	1,298.00	1,304	1,285	----------	−48.95
		4.813	4.813	28.92	119.7	1,274.00	1,279	1,285	−.47	−48.95
30°----------	±29.1	4.84	31.28	45.165	69.7	1,051.00	1,055	1,045	----------	±28.47
		4.836	4.836	45.165	69.6	1,049.00	1,050	1,045	+.48	±28.47
30°----------	±90.0	4.81	18.73	34.517	78.7	783.00	797	770	----------	±90(±0.02)
		4.805	4.827	34.517	78.7	783.00	784	770	+1.82	±90(±0.02)
		4.806	4.814	32.409	79.17	----------	----------	----------	----------	+67.31
0°----------	----------	4.806	4.826	32.409	79.007	696.03	697.7	691	+.97	+71.56
		4.805	4.834	32.409	79.242	----------	----------	----------	----------	+73.74

* $k = \dfrac{1}{1 - \frac{\pi^2}{6}\frac{a^2}{l^2}(a^2\sigma_1^2 + b^2\sigma_2^2)}$ where a is the thickness, b the breadth, σ_1 and σ_2 respective values of Poisson's ratio, and l is the length.

(f) COMMENTS CONCERNING AIR CURRENT PATTERNS

An interesting fact, indicated first by the study of surface patterns and then well substantiated by studies of air current patterns, is that a quartz plate of a given cut will vibrate in much the same way regardless of its shape. The elastic properties appear to be the dominant factor in determining the type of vibration which a quartz plate will execute. Even in the case of the relatively long rod-like

plate shown in Figure 15, the direction of the principal displacement is inclined toward the direction of the minimum Young's modulus. In the case of longer rods this tendency persists. This fact has an interesting bearing on the practice of clamping of 0° rods. It has been demonstrated that the decrement of 0° rods may be reduced by clamping at an angle indicated by the "nodal" line. It indicates also, of course, that improvement may be obtained by cutting the 0° rod either parallel to the maximum or minimum Young's modulus. Rods are being prepared not in these directions, but oriented parallel to the direction $\gamma = -45°$, in which Poisson's ratio for the 0° plane (YZ-plane) is seen (in fig. 22) to be about zero. A rod cut in this direction is very nearly parallel to the direction of the maximum Young's modulus. Thirty-degree rods are being prepared also, parallel to $\gamma = \pm 45°$, in which Poisson's ratio for the 30° plane (XZ-plane) is practically zero. A rod cut in this direction is not very far from the direction of maximum Young's modulus for the 30° plane, but as a matter of fact almost as far as an ordinary 0° rod is from the minimum Young's modulus. Clamping experiments will be performed on these rods.

It was found in these studies of air currents that when plates of various cuts and shapes are caused to oscillate vigorously at one of their strong modes of high-frequency vibration, very pronounced air currents emanate from their uppermost major face. Although more difficult to produce, patterns of lycopodium powder blown from a major face give an excellent insight into the type and configuration of displacement of these higher frequency modes. To produce patterns of this nature the plate is caused to oscillate while in such a position that the major faces lie in vertical planes. A plane metallic surface may serve as one electrode. A screen was found quite convenient for the other. Obviously the wires forming the mesh should be spaced quite far apart, and should be strung only in a horizontal direction. Thus a heavy sheet of paper upon which a layer of lycopodium is sprinkled may be placed close to the major face behind the screen, in a position perpendicular to this face. If the process is carried out at various levels much information may be obtained concerning the displacement of this surface.

Studies of this nature have been carried on, but further work is required before results may be set forth with safety. Indisputable evidence has, however, been obtained through these initial studies that, as must be expected, the major surfaces break up into various antinodal areas at that relatively strong mode responding at the highest frequency, both for 0° and 30° plates. This precludes definitely the possibility of the frequency of response of a mode of this nature being any simple function of Young's modulus, in the direction of the thickness, and the thickness dimension.[23]

[23] As has already been pointed out, Crossley found evidence of this breaking up of the major faces. But notwithstanding this evidence, which he describes in the publication referred to in note 8, he proceeds, as reported in this publication, to measure quantitatively Young's modulus by means of measurements of the thickness of the plate and the frequency of vibration, which values he substitutes in the equation he gives for Young's modulus, namely, $E = V^2D$, in which D is the density, and $V = {}^1TF$, F being the frequency and T the thickness. In so doing he presupposes a half wave length distribution; in fact, he makes the statement: "The thickness of the crystal as previously stated is equal to one-half wave length of sound in quartz for the X-axis oscillation." This is undoubtedly a fallacious conception of the type and configuration of displacement obtaining. As may be expected, therefore, the value of Young's modulus as derived by him does not closely agree with the computed value corresponding to the direction parallel to the thickness dimension of a 0° plate, which computed value has been checked within 2 per cent by the conventional method. Such a conception appears to lead him and others to consider Young's modulus as a constant of the type or mode of vibration rather than a constant of the material itself.

III. EXPERIMENTS OF A MORE SPECIFIC NATURE

1. STUDY OF THE AIR CURRENTS EMANATING FROM THE PERIPHERY OF CIRCULAR 0° PLATES

With the view in mind of determining with greater accuracy the angles of maximum radial displacement for the first and second modes of vibration of a 0° cut circular plate, apparatus illustrated in Figure 16 (*a*) and (*b*) and Figure 17 was set up. The annular scale, *A*, in Figure 16 (*a*) and (*b*), graduated in thirds of a degree, is fixed to a heavy insulating base. Riding on a tapered shaft concentric with the annular scale, *A*, is the rotating member, *B*, in Figure 16 (*b*), with arms, *B'* and *B''*, serving as verniers with which the angular position may be read to within one minute of arc. The revolving member, *B*, is also fitted with an insulated arm, *H*, by which it may be rotated. A cap, *C*, rests on top of the member *B* serving as the final support for the quartz plate, *P*. At the center of the supporting cap, *C*, is a small circular face raised 0.2 mm, upon which the quartz plate, *P*, rests, fixed in position with collodion. Above the quartz plate is the upper electrode *E*, supported on an adjustable arm, *F*. The supporting members, *C*, *B*, and *A*, below the quartz plate serve as the second electrode.

Suspended separately from the rest, on an adjustable supporting arm, *G*, hangs a celluloid vane, *V*, which is in length, measured horizontally, about equal to the diameter of the quartz plate, and in width, measured vertically, about equal to the thickness of the quartz plate. In other words, the effective area of the vane, *V*, is about equal to the projected area of the plate. The vane itself is about one-sixteenth inch thick. It is suspended on a fine tungsten wire which is held by a clamping device, *K*, designed to allow rotation. Centrally fixed to the vane, *V*, is a small mirror, *M*.

Referring now to Figure 17, a condensing lens, *L*, is so interposed between a light source, *L'*, which is some 6 feet distant from the mirror, *M*, attached to the vane, *V*, that a sharp image of the vertical filament appears on a screen, *S*, placed about 15 feet from the mirror, *M*.

Means are provided for determining the angular position the member *B* must take in order that the diameter passing through the centers of the verniers, *B'* and *B''*, on its arms shall pass through the center of the vane, *V*, as well as for holding the vane accurately perpendicular to that radius passing through its center.

When the vane is thus centered by rotation of the member *B*, whose angular position is noted, it is held by the means provided, accurately perpendicular until the light source, *L'*, or the screen, *S*, may be so adjusted that the image of the filament is centered on the screen. The vane is then allowed to hang freely, and is rotated until the filament image is centered on the screen. The quartz plate is then set in oscillation by a single tube (UX210) circuit without regeneration. And the member *B*, is rotated until the filament image again returns to the center of the screen. The angular position of the member *B* is again noted. Of course, steps must be taken to determine, in the case of the first mode of vibration of 0° plates, which of the antinodes is being measured. With the size of vane used measurements of the antinodes of lesser amplitude did not prove practicable.

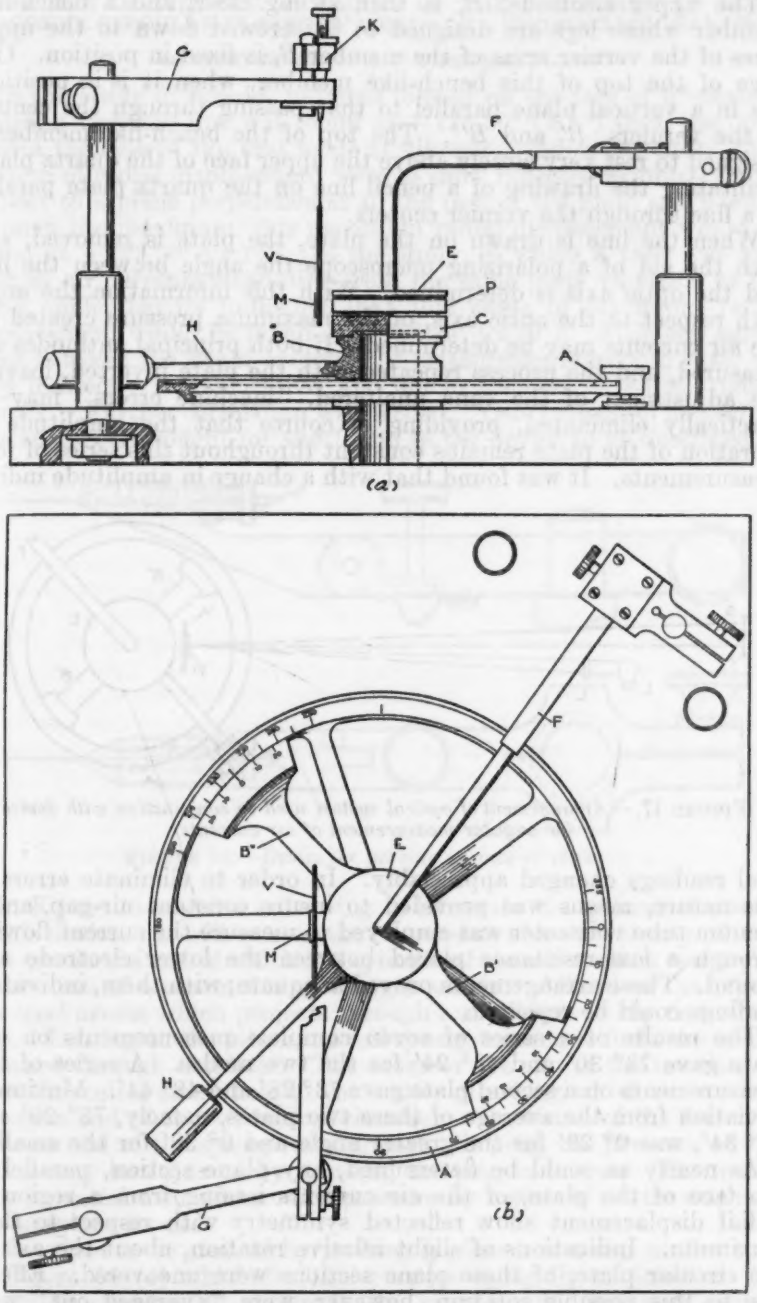

FIGURE 16.—*Device for angular measurements of air currents emanating from periphery of circular plate*

(*a*), elevation; (*b*), plan view.

The upper electrode, E, is then swung clear, and a bench-like member whose legs are designed to be screwed down to the upper faces of the vernier arms of the member B, is fixed in position. One edge of the top of this bench-like member, when it is in position, lies in a vertical plane parallel to that passing through the centers of the verniers, B' and B''. The top of the bench-like member is designed to rest very closely above the upper face of the quartz plate, facilitating the drawing of a pencil line on the quartz plate parallel to a line through the vernier centers.

When the line is drawn on the plate, the plate is removed, and with the aid of a polarizing microscope the angle between the line and the optic axis is determined. With this information the angle with respect to the optic axis, of the maximum pressure created by the air currents may be determined. If both principal antinodes are measured, and the process repeated with the plate inverted, leaving the adjustment of the vane unaltered, "machine errors" may be practically eliminated, providing of course that the amplitude of vibration of the plate remains constant throughout this series of four measurements. It was found that with a change in amplitude indivi-

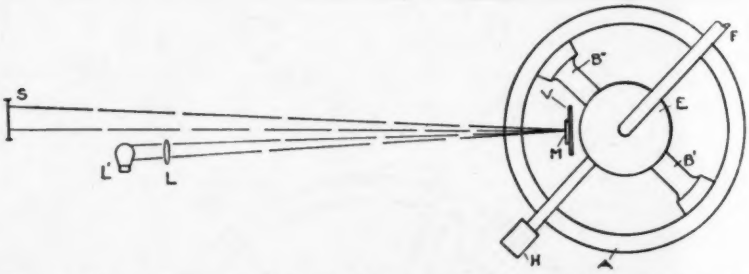

FIGURE 17.—*Arrangement of optical system used in conjunction with device for angular measurement of air currents*

dual readings changed appreciably. In order to eliminate errors of this nature, means was provided to insure constant air-gap, and a vacuum tube voltmeter was employed to measure the current flowing through a low resistance placed between the lower electrode and ground. These arrangements proved adequate; with them, individual readings could be repeated.

The results of a series of seven complete measurements on one plate gave 73° 30′ and 48° 24′ for the two modes. A series of five measurements on a second plate gave 73° 28′ and 48° 44′. Maximum deviation from the average of these two plates, namely, 73° 29′ and 48° 34′, was 0° 29′ for the greater angle and 0° 38′ for the smaller.

As nearly as could be determined, any plane section, parallel to the face of the plate, of the air currents issuing from a region of radial displacement show reflected symmetry with respect to their maximum. Indications of slight relative rotation, about the axis of the circular plate, of these plane sections were uncovered. Effects due to this possible rotation, however, were "averaged out" with the "machine errors." Thus it appears that these measurements should represent quite accurately the angle of maximum radial displacement.

2. STUDIES OF THE DISPLACEMENT OF THE PERIPHERY OF ZERO-DEGREE CIRCULAR PLATES BY MEANS OF A PROBING MECHANISM

(a) FIRST MODE OF A 0° CIRCULAR PLATE

In the study of powder patterns formed on the face of 0° circular plates, a "nodal" line was found at $-17°\ 30'$ ($\pm 1°$) from the optic axis in the case of the first mode of vibration, indicating that, if the pattern of radial displacement were to show reflected symmetry with respect to a plane perpendicular to the face of the plate and passing through the maximum, this maximum radial displacement would be found at $+72°\ 30'$ ($\pm 1°$). In the study, in which a vane was utilized, of air currents emanating from the same plate vibrating at the same mode, results indicated that this angle of maximum radial displacement would be found at $+73°\ 29'$ ($\pm 29'$). Although agreement between the two is evident, the measurements in both cases are only indirectly representative, and not in themselves entirely trustworthy. Further correlation was needed. Other means of measuring this angle were sought for and found in the device to be described.

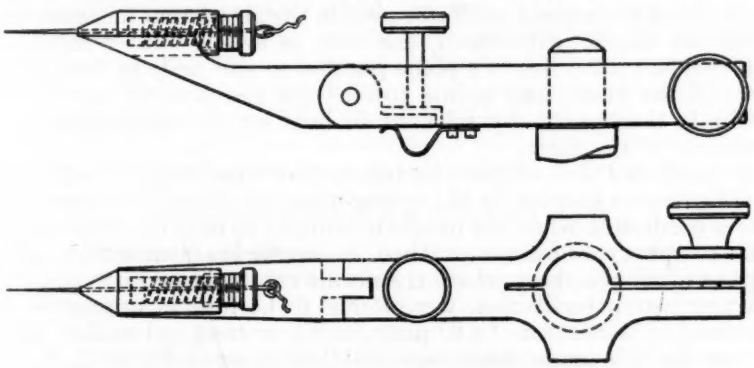

FIGURE 18.—*Device for probing surface of plates*

In Figure 18 is given a drawing to illustrate the general character of this device. It will be seen that it consists of a very sturdy adjustable arm in the end of which is a cylindrical chamber which constrains the motion of a piston fitting snuggly within. Affixed to the piston is a steel needle which projects through a small hole in the end of the arm. Bearing on the piston is a coil spring, tending to force the needle outward through this hole. The other or eye end of the needle projects through a small hole in the center of a plug which screws into the open end of the cylindrical chamber. By virtue of the fact that the rear end of the spring rests against this plug, the pressure on the piston may be adjusted by screwing the plug in or out. The needle may be withdrawn against this pressure by means of a wire attached to the eye in its end.

The plate to be studied by probing is placed on a cap similar to *C* in Figure 16 (*a*) which for this purpose is rigidly attached to the revolving member *B*, shown in the same figure, to insure against relative rotation of the two. In the center of the upper face of this cap is a small raised surface, as before, upon which the quartz plate rests. The cap used in this instance, however, differs from the one used previously in that it embodies two arms. The purpose of these

arms is to allow clamping of the quartz plate, which is obviously necessary if probing operations, with a device such as described, are to succeed. Another cap with corresponding arms is rigidly supported above the one fixed to the member *B*. The means of support consists simply of suitable spacers placed between the arms, which are flat bars, one running across above the upper cap and one running below the lower; with bolts drawing the two bars or arms together. Adequate electrical insulation between the two caps, of course, is provided so that each may serve as an electrode. A screw through the center of the upper cap bears down on the center of the upper face of the quartz plate, pressing the plate down on the small raised surface in the center of the lower cap, thus rigidly clamping the plate.[24] It was found that the plate can be clamped in this manner with sufficient force to prevent it from moving when being probed, without interfering seriously with its oscillation at several modes of low-frequency response.

The probing device is firmly mounted within range of the periphery of the plate thus clamped. The plate is set in oscillation, using the same tuned-plate piezo oscillator used in the air current measurements. With the needle withdrawn, the arm is swung into position and adjusted so that it lies in a plane parallel to and midway between the faces of the plate, and points toward the geometrical center. The needle is then gradually released to bear on the midportion of the periphery of the plate.

It was found that within a certain rather broad range of adjustment of the pressure exerted by the spring upon the piston, the quartz plate ceases oscillation when the needle is brought to bear on certain regions of its periphery, but does not when the needle bears on others. Those regions of its periphery where the needle can be brought to bear without preventing oscillation, were found to be four in number for the first mode of virbation of a 0° plate, and to correspond to the "nodal" regions for this mode, which are well illustrated in Figure 9, *A*. The centers of these "nodal" regions are nodes of radial displacement, but not necessarily points at which displacements of all types vanish.

According to the procedure finally adopted, one of the "nodal" regions is sought out by continued trial, care being taken that the needle is withdrawn each time before the member *B* is rotated, in order to avoid rotation of the plate in the mounting. When one of these regions is located it is probed in minute successive steps, working outward from the center until the point is reached at which the quartz plate first falls out of oscillation. The angular position of the member *B* at this point is recorded. The same "nodal" region is then probed from the center outward in the opposite direction until a second similar point is found, at which the position of the member *B* is again recorded.

The four "nodal" regions are probed numerous times, for individual readings vary as much as 2° or 3°, on the average. The needle is then released to bear on the plate at some point for which the angular position of the member *B* is recorded, and by means of the adjusting screw it is raised vertically while still bearing on the plate, thus marking the periphery of the plate with a very fine line perpendicular to the faces. This process is repeated for the position of the plate

[24] Doctor Hund, while working at the National Bureau of Standards, built a plate holder incorporating this principle of rigid mounting.

represented by a rotation of member B through 180°. These marks are run to the upper face of the plate so that with a straight-edge and a magnifying glass a line may be drawn between them on the face of the plate without the introduction of any appreciable error. With the determination of the angle between the line and the optic axis, which is readily accomplished with a polarizing microscope, the measurement is completely determined.

Six series of such measurements were performed at the first mode. The average of the six series places the "nodes" at $+20° 4'$, $+126° 54'$, $-53° 6'$, and $-159° 56'$ from the optic axis. The "nodes" referred to are, of course, the points midway between the pairs of points at which the plate first falls out of oscillation. Assuming reflected symmetry of the amplitude of displacement with respect to the maximum amplitude, the maximum of one of the principal antinodes would fall at $+73° 29'$. This is exactly the value obtained through measurement of air currents. The fact that the air-current measurements were somewhat more closely related to the maximum displacement than to the minimum, while the probing results are more closely related to the "nodal" regions, which measured on the average with the particular spring used some 8° to 10° in extent, rather than to the antinodal ones, indicates reflected symmetry of amplitude of radial displacement. The maximum deviation from the above average of $+73° 29'$ was $0° 28'$ for the six series. Three of the six series were performed on one plate and three on another. No difference between the two plates was detected in these measurements.

(b) SECOND MODE OF A 0° CIRCULAR PLATE

A similar probing study was made of the second mode of 0° circular plates. Seven series, each consisting of a number of individual readings, averaged $+44° 26'$ ($\pm 48'$) for a line joining the two "nodal" points, indicating that if the displacement were to show reflected symmetry with respect to the maximum, the maximum displacement would take place at $-45° 34'$ ($\pm 48'$). The "nodal" points referred to here as before are the points midway between the pairs of points at which the plate first ceases oscillation. This angle does not agree closely with results obtained through angular measurement of the air currents, namely, $-48° 34'$ ($\pm 38'$). Here we have indication of dissymmetry of radial displacement, made particularly evident, if the measurements are to be trusted, by the fact that the "nodal" regions as measured in this manner averaged in this case approximately 80° in extent, with the particular spring pressure used. Further indication may be found in Figure 9, B, in which the pattern formed by the air currents indicates that the maximum radial displacement is to be found farther from the optic axis than would be the perpendicular bisector of the "nodal" line. Four of the seven series were performed on one plate and three on another. As before, no difference between the two plates was evident.

(c) THE MODE OF A 36.03 BY 4.805 MM 0° CIRCULAR PLATE RESPONDING AT 136 KC

A third probing study was made on the 136 kc mode of oscillation of a 36.03 by 4.805 mm 0° circular plate. Only one series of measurements was carried out. It indicated the presence of a "nodal" point of radial displacement at $+13° 14'$ and another at $-82° 29'$,

the former being somewhat strictly nodal in nature, while the latter appears to be perhaps an antinode of tangential displacement. The surface powder pattern for this mode is given in Figure 3, *F*.

(d) COMMENTS CONCERNING RESULTS OF PROBING STUDIES

The probing operations not only proved successful in themselves as means of studying the oscillations of plates, but, in addition, they help to substantiate the results obtained in the studies of air currents emanating from the plate, in which a vane was utilized. The exact agreement between the results of the two methods of measurement in the case of the first mode of vibration is fairly good reason to believe that this maximum does take place at $+73°\ 29'$ ($\pm 29'$) and that the amplitude of radial displacement closely approaches reflected symmetry with respect to its maximum.

This agreement in the case of the first mode is also a reason for accepting with some confidence the results of the two methods of measurement obtained for the second mode of vibration, which indicate dissymmetry of the amplitude of radial displacement, and a maximum at $-48°\ 34'$ ($\pm 38°$).

Although they have not been thus applied, it is believed that probing methods may be profitably employed as a means of studying the third mode of 0° plates.

IV. COMMENT AND CONCLUSION

Many conclusions may be drawn quite readily from the results of the various methods of study of the vibrations of quartz plates described above. First of all it is increasingly evident that the production and observation of luminous discharge phenomena constitute a relatively poor method of studying these modes of vibration. Certainly no reasons were discovered showing necessity or even desirability of reversion to that method of attack. Another conculsion to be drawn is that there are at our command several quite direct methods for studying modes of vibration of quartz plates which may be employed with greater ease than the optical method involving the production of figures caused by interference of light waves. This optical method, moreover, it not as readily adapted to the study of different modes of vibration.

A third conculsion of a general nature to which attention was called in a preceding section, is that the magnitude and direction of critical values of Young's modulus play an exceedingly important rôle in the determination of the nature of various modes of vibration of plates of an anistropic material.

Turning now to the more specific aspects of these various studies, it is to be concluded that the magnitude of all computed critical values of Young's modulus in the 0° plane, and the maximum value and that one of the two minima which is to be found perpendicular to the optic axis, in the 30° plane, have been experimentally verified within 2 per cent.

In addition to these verifications in magnitude, the direction of one of the critical values of Young's modulus has been verified within about a degree. This critical value is the maximum. The fact that the magnitudes of all critical values except that in the direction of the optic axis (for the 30° plane) have been quite closely verified,

and that one has been verified as to its direction, should be considered as very good reason for accepting the other predicted directions of critical values as accurate within close limits. In other words, it is to be concluded that from the various measurements and observations, the equation for Young's modulus as originally derived and evaluated by Voigt [25] has been found to be quite accurate in all respects.

In general, a large amount of information was gained concerning the oscillation of rods [26] and plates. The relating of the frequencies of the three modes of strongest response of a rectangular plate to its three dimensions is shown to be prompted by misconceptions. [27] Of particular interest were the more specialized studies of the first and second modes of 0° circular plates. These two cases presented convenient sources of detailed information concerning the oscillation of quartz plates. Just why a 0° circular plate oscillates as it does at these two frequencies, to say nothing of other frequencies or other plates, is yet to be learned, of course.[28] But facts have been uncovered which have important bearing on the subject. For instance, the fact that Poisson's ratio for the 0° plane is very small in the directions $\gamma = \pm 45°$, whereas its value in the vicinity of $\gamma = -16°$ is relatively large, is good reason why the two modes may be expected to differ. Furthermore, in view of knowledge concerning these two modes gained experimentally, it must be considered as somewhat of a coincidence that the two frequencies bear the relation of approximately $1 : \sqrt{2}$ despite the fact that the values of Young's modulus in the direction of the maximum radial displacement for the two cases are to each other quite closely as 2 : 1.

In the course of the various experiments seven 0° circular plates were broken during oscillation. Without exception the cleavage planes were found to be roughly perdendicular to the faces of the plate. Whenever a plate cracked in such a manner that two cleavage planes were not parallel, it was found that these planes always intersected the face of the plate at about equal angles from the optic axis, on the average ± 38.1. Three of these plates cracked into but two pieces with a fairly smooth uniform cleavage plane through a diameter, or nearly so, in each case. Unfortunately two of these plates included considerable twinning. As nearly as could be determined, however, all parted at planes intersecting the face of the plate in a direction for which, roughly, $\gamma = +38.1°$. Reasons for these phenomena are not apparent.

As a result of information gained and intimations found in the various studies carried on, experiments are now being performed on the various means of mounting plates and rods which have suggested themselves. Although it is not clear at this point how present general practice may be much improved upon, certain possibilities of improvement in methods of mounting plates and rods which are to be used as standards of frequency, have presented themselves. The experi-

[25] W. Voigt, Bestimmung der Elasticitatsconstanten von Beryll und Bergkrystall, Ann. der Phys., **31**, pp. 474–501 and 701–724; 1889.

[26] Our observations explain very well, for instance, the reason for the variation in intensity, over the end of a 0° rod noticed and reported by E. P. Tawil, Les Ondes Stationnaires Ultra-Sonores Rendues Visibles dans les Gaz par la Méthode des Stries, Compt. Rend. **191**, pp. 92–95; 1930; of the supersonic waves emanating therefrom.

[27] Results of these various studies anwer in a very definite manner many questions such as those brought up by P. T. Kao, Sur les Vibrations du Quartz Piézoélectrique Suivant l'Axe Optique, Compt. Rend. **191**, pp. 768–770; 1930.

[28] See supplementary note, p. 544.

ments on the clamping of rods has already been mentioned. The possibilities offered through the clamping of circular plates at the center, both 0° and 30°, look quite promising. One very interesting method of accomplishing this end involves the drilling of a small hole in the center of each face of the plate to a depth of nearly one-half its thickness. The plate may then be rigidly held by means of two rods fixed to the electrodes. This method, among others, is being tried at present.

The authors wish to acknowledge the inestimable assistance in these studies given them by J. E. Williard, who with the greatest of care cut and ground all the plates and rods with great accuracy, and by E. F. Webb, under whose very capable direction the cutting and grinding was done.

V. SUPPLEMENTARY NOTE

A. Meissner has attempted to relate the preferred angle of radial displacement; that is, the angle of maximum radial displacement, at the two lower modes of response of 0° circular plates, to certain directions determined by the silicon atoms in the lattice structure of quartz, by assuming that the smaller one of the two angles, namely, the angle of maximum radial displacement during oscillation at the second mode, corresponds to that direction in the planes of greatest "atomic density" parallel to the intersection of these planes with the YZ-plane or 0° plane. By "atomic density" he apparently means the number of atoms in a given plane per unit area, times the atomic weight. He tacitly assumes that the other favored angle of radial displacement; that is, the angle of maixmum displacement in the case of first mode, corresponds to that direction determined by the intersection with the 0° plane of planes which have a very low value of this "atomic density." It is rather difficult to conceive how this low value of "atomic density" would bring about angular stability of oscillation.

However this may be, he proceeds to explain, referring to that element of the silicon atom lattice structure which, according to some indications (see Sosman, Properties of Silica), somewhat closely resembles a cube, one of whose diagonals lies parallel to the principal crystallographic axis, that if that diagonal of the rhombohedron parallel to the optic or principal axis is sufficiently reduced in dimension relative to the interatomic distances, which are left undisturbed, measured in planes perpendicular to the optic axis, planes of maximum "atomic density" will be inclined about −37° with respect to the optic axis. The "complementary" angle would be in this case about +58°. This is the angle at which planes which pass through approximately $1/\sqrt{2}$ as many silicon atoms as do the planes of maximum "atomic density" intersect the YZ or 0° plane. He found that the smaller one of these two angles corresponded well with the lowest values of the angles of maximum radial displacement for the two modes of oscillation, measured by various means experimentally, and reported by him variously as +71° (±2°) and −48° (±2°) in the publication referred to in note 5; as about −46°in the publication referred to in note 17; and as −44°, −39°, −37°, or −34.5° in the publication referred to in note 7. He lightly passes over the large discrepancy between the larger of these two angles and the measured angle of +71° (±2°), whereas this angular measurement and the corresponding measurement for the other mode, namely −48° (±2°), which were the first reported, agree nicely with those described here. Therefore, if the angles at which these planes intersect the 0° plane are to correspond to the angles of maximum radial displacement for the two modes of oscillation, the length of the diagonal of the rhombohedron parallel to the optic axis must be still further reduced relative to interatomic distances in planes perpendicular thereto. As a matter of fact, the diagonal would have to be reduced to a value less than the interatomic distance in these planes perpendicular to the optic axis, a condition widely different from what is indicated by X-ray and other measurements.

What would appear a more logical attempt, with the purpose in mind of gaining information concerning the ratio $\frac{a}{c}$ would be that to disclose relations which obviously must exist between the well-established elastic characteristics of quartz and the lattice structure. If the dependence of the elastic and piezo-electric

characteristics upon the lattice structure could be entirely disclosed the lattice structure would obviously be determined.

Considering again the rhombohedron, we find indicated dissymmetry in the zero plane (parallel to the diagonal plane cutting two edges and four diagonally opposite corners, and, therefore, including two diagnoals, one of which is that one parallel to the optic axis), and reflected symmetry in the 30° planes. We find that the equatorial plane has a simple relation, easily definable in terms of the atoms it intersects, to the lattice structure. The 0° plane also is seen to be simply or critically related to the lattice structure. The 30° plane is seen, moreover, not to be so critically related, particularly if the presence of two oxygen atoms in the near vicinity of each silicon atom is considered. We find planes of such critical nature making angles of some 30° to 40° and some 50° to 60° with respect to the optic axis, which planes include an X axis, or electric axis. All these critical planes, overlooking the discrepancy in the case of the last two, include directions of critical values of Young's modulus. All in all, we find indications of the intimate relationship which must exist. But discrepancies show that there are probably other factors which must be considered. One of these is no doubt the presence of two similar lattice structures of oxygen atoms. Explanations of why a plane, including the electric axis, which makes an angle of about 11° with the optic axis includes a critical direction of Young's modulus; of why the value of this modulus is the same for all directions in the equatorial plane; and of why the angles at which the two critical planes intersect the YZ plane do not correspond to the angles of maximum and minimum Young's modulus, may all be found if the presence of the oxygen atoms is taken into account.

VI. Appendix I.—THE DEVELOPMENT OF POISSON'S RATIO AND THE MODULUS OF RIGIDITY FOR CRYSTALLINE QUARTZ

When the experimental studies described above were first undertaken it became increasingly evident that the expression for Young's modulus of quartz as a function of direction was practically the only mathematical development available as an aid to the interpretation and understanding of the results. It was deemed very expedient, therefore, to develop and numerically evaluate like expressions for Poisson's ratio and the modulus of rigidity for quartz as functions of orientation.

In general form Love [29] expresses Young's modulus, the modulus of rigidity, and Poisson's ratio in terms of the elastic moduli, respectively, as

$$E=\frac{\Delta}{\phi} \tag{1}$$

$$\mu=\frac{\Delta}{\phi'} \tag{2}$$

and

$$\sigma=-\frac{1}{2\phi}\left[l'^2\frac{\partial\phi}{\partial(l^2)}+m'^2\frac{\partial\phi}{\partial(m^2)}+n'^2\frac{\partial\phi}{\partial(n^2)}\right.$$
$$\left.+m'n'\frac{\partial\phi}{\partial(mn)}+n'l'\frac{\partial\phi}{\partial(nl)}+m'l'\frac{\partial\phi}{\partial(ml)}\right] \tag{3}$$

in which

$$\phi=(S_{11}, S_{22}, \cdots S_{12}, \cdots)\ (l^2, m^2, n^2, mn, nl, lm)^2 \tag{4}$$

and

$$\phi'=(S_{11}, S_{22}, \cdots S_{12}, \cdots)\ (2ll', 2mm', 2nn', mn'+m'n, nl'+n'l, lm'+l'm)^2 \tag{5}$$

[29] A Treatise on the Mathematical Theory of Elasticity.

In these expressions the terms S_{rs} are the various minors [30] of the determinant, Δ, of the elastic constants, and l, m, n, and l', m', n' are direction cosines. In the expression for Young's modulus the direction (l, m, n) is that of the related simple stress. In the expression for the rigidity the directions (l, m, n) and (l', m', n') correspond to the normals to the pair of orthogonal planes across which the related stress is considered. And in the expression for Poisson's ratio the direction (l, m, n) is to be indentified with that of the principal stress and (l', m', n') that of the accompanying lateral stress, or vice versa.

Voigt,[31] through considerations of symmetry, determined the following relations among the elastic constants of quartz:

$$\begin{aligned} c_{22} &= c_{11} & c_{55} &= c_{44} \\ c_{23} &= c_{13} & c_{56} &= c_{14} \\ c_{24} &= -c_{14} & c_{66} &= \frac{c_{11}-c_{12}}{2} \end{aligned}$$

and

$$c_{15}=c_{16}=c_{25}=c_{26}=c_{34}=c_{35}=c_{36}=c_{45}=c_{46}=0 \tag{6}$$

The orientation assumed by him in determining these relations involved the coincidence of the principal crystallographic axis with the Z axis, electric axis with the X axis, and "mechanical" axis with the Y axis, as illustrated in Figure 25.

The corresponding relations among minors is then:

$$\begin{aligned} S_{22} &= S_{11} & S_{55} &= S_{44} \\ S_{23} &= S_{13} & S_{56} &= 2S_{14} \\ S_{24} &= -S_{14} & S_{66} &= 2(S_{11}-S_{12}) \end{aligned} \tag{7}$$

and

$$S_{15}=S_{16}=S_{25}=S_{26}=S_{34}=S_{35}=S_{36}=S_{45}=S_{46}=0$$

With these relations (7) the function ϕ given in (4) may be expanded in the form

$$\begin{aligned} \phi = {} & S_{11}l^4+S_{11}m^4+2S_{11}l^2m^2+S_{33}n^4+(S_{44}+2S_{13})\ (l^2n^2+m^2n^2) \\ & +2S_{14}mn\ (3l^2-m^2) \end{aligned} \tag{8}$$

$$\begin{aligned} = {} & S_{11}+(S_{11}+S_{33}-S_{44}-2S_{13})\cos^4\gamma-(2S_{11}-S_{44}-2S_{13})\cos^2\gamma \\ & -2S_{14}\sin^3\gamma\cos\gamma\cos 3C \end{aligned} \tag{9}$$

where γ represents the angle measured from the optic axis (Z axis), and C, the "angle of cut," is measured from a mechanical axis (Y axis), as shown diagrammatically in Figure 19. This in turn may be written

$$\begin{aligned} \phi = \Delta[& s_{11}+(s_{11}+s_{33}-s_{44}-2s_{13})\cos^4\gamma-(2s_{11}-s_{44}-2s_{13})\cos^2\gamma \\ & -2s_{14}\sin^3\gamma\cos\gamma\cos 3\ C] \end{aligned} \tag{10}$$

where

$$s_{rs}=S_{rs}/\Delta \tag{11}$$

Then from (1)

$$\begin{aligned} \frac{1}{E} = {} & s_{11}+(s_{11}+s_{33}-s_{44}-2s_{13})\cos^4\gamma-(2s_{11}-s_{44}-2s_{13})\cos^2\gamma \\ & -2s_{14}\sin^3\gamma\cos\gamma\cos 3C \end{aligned} \tag{12}$$

[30] The quantities $\frac{1}{2}S_{11}/\Delta, \ldots S_{12}/\Delta, \ldots$ are the coefficients of the strain-energyfunction, which is in this case a function of the stress components. The quantities $S_{11}/\Delta, \ldots 2S_{12}/\Delta, \ldots$ are termed by Voigt the elastic moduli, and denoted by him S_{rs}.

[31] See footnote 25, p. 543.

In a similar manner, from (5)

$$\begin{aligned}\phi' = {} & 4S_{11}\ (l^2l'^2+m^2m'^2)+2S_{11}\ (lm'+l'm)^2-2S_{12}\ \ (lm'-l'm)^2 \\ & +8S_{13}nn'\ \ (ll'+mm')+4S_{33}n^2n'^2 \\ & +S_{44}[(mn'+m'n)^2+(nl'+n'l)^2] \\ & +4S_{14}[ll'(mn'+m'n)-mm'(mn'+m'n)+(nl'+n'l)(lm'+l'm)]\end{aligned} \tag{13}$$

$$\begin{aligned}= {} & \Delta\{s_{44}+(s_{11}+s_{33}-s_{44}-2s_{13})\ \cos^2B\ \sin^2 2\gamma+(2s_{11}-s_{14} \\ & -2s_{12})\ \sin^2B\ \sin^2\gamma+s_{14}[-\cos^2B\ \sin 4\gamma\ \cos 3C \\ & +2\ \sin^2B\ \sin\ 2\gamma\ \cos\ 3C+2\ \sin\ 2B\ \sin\ \gamma(2\cos^2\gamma-\sin^2\gamma)\ \sin\ 3C]\}\end{aligned} \tag{14}$$

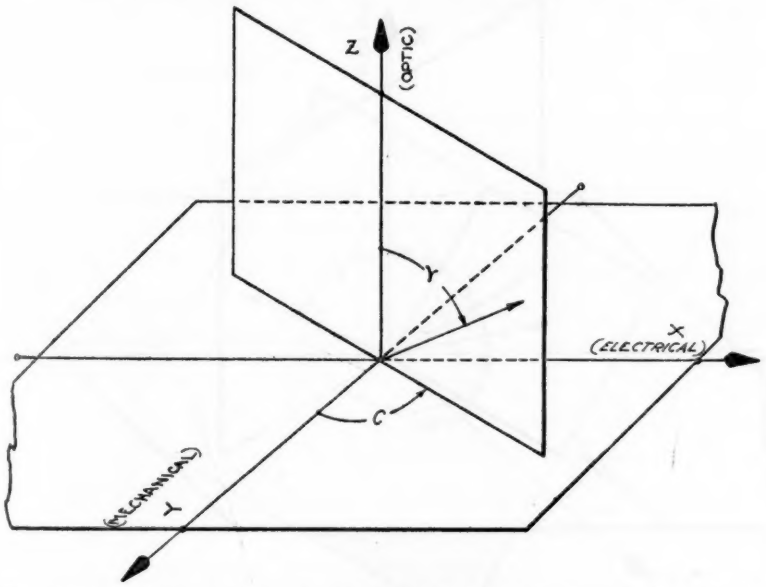

FIGURE 19.—*Diagrammatic illustration of the angles represented by* γ *and* C.

In this expression the angle B is that illustrated in Figure 20.

From (2) then

$$\begin{aligned}\frac{1}{\mu} = {} & s_{44}+(s_{11}+s_{33}-2s_{13})\ \cos^2B\ \sin^2 2\gamma+(2s_{11}-s_{44}-2s_{12})\ \sin^2B\ \sin^2\gamma \\ & +s_{14}[-\cos^2B\ \sin\ 4\gamma\ \cos\ 3C+2\ \sin^2B\ \sin\ 2\gamma\ \cos\ 3C \\ & +2\ \sin\ 2B\ \sin\gamma\ (2\cos^2\gamma-\sin^2\gamma)\ \sin\ 3C]\end{aligned} \tag{15}$$

Having expanded the function ϕ, we proceed with the expansion of the expression for Poisson's ratio, (3)

$$\begin{aligned}\sigma = -\frac{1}{\phi}\Big\{ & S_{11}\ (ll'+mm')^2+S_{12}\ (ml'-lm')^2+s_{13}\ [n^2(l'^2+m'^2) \\ & +n'^2(l^2+m^2)]+S_{14}\ [mn\ \ (l'^2-m'^2)+m'n'\ \ (l^2-m^2) \\ & +2ll'\ \ (mn'+m'n)]+S_{33}n^2n'^2+S_{44}nn'\ (mm'+ll')\Big\}\end{aligned} \tag{16}$$

Using the relation $s_{rs}=S_{rs}/\Delta$, this becomes

$$\sigma=-\Big\{s_{13}+\frac{1}{4}(s_{11}+s_{33}-s_{44}-2s_{13})\ \cos^2B\ \sin^2 2\gamma+(s_{12}-s_{13})\ \sin^2B\ \sin^2\gamma$$

$$+\frac{1}{4}s_{14}\,[-\cos^2B\ \sin\ 4\gamma\ \cos\ 3C+2\ \sin^2B\ \sin\ 2\gamma\ \cos\ 3C+2\ \sin\ 2B\ \sin\gamma$$

$$(2\ \cos^2\gamma-\sin^2\gamma)\ \sin\ 3C]\} \tag{17}$$

$$+[s_{11}+(s_{11}+s_{33}-s_{44}-2s_{13})\ \cos^4\gamma-(2s_{11}-s_{44}-2s_{13})\ \cos^2\gamma-s_{14}\sin^3\gamma\cos\gamma$$

$$\cos\ 3C]$$

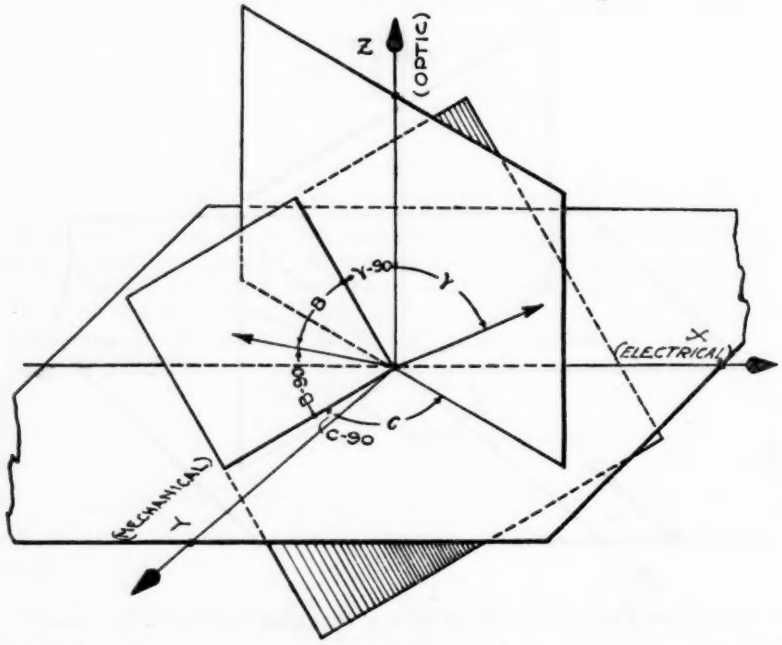

FIGURE 20.—*Diagrammatic illustration of the angles represented by* γ, C, *and* B.

Voigt experimentally determined the following values of the six elastic constants for quartz

$$s_{11}=12.734\times10^{-10}(\pm0.001)\ \text{cm}^2/\text{g}\qquad -s_{12}=1.629\times10^{-10}\ (\pm0.019)\ \text{cm}^2/\text{g}$$

$$s_{33}=\ 9.705\times10^{-10}(\pm0.011)\ \text{cm}^2/\text{g}\qquad -s_{13}=1.486\times10^{-10}\ (\pm0.015)\ \text{cm}^2/\text{g} \tag{18}$$

$$s_{44}=19.665\times10^{-10}(\pm0.018)\ \text{cm}^2/\text{g}\qquad -s_{14}=4.230\times10^{-10}\ (\pm0.10)\ \text{cm}^2/\text{g}$$

Using the mean values, and the value $g=980.6$

$$s_{11}=12.985\times10^{-13}\ \text{cm}^2/\text{dyne}\qquad -s_{12}=1.661\times10^{-13}\ \text{cm}^2/\text{dyne}$$

$$s=_{33}\ 9.897\times10^{-13}\ \text{cm}^2/\text{dyne}\qquad -s_{13}=1.515\times10^{-13}\ \text{cm}^2/\text{dyne} \tag{19}$$

$$s_{44}=20.054\times10^{-13}\ \text{cm}^2/\text{dyne}\qquad -s_{14}=4.314\times10^{-13}\ \text{cm}^2/\text{dyne}$$

With these values, (12) becomes

$$\frac{10^{15}}{E} = 1298.5 + 585.8 \cos^4\gamma - 894.6 \cos^2\gamma + 862.8 \sin^3\gamma \cos\gamma \cos 3C \quad (20)$$

giving E in dynes/cm². Similarly, (15) becomes

$$\frac{10^{15}}{\mu} = 2005.4 + 585.8 \cos^2 B \sin 2\gamma + 923.8 \sin^2 B \sin^2\gamma + 431.4$$
$$[\cos^2 B \sin 4\gamma \cos 3C - 2 \sin^2 B \sin 2\gamma \cos 3C - 2 \sin 2B \sin\gamma \quad (21)$$
$$(2\cos^2\gamma - \sin^2\gamma) \sin 3C]$$

giving μ in dynes/cm².

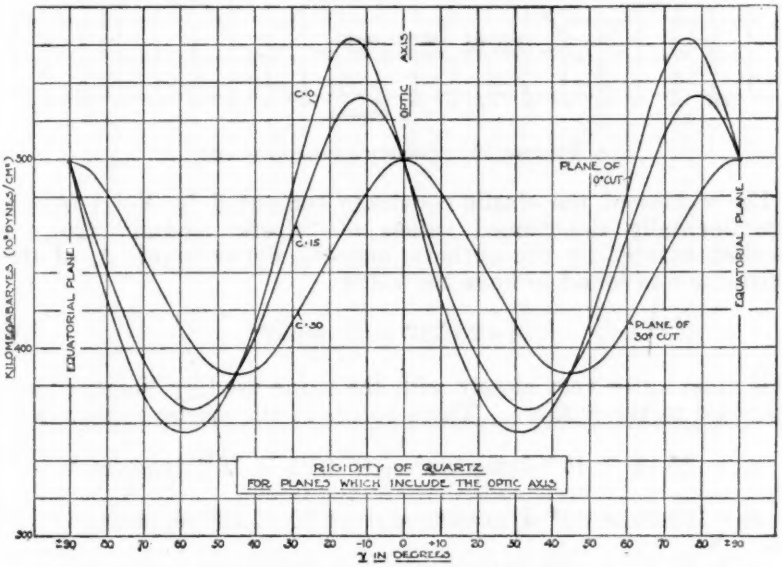

FIGURE 21.—*Modulus of rigidity of quartz*

This when simplified for planes containing the optic axis, becomes

$$\frac{10^{15}}{\mu} = 2005.4 + 585.8 \sin^2 2\gamma + 431.4 \sin 4\gamma \cos 3C \quad (22)$$
giving μ in dynes/cm²

A graph of this is given in Figure 21. And the expression (17) for Poisson's ratio becomes

$$\sigma = \{151.5 - 146.4 \cos^2 B \sin^2 2\gamma + 14.6 \sin^2 B \sin^2\gamma - 1.078$$
$$[\cos^2 B \sin 4\gamma \cos 3C - 2 \sin^2 B \sin 2\gamma \cos 3C - 2 \sin 2B \sin\gamma$$
$$(2\cos^2\gamma - \sin^2\gamma) \sin 3C]\} \quad (23)$$
$$\div [1298.5 + 585.8 \cos^4\gamma - 894.6 \cos^2\gamma + 862.8 \sin^3\gamma \cos\gamma \cos 3C]$$

For planes including the optic axis, this reduces to

$$\sigma = \frac{151.5 - 146.2 \sin^2 2\gamma - 1.078 \sin 4\gamma \cos 3C}{1298.5 - 585.8 \cos^4\gamma - 894.6 \cos^2\gamma + 862.8 \sin^3\gamma \cos\gamma \cos 3C} \quad (24)$$

a graph of which is given in Figure 22.

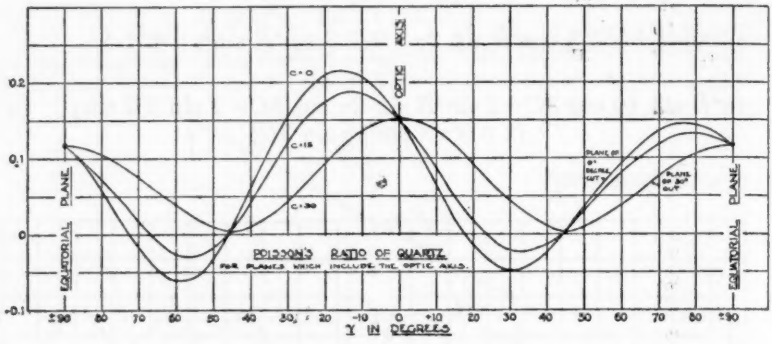

FIGURE 22.—*Poisson's ratio of quartz*

The values of the elastic constants computed by Voigt from his experimentally determined values of "elastic moduli" (20) were checked exactly by the authors, and the determinant, Δ, of these constants was found to have the value

$$\Delta = 7.0727 \text{ (cm}^2\text{/dyne)}^6 \quad (25)$$

This must agree very closely with the value used by Voigt, which is unknown to the authors. These values of the elastic constants are:

$$\begin{aligned} c_{11} &= 85.14 \times 10^{10} \text{ dynes/cm}^2 & c_{12} &= 6.95 \times 10^{10} \text{ dynes/cm}^2 \\ c_{33} &= 105.36 \times 10^{10} \text{ dynes/cm}^2 & c_{13} &= 14.10 \times 10^{10} \text{ dynes/cm}^2 \\ c_{44} &= 57.10 \times 10^{10} \text{ dynes/cm}^2 & c_{14} &= 16.82 \times 10^{10} \text{ dynes/cm}^2 \end{aligned} \quad (26)$$

It might be well to point out that within the limits of error, as specified by Voigt, of measurement of the elastic constants, Poisson's ratio is always greater than zero for the 30° plane. However, interestingly enough, if values of these constants are chosen with the end in view of reducing as much as possible within these limits the minimum value of the ratio for this plane, the smallest value thus obtainable is found to be about half as large as the minimum obtained by using the mean value of these elastic constants. In other words, if the limits of error happened to be slightly wider, the minimum could then be caused, through proper choice of values of the constants, to become zero at $\gamma = \pm 45°$, which, because of the form of the equation, would then cause the curve for the 0° plane to pass through zero at this same angle. If it could be demonstrated that this ratio should be zero at $\gamma = \pm 45°$ for any or all planes that include the optic axis, the number of independent elastic constants would thereby be reduced to five.

VII. Appendix II.—THE EVALUATION OF YOUNG'S MODULUS

Using the equation[32] $\frac{10^{15}}{E} = 1298 + 587 \cos^4\gamma - 895 \cos^2\gamma + 862 \sin^3\gamma \cos\gamma \cos 3C$ expressing E in dynes/cm^2, values of Young's modulus were computed for planes passing through the optic axis at various angles, C, from the YZ plane, and for various angles, γ, measured from the optic axis, in these planes. (See again fig. 19.) These values are to be found tabulated in Table 2, and prepared in the form of a graph in Figure 23. In Figure 24 is reprinted[33] a photograph showing a surface constructed to represent the locus of Young's modulus as a radius vector.

TABLE 2

γ	$C=0°$	$C=5°$	$C=10°$	$C=15°$	$C=20°$	$C=25°$	$C=30°$
−90°	770	770	770	770	770	770	770
−80°	886	882	871	855	833	810	786
−70°	1,045	1,036	1,011	972	927	879	833
−60°	1,203	1,189	1,151	1,095	1,030	963	900
−50°	1,283	1,269	1,230	1,173	1,106	1,037	972
−40°	1,251	1,241	1,215	1,175	1,127	1,076	1,026
−30°	1,158	1,154	1,141	1,122	1,099	1,072	1,045
−20°	1,072	1,071	1,067	1,061	1,053	1,045	1,036
−10°	1,023	1,023	1,022	1,021	1,020	1,019	1,018
0°	1,010	1,010	1,010	1,010	1,010	1,010	1,010
10°	1,014	1,014	1,014	1,015	1,016	1,017	1,018
20°	1,002	1,003	1,006	1,012	1,019	1,027	1,036
30°	952	955	963	977	996	1,019	1,045
40°	869	874	888	910	942	980	1,026
50°	783	789	804	830	868	916	972
60°	719	724	739	764	799	845	900
70°	692	696	708	728	755	790	833
80°	707	710	717	728	745	764	786
90°	770	770	770	770	770	770	770

The maxima and minima of these curves of Young's modulus as an angular function are found to fall at

$$\gamma = -48°15' \qquad \gamma = 0° \qquad \gamma = +10°50' \qquad \gamma = +71°35'$$

for $C=0°$, in which directions the modulus takes the respective values

$$E = 1285 \times 10^9 \qquad E = 1010 \times 10^9 \qquad E = 1014 \times 10^9 \qquad E = 691 \times 10^9$$

the units being dynes/cm^2.

The maxima and minima for $C=30°$ are to be found at

$$\gamma = \pm 90° \qquad \gamma = \pm 29°\ 6' \qquad \gamma = 0°$$

where the corresponding values of Young's modulus are, respectively,

$$E = 770 \times 10^9 \qquad E = 1045 \times 10^9 \qquad E = 1010 \times 10^9$$

in dynes/cm^2.

In Figure 25 is shown the sense in which the angle γ is to be taken with respect to the polarization and sense of optical rotation of a crystal. The figure shows that the sense of optical rotation of a given piece of quartz may be determined by the orientation of its elastic properties with respect to the sense of its piezo-electric polarization.

[32] Based on g=981 dynes, and Voigt's experimentally determined "moduli." This equation agrees with that given by Sosman, Properties of Silica.

[33] This figure appeared with three similar ones, illustrating changes of Young's modulus with temperature. The one reprinted here represents conditions at 15° C. The four were originally presented by A. Perrier and R. de Maudrot, Elasticité et Symétrie du Quartz aux Températures Élevées, Mémoires de la Société Vaudoise des Sciences Naturales, **1**, pp. 333-363; 1923.

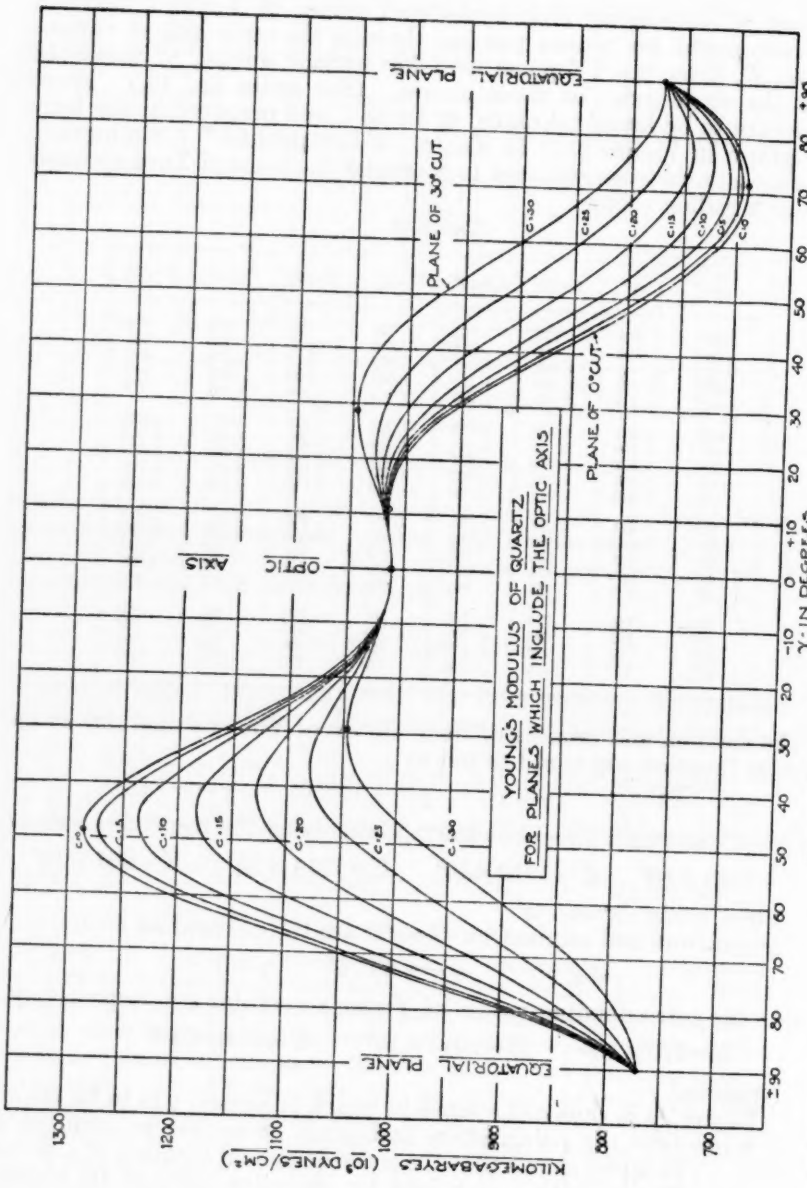

FIGURE 23.—*Linear modulus of elasticity of quartz*

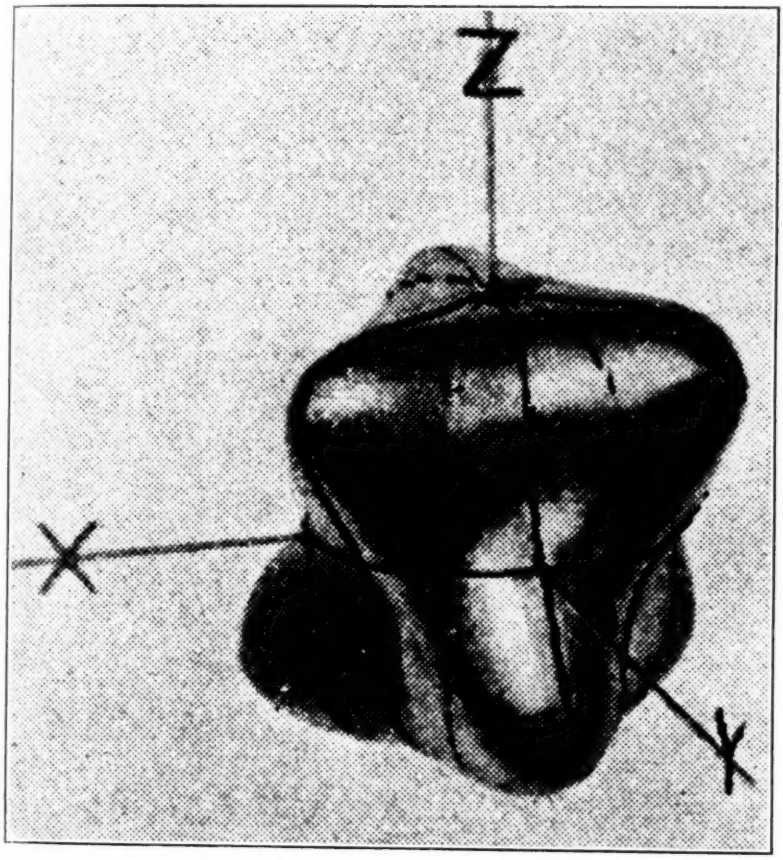

FIGURE 24.—*Surface representing the locus of Young's modulus as a radius vector*

(See Note 33.)

Or, with knowledge of any two or these three characteristics, the other is determined.[34]

It has been found that a very convenient means of determining the sense of the piezo-electric polarization lies in the application of stresses. As may be easily seen, a very large rate of change of stress may be obtained by the sudden releasing of the crystalline plate from forces exerted through a device of high mechanical leverage. And the vacuum tube circuit lends itself quite readily to the measure-

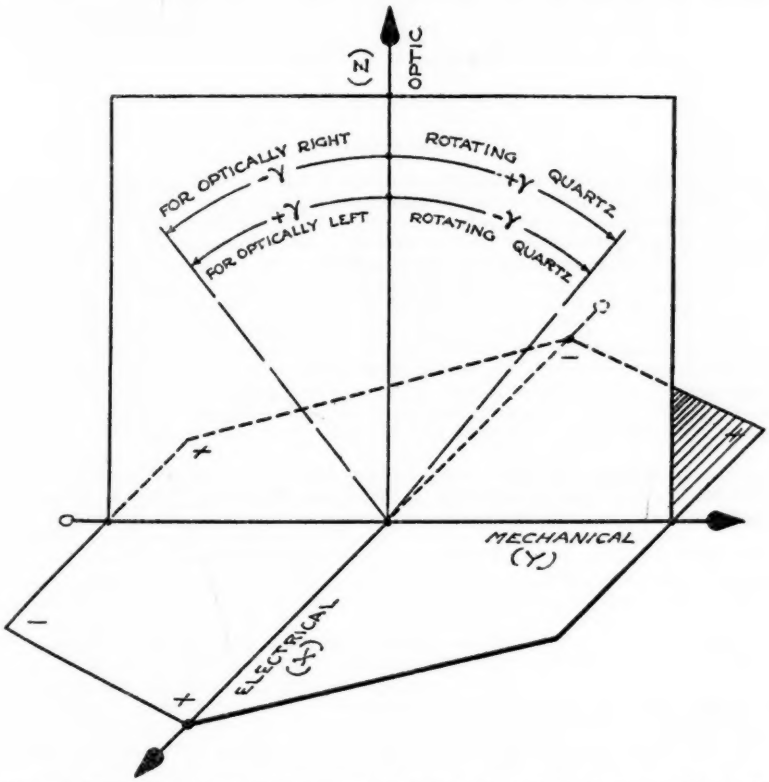

FIGURE 25.—*Diagrammatic representation of orientation of the angle γ with respect to sense of optical rotation (facing source) and piezo-electric polarization*

ment of the time rate of change of the accompanying polarization. Thus, for the case in which the time derivative of the polarization is measured, the polarity accompanying a decrease of pressure applied parallel to an electric axis is to be identified with a corresponding opposing polarity shown in Figure 25 for the orientation of the elastic properties shown therein.

WASHINGTON, June 18, 1931.

[34] This is in accord with observations of A. Meissner to be found in the publication by him, Uber Piezo-Elektrische Kristalle bei Hochfrequenz. Zs. f. techn. Phys., *8*, pp. 74–77; 1927.

AQUEOUS SOLUTIONS OF ETHYLENE GLYCOL, GLYCERIN AND SODIUM SILICATE AS QUENCHING MEDIA FOR STEELS

By Thomas E. Hamill

ABSTRACT

The quenching characteristics of aqueous solutions of ethylene glycol, glycerin, and sodium silicate were studied by means of temperature-time cooling curves on small cylinders of a 0.96 per cent carbon steel quenched in solutions of various concentrations and temperatures. Center cooling curves are given for cylinders one-half inch in diameter by 2 inches long, quenched in aqueous solutions of ethylen glycol and glycerin at atmospheric temperature. Surface and center cooling curves are given for aqueous solutions of two lots of sodium silicate having different soda-to-silica ratios, namely, 1:4 and 1:2.5. These two silicates are designated in this report by these ratios. The effect of increasing the temperature of solutions of the 1:4 soldium silicate from 20° to 80° C. was also studied. The characteristics of these cooling curves and a study of the hardnesses and structures produced suggest that these sodium silicate solutions would be useful for obtaining cooling rates from slightly less than that obtained with water tc that of oil.

Four concentrations of the 1:4 sodium silicate having specific gravities corresponding to 4.6°, 9.5°, 13.2°, and 16.7° B. and two of the 1:2.5 sodium silicate, 12.4° and 28.8° B., were found which gave intermediate cooling rates between those obtained with water and with oil at atmospheric temperature.

Some trouble was experienced with the instability of certain of the aqueous solutions of the 1:4 sodium silicate. The stability of these solutions was greatly increased by the addition of 2 per cent by volume of a solution of sodium hydroxide of specific gravity 1.065.

The wide variations in cooling produced by check tests on aqueous solutions of ethylene glycol and of glycerin indicate that these solutions may not be particularly useful as media for the quenching of steels.

Quenching experiments with "stepped" bars of a 1.06 per cent carbon steel indicate that sodium silicate solutions can be used at atmospheric temperature to provide coolants with graded cooling speeds between those of water and oil.

CONTENTS

	Page
I. Introduction	556
II. Experimental methods and materials	556
III. Quenching experiments with glycol and with glycerin solutions	558
IV. Quenching experiments with soldium silicate solutions	561
1. Effect of varying concentrations of sodium silicates	561
(*a*) Cooling times and cooling rates	561
(*b*) Hardness and microstructure	564
2. Effect of varying the temperature of sodium silicate solutions	565
3. Structure and hardness of "Stepped" specimens quenched in sodium silicate solutions	568
V. Stability of sodium silicate quenching solutions	570
VI. Summary	571
VII. Acknowledgments	571

I. INTRODUCTION

The structure and properties of a quenched steel depend upon both the critical cooling rate of the particular steel in question and the cooling characteristics of the media in which the steel is quenched. In recent years plain carbon steels have been supplemented by alloy steels in which the alloying additions have changed the critical cooling rates. The simplest and most widely used quenching media are water and oil. The cooling characteristics of these two media have been modified by adding salts, alkalis, acids, or other chemical compounds to water, by using water or aqueous solutions at temperatures below or above room temperatures, and by employing emulsions of oil and water.

With quenching solutions available giving a complete graded series of cooling rates, the control of the results to be obtained from quenching both plain carbon and alloy steels is obviously made much more simple. Oil-water emulsions, concentrated sulphuric acid, and hot aqueous solutions have been used in the attempt to supply this need.

Experiments previously made at the National Bureau of Standards on emulsions of water and machine oil showed that the addition to water of only 0.1 per cent of oil, by volume, decreased the cooling rate of the water almost to that of the oil alone. The extreme accuracy that apparently is required in preparing and maintaining emulsions of this type in order to secure quenching solutions of known cooling rates appears seriously to limit the usefulness of such emulsions.

Concentrated sulphuric acid has been used successfully to give cooling rates between those obtained with oil and water.[1] Its disadvantages are its hydroscopic nature. making maintenance of its concentration difficult, and the very great danger to workmen from splashing.

Hot water and hot aqueous solutions are sometimes used to give cooling rates intermediate between those of oil and water.[2] Such solutions require good circulation and accurate control of temperature and concentration.

Solutions of glycerin also have been used as quenching media. Scott[3] reported that glycerin-water solutions "effectively bridge the gap between oil and water."

The present investigation was directed chiefly toward a study of solutions of sodium silicate as quenching media which it was expected might give cooling rates intermediate between those of oil and of water. Some attention was also given to the behavior of solutions of ethylene glycol and of glycerin when used as quenching media.

II. EXPERIMENTAL METHODS AND MATERIALS

The experimental method employed in the present investigation was based on the classical work of LeChatelier,[4] who first succeeded in devising means for recording photographically the temperature changes taking place over the period of a few seconds in small speci-

[1] H. J. French and O. Z. Klopsch, Quenching Diagrams for Carbon Steels in Relation to Some Quenching Media for Heat Treatment, Trans. Am. Soc. Steel Treating, **3**, p. 284; 1924.

[2] H. J. French and T. E. Hamill, Hot Aqueous Solutions for the Quenching of Steels, B. S. Jour. Research, **3** (RP103), p. 399; 1929; Trans. Am. Soc. Steel Treating, **16**, p. 711; 1929.

[3] H. Scott, Quenching Properties of Glycerin and its Water Solutions, Trans. Am. Soc. Steel Treating, **6**, p. 31; 1924.

[4] H. LeChatelier, "Etudes sur la trempe de l'acier," Revue de Métallurgie, **1**, p. 473; 1904.

mens of steel quenched in various coolants. LeChatelier's method was further developed by Benedicks[5] and employed in studying the influence on quenching rates of the surface of the steel, the rate of motion of the steel, the dimensions, mass, and chemical composition of the specimen, the temperature of the quenching bath, and other factors.

In the present work determinations were made of surface and center cooling curves of steel cylinders one-half inch diameter by 2 inches long, quenched from 875° C. in several coolants at various temperatures from 20° to 80° C. The quenching media were moving with a velocity of 3 feet per second. The time-temperature curves were obtained on a moving photographic film by a method previously described in detail[6] in which thermocouples suitably mounted at the center or on the surface of the steel specimen were connected to an Einthoven "string galvanometer."

In addition to the determination of cooling curves on the plain cylindrical specimens, hardness determinations was made on the steel at the surface and at the center of the specimens. A study was also made of the hardness and microstructure developed in cylindrical "stepped" bars (fig. 13) which were machined to have abrupt changes in diameter from one-fourth to one-half inch to 1 inch.

The surface hardness of the quenched cylinders was taken as the average of six determinations made along the length of the cylinder on the side meeting the direct flow of the liquid during quenching. These tests were made after removing about 0.01 inch of metal from the surface by wet grinding to form a narrow flat strip along the length of the cylinder. The center hardness was determined from tests made after cutting the cylinders in half (transversely) under a water spray.

Two steels were used in the preparation of specimens, one for the plain cylindrical specimens for cooling curves and second for the "stepped" bars. They differed but slightly in composition both being practically a 1 per cent plain carbon steel.

TABLE 1.—*Chemical composition of steel specimens*

	Carbon	Manganese	Silicon	Phosphorus	Sulphur
Plain cylinders	0.96	0.28	0.18	0.016	0.028
"Stepped" bars	1.06	.24	.18	.014	.016

Commercial sodium silicate from two sources was used in the preparation of the silicate quenching solutions. The two lots differed in soda-to-silica ratios. One contained approximately 6 per cent Na_2O, 25 per cent SiO_2 by weight, and the other approximately 11 per cent Na_2O, 27 per cent SiO_2, the balance being water in each case. The ratios of soda to silica were thus nearly 1:4 and 1:2.5. The two solutions are referred to in this report by these ratios. While the 1:4 silicate was cloudy the 1:2.5 silicate was quite clear, apparently due to its higher proportion of Na_2O.

The diluted solutions of sodium silicate, ethylene glycol, and glycerin were prepared in the concentrations shown in Table 2. The

[5] C. Benedicks, The Cooling Power of Liquids, Quenching Velocities, J. Iron and Steel Inst., **2**, p. 153; 1908.

[6] See footnote 1, p. 556.

thoroughly stirred solutions were allowed to stand for several hours and again stirred in order to cause complete solution before they were used in the quenching experiments.

The prepared quenching oil was the same commercial quenching oil that has been used in previous studies on quenching at the National Bureau of Standards and designated there as No. 2 oil. Its physical properties have been given in a previous publication.[7]

TABLE 2.—*Concentrations and specific gravities of the sodium silicate, glycol, and glycerin quenching solutions*

SOLUTIONS OF 1:4 SODIUM SILICATE

Per cent by volume		Specific gravity at 20° C./15.6° C.	° B.
Sodium silicate	Water		
10	90	1.030	4.6
20	80	1.070	9.5
30	70	1.100	13.2
40	60	1.130	16.7
60	40	1.190	23.2
100	0	1.300	33.5

SOLUTIONS OF 1:2.5 SODIUM SILICATE

20	80	1.093	12.4
60	40	1.248	28.8
100	0	1.405	41.8

ETHYLENE GLYCOL SOLUTIONS

Ethylene glycol	Water	Specific gravity at 20° C./15.6° C.	° B.
20	80	1.033	-------
60	40	1.083	-------
100	0	1.113	-------

GLYCERIN SOLUTION

Glycerin	Water	Specific gravity at 20° C./15.6° C.	° B.
60	40	1.165	

III. QUENCHING EXPERIMENTS WITH GLYCOL AND WITH GLYCERIN SOLUTIONS

The center cooling curves of the one-half by 2 inch cylinders of the 0.96 per cent carbon steel quenched in ethylene glycol and aqueous solutions of 20 and 60 per cent glycol and of 60 per cent glycerin are shown in Figure 1. The velocity of the quenching medium was 3

[7] See footnote 2, p. 556.

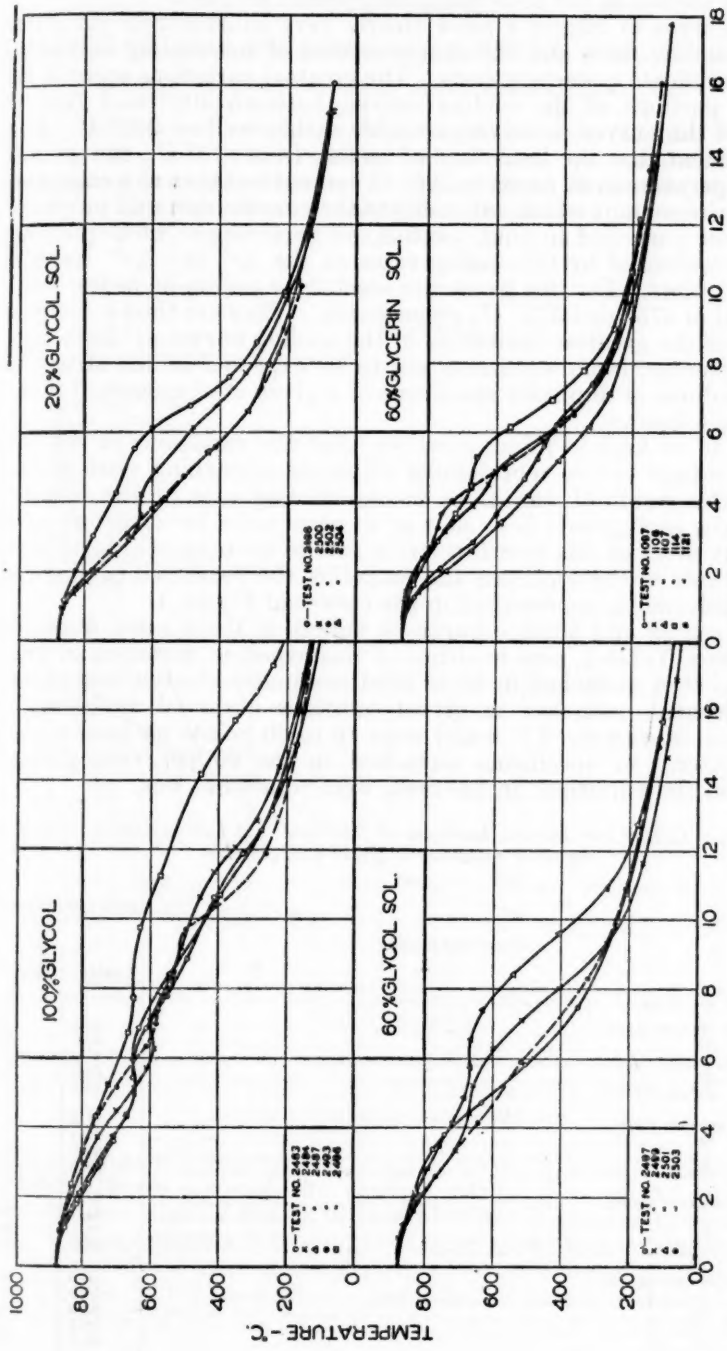

FIGURE 1.—*Center cooling curves of 0.96 per cent carbon steel cylinders quenched into aqueous solutions of glycol and glycerin at 20° C.*

feet per second in the tests with glycol and the glycol solutions and 1 foot per second in the tests with the glycerin solution.

The curves of Figure 1 show clearly very considerable variations in the cooling rates and the characteristics of the cooling curves between duplicate quenching tests. The greatest variations occur in the middle portions of the cooling curves, between 300° and 700° C. Most of the curves, however, coincide rather well at 200° C. It is thus evident that the total time of cooling from 875° C., the quenching temperature in all cases, to 200° C. can not be taken as a characteristic of the coolant which will indicate the constitution and properties of a steel quenched in that solution. The structure of a quenched steel is controlled by the cooling rates at the Ar′ and Ar″ transformation points. For this particular steel these points lie in the neighborhood of 675° and 375° C., respectively. They are thus in the very region of the greatest variations in the cooling curves of check tests. Consequently, large variations are to be expected in the structures and hardness of duplicate specimens of a given steel quenched in any of these solutions.

It is to be kept in mind, however, that the variations in the temperature-time curves representing duplicate quenching tests are not solely the result of variations in the cooling rate of the solution. When the cooling rate is so slow as to permit the Ar[1] transformation the heat effect of this transformation acts to decrease still further the cooling rate of the specimen and magnifies the decreased cooling rate of the solution as represented in the curves of Figure 1.

The center and surface hardness values of these same quenched specimens, Table 3, give evidence of this expected variation in properties of steel quenched in these solutions under identical conditions. In specimens quenched in glycol solutions observed variations in hardness (Rockwell "C" scale) were 10 to 20 points on both surface and center. In specimens quenched in the 60 per cent glycerin solution, the variations in hardness were somewhat less.

TABLE 3.—*Center and surface hardness of 0.96 per cent carbon steel quenched in aqueous solutions of glycol and glycerin*

Test No.	Quenching medium	Rockwell hardness, "C" scale	
		Center [1]	Surface [2]
2483	100 per cent glycol	44.1	45.2
2484	do	46.6	65.1
2487	do	43.0	50.7
2493	do	52.8	53.6
2496	do	42.6	46.4
2497	60 per cent glycol	66.2	66.4
2499	do	45.4	66.0
2501	do	46.0	47.8
2503	do	63.1	63.9
2498	20 per cent glycol	57.1	55.0
2500	do	44.1	48.6
2502	do	64.4	64.4
2504	do	65.0	66.2
1097	60 per cent glycerin	58.8	63.8
1106	do	56.9	63.4
1107	do	62.2	64.3
1114	do	58.3	61.5
1121	do	63.2	63.6

[1] Average of 3 tests. [2] Average of 6 tests.

IV. QUENCHING EXPERIMENTS WITH SODIUM SILICATE SOLUTIONS

1. EFFECT OF VARYING CONCENTRATIONS OF SODIUM SILICATES

(a) COOLING TIMES AND COOLING RATES

The surface and center cooling curves obtained on the 0.96 per cent carbon steel cylinders quenched into various concentrations of the 1:4 and the 1:2.5 sodium silicates at 20° C. are shown in Figures 2 and 3. Cooling curves obtained on quenching in water and in oil at 20° C. are also given for comparison.

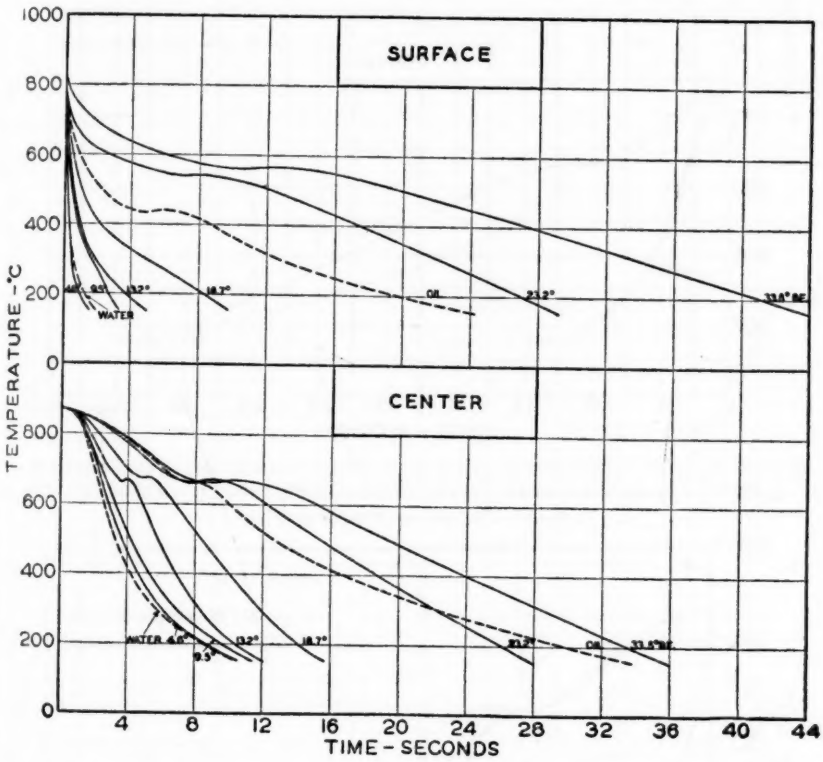

FIGURE 2.—*Surface and center cooling curves of 0.96 per cent carbon steel cylinders quenched into solutions of the 1:4 sodium silicate, water, and oil at 20° C.*

Each curve is the average of two or three tests.

Increasing the concentration of solutions of both the 1:4 and 1:2.5 sodium silicates lowered the cooling rates. The cooling times increased from slightly less than that of water to greater than that of oil. The comparison between the cooling times and cooling rates of oil and one of the more concentrated sodium-silicate solutions is more readily seen in Figure 4 which shows the surface and center cooling curves of the oil and the 23.2° B. solution of the 1:4 sodium silicate.

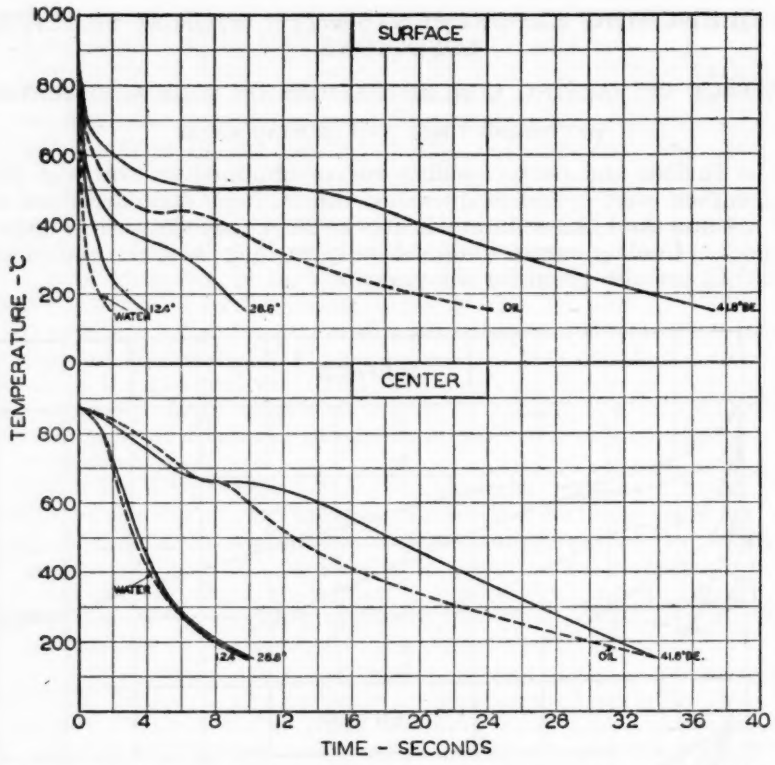

FIGURE 3.—*Surface and center cooling curves of 0.96 per cent carbon steel cylinders quenched into solutions of the 1:2.5 sodium silicate, water, and oil at 20° C.*

Each curve is the average of two or three tests.

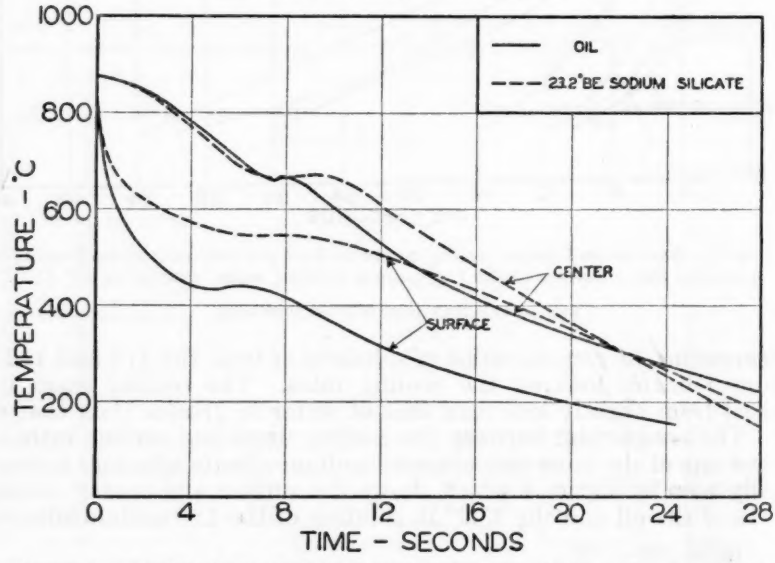

FIGURE 4.—*Replot of surface and center cooling curves of Figure 2, comparing the cooling curves of the oil and2 3.2° B. solution of the 1:4 sodium silicate at 20° C.*

The surface cooling in the 23.2° B., solution is much slower than in the oil, while the center cooling was about the same for both quenching media.

Figures 2 and 3 also show that three concentrations of the 1:4 sodium silicate and two of the 1:2.5 sodium silicate gave cooling rates intermediate between water and oil. These were the 9.5°, 13.2°, and 16.7° B. solutions of the 1:4 sodium silicate and 12.4° and

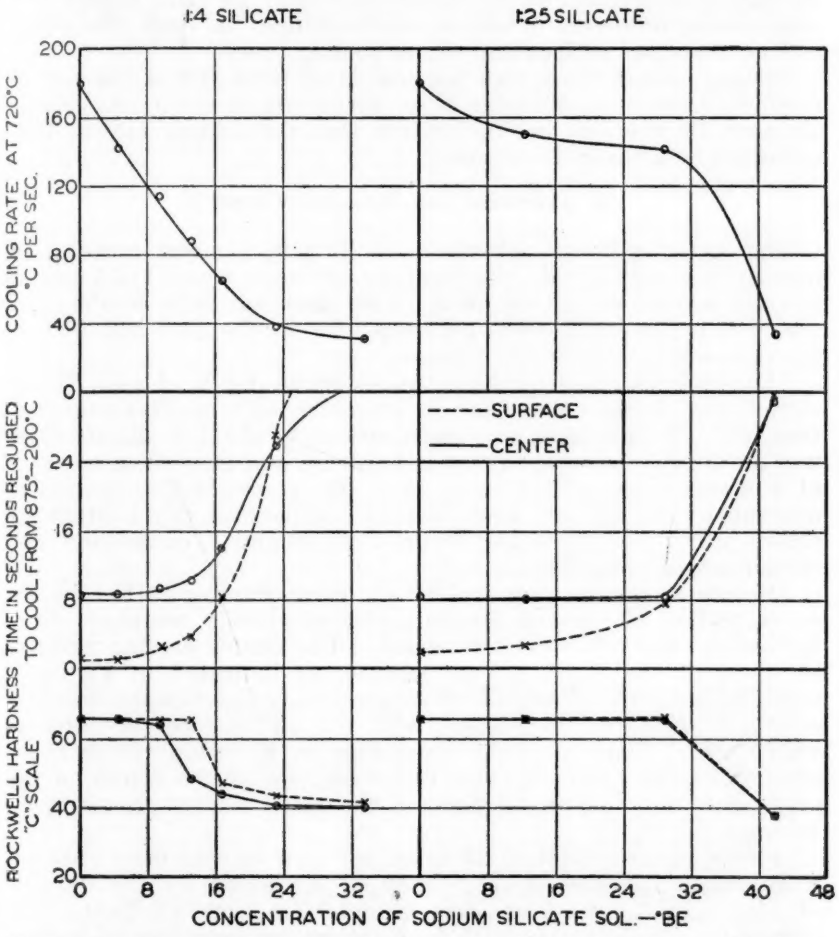

FIGURE 5.—*Center cooling rates and center and surface cooling times and hardness of 0.96 per cent carbon steel cylinders quenched into different concentrations of sodium silicates at 20° C.*

28.8° B. solutions of the 1:2.5 sodium silicate. The 4.6° B. solution of the 1:4 sodium silicate also gave slightly slower cooling than water at the center, but at the surface both cooled about the same except at lower temperatures.

The decrease in center cooling rate and increase in surface and center cooling times with increasing concentrations of the sodium silicate solutions is better shown in Figure 5. The relation between

the center cooling rate and the concentration of the 1:4 sodium silicate is almost linear up to concentrations of approximately 20° B. At higher concentrations the cooling rate changes relatively little with increasing concentration. On the other hand, the 1:2.5 sodium silicate containing the higher soda to silica ratio shows quite different results. With solutions of the 1:2.5 silicate the center cooling rate and surface and center cooling times are very little affected by increasing concentrations up to approximately 28° B. Higher concentrations, however, produced rapid changes in both the center cooling rates and surface and center cooling times.

Surface cooling rates were not calculated from any of the surface cooling curves in as much as these curves are so steep and contain so many fluctuations in temperature that the cooling rate at 720° could not be measured accurately.

(b) HARDNESS AND MICROSTRUCTURE

The center and surface hardness of the 0.96 per cent carbon steel quenched in the several concentrations of the 1:4 and 1:2.5 sodium silicates are shown in Figure 5. The steel was fully hardened at the center (Rockwell C65) on quenching in the 4.6° and 9.5° B. solutions of the 1:4 sodium silicate.

The steel quenched in these two solutions (fig. 6, *A* and *B*) was almost completely martensitic in structure with small amounts of troostite. With increasing concentrations of the 1:4 silicate there was an abrupt decrease in center hardness and in surface hardness at concentrations of 9.5° and 13.2° B., respectively. Increasing amounts of troostite and finally sorbite and pearlite, in the structures shown in Figure 6, *C*, and in Figure 7, *D*, *E*, and *F*, correspond with these changes in hardness.

The center cooling rate at 720° C., corresponding to the highest concentration of the 1:4 silicate giving practically complete center hardening, was 115° C. per second. The center cooling rates in solutions of the 1:2.5 sodium silicate, as indicated in Figure 5, exceeded this critical rate in all concentrations up to approximately a 34° B. solution. Consistent with this are the center hardness values which show complete hardening on quenching in 28.8° B. solution of the 1:2.5 silicate. The structures at the center of the specimens quenched in solutions of the 1:2.5 silicate are shown in Figure 8.

It appears possible that the relatively slow cooling rates obtained with sodium silicate solutions may be explained by the deposits of silica which formed on steel quenched in such solutions. The decrease in cooling rate with increase in concentration of sodium silicate may be due to the increase in thickness of the layer of silica that deposits on the steel during quenching. While no definite measurements were taken, it was observed that cylinders quenched in low concentrations of sodium silicate had a much thinner layer of silica than those quenched into highly concentrated solutions. Photographs of quenched "stepped" bars (fig. 14) verify this observation.

The only known difference between the two sodium silicates used in these experiments is that of the soda-to-silica ratios, the 1:2.5 silicate having the higher ratio—a greater proportion of alkali. This may account for the greater cooling rates observed in the lower

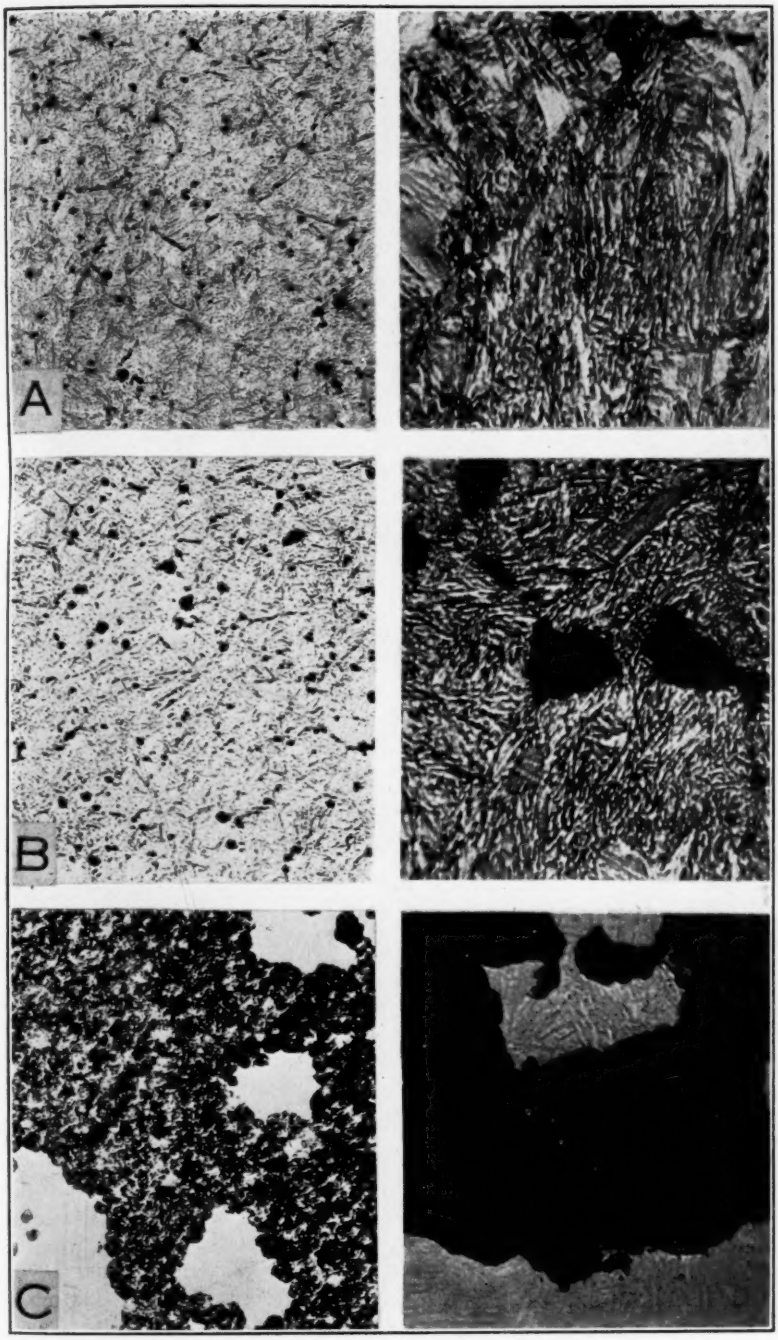

FIGURE 6.—*Microstructures at the center of 0.96 per cent carbon steel cylinders quenched from 875° C. into different concentrations of the 1:4 sodium silicate at 20° C.*

Etched in 2 per cent nitric acid in alcohol. Magnification, left ×100 and right ×1,000. *A*, quenched into 4.6° B. solution; *B*, quenched into 9.5° B. solution; *C*, quenched into 13.2° B. solution.

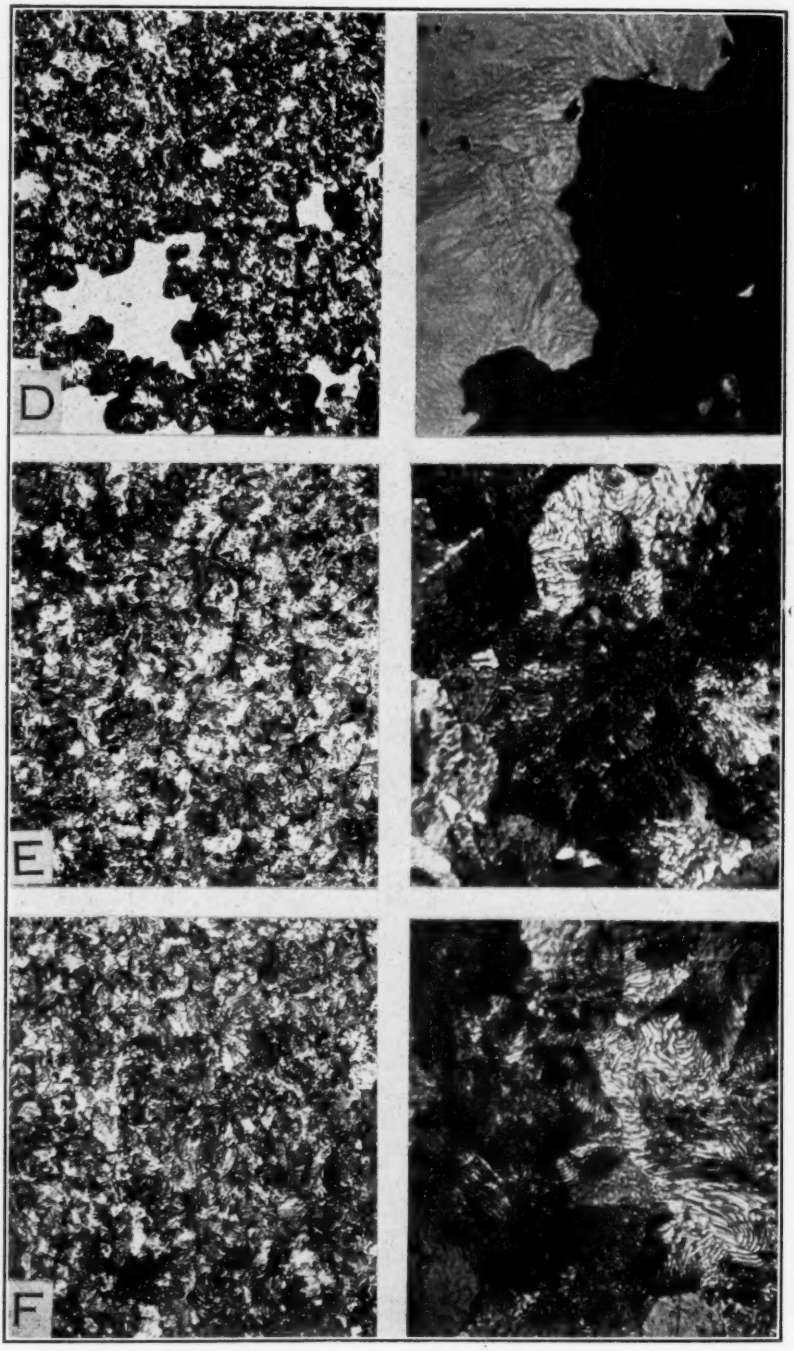

FIGURE 7.—*Microstructures at the center of 0.96 per cent carbon steel cylinders quenched from 875° C. into different concentrations of the 1:4 sodium silicate at 20° C. Magnification left × 100 and right × 1,000*

Etched in 2 per cent nitric acid in alcohol. *D*, quenched into 16.7° B. solution; *E*, quenched into 23.2° B. solution; *F*, quenched into 33.5° B. solution.

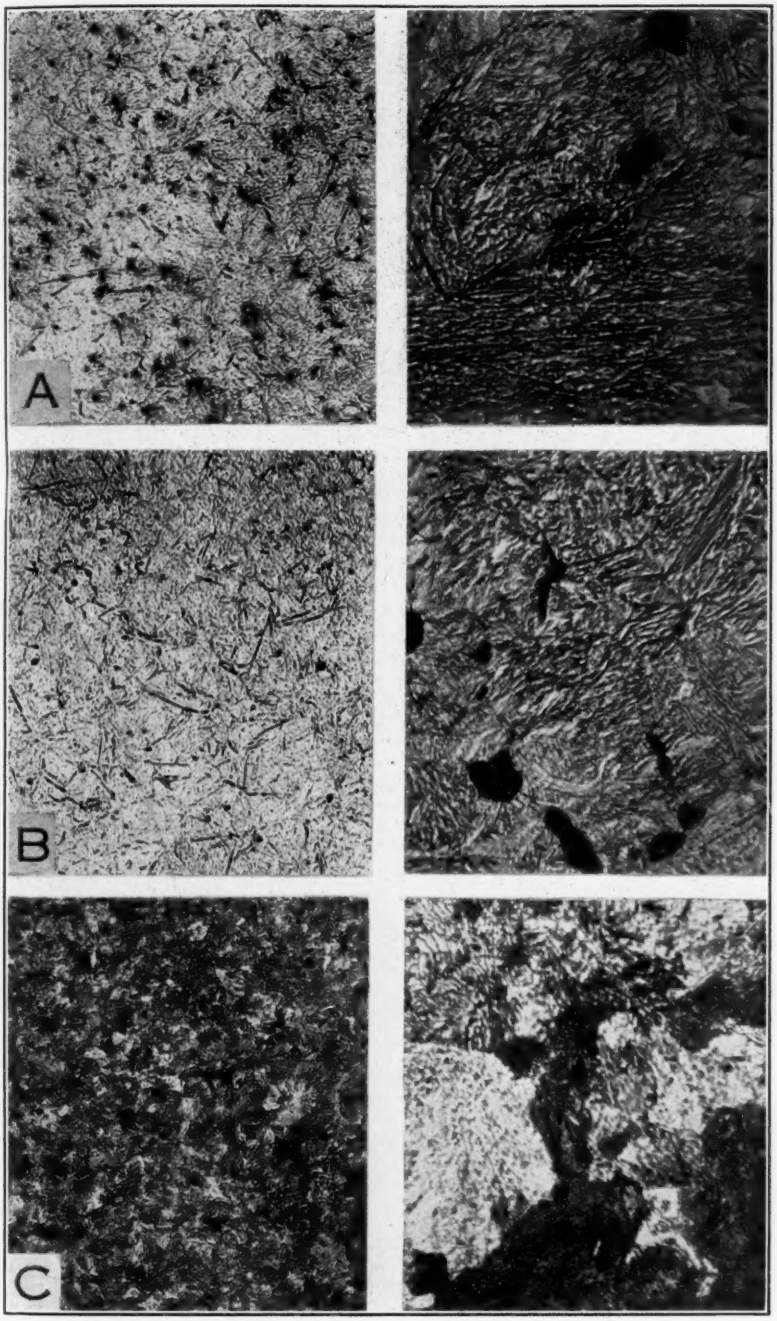

FIGURE 8.—*Microstructures at the center of 0.96 per cent carbon steel cylinders quenched from 875° C. into different concentrations of the 1: 2.5 sodium silicate at 20° C. Magnification, left × 100 and right × 1,000*

Etched in 2 per cent nitric acid in alcohol. *A*, Quenched into 12.4° B. solution; *B*, quenched into 28.8° B. solution; *C*, quenched into 41.8° B. solution.

concentrations of the 1:2.5 silicate in that such solutions may exhibit to a greater degree than solutions of the 1:4 silicate, the rapid cooling of which is characteristic of aqueous caustic alkali solutions. It may also be assumed that solutions of the 1:2.5 silicate made up to specific gravities of between 30° and 42° B. will give cooling curves intermediate between those of water and of oil corresponding to the intermediate rates obtained with solutions of the 1:4 silicate of specific gravities between 10° and 24° B.

2. EFFECT OF VARYING THE TEMPERATURE OF SODIUM SILICATE SOLUTIONS

The effect of temperature on the cooling characteristics of the various concentrations of the 1:4 sodium silicate was studied, chiefly in order to determine what variation in temperature of the quenching media could be allowed without producing excessive variations in the properties of the quenched steel.

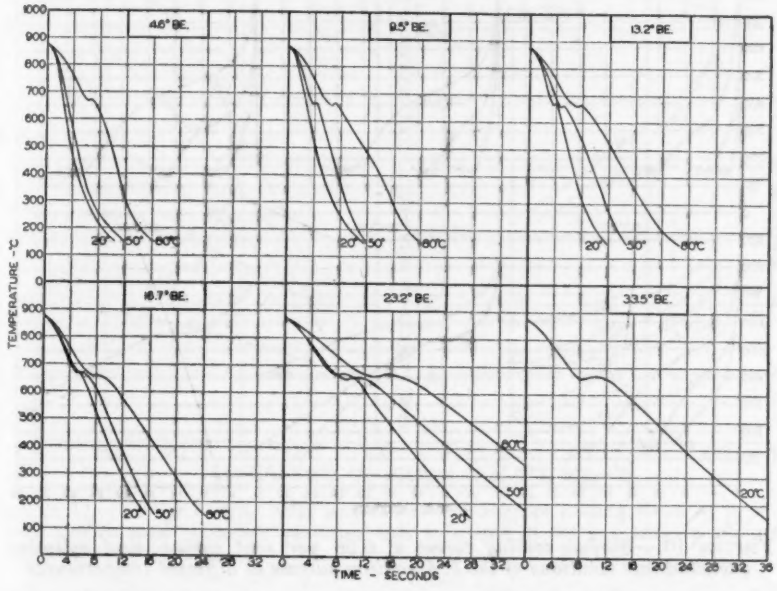

FIGURE 9.—*Center cooling curves of 0.96 per cent carbon steel cylinders quenched into solutions of the 1:4 sodium silicate at different temperatures*

Figures 9 and 10 show the center and surface cooling curves obtained with the various concentrations of the 1:4 sodium silicate (4.6° to 23.2° B.), when heated to temperatures between 20° and 80° C. The center cooling rates and surface and center cooling times, taken from the curves are given in Figure 11. Increasing the temperature of the sodium silicate solutions from 20° to 80° C., decreased the center cooling rates and increased the surface and center cooling times in all concentrations investigated. (Fig. 9 and 10.) This change is smaller, however, between 20° and 50° C. than between 50° and 80° C. This behavior is a distinct advantage, since it indicates that some increase in temperature of the media can be

allowed without expecting large changes in the properties of the quenched steel.

The fact that this temperature increase from 20° to 50° C. had less effect on cooling rates and times than from 50° to 80° C. is more readily seen in Figure 11. If the slopes of the cooling rate curves are compared, it is obvious that for all concentrations the slope is greater between 50° and 80° C. than between 20° and 50° C. and is greater for the lower concentrations than for the higher concentrations. This means that when using solutions of low concentration the variation in the temperature of the medium must be kept to a minimum if no variation in the quenched sample is to be expected. When using higher concentrations the cooling rate is much less affected by changes in temperature, but the cooling times change considerably.

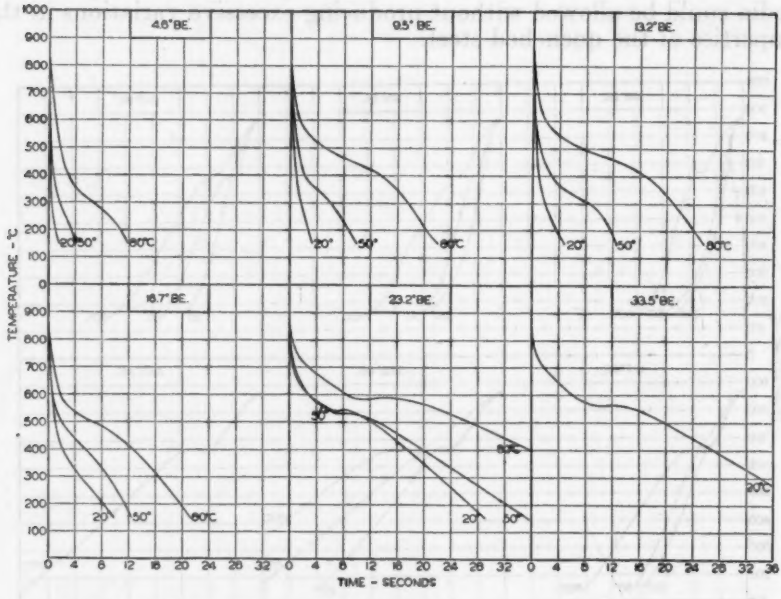

FIGURE 10.—*Surface cooling curves of 0.96 per cent carbon steel cylinders quenched into solutions of the 1:4 sodium silicate at different temperatures*

If the center cooling rates of the high concentrations are compared with their respective center cooling times, the cooling rate is the more important factor because slow cooling at the Ar′ will cause a partial transformation of the austenite while variations in cooling rate below this point will not produce large variations in hardness.

It will be noticed that considerable importance has been attached to the center cooling rate at 720° C., but it is well realized that the final structure and hardness of a quenched specimen depends on other factors of equal importance. The cooling times from the quenching temperature down to 100° C. and the cooling rates at the Ar″ point are also of considerable importance. However, the cooling rate just preceding the Ar′ point determines whether austenite will change into martensite, troostite, sorbite, or pearlite. If the center cooling rate at this point does not exceed the "critical cooling rate" of the

steel, a combination of two or more of the following structures, martensite, troostite, sorbite, or pearlite, will be formed depending on that rate. If the center critical cooling rate is exceeded, the austenite remains stable until the Ar'' transformation is reached where either all or part of it is transformed into martensite. When the latter change occurs, it will be accompanied by an increase in volume which sets up internal stresses if the change does not occur simultaneously throughout the entire specimen. Thus, when the critical cooling rate at the Ar' transformation is exceeded, the cooling rate at the Ar'' point would then determine the final structure provided the cooling below this latter point is not too slow.

Some rather peculiar results are seen on close examination of certain of the center and surface cooling curves of Figures 9 and 10. Some of the surface cooling curves cross the center cooling curves at temper-

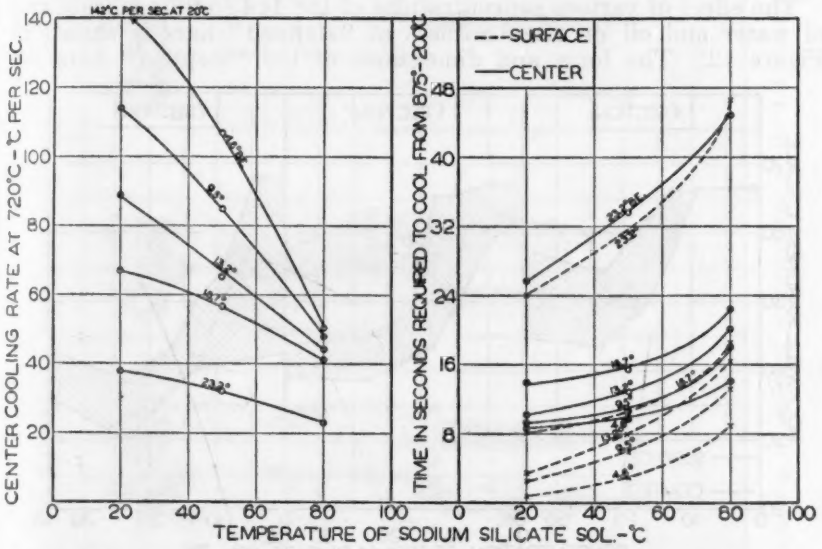
142°C PER SEC AT 20°C
CENTER COOLING RATE AT 720°C - °C PER SEC.
TIME IN SECONDS REQUIRED TO COOL FROM 875°-200°C
---SURFACE
—CENTER
TEMPERATURE OF SODIUM SILICATE SOL.-°C

FIGURE 11.—*Center cooling rates and center and surface cooling times of 0.96 per cent carbon steel cylinders quenched into solutions of the 1:4 sodium silicate at different temperatures*

atures of 500° C. or lower. It is impossible that the center of the cylinder actually could cool faster than the surface, since the cooling of the cylinder in contact with the quenching medium must take place through the surface. It must be remembered that these surface and center cooling curves were obtained by using different samples and that each cooling curve represents the average of two or three different curves, or two or three different samples. Also, the cooling at the surface of the quenched cylinder was measured by spot welded thermo-couple wires on the cylinder approximately one-quarter inch apart. This thermocouple, therefore, measures only the temperature of the area where it is spot welded to the cylinder, whereas the actual cooling of the cylinder takes place through the whole surface in contact with the quenching medium. A second and more probable explanation is that this slow cooling of the surface at

the lower temperatures may be due to the formation of silica around the thermocouple wires at the point where they were spot welded to the cylinder. This layer of silica appears to be thicker at this point of contact of the thermocouple wires than the layer left on the smooth sample after quenching.

The effect of temperature on the concentrated sodium silicate solution (33.5° B.) was not investigated. The undiluted sodium silicate showed no promise of practical application as a quenching medium. Its very high viscosity hinders circulation of the coolant and movement of the quenched piece and also leaves a rather heavy coating of silica on the quenched steel.

3. STRUCTURE AND HARDNESS OF "STEPPED" SPECIMENS QUENCHED IN SODIUM SILICATE SOLUTIONS

The effect of various concentrations of the 1:4 sodium silicate and of water and oil on the hardness of "stepped" bars is shown in Figure 12. The form and dimensions of the "stepped" bars are

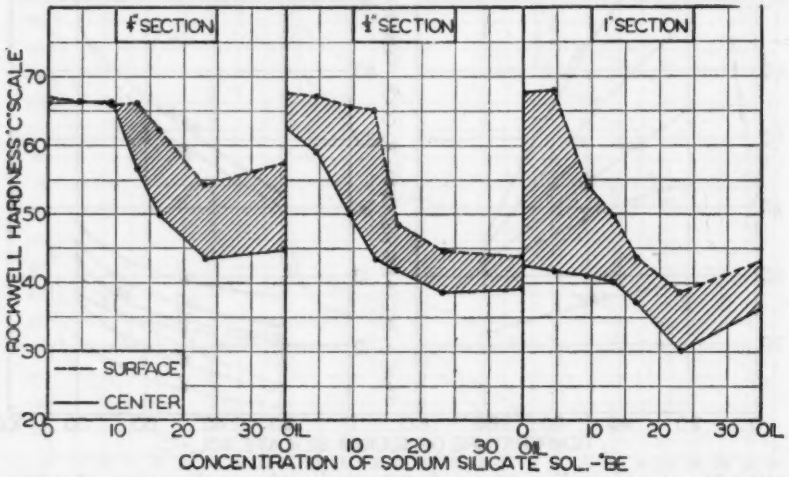

FIGURE 12.—*Center and surface hardness of the different sections of stepped bars quenched in the coolants indicated in Figure 13*

Area between surface and center curves shows range of hardening of each section.

shown in Figure 13. They were machined from a 1.06 per cent carbon steel having the chemical composition given in Table 1.

It was expected that some of these bars, with their sharp corners and large variations in size, would crack when quenched in some of the cooling media used. Such cracking frequently occurs on rapid cooling caused by the high internal stresses set up as a result of the volume changes which accompany the structural changes during the hardening of steel.

The material from which the "stepped" bars were machined was first given a preliminary heat treatment in order to secure an even carbide distribution and proper grain refinement. The bars were normalized by heating to 850° C., holding for one hour and cooling in air. They were then annealed at 760° C. for one hour and cooled in the furnace.

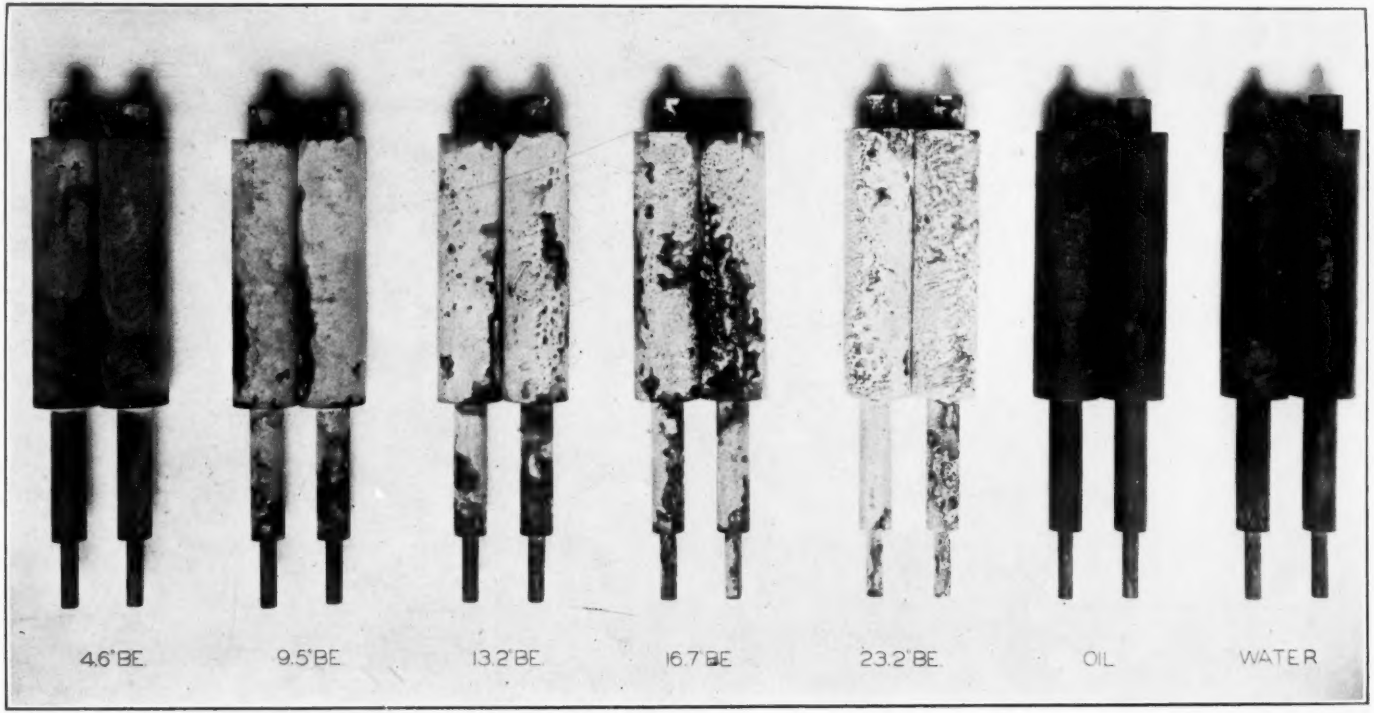

FIGURE 14.—*Stepped bars after quenching in different concentrations of the 1:4 sodium silicate, water, and oil at 20° C.*

The "stepped" bars so prepared for quenching were placed in an electric muffle furnace at a temperature of 800° C., held at this temperature for one hour, and then quenched (two bars each) into the various media. The quenching was carried out by gripping the end of the bar at *A* (fig. 13) in tongs and rapidly lowering it vertically into the desired medium. All quenching media were at a temperature of 20° C. and moving at a velocity of 3 feet per second. The floor of the furnace was covered with a layer of granular carbon about 1½ inches deep to reduce oxidation. The bars were laid on bricks in the furnace and did not touch the carbon. Figure 14 shows the bars after quenching.

It was rather surprising that none of the bars cracked immediately on quenching. However, specimens for hardness tests and microscopic examination cut from the bars that were quenched into the two fastest quenching media; that is, water and the 4.6° B. solution did crack later.

The tendency of these bars to distort and crack could no doubt have been somewhat reduced if the bars had been moved rapidly up and down in a vertical position during the quenching instead of keeping the bar still while the quenching medium was flowing past the bar. The latter method was used, however, because it had been used in the previous experiments and it was desired to keep the conditions approximately the same.

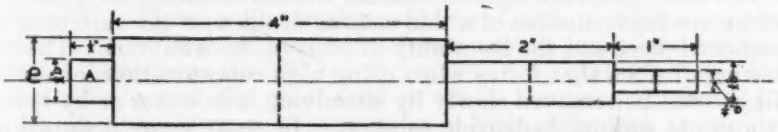

FIGURE 13.—*Design of the stepped bar used in quenching experiments*

The rapid movement of the specimen vertically during quenching would also doubtless have reduced the thickness of the layer of silica which formed on the sample, especially when quenching in the higher concentrations of sodium silicate. These layers appear to be rather thick (see fig. 14), but were never found to be over 0.005 to 0.01 inch, and then only when quenching in solutions of the highest concentrations.

Hardness tests were made on specimens, one-fourth inch thick, cut from the middle of each section, as indicated by the dotted lines in Figure 13. Figure 12 shows the results of the hardness tests taken at the center and surface of these samples.

A surface hardness of over 65 Rockwell was obtained on the one-fourth and one-half inch diameter samples, that had been quenched in water, and in 4.6°, 9.5°, and 13.2° B. sodium silicate solutions. Approximately the same surface hardness was also obtained on the 1-inch samples quenched in water and in the 4.6° B. sodium silicate solution. On the other hand, a center hardness of over 65 was obtained only on the one-fourth inch diameter samples that had been quenched in water, and in 4.6° and 9.5° B. sodium silicate solutions. Increase in concentration of the sodium silicate solutions or change in size to one-half or 1 inch produced a rapid decrease in hardness at the center. This rapid decrease was accompanied by changes in structure from martensite with a small amount of primary troostite,

to martensite with a large amount of troostite, then to troosto-sorbite with some lamellar pearlite, and finally to sorbite with large amounts of lamellar pearlite. Free carbides were also evident in all of these microstructures.

The one-fourth inch sections of the bars that had been quenched in water and in the 4.6° B. sodium silicate solution were the only sections that hardened completely throughout; that is, whose structure was martensite free from troostite. These samples had a center hardness of about 66.

It is evident from the hardness tests and their corresponding microstructures that samples having a martensitic structure with some primary troostite had practically the same hardness as those samples having a martensitic structure free from primary troostite. It may be concluded, therefore, that hardness tests alone can not be used as a means of determining whether the steel is completely martensitic or not. Microscopic or other tests are also necessary.

V. STABILITY OF SODIUM SILICATE QUENCHING SOLUTIONS

Sodium silicate solutions like nearly all quenching solutions have advantages and disadvantages. Among their advantages are their low cost and the fact that they do not readily corrode the steel.

The chief disadvantages of sodium silicate solutions as quenching media are the formation of a thin coating of silica on the surface of the quenched piece and the instability of some of the solutions. The thin coating of silica that forms when using high concentrations of sodium silicate can be removed slowly by dissolving it in water or by boiling in a dilute sodium hydroxide solution. In most cases it should not be necessary to remove this coating.

Some trouble was experienced with the instability of certain of the solutions of the 1:4 sodium silicate. A flocculent precipitate formed in the 9.5°, 13.2°, and 16.7° B. solutions on standing from six weeks to two months. However, solutions of these same concentrations made up with the addition of 2 per cent of sodium hydroxide of specific gravity 1.065 at 20° C. showed no evidence of instability and breaking down after three months. The addition of sodium hydroxide was without effect on the cooling rates of these solutions. Sodium silicate solutions of 4.6° and 23.2° B. remained stable for more than three months, even without additions of sodium hydroxide. The stability of solutions of the 1:2.5 sodium silicate was not investigated. Presumably these solutions are more stable than solutions of the 1:4 sodium silicate on account of the higher soda content.

A test was also made to determine the stability of solutions of the 1:4 sodium silicate at temperatures of from 20° to 60° C. This test consisted of adding 2 per cent of a solution of sodium hydroxide of the concentration given above to the sodium silicate solutions. The solution was then allowed to stand in a closed container for about three weeks. No precipitate had formed at the end of this time. A definite amount of red-hot steel was quenched in these solutions so that their temperature was raised from 20° to 60° C. This test was repeated eight times on each solution. The solutions were then allowed to stand for three more weeks. No precipitate had formed in any of them.

The cooling rates of the solutions were then tested and found to be unchanged thus showing that no breakdown had occurred. This test indicates that these solutions are fairly stable up to 60° C.

VI. SUMMARY

1. Center cooling curves were obtained and hardness tests made on cylinders of 0.96 per cent carbon steel, one-half inch in diameter and 2 inches long, when quenched from 875° C. in 20, 60, and 100 per cent glycol-water and 60 per cent glycerin-water solutions at 20° C. The results obtained are believed to justify the conclusion that these solutions can not be used successfully as quenching media for intermediate cooling between the rates obtained with water and with oil.

2. Similar cooling curves were determined for solutions of two sodium silicates having ratios of Na_2O to SiO_2 of 1:4 and 1:2.5, respectively. Concentrations ranging from 4.6° to 23.2° B. for the 1:4 silicate and 12.4° to 41.8° B. for the 1:2.5 silicate were used. Increasing the concentration and the temperature of the 1:4 sodium silicate and the concentration of the 1:2.5 sodium silicate lowered the cooling rates and increased the cooling times. The changes in cooling rates and times of the 1:4 sodium silicate were smaller at temperatures between 20° and 50° C. than between 50° and 80° C.

3. Sodium silicate solutions can be used successfully to obtain intermediate cooling rates between those obtained with water and with oil at 20° C. Three concentrations of the 1:4 sodium silicate and two of the 1:2.5 sodium silicate were found which gave intermediate cooling. These were the 9.5°, 13.2°, and 16.7° B. solutions of the 1:4 sodium silicate and the 12.4° and 28.8° B. solutions of the 1:2.5 sodium silicate. However, there is very little difference in cooling between the latter two solutions.

4. No correlation was found between the results obtained with the various concentrations of the 1:4 and the 1:2.5 soldium silicates.

5. The stability of solutions of the 1:4 sodium silicate was considerably increased by the addition of 2 per cent of a solution of sodium hydroxide (specific gravity of 1.065 at 20° C.) without changing the cooling speeds of the silicate solutions.

6. Quenching experiments on "stepped" bars of a 1.06 per cent carbon steel were made to determine the relation between the hardness and microstructures produced by the various concentrations of the 1:4 sodium silicate, water and oil at 20° C.

7. It is possible that the aqueous solutions of other sodium silicates having different soda-to-silica ratios may be more stable and give better results than the ones used in the present investigation.

VII. ACKNOWLEDGMENTS

Acknowledgments are made to the Philadelphia Quartz Co., who donated the two lots of sodium silicate, and the Carbide & Carbon Chemical Corporation, who donated the ethylene glycol for these tests.

Grateful acknowledgment is also made to Dr. R. L. Dowdell, formerly of this bureau for his helpful suggestions and criticisms throughout the progress of the work reported in this paper.

WASHINGTON, July 6, 1931.

OPTICAL ROTATION AND ATOMIC DIMENSION—HALOGENO-TETRA-ACETYL-DERIVATIVES OF MANNOSE. THEIR CONFIGURATIONAL PECULIARITIES

By D. H. Brauns

ABSTRACT

The pure crystalline fluoro and iodo derivatives of acetylated mannose have been prepared. The specific rotation values in combination with the revised values of the chloro and bromo derivatives of acetylated mannose show a disagreement with the atomic dimension relationship established for the halogen derivatives of other monosaccharides.

An explantion of this behavior is obtained by model studies which show that the hydrogen of the first asymmetric carbon (to which the halogen is also attached) is influenced by atoms of the second carbon acetyl group, whereas, such an influence does not exist for the other investigated halogen derivatives of monosaccharides.

This result gives a suggestion for the configuration of other acetyl groups. These results show also that the study and testing of the principle of optical superposition should be carried out in the light of these configurational peculiarities.

CONTENTS

	Page
I. Introduction	573
II. Discussion of results and conclusions	575
III. Description of stereo-formulas	578
IV. Experimental part	580

I. INTRODUCTION

NOTE.—This article is the ninth contribution to a series on optical rotation and atomic dimension which has appeared in the Journal of the American Chemical Society. The eighth article was published in Journ. Am. Chem. Soc., **51**, p. 120; 1929.

The study of mannose has been impeded by the difficulty of obtaining its derivatives in crystalline form. This difficulty also delayed the comparison of the rotations of the halogeno-acetyl derivatives of this sugar. Only recently fluro-tetra-acetyl mannose was obtained in the form of crystals, whereas iodo-tetra-acetyl mannose crystallizes readily, if prepared according to the method described later in this paper. Bromo-tetra-acetyl mannose has been obtained in crystalline form by Micheel [1] and also by Levene and Tipson. [2] The compound has been prepared again and its rotation revised. Since the writer prepared crystalline α-chloro-tetra-acetyl mannose [3] several years ago a series of rotational values is available for comparison with the atomic dimension values. It has been established in the writers previous investigations on this subject that for all the investigated halogen derivatives of the mono-saccharides (glucose, fructose, xylose, and arabinose) the differences in specific rotations Cl–F, Br–Cl, and I–Br, have the same ratio 41 : 17 : 21, and further that this ratio agrees approximately with that for the respective differences in atomic diameter as given by Bragg (41 : 16 : 24). Later it was found [4]

[1] Micheel, Ber., **63**, p. 390; 1930.
[2] Levene and Tipson, J. Biol. Chem., **90**, p. 93; 1931.
[3] Brauns, J. Am. Chem. Soc., **44**, p. 401; 1922.
[4] Brauns, J. Am. Chem. Soc., **49**, p. 3170; 1927.

that close agreement is obtained by replacing Bragg's values of ionized halogens (in inorganic salts) by the values derived by van Arkel and de Boer[5] for the distance of the carbon to the halogen atoms as occurring in organic (homopolar) compounds. From these values the ratio 41 : 17 : 22.6 is found. Lately these values for neutral atomic diameters have been derived by Goldschmidt,[6] which yield as an average the ratio 41 : 14 : 20. If we take an average between these ratios of van Arkel and de Boer, and of Goldschmidt, we obtain 41 : 16 : 21, in close agreement with that for the differences in specific rotations of these four mono-saccharides. However, as seen from the compiled data in Table 1, the values for the mannose derivatives give an abnormal ratio 41 : 25 : 35. It is noteworthy, furthermore, that whereas for the β-bioses [7] an agreement is obtained by excluding the fluoro-derivatives, such an agreement is not obtained for the mannose derivatives, as the ratio is in this case 17 : 24.5 instead of 17 : 21.

TABLE 1.—*Comparison of the ratio of the differences of specific rotations with the ratio of the differences of neutral atomic diameters, for halogen derivatives of monosaccharides*

Specific rotations; derivatives of—						Specific rotation differences; derivatives of—						Reduced specific rotation differences; derivatives of—					Ratio of differences of neutral atomic diameter.
	Xylose	*l*-Arab.	Fruct.	Gluc.	Mann.		Xylose	*l*-Arab.	Fruct.	Gluc.	Mann.	Xylose	*l*-Arab.	Fruct.	Gluc.	Mann.	
1						2						3					4
F	67.2	138.2	−90.4	90.1	21.5												
						Cl-F	104.0	106.2	70.5	76.0	68.5	41.0	41.0	41.0	41.0	41.0	41
Cl	171.2	244.4	−160.9	166.1	90.0												
						Br-Cl	40.7	42.7	28.2	31.7	41.6	16.0	16.5	16.4	17.1	24.9	16
Br	211.9	287.1	−189.1	197.8	131.6												
						I-Br	-----	52.0	-----	39.6	58.9	-----	20.0	-----	21.4	35.2	21
I	-----	339.1	-----	237.4	190.5												

Explanation of table.—Sec. 1 gives the observed specific rotations of the halogen-acetyl derivatives of xylose, *l*-arabinose, fructose, glucose and mannose.

Sec. 2 gives the differences in specific rotation of sec. 1, between the Cl and F derivatives, the Br and Cl derivatives and the I and Br derivatives.

Sec. 3. The values given in this section have been obtained from those in sec. 2 by dividing each column by a factor which will reduce the first member of each column to the value 41. This value has been chosen in order to conform to the values given in sec. 4 for the ratio of the differences between the neutral atomic diameters.

Sec. 4. The ratio of the differences between the neutral atomic diameters of the halogens are obtained by averaging the values given by van Arkel and de Boer, and by Goldschmidt.

TABLE 2.—*Comparison of molecular rotations (divided by 100) of monosaccharide derivatives*

	Derivatives of—					Respective molecular rotation difference				
	Xylose	*l*-Arab.	Fruct.	Gluc.	Mann.	Xylose	*l*-Arab.	Fruct.	Gluc.	Mann.
F	187	384	−316	315	75					
						317	336	274	294	255
Cl	504	720	−590	609	330					
						214	253	187	204	211
Br	718	973	−777	813	541					
						-----	336	-----	274	332
I	-----	1309	-----	1,087	873					

[5] van Arkel and de Boer, Z. f. Physik, **41**, p. 27; 1927.
[6] See Wherry Am. Mineralogist, **14**, p. 54; 1929.
[7] J. Am. Chem. Soc., **51**, p. 1820; 1929.

II. DISCUSSION OF RESULTS AND CONCLUSIONS

In order to arrive at an explanation of the different results obtained for the halogeno-acetyl compounds of glucose, fructose, xylose, and *l*-arabinose on the one hand and for the halogeno-acetyl derivatives of mannose on the other, consider first their structural formulas (X representing a halogen).

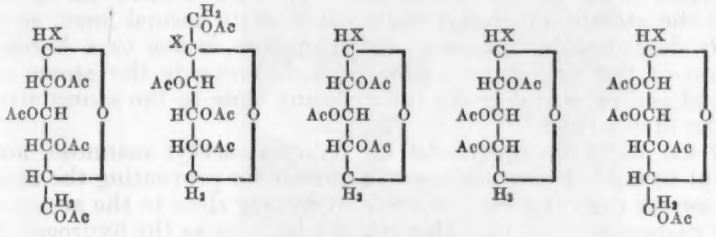

α-d hal. tetra-acet. glucose | *β-d* hal. tetra-acet. fructose | *α-d* hal. tri-acet. xylose | *β-l* hal. tri-acet. arabinose | *α-d* hal. tetra-acet. mannose

As the index *d* refers to position of groupings on the last asymmetric carbon atom and *α* refers to the position of the hydroxyl group (or its substituent) attached to the reducing carbon, *α-d* compounds must be similar in structure regarding the position of the groups attached to these two carbon atoms. As a result of the system of nomenclature and of the chemical behavior,[8] *β-d* halogeno-acetyl arabinose is similar in structure to *α-d* halogeno-acetyl galactose, consequently in this compound also the halogen occupies the same position as it does in the *α-d* compounds. However, for the *β-d* derivatives as represented by the fructose derivatives, the halogen must take an opposite place in comparison with the other compounds under discussion. For that reason halogeno-acetyl fructose will not be considered at this time, but will be discussed later. This is also warranted by its exceptional structure as a ketose. If we now compare the structural formulas for the halogeno-acetyl derivatives of glucose, xylose and *l*-arabinose on one hand and the structural formula for halogeno-acetyl mannose on the other, it is easily found that the difference in the position of the acetyl group of the second carbon is the only difference between the glucose and mannose derivatives, whereas additional differences in other groups have to be taken in account for the xylose, arabinose and fructose derivatives. The influence of the configuration or the direction [9] of the acetyl group of the second carbon can account for the different results for the glucose and mannose derivatives by considering the influence of the residual affinities of the double bond oxygen atom of the ring. The important part, which the residual affinities of this ring oxygen atom plays in the behavior of carbohydrates and their derivatives is illustrated by the frequent formation of the aldehyde form of the sugars as an intermediate in several reactions including the mutarotation.[10]

[8] Hudson and Phelps, J. Am. Chem. Soc., **46**, p. 2593; 1924.

[9] The written structure formula can give on the position of a group. The stereo-formula can clearly indicate position and also "configurational direction" or in short the "direction" of a group. The word direction will be used in that sense.

[10] Wolfrom, J. Am. Chem. Soc., **53**, p. 622; 1931. Lowry, Z. physik. Chem., **130**, p. 1928.

If we take the model of halogeno-tetra-acetyl glucose in which the second carbon acetyl group is represented in full by blocks, and turn this acetyl group in all possible directions, then we find that the hydrogen atoms of this acetyl group can come quite close to the ring oxygen atom (fig. 1, upper) and, therefore, possibly come under the influence of this atom. In this particular position of the acetyl group "all the atoms of this group are kept well away from the atoms attached to the first carbon atom." Thus we come to the conclusion that the atomic dimension relationship in its normal form, as previously described for halogeno-acetyl glucose, is due to a barrier-like action of the ring oxygen atom, which prevents the atoms of the second carbon acetyl group from coming close to the atoms attached to the first carbon.

If we also take the model for halogeno-acetyl mannose, and attempt to use the ring oxygen as a barrier for preventing the atoms of the second carbon acetyl group from coming close to the atoms of the first carbon, we find that this can not be done as the hydrogen atoms of the second carbon acetyl group will never come closer than two carbon diameters to the ring oxygen atom for any direction of the acetyl group. If the abnormal atomic dimension relationship for halogeno-tetra-acetyl mannose is due to the action of other atoms in the vicinity of the first carbon, then these disturbing atoms must be those of the second carbon acetyl group.

The results of Freudenberg [11] and Haworth [12] (which will be discussed below) show that the double bond oxygen of the second acetyl group must be in the vicinity of the halogen as it yields derivatives with a ring formation (orthoacetic acid ring) between the first and second carbon atom. These facts gave the following clue. It was found probable that not only the hydrogen atoms of the second carbon acetyl group of halogeno-tetra-acetyl glucose are directed to a definite oxygen atom, but also that other acetyl groups influence each other by the same principle, the hydrogens of the one group being attracted by the double bond oxygen of another acetyl group.[13] It was possible to find the particular most probable position of the groups by trying out all possibilities and taking those configurational directions as the most probable, in which most of the active groups are saturated, preferably not allowing two CH_3 groups to act on the same oxygen atom. On this basis it was found that for halogeno-tetra-acetyl mannose the hydrogen atoms of the third carbon acetyl group are directed to the oxygen atom of the sixth carbon acetyl group; further, that the hydrogen atoms of the sixth carbon acetyl group are directed to the oxygen atom of the third acetyl group and the hydrogen atom of the fourth carbon to the ring oxygen atom. This arrangement left the oxygen affinities of the second carbon acetyl group still available and it seemed plausible that they are directed to the hydrogen atom of the first carbon atom, which brings the double bond oxygen atom in the vicinity of the halogen. This arrangement for halogeno-tetra-acetyl mannose is shown in Figure 1, lower.

The following experimental facts lend support to the above conclusions. First consider the facts relating to the structural formula of

[11] Freudenberg, Naturwissenschaften, 18, p. 393; 1930.
[12] Haworth, J. Chem. Soc., p. 1395; 1930.
[13] In general, the direction of a group will be determined by the direction of the strongest secondary valence acting on it.

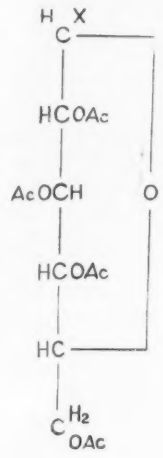

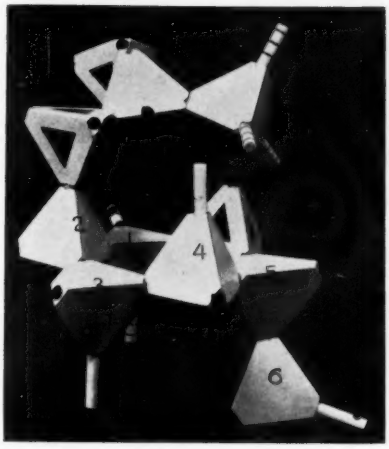

α-HALOGENO - TETRA-ACETYL- GLUCOSE

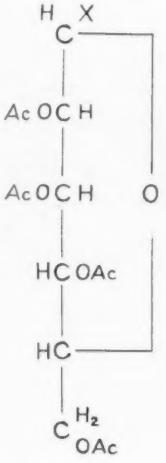

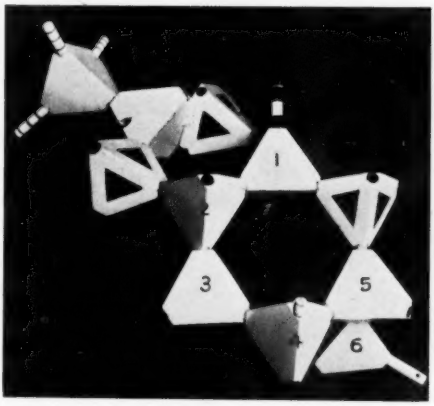

α-HALOGENO - TETRA-ACETYL-MANNOSE

CARBON ATOM

OXYGEN ATOM

ACETYL GROUP

HALOGEN (ALWAYS IN α-POSITION)

HYDROGEN ATTACHED TO THE FIRST CARBON AND SECOND CARBON-ACETYL-GROUP, ALL OTHERS OMITTED.

FIGURE 1

halogeno-acetyl-glucose and then to the structural formula of halogeno-acetyl mannose. Brigl [14] found that intense halogenation of acetylated glucose, maltose and cellobiose yields derivatives, which contain four chlorine atoms, the acetyl group of the first carbon being replaced by chlorine and also "the three hydrogen atoms of the second carbon acetyl group, which in our model come near to the ring atoms. This 1-chloro-2-tri-chloro-acetyl-glucose was shown by Brigl to be a stable β-derivative." The study of our model can account for this result as the three chlorine atoms are free from the attraction of the ring oxygen and consequently the double bond oxygen of the second carbon acetyl group can exert its action on the hydrogen of the first carbon and make it possible that a stable β derivative is formed. The mechanism of the Brigl reaction is undoubtedly of a complicated nature (see Brigl l. c.) as often found for similar reactions (Wolfrom l. c.), but "the β configuration of the final product as an equilibrium form of the affinities of all the groups support our stereo-formula." Further evidence in support of that formula is given by the following considerations and facts.

If it were possible to apply a certain halogenating reaction on glucoselike compounds, which could (if only temporarily) saturate the affinities of the ring oxygen atom, results should be obtained similar to those for the mannose compounds. Now Freudenberg [15] has found that maltose oct-acetate can be converted by an exceptional method of chlorination [16] to a compound with a ring formation which includes the chlorine and the acetyl group of the second carbon (ortho-acetic acid ring). However, chloro-hepta-acetyl maltose prepared by ordinary methods of chlorination (as applied for glucose and mannose derivatives) does not show a tendency for such a ring formation as it does not even yield derivatives with such a ring structure. It displays in combination with the fluorine and bromine derivatives of maltose an abnormal atomic dimension relationship.[17] Hence, an exceptional halogeno-acetyl maltose (with ortho-acetic acid structure) is obtained only by applying an extraordinary method of halogenation. However, a different result is obtained for the mannose derivatives. Freudenberg [18] and Haworth [19] came both to the conclusion that bromo-tetra-acetyl mannose [20] (prepared by the common method of halogenation) yields derivatives, which have a ring formation between the first and second carbon atom of the same type as the above-mentioned ortho-acetic acid ring structure. This shows then that the groups of the first and second carbon atoms for mannose can interact, which is in agreement with our conclusions of the proximity of the groups in the halogen derivatives

Before making other conclusions, we will summarize as follows:

1. The "normal" ratio for the specific rotation differences of the halogeno-acetyl derivatives of glucose, as revealed by the atomic dimension relationship, can be displayed on account of the ring

[14] Brigl, Ber., **58**, p. 1588; 1926, and subsequent articles also Ber., **62**, p. 1717; 1929.
[15] Freudenberg, Naturwissenschaften, **18**, p. 393; 1930.
[16] The absolute ether used in the reaction of Freudenberg may have as active a part in it as in the Grignard reaction.
[17] Brauns, J. Am. Chem. Soc., **51**, p. 1820; 1929.
[18] See footnote 11, p. 576.
[19] See footnote 12, p. 576.
[20] Chloro-tetra-acetyl mannose behaves in the same manner as the bromo-derivative.

oxygen atom, which attracts the hydrogen atoms of the second carbon acetyl group, preventing the action of the double-bond oxygen of this group on the hydrogen of the first carbon.

2. The "abnormal" ratio for the specific rotation differences of the halogeno-acetyl derivatives of mannose as revealed by the atomic dimension relationship is due to the secondary valence action of the double-bond oxygen atom of the acetyl group attached to the second carbon atom upon the hydrogen of the first carbon atom.

The orientation of acetyl groups in the stereo-formula of all the discussed halogeno-acetyl derivatives are described below as a guide, but a clear insight can be obtained only by actually manipulating the models. Without models an idea can be obtained by viewing the picture of the ring structure. The acetyl group can be represented by four blocks, one for the binding oxygen, one for the double-bond oxygen, and two for carbons; the hydrogens can be omitted. The model of each compound is tested on its own possibilities, without taking into consideration the result of even closely-related substances. These will often give entirely different results, as illustrated by xylose tetra-acetate and glucose penta-acetate. The model of the definite six atomic ring structure described in Part VIII for glucose [21] will be kept, as it is interesting to see how far this arrangement can explain the facts.

III. DESCRIPTION OF STEREO-FORMULAS

α-d-halogeno-tetra-acetyl glucose: 2 CH_3 to ring O; 3 CH_3 to 6 O; 4 CH_3 to 2 O; 6 CH_3 to 3 O.

Remarks.—This means that the three hydrogen atoms of the second carbon acetyl group are directed to the vicinity of the ring oxygen atom. Further that the three hydrogens of the third carbon acetyl group are directed to the vicinity of the double bond oxygen atom of the sixth carbon acetyl group, etc. The acetyl residual affinities of the groups of the third and sixth carbon saturate each other. The discussion for obtaining the direction of the second carbon acetyl group has been made as well as the discussion for obtaining the directions of the others. The possibility of: 2 CH_3 to 4 O; 3 CH_3 to 6 O; 4 CH_3 to ring O and 6 CH_3 to 3 O also exists. This arrangement does not change the conclusions made, but does not explain the Brigl reaction.

α-d halogeno-tetra-acetyl mannose: 2 O to β hydrogen and α halogen; 3 CH_3 to 6 O; 4 CH_3 to ring O; 6 CH_3 to 3 O.

Remarks.—The discussion for obtaining the direction of the second carbon acetyl group has been made.

α-d halogeno-tri acetyl xylose: 2 CH_3 to 4 O; 3 CH_3 to ring O; 4 CH_3 to 2 O.

Remarks.—The atoms of acetyl groups do not come into the vicinity of the α-halogen.

β-l halogeno-tri-acetyl arabinose: 2 CH_3 to ring O; 3 CH_3 to 4 O; 4 CH_3 to 3 O.

Remarks.—The atoms of acetyl groups do not come into the vicinity of the β halogen, which has an upper position at the first carbon because the arabinose is an *l*-sugar.

β-d halogeno-tetra-acetyl fructose: 1 CH_3 to 4 O; 3 CH_3 to 1 O; 4 CH_3 to 3 O; 5 CH_3 to ring O.

Remarks.—The atoms of acetyl groups do not come into the vicinity of the β halogen, which has a lower position at the second carbon because the fructose is a *d*-sugar.

[21] Brauns, J. Am. Chem. Soc., **51**, 1824; 1929.

We will now discuss the fully acetylated sugars.

In Hudson's method of studying the principle of optical superposition the first carbon is indicated by + A and − A for the α and β derivatives, respectively, and the rest of the molecule by B. The difference in the molecular rotations of the fully acetylated sugars is thus required to be equal (2A). The experimental results [22] for the mono-saccharides are given in Table 3.

TABLE 3.—*Molecular rotations of α and β forms of fully acetylated sugars*

	α	β	Difference
d-Glucose-penta-acetate	+39, 600	+1, 500	+38, 100
d-Mannose-penta-acetate	+21, 400	−9, 800	+31, 200
d-Galactose-penta-acetate(1 and 2)	+41, 600	+8, 900	+32, 700
d-Galactose-penta-acetate (3 and 4)	+23, 800	−16, 400	+40, 200
d-Xylose-tetra-acetate	+28, 300	−7, 900	+36, 200
l-Arabinose-tetra-acetate	+13, 400	+46, 800	−33, 400

It is seen from the table that the differences are not quite constant We will consider this lack of constancy from a viewpoint which takes into account the influence of the direction of the acetyl groups.

If we view the model for α glucose as described, so that the ring is horizontal and the first carbon is situated farthest away from the observer with the second carbon at the left and the oxygen atom at the right, then it is not only assumed (as is generally done) that the upper position of an acetyl group (replacing a hydroxyl group of the original sugar) will make the particular carbon atom to which the acetyl group is attached positive rotating but also that the direction of the acetyl group to the right of the whole model has a positive rotating influence, and that a left direction has a negative rotating influence. The strongest positive influence, which an acetyl group can have is therefore to be up to the right and the strongest negative to be down to the left. Other intermediate values are dependent on the degree of left or right direction of the group.

The discussion is made easier, if we indicate the rotations of the first carbon for the α and β derivatives by A_α and A_β respectively, keeping in mind that A_α is the more positive rotating for the *d*-sugars and the more negative for the *l*-sugars. The rotations of the rest of the molecule are, respectively, B_α and B_β.

α-Glucose-penta-acetate: 1 CH_3 to ring O; 2 CH_3 to 4 O; 3 CH_3 to 6 O and to 4 O; 4 CH_3 to 2 O; 6 CH_3 to 3 O.

β-Glucose-penta-acetate: 1CH_3 to 3 O; 2 CH_3 to 4 O; 3 CH_3 to 4 O; 4 CH_3 to 2 O; 6 CH_3 to ring O.

Remarks.—The place of the first acetyl group for the α derivative changes to a diametrically opposite place for the β derivative, hence A_α and A_β can be represented by $+A$ and $-A$. The direction of the first acetyl group of the β derivative is also determined by the action of the hydrogen directly attached to the second column. The B_α value is not changed in comparison with the B_β value as the change of the sixth acetyl group which is not asymmetric does not change the rotation, hence the calculated difference (+38,100) truly represents $2A$.

α-Mannose-penta-acetate: 1 CH_3 to 2 O; 2 CH_3 to 1 O; 3 CH_3 to 6 O; 4 CH_3 to ring O; 6 CH_3 to 3 O.

β-Mannose-penta-acetate: The same as for the α compound. The first or β acetyl-group is here also directed to the second oxygen.

[22] Hudson, B. S. Sci. Paper, No. 533, p. 259.

Remarks.—It is seen that the arrangement in space of the groups attached to the first carbon is slightly more positive for the β form of the mannose compound than for the β forms of the glucose which will make the calculated difference for the mannose derivative smaller than for the glucose compound. Further, the direction of this acetyl group in the case of the α mannose compound (being up and to the left) is such as to give a more negative rotation to this first carbon atom than in the case of the α glucose compound where the direction of the acetyl group is up and to the right thus making A_α for mannose-penta-acetate smaller than for glucose-penta-acetate, which will make again the calculated difference for the mannose derivatives (+31,200) smaller than the difference for the glucose derivatives, which agrees with experiment. (See Table 3.) The two pairs of galactose-penta-acetates are not considered on account of the uncertainty in their ring structure.

α-Xylose-tetra-acetate: 1 CH_3 to 3 O; 2 CH_3 to 4 O; 3 CH_3 to ring O; 4 CH_3 to 2 O.

β-Xylose-tetra-acetate: 1 CH_3 to 3 O; 2 CH_3 to 4 O; 3 CH_3 to ring O; 4 CH_3 to 2 O, or the same as for the α derivative.

Remarks.—The explanation for the discrepancy in the 2 A value for the xylose derivatives is the same as that given for the mannose derivatives, The $B\alpha$ and B_β value for the xylose derivatives is the same. The models also show that the discrepancy is here not as large as for the mannose derivatives as the $A\beta$ value is more negative for the xylose derivatives.

α-l Arabinose-tetra-acetate: 1 O to 5 H, 2 CH_3 to ring O; 3 CH_3 to 4 O; 4 CH_3 to 3 O.

β-l Arabinose-tetra-acetate: 1 CH_3 to ring O; 2 CH_3 to 1 O; 3 CH_3 to 4 O; 4 CH_3 to 3 O.

Remarks.—The α acetyl group of the first carbon, which has here a lower position at that carbon (because the arabinose is an l-sugar), has a direction which is more positive than the β acetyl group of the glucose compound, whereas the β acetyl group of the arabinose compound occupies the same place as the α acetyl group of the glucose compound. Hence the calculated difference must be smaller than for the glucose compounds. Further the $B\alpha$ value is different from the B_β value. The change in direction of the second carbon acetyl group makes the absolute value of the difference too low as found. (See Table 3.)

It is not intended to enter the field of investigation of the principle of optical superposition, however, the configurational peculiarities found by applying the atomic dimension relationship warrant the suggestion that the principle of optical superposition should be carefully tested and studied in the light of these results, taking into account the configurational peculiarities as illustrated for the acetylated sugars.

IV. EXPERIMENTAL PART

General remarks.—For all determinations of the specific rotation purified chloroform [23] was used. The volume of the solution was made up in the same flask to 24.9767 cc at 20°, which requires multiplication by the factor 4.0038 for obtaining 100 cc. The reading, which was made in the same 4 dm tube at 20°, is given in circular degrees.

β-Penta-acetyl mannose was prepared by acetylating mannose with acetic anhydride and zinc chloride according to the method of Hudson and Sawyer.[24] The time of reaction could be appreciably shortened (even when working with 80 g of mannose at a time) by taking the stoppered Erlenmeyer flask out of the cooling bath and rotating. As soon as the reaction mixture heated up it was cooled again. A

[23] Brauns, J. Am. Chem. Soc., **46**, p. 1486; 1924.
[24] See Hudson and Dale, J. Am. Chem. Soc., **37**, p. 1281; 1915.

few recrystallizations gave a product of constant specific rotation in chloroform of −25.15° and m. p. 117° to 118° agreeing with the values reported by Hudson and Dale:[24] $[\alpha]_D^{20} = -25.3$; m. p. 117° to 118°.

α-Fluoro-tetra-acetyl mannose was prepared from β-penta-acetyl mannose in the manner previously described.[25] The distillation was finished in about 40 minutes and the reaction product was directly worked up. The sirup resulting from the extraction with chloroform did not crystallize by stirring with petroleum ether. After many unsuccessful attempts to crystallize the sirup it was kept in a vacuum desiccator over fresh sodium hydroxide and stirred repeatedly for removing the petroleum ether. After a few days the sirup crystallized. The solid mass was broken up and some of the substance saved for seeding. The larger part was dissolved in a small amount of absolute ether and filtered clear through a hardened filter paper. To the concentrated solution petroleum ether was added until a sufficient amount of crystals had separated. Many recrystallizations are required before a constant rotating pure substance is obtained. Large crystals can be separated by crystallizing from ether alone. The pure product crystallizes in prismatic needles and is stable colorless and slightly bitter. It is very soluble in most solvent except water and petroleum ether. m. p. 68° to 69°. The determination of the specific rotation in purified chloroform solution gave the following results:

Rotation.—Second recrystalization: Subs., 0.6695; $\alpha = +2.042°$; $[\alpha]_D^{20} = +19.05°$. Third recrystallization: Subs., 0.6049: $\alpha = +1.946°$; $[\alpha]_D^{20} = +20.08°$. Fourth recrystallization: Subs., 0.6220: $\alpha = +2.077°$; $[\alpha]_D^{20} = +20.85°$. Fifth recrystallization: Subs., 0.6166: $\alpha = +2.112°$; $[\alpha]_D^{20} = +21.38°$. Sixth recrystallization: Subs., 0.6184: $\alpha = +2.129°$; $[\alpha]_D^{20} = +21.50°$. Therefore, +21.50 is taken as the specific rotation of the pure substance.

Analyses.—Subs., 0.2171: CO_2, 0.3840; H_2O, 0.1083. Subs., 0.5000: CaF_2, 0.0524. Calcd. for $C_{14}H_{19}O_9F$: C, 47.98; H, 5.47; F, 5.43. Found: C, 48.24; H, 5.58; F, 5.10.

α-Chloro-tetra-acetyl-mannose.—This compound has been prepared and described before.[26] It was prepared again and the specific rotation measured under the same conditions as for the other halogen derivatives of mannose. The melting point (81°) and specific rotation were found identical with those recorded before. The specific rotation was determined in purified chloroform.

Rotation.—First recrystallization: Subs., 0.6027: $\alpha = +8.672°$; $[\alpha]_D^{20} = +89.84°$. Second recrystallization: Subs., 0.6140: $\alpha = +8.863°$; $[\alpha]_D^{20} = +90.13°$. Third recrystallization: Subs., 0.6202: $\alpha = +8.932°$ $[\alpha]_D^{20} = +89.92°$. Therefore $[\alpha]_D^{20} = +90.13$ is taken as the rotation of the pure substance.

α-Bromo-tetra-acetyl-mannose.—This compound has been prepared by Micheel and Micheel [27] and also by Levene and Tipson.[28]

The method by Micheel and Micheel was followed. Ten grams of powdered β penta-acetyl-mannose was added to 14.5 cc of a saturated solution of hydrobromic acid in glacial acetic acid, which had been

[25] Brauns, J. Am. Chem. Soc., **45**, p. 834; 1923.
[26] Brauns, J. Am. Chem. Soc., **44**, p. 401, 1922.
[27] Micheel and Micheel, Ber., **63**, p. 390, 1930.
[28] Levene and Tipson, J. Biol. Chem., **90**, p. 93, 1931.

cooled to 0° in a glass stoppered Erlenmeyer flask. After the substance had dissolved, the solution was allowed to stand for two hours at room temperature, then dissolved in 60 cc of chloroform and poured into 60 cc of ice water. The separated chloroform solution was shaken out three times with ice water; dried with calcium chloride and filtered and the chloroform evaporated with a current of dry air. The slightly yellow sirup, kept in a vacuum dessicator over fresh sodium hydroxide in the ice box solidified after a few weeks standing. Subsequent preparations crystallized easily by seeding. It was recrystallized by dissolving in a small amount of absolute ether, filtering through hardened filter paper and allowing the seeded solution to evaporate slowly in the ice box. Yield about 6 gm. A few recrystallizations gave a constant rotating pure product. The pure substance crystallizes in long colorless needles, which have a bitter taste. It is easily soluble in all ordinary solvents, except petroleum ether and water. m. p. 62°. Micheel and Micheel 48 to 50°. Levene and Tipson 53 to 54°. The rotation was measured in purified chloroform solution.

Rotation.—First recrystallization: Subs., 0.6690: $\alpha = +14.004°$; $[\alpha]_D^{20} = +130.70°$. Second recrystallization: Subs., 0.6392: $\alpha = +13.450°$; $[\alpha]_D^{20} = +131.38°$. Large clear crystals from a second separation of second recrystallization: Subs., 0.6506: $\alpha = +13.709°$; $[\alpha]_D^{20} = +131.57°$. Third recrystallization: Subs., 0.6230: $\alpha = +13.104°$; $[\alpha]_D^{20} = +131.33°$. Therefore, +131.57° is taken as the specific rotation of the pure substance. Micheel and Micheel found for the specific rotation in chloroform +122.1° and Levene and Tipson +123.1°.

Analyses.—Subs., 0.2136: CO_2, 0.3206; H_2O, 0.0908. Subs., 0.2200: AgBr, 0.1016. Calcd. for $C_{14}H_{19}O_9Br$: C, 40.87; H, 4.66; Br, 19.44. Found: C, 40.93; H, 4.76; Br, 19.65.

α-Iodo-tetra-acetyl-mannose.—Eight grams of β mannose-penta-acetate was dissolved in 14 cc purified chloroform in a Pyrex test tube and a minute amount of zinc chloride was added. The solution was cooled in an ice and salt bath. Hydriodic acid (which was first passed through asbestos mixed with red phosphorus, then through a calcium chloride tower, then through a phosphorus pentoxide tube and finally thorugh a spiral tube cooled in ice and salt) was passed in a slow stream through the mannose-penta-acetate solution for 10 to 15 minutes. The solution was poured into a dish and evaporated with a current of dry air under a belljar. A mixture of equal amounts of ether and petroleum ether was added and by scratching the sides of the dish crystallization started. The crystals were separated by suction and washed with ether—petroleum ether mixture. Recrystallization was produced by dissolving in a small amount of absolute ether adding half the amount of petroleum ether and seeding. Clear large size crystals were obtained by keeping the solution in a dessicator in a partial vacuum and cooling in the refrigerator. The pure compound crystallizes in short prisms and is slightly bitter and colorless. It is not stable but can be kept in pure condition for many months in a dessicator over sodium hydroxide in an ice box. It is readily soluble in ordinary solvents except water and petroleum ether. A sharp melting point can be obtained by quickly heating the substance

to near its melting point. It melts at 95° to a slightly yellowish liquid. The determination of the specific rotation in purified chloroform gave the following results:

Rotation.—First recrystallization: Subs., 0.6288: $\alpha = +18.799°$; $[\alpha]_D^{20} = +186.67°$. Second recrystallization: Subs., 0.6042: $\alpha = +18.418°$; $[\alpha]_D^{20} = +190.34°$. Third recrystallization: Subs., 0.6129: $\alpha = +18.608°$; $[\alpha]_D^{20} = +189.57°$. As other preparations gave final values of about +190.50, this value is taken as the specific rotation of the pure substance.

Analyses.—Subs., 0.2299: CO_2, 0.3088; H_2O, 0.0872, Subs. 0.2977 AgI, 0.1530. Calcd. for $C_{14}H_{19}O_9I$: C, 36.67; H, 4.18; I, 27.71. Found: C, 36.63; H, 4.24; I, 27,78.

WASHINGTON, June 30, 1931.

RP359

SOIL-CORROSION STUDIES

NONFERROUS METALS AND ALLOYS, METALLIC COATINGS AND SPECIALLY PREPARED FERROUS PIPES REMOVED IN 1930

By K. H. Logan

ABSTRACT

This paper presents the results of the examination of specimens of nonferrous materials and metallic protective coatings removed from 45 soils after exposure of from four to six years. Included in the test were specimens of copper and brass pipe, cast and forged brass fittings, galvanized pipe and sheet steel, lead sheet, lead-coated pipe, and lead-coated and galvanized bolts. Data on the rates of corrosion of steel pipe are also presented as a basis for comparison. The nonferrous metals tested were found to resist corrosion somewhat better than steel but they were not unaffected by soil action.

CONTENTS

	Page
I. Introduction	585
II. Tests of nonferrous metals and alloys	588
1. Copper alloy castings	588
2. Effect of connecting brass to other metals	589
3. Copper and copper alloy pipe and rod	590
4. Lead cable sheaths	592
5. Miscellaneous alloys	593
6. Parkway cable	594
III. Tests of metallic coatings	595
1. Lead-coated pipe	595
2. Galvanized pipe and sheet	597
3. Lead and zinc coated bolts	602
4. Calorized pipe	602
IV. Tests of high copper steel and of ground specimens	602
V. Summary	604

I. INTRODUCTION

When the National Bureau of Standards soil corrosion investigation started in 1922 attention was called to soils as possible causes of corrosion, and questions were raised as to the best methods of preventing the deterioration of pipe lines. Recognizing the close relation between this problem and the investigation already started, the bureau undertook to determine the corrosion-resisting properties of a considerable variety of materials when buried in the soil. In most cases these materials were supplied by their makers or users. Some of the difficulties involved in the work were recognized, while others were underestimated.

The principle governing the acceptance or rejection of specimens was to test such offered materials as could be tested without materially increasing the cost of the investigation, with the understanding that such data would be secured as circumstances permitted.

A list of the materials tested will be found on page 453 of Technologic Paper No. 368.[1] That paper also gives a description of the soils to which the materials were exposed, a list of organizations cooperating in the tests, and the results of the tests after periods of exposure of from two to four years; that is, for the specimens removed in 1924 and 1926. Almost no nonferrous specimens were removed in 1928, but sets of all kinds of specimens, with the exception of one metallic and four bituminous coatings, were removed in 1930. The results of the examinations of the ferrous materials removed in 1930 will be found in Research Paper No. 329 entitled "Soil Corrosion Studies 1930, Rates of Corrosion and Pitting of Bare Ferrous Specimens." That report[2] is the third report on ferrous materials. The present report deals mainly with the nonferrous materials used to reduce corrosion losses, but includes a few data on rates of corrosion of ferrous materials for purposes of comparison.

As some of the tables require considerable space, it has been found advisable to refer to the test locations by number only. Table 1 gives the numbers of the soils and their approximate locations. The numbers are the same as those used in the other National Bureau of Standards reports on soil corrosion. Table 1 also gives the weighted average rates of corrosion and pitting for all the 6-year-old ferrous specimens. The weighting is based on the total exposed areas of the several kinds of specimens.

In using this table for comparing the rates of corrosion of ferrous and nonferrous materials, it should be remembered that the rate of corrosion is influenced by the time of exposure, and that on account of irregularities in soils and in commercial materials the performance of a single specimen may be either better or worse than the average performance of a group of specimens of the same material. In the case of pitting it can be shown that for relatively small specimens with only a few pits the chances are that other things being equal, the largest specimen will have the deepest pit. The effects of irregularities in soils and the difficulties arising from comparing specimens of different sizes and ages are discussed in the 1930 report on ferrous materials. On account of the nature of the tests no positive conclusions as to relative merits of materials should be drawn from the performance of individual specimens, but the average performance of the material may be taken as indicative of the usefulness of that material under the conditions of the test. Obviously, the material best suited for some soil conditions may not be the best material under radically different conditions.

---

[1] Bureau of Standards Soil Corrosion Studies. I. Soils, Materials, and Results of Early Observations. B. S. Tech. Paper No. 368. For sale by Superintendent of Documents, Washington, D. C., 50¢ per copy.

[2] B. S. Jour. Research, 7 (PP329), p. 1.

TABLE 1.—*Soils, locations of tests, and rates of corrosion of ferrous materials for the first six years after burial*

No.	Name	Location	6-year weighted rates of corrosion	
			Loss of weight in ounces per square foot per year	Penetration in mils per year
1	Allis silt loam	Cleveland, Ohio	0.939	10.7
2	Bell clay	Dallas, Tex	.689	7.4
3	Cecil clay loam	Atlanta, Ga	.592	11.5
4	Chester loam	Jenkintown, Pa	.743	8.7
5	Dublin clay adobe	Oakland, Calif	.849	8.0
6	Everett gravelly sandy loam	Seattle, Wash	.126	2.1
7	Fairmount silt loam	Cincinnati, Ohio	(1)	(1)
8	Fargo clay loam	Fargo, N. Dak	.621	10.7
9	Genesee silt loam	Sidney, Ohio	.496	5.3
10	Gloucester sandy loam	Middleboro, Mass	.532	6.7
11	Hagerstown loam	Baltimore, Md	.192	9.3
12	Hanford fine sandy loam	Los Angeles, Calif	.440	8.3
13	Hanford very fine sandy loam	Bakersfield, Calif	1.377	14.2
14	Hempstead silt loam	St. Paul, Minn	.563	13.0
15	Houston black clay	San Antonio, Tex	1.028	10.4
16	Kalmia fine sandy loam	Mobile, Ala	.836	14.8
17	Keyport loam	Alexandria, Va	.981	6.0
18	Knox silt loam	Omaha, Nebr	.526	12.4
19	Lindley silt loam	Des Moines, Iowa	.381	10.0
20	Mahoning silt loam	Cleveland, Ohio	.515	5.6
21	Marshall silt loam	Kansas City, Mo	.799	9.9
22	Memphis silt loam	Memphis, Tenn	.786	13.1
23	Merced silt loam	Buttonwillow, Calif	3.144	22.0
24	Merrimac gravelly sandy loam	Norwood, Mass	.160	2.2
25	Miami clay loam	Milwaukee, Wis	.292	7.9
26	Miami silt loam	Springfield, Ohio	.302	11.1
27	Miller clay	Bunkie, La	.637	7.4
28	Montezuma clay adobe	San Diego, Calif	1.569	12.2
29	Muck	New Orleans, La	1.599	13.5
30	Muscatine silt loam	Davenport, Iowa	.455	3.9
31	Norfolk sand	Jacksonville, Fla	.355	6.6
32	Ontario loam	Rochester, N. Y	.409	6.2
33	Peat	Milwaukee, Wis	.673	6.7
34	Penn silt loam	Norristown, Pa	.469	5.2
35	Ramona loam	Los Angeles, Calif	.185	2.6
36	Ruston sandy loam	Meridian, Miss	.245	8.8
37	St. Johns fine sand	Jacksonville, Fla	.758	7.4
38	Sassafras gravelly sandy loam	Camden, N. J	.175	3.6
39	Sassafras silt loam	Wilmington, Del	.568	6.9
40	Sharkey clay	New Orleans, La	1.102	12.2
41	Summit silt loam	Kansas City, Mo	.575	7.9
42	Susquehanna clay	Meridian, Miss	1.322	16.6
43	Tidal marsh	Elizabeth, N. J	1.132	12.0
44	Wabash silt loam	Omaha, Nebr	.320	10.3
45	Unidentified alkali soil	Casper, Wyo	.493	6.9
46	Unidentified sandy loam	Denver, Col	.458	9.8
47	Unidentified silt loam	Salt Lake City, Utah	.342	1.7
	Average for all soils		.690	8.9

[1] No 6-year-old specimens.

II. TESTS OF NONFERROUS METALS AND ALLOYS

1. COPPER ALLOY CASTINGS

At the time the soil corrosion tests were started, the American Water Works Association and certain manufacturers were considering the proper specification for the composition of the cocks to be used in connection with water-service lines. On this account the bureau was asked to determine the corrosion-resisting properties of four brasses, and the effect of connecting these to steel, brass, and lead service pipes. The compositions of the brasses are given in Table 16 of Technologic Paper 368, previously referred to. Roughly, the copper content of the castings ranged between 94 and 75 per cent, the tin content between 6 and 0 per cent, and the zinc content between 20 and 5 per cent. All of the castings contained small amounts of lead. Short lengths of three materials—brass, lead, and galvanized iron—were connected to castings of each composition for the purpose of studying possible galvanic corrosion caused by connecting together two two different metals. Figure 1 shows the appearance of these specimens.

Table 2 gives the rates of loss of weight of the castings and of the nipples attached to the castings. While there are some apparent differences between the rates of corrosion of the castings of different compositions, the corrosion was in nearly all cases slight and the differences in the losses may well be attributed to variations in the castings or to variations in the soil conditions to which they were exposed. On this account it does not seem worth while to report the rates of loss of weight of each compositon separately. In so far as inspection can be depended upon, castings of any of the compositions under test appear to be satisfactory from a corrosion standpoint.

TABLE 2.—*Rates of loss of weight of cast brass caps, and of brass, lead, and galvanized steel nipples attached to the caps*

[In ounces per square foot per year]

Soil No.[1]	Average of 12 cast brass caps	Average of 4 brass nipples	Average of 4 lead nipples	Average of 4 galvanized steel nipples	Soil No.[1]	Average of 12 cast brass caps	Average of 4 brass nipples	Average of 4 lead nipples	Average of 4 galvanized steel nipples
1	0.0581	0.198	0.883	1.971	26	0.0190	0.123	0.447	0.330
2	.0074	.084	.415	.177	27	.0070	.124	.620	.243
3	.0228	.085	.740	.434	28	.0097	(3)	(3)	2.072
4	.0230	.239	.704	.933	29	.0354	.567	1.937	1.384
5	.0097	.199	1.020	1.118	30	.0123	.079	.323	.442
6	.0142	.024	.168	.219	31	.0124	.084	.691	.301
7	.0127	.189	.717	.420	32	.0155	.086	.332	.165
8	.0176	.130	.273	.556	33	.0355	.284	.384	.723
9	.0228	.156	.570	.357	34	.0239	.123	.341	.238
10	.0131	.127	.722	.375	35	.0112	.008	.074	.076
11	.0158	.075	.546	.295					
12	.0953	.111	.833	.168	36	.0133	.039	.408	.133
13	.0149	.172	.301	1.876	37	.0806	.407	1.608	1.510
14	.0103	.047	1.129	.519	38	.0072	.053	.241	.082
15	.0085	.073	.376	.369	39	.0198	.336	.397	.416
16	.0185	.151	.951	.594	40	.0146	.206	.666	.420
17	.0218	.181	.666	.880	41	.0129	.063	.462	.253
18	.0135	.120	.601	.282	42	.0181	.129	.908	.734
19	.0211	.140	.620	.320	43	.3318	.037	.083	1.687
20	.0226	.153	.691	.620	44	.0095	.036	.177	.282
21	(2)	(2)	(2)	(2)	45	.0314	.623	.102	4.201
22	.0209	.178	.697	.649	46	.0113	.052	.646	.884
23	.1910	1.678	.161	(3)	47	.0088	.020	.104	.240
24	.0138	.027	.156	.048					
25	.0106	.112	.546	.191	Average	.0309	.180	.552	.671

[1] See Table 1 for names and locations of soils. [2] No specimens. [3] Specimens destroyed by corrosion.

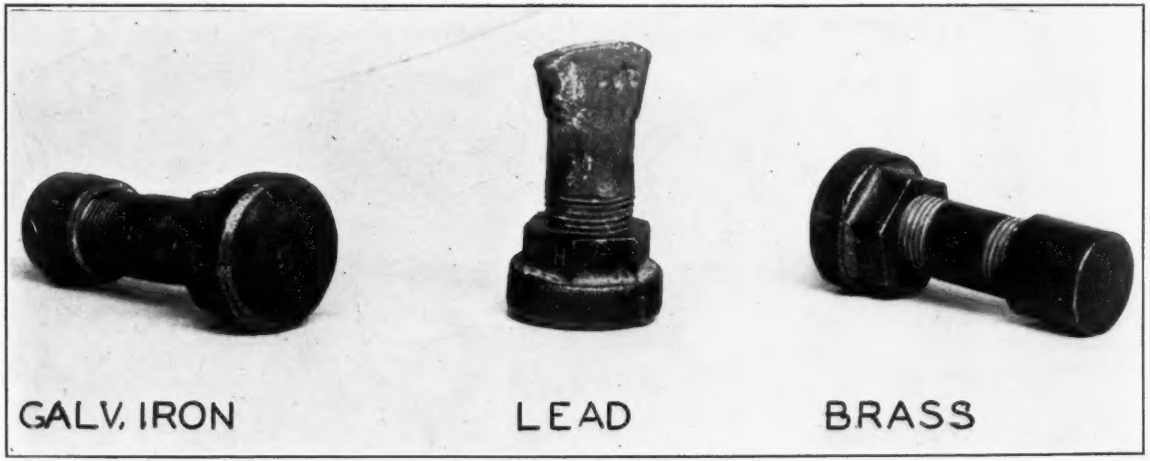

FIGURE 1.—*Brass caps attached to brass, lead, and galvanized steel nipples*

2. EFFECT OF CONNECTING BRASS TO OTHER METALS

Table 2 shows also the rates of corrosion of the nipples attached to the brass caps. In every soil the rates of corrosion of the galvanized nipples were greater than those for the brass nipples. In many soils the coating of zinc was almost or entirely destroyed. Unfortunately, the weight of the zinc coating was not determined. There is evidence of some pitting of the lead nipples which may be attributed to galvanic action. That the corrosion of the lead nipples was caused in part by galvanic action is indicated by the fact that in all soils the rates of corrosion of the lead nipples were greater than the rates of loss of weight of the commercial lead cable sheath shown in Table 6. It is probable, however, that the compositions of the two leads are not identical, since they were obtained from different sources.

Dezincification was observable in some of the brass nipples; but as this occurs also in brass pipe of approximately the same composition not connected with another metal the dezincification should not be attributed to galvanic action. There was no roughening of the brass nipples, but in one soil dezincification so weakened one of them that it crushed when an attempt was made to unscrew it from the casting.

It is somewhat doubtful whether the experiment simulates working conditions closely enough to warrant definite conclusions as to the effect of connecting together different metals. In the experiment the anodic and cathodic metals had approximately the same areas, while in service the anodic area is usually very large when compared with the cathodic area. Polarization which tends to limit galvanic corrosion is in most soils largely a cathodic phenomenon and increases as the current density at the cathode increases. Galvanic action would, therefore, be less affected by polarization when the cathodic area is relatively large, as in the test, than in actual service. This may account for the fact that there are few reported cases of corrosion of iron and steel pipes adjacent to the brass cocks which are screwed into them.

To study further the question of corrosion of iron adjacent to brass, several pairs of cast-iron strips about 2 inches wide and 8 inches long were joined by brazing and buried in a corrosive soil. After about six years the strips were removed. The specimens were irregularly pitted, but the corrosion with one exception did not appear greater at the joint than elsewhere. Thus the results of the test indicate that a small amount of brass in an iron pipe line does not increase its rate of corrosion. On the other hand, a case has recently been called to the bureau's attention in which a steel coupling in a brass water-service pipe failed within a comparatively short time. In this case, however, there was the unusual condition of a large cathodic area and a small anode. Corrosion caused by galvanic action has been reported in a number of cases where ferrous and nonferrous materials have been joined. No positive demonstration has been made showing the conditions under which such corrosion does or does not occur. Apparently galvanic corrosion may be expected if a film of corrosion products or if polarization at the cathodic surface does not interfere. Moving water tends to remove corrosion products and a relatively small cathodic area tends to increase the amount of polarization.

3. COPPER AND COPPER ALLOY PIPES AND RODS

The question as to the resistance of copper and brass pipe to soil action resulted in the burial in 1926 of three varieties of copper pipe, two kinds of brass pipe, a forged leaded brass ell, and two kinds of copper alloy rods. Analyses of these materials are given in Table 3. The rates of loss of weight of most of these materials are shown in Table 4. The figures represent the average for two specimens in each soil except where a specimen was lost. This table also indicates whether or not the specimens were pitted. In most cases the pits were too shallow to permit their accurate measurement. In addition to the pits on the Muntz metal pipe, there were, in most cases, numerous reddish spots where dezincification occurred, leaving the metal week and spongy. The bottoms of the larger pits also contained some of this dezincified metal. Of the materials for which data are shown in Table 4, the alloy (A) appears to be the poorest in most soils. Table 5 shows similar data for two materials which were buried in six soils only.

It is doubtful whether there is a significant difference between the performances of similar materials included in the two tables. Comparison of the data in Tables 4 and 5 with the average rates of corrosion of ferrous materials shown in Table 1 indicates that, in most soils, copper and its alloys corroded much more solwly than did the ferrous pipe materials. It is probable, however, that the reduction in the strength of the Muntz metal pipe, material B, is considerably greater than would be indicated by the loss of weight.

TABLE 3.—*Compositions of copper and copper alloy pipes and rods*

Class	Form	Length	Cu	Zn	Pb	Al	Fe	Ni	P
		Inches	*Per cent*	*Per cent*	*Per cent*	*Per cent*	*Per cent*	*Per cent*	*Per cent*
A	7/16-inch rod	12	47	[1] 40.5	2.5	----	----	10	----
B	½-inch I. P. S. pipe	12	60	40	----	----	----	----	----
E	1-inch pipe	17	99.97	----	----	----	----	----	----
H	----do	17	84.99	14.97	.01	----	0.03	----	----
M	¾-inch pipe	12	99.93	----	----	----	----	----	----
Me	½-inch S.A.E. forged ell	2	59	[1] 38.5	2.5	----	----	----	----
N	7/16-inch rod	12	87	----	----	[1] 9.5	3.5	----	----
P	¾-inch pipe	12	99.94	----	----	----	----	----	0.015

[1] By difference.

NOTE.—These analyses were furnished by the manufacturers of the materials.

TABLE 4.—*Corrosion of copper and copper alloy pipes and rods*

[Two specimens of each material in each soil except as noted]

Soil No.[1]	Age (years)	Rates of loss of weight in ounces per square foot per year						Pitting					
		A[2]	N	M	P	Me	B	A	N	M	P	Me	B
1	4.11	0.0155	0.0085	0.0179	0.0113	0.0453	0.0165	[3] P	----	----	----	----	----
2													
3	3.90	.2237	.0666	.0538	.0530	.1557	.0917	P	----	P	P	----	P
4	3.93	.0479	.0290	.0218	.0205	[4] .2114	.0146	P	----	----	----	----	----
5	3.93	.1895	.0441	.0402	.0323	.4323	.0260	P	----	----	----	----	----
6	3.92	.0539	.0031	.0207	.0185	.0351	.0250	P	----	----	----	----	----
7													
8	3.94	.1983	[4] .0401	.0413	.0413	[4] .2122	.0686	P	----	P	P	----	P
9	4.19	.2053	.0141	.0576	.0742	.2100	.3070	P	P	P	P	----	P
10	3.92	.2171	.0628	.0841	.0731	.1466	.1155	P	----	P	P	----	P

[1] See Table 1 for names and locations of soils.
[2] See Table 3 for significance of the letters at the tops of each column.
[3] P signifies pitted.
[4] One specimen only.

TABLE 4.—*Corrosion of copper and copper alloy pipes and rods*—Continued

Soil No.	Age (years)	Rates of loss of weight in ounces per square foot per year						Pitting					
		A	N	M	P	Me	B	A	N	M	P	Me	B
11	3.88	0.1528	0.0255	0.0395	0.0422	0.0952	0.0810	P	----	P	P	----	P
12	3.92	[4].0659	[4].0302	.3576	.3421	[4].3077	[4].0721	P	----	P	P	----	P
13	3.84	.0570	.0515	.0320	.0349	.4119	.2727	----	----	P	P	----	P
14	3.92	.1368	.0290	.0200	.0225	.2559	.0505	P	----	----	----	----	----
15	3.90	.0845	.0374	.0264	.0262	.0669	.0533	P	----	----	----	----	----
16	3.90	.2782	.1032	.0885	.1015	.1509	.1818	P	----	P	P	----	P
17	3.89	.2704	.0953	.0665	.0678	[4].2761	.1419	P	----	P	P	----	P
18	3.92	.0287	.0166	.0103	.0132	.1090	.0245	P	----	P	----	----	----
19	3.92	.2842	.0752	.0792	.0855	[4].1444	[4].2211	P	----	P	P	----	P
20	4.12	.1391	.0476	.0358	.0445	.2559	.0329	P	----	P	P	----	----
21													
22	3.91	.2884	.0739	.0939	.0957	[4].1452	.1795	P	----	P	P	----	P
23	3.89	.2606	.1973	.0540	.0332	1.3259	.5801	----	----	P	P	----	P
24	3.92	.0570	.0201	.0249	.0223	.0485	.0362	P	----	P	P	----	----
25	3.91	.1741	.0400	.0193	.0173	.1586	.0564	P	----	----	----	----	P
26	4.18	.1261	.0251	.0274	.0241	.1089	.0780	P	----	----	----	----	----
27	3.85	.1457	.0513	.0369	.0471	----	.0856	P	----	----	----	----	----
28	3.99	.1628	.1202	.0534	.0671	1.1783	.0684	P	----	P	P	----	----
29	3.90	.2213	.1021	.1645	.1585	.5563	.1590	P	P	P	P	----	P
30	4.52	.0104	.0054	.0078	.0079	----	.0053	----	----	----	P	----	----
31	3.91	.0898	.0377	.0293	.0287	.0053	.0646	P	----	----	----	----	----
32	3.92	.2070	.0449	.0129	.0166	.3481	.1167	P	----	----	----	----	P
33	3.92	.1167	.0329	.0646	.0731	.2456	.0593	P	----	P	P	----	P
34	3.93	.1446	.0305	.0259	.0306	.0416	.0648	P	----	----	----	----	P
35	3.92	.0205	.0140	.0175	.0173	.0754	.0103	P	----	----	----	----	----
36	3.94	.1686	.0254	.0379	.0376	.0900	.0801	P	----	P	P	----	P
37	3.91	.2663	.0796	.2441	[4].2199	[4].4906	.1994	P	----	P	P	----	P
38	3.93	.0560	.0278	.0323	.0296	.0826	.0302	P	----	P	P	----	P
39													
40	3.90	.4252	.0098	.1009	[4].0948	[4].3531	.3030	P	P	P	P	----	P
41	3.92	.2326	.0100	.0405	.0453	.1432	.0926	P	----	----	P	----	P
42	3.94	.3128	.1273	.0948	.0866	.2334	.2249	P	----	P	P	----	P
43	3.92	.0054	.0969	.5189	.6305	.0221	.0550	----	P	P	P	----	----
44	3.92	.1593	.0438	.0417	.0390	.3575	.0735	P	----	P	P	P	P
45	3.91	.0960	.0579	.0207	.0308	.3070	.0488	P	----	P	P	----	----
46													
47	3.91	.0105	.0066	[4].0065	[4].2830	[4].0240	.0060	----	----	----	----	----	----

[4] One specimen only.

TABLE 5.—*Corrosion of 1-inch copper and red brass pipe in six soils*

[Two specimens of each kind in each soil except soil 42]

Soil No.[1]	Age (years)	Rates of loss of weight in ounces per square foot per year		Pitting		Soil No.[1]	Age (years)	Rates of loss of weight in ounces per square foot per year		Pitting	
		E[2]	H	E	H			E[2]	H	E	H
13	3.84	0.0346	0.0275	[3]P		42	3.94	[4]0.0826	[4]0.1373	P	P
24	3.92	.0264	.0267	P		43	3.92	.4088	.0913	P	P
29	3.90	.1563	.1717	P	P	45	3.91	.0418	.0614	P	P

[1] See Table 1 for names and locations of soils.
[2] See Table 3 for significance of letters at the top of each column.
[3] P signifies pitted.
[4] One specimen only.

4. LEAD CABLE SHEATHS

Samples of two kinds of lead cable sheaths were buried in 1922 and 1924. The sheaths were split and flattened to form sheets. One set of samples contained approximately 1 per cent of antimony; the other sheath was made from commercial lead. The standard size of the alloy sheets was 22 by 8½ inches and that of the commercial lead samples was 22 by 3½ inches. The thicknesses of the specimens were 0.12 and 0.11 inch, respectively. In comparing the performances of the two materials it should be kept in mind that the larger sheets afford a greater opportunity for unusually deep pits. Table 6 shows the rates of corrosion of the two materials. Both the rates of loss of weight and the rates of pitting indicate that the samples containing 1 per cent of antimony corroded more rapidly than those without it.

There appears to be no close relation between the corrosive actions exerted by the soils upon lead and steel. The shaley subsoil of Allis loam causes bad pitting of both steel and lead. Merced silt loam (soil 23), an alkali soil which is the most corrosive soil under investigation with respect to ferrous materials, is relatively noncorrosive with respect to lead.

TABLE 6.—*Corrosion of lead cable sheath*

[One specimen of each material in each soil]

Soil No.[1]	Age (years)	Rates of loss of weight in ounces per square foot per year		Rates of penetration in mils per year		Soil No.[1]	Age (years)	Rates of loss of weight in ounces per square foot per year		Rates of penetration[4] in mils per year	
		A[2]	H[3]	A	H			A[2]	H[3]	A	H
1	7.68	0.45	0.30	14.8	12.1	26	7.67	0.06	0.03	3.4	2.0
2	5.84	.11	.09	3.1	2.4	27	6.01	.12	.07	3.5	4.0
3	5.97	.07	.06	(5)	(5)	28	5.56	.19	.14	4.9	3.6
4	7.96	.24	.26	4.4	3.1	29	7.96	.24	.29	(5)	1.4
5	6.13	.25	.15	5.9	2.9	30	8.17	.15	.11	4.4	3.8
6	6.13	.04	.04	(5)	(5)	31	5.98	.05	.04	2.2	(5)
7	7.68	.17	.12	4.2	2.3	32	7.65	.05	.03	(5)	(5)
8	7.74	.09	.04	6.8	1.8	33	7.63	.12	.14	2.5	2.0
9	7.67	.11	.11	(5)	4.2	34	7.96	.22	.19	5.2	3.1
10	7.93	.08	.04	(5)	(5)	35	6.12	.02	.03	(5)	(5)
11	7.84	.05	.03	3.8	(5)	36	6.02	.06	.05	(5)	(5)
12	6.12	.23	.15	2.3	4.7	37	5.98	.30	.31	7.0	3.3
13				(5)	(5)	38	7.97	.04	.03	(5)	(5)
14	7.72	.13	.06	3.6	(5)	39	7.95	.13	.11	5.5	2.6
15	5.99	.08	.08	3.7	2.8	40	6.01	.26	.17	3.7	3.2
16	5.98	.09	.11	(5)	3.2	41	7.94	.04	.04	(5)	(5)
17				(5)	(5)	42	6.02	.11	.10	(5)	3.0
18	7.67	.06	.02	2.2	(5)	43	7.98	.06	.03	2.5	2.0
19	7.58	.12	.07	3.8	1.5						
20	7.68	.23	.17	5.6	3.6	44	7.58	.08	.05	(5)	(5)
21				(5)	(5)	45	7.68	.04	.03	6.0	(5)
22				(5)	(5)	46				(5)	(5)
23	7.95	.03	.02	(5)	(5)	47	7.99	.27	.06	6.8	3.3
24	7.93	.04	.02	(5)	(5)						
25	7.62	.04	.04	4.2	(5)						

[1] See Table 1 for names and locations of soils.
[2] Lead + 1 per cent of antimony.
[3] Commercial lead.
[4] Average of the 2 deepest pits; one on each side of a single specimen.
[5] No measurable pits.

By comparing Tables 1 and 6 it will be seen that the rates of loss of weight of the lead sheaths are about one-tenth of those of ferrous materials in the same soils, and the rates of pitting of the lead about half those of iron and steel. However, in most soils the ratio of the maximum to the average penetration by corrosion is much greater for lead than for steel. If the rates of loss of weight of lead are compared with the corresponding rates for copper and brass pipe, as shown in Tables 4 and 6, it will be seen that the latter materials corrode somewhat more slowly in most soils, but not in all. As the specimens of the different materials are of different sizes and have been buried for different lengths of time, and as the duration of the test is short when compared to the life of any of the materials, too much weight should not be given to the results of comparison made at this time.

5. MISCELLANEOUS ALLOYS

At the request of the Bureau of Mines there were included with the specimens buried in five soils in 1924 specimens of a number of alloys. These were 6 inches long and 2 inches wide and of different thicknesses. Such data as are available concerning these specimens are given in Table 7. This table also includes descriptions of some materials that will be discussed in later parts of this paper. Table 8 gives the rates of losses of weight of the specimens and indicates the maximum pit depths in mils per year. The corrosion of some of the aluminum and aluminum alloy specimens occurred beneath their surfaces and produced ridges or blisters. The corrosion products were not completely removed from these blisters before the specimens were weighed. It has been suggested that the aluminum specimens represented poor material, but at this time no evidence as to this is available.

TABLE 7.—*Character and dimensions of miscellaneous specimens*

Symbol	Description
A	Pure open-hearth iron, 2 by 6 by 0.125 inches.
S	Copper-bearing steel, 2 by 6 by 0.0625 inches.
Z1	Zinc sheet, 99.5 per cent pure, 2 by 6 by 0.0625 inches.
Z2	Zinc plate, 99.5 per cent pure, 2.5 by 6.5 by 0.25 inches.
Z3	Corrugated zinc sheet, 12 by 12 by 0.027 inches.
P	"Standard" zinc sheet, 2 by 6 by 0.0625 inches.
I	Bronze 90-10 Cu-Sn, 2 by 6 by 0.25 inches.
B	Brass 70-30 Cu-Zn, 2 by 6 by 0.050 inches.
H	Copper sheet, 2 by 6 by 0.050 inches.
N	Chemical lead (0.05–0.08 per cent Cu, about 0.005 per cent Ag), 2 by 6 by 0.25 inches.
NN	Hearth refined lead (less than 0.001 per cent each of Cu and Ag), 2 by 6 by 0.25 inches.
C1	Commercial aluminum, 2 by 6 by 0.0625 inches.
C2	Aluminum with 1.5 per cent Mn, 2 by 6 by 0.0625 inches.
C3	Duralumin, 2 by 6 by 0.0625 inches.
D	Wrought-iron nuts and bolts, 2 by 0.75 inches.
F	Lead-coated nuts and bolts, 2 by 0.75 inches.
G	Sherardized nuts and bolts, 2 by 0.75 inches.

68723—31——12

TABLE 8.—*Corrosion of miscellaneous specimens*

[Average of 2 specimens]

Material	Soil number									
	13		29		42		43		45	
	Age (years)									
	6.13		6.01		6.02		6.70		6.50	
	Loss [1]	Pits [2]	Loss	Pits	Loss	Pits	Loss	Pits	Loss	Pits
A	0.7632	6.85	0.5938	11.65	0.5628	H	1.4166	H	1.4470	H
B	.0537	[3]	.1654	[3]	.0247	[3]	.0101	[3]	.0773	[3]
C1	.0071	3.59	.0635	H	.0191	5.81	.0535	[4] 1.94	[5] .0410	4.0
C2	.0351	H	.1705	H	.0024	.92	.0007	[3]	.0363	2.54
C3			[5] .5755	H	.1816	H	.0018	[3]	.0529	H
H	.0042	[3]	.1369	1.33	.0267	[3]	[4] .4818	[3]	.0341	[3]
L	.0090	[3]	.0883	1.75	.0389	.83	.5308	[3]	.0640	2.00
N	.0475	[3]	.3781	2.49	.1880	3.24	.0502	1.19	.0750	4.08
NN	.0063	[3]	.2386	2.00	.1066	[3]	.0568	2.31	.0287	3.0
P									[5] .2037	[3]
S	.8023	H	.8058	H	.6604	H	[5] 1.7365	H	1.1243	H
Z1	.1140	2.69	.2447	1.75	.0424	.83	.1752	4.63	.1187	3.23
Z2	.1542	4.98	.2683	3.58	.0367	1.66	.1842	11.42	.1319	7.00

[1] Loss in ounces per square foot per year.
[2] Maximum pits in mils per year.
[3] No measurable pits.
[4] Pitting under asphalt only.
[5] One specimen only.
H = Hole in at least one specimen.

6. PARKWAY CABLE

Specimens of parkway cable were buried in most of the test locations in 1924. This material consists of a rubber-covered copper wire surrounded by a lead sheath. The sheath is wrapped with jute partially impregnated with a bituminous material. This is protected by two spirally wound ribbons of galvanized steel which in turn are covered by an asphalt-coated jute wrapper. The cable is intended to be buried directly in the earth. It is not practicable to determine the deterioration of the cable by measurements of loss of weight or depth of pits. Table 9 is an attempt to indicate the condition of each part of each specimen. It will be noted that while the outer steel sheath is rusted in a large percentage of the soils in which the cable was buried, the sheath was pitted in but two soils. In most cases the lead sheath was coated with a thin layer of white material, possibly lead carbonate.

It seems probable that the use of a wrapper which would not separate on being bent and one more thoroughly impregnated with bituminous material would offer more protection to the steel ribbons, but the condition of the lead sheath indicates that the present construction results in quite effective protection of the copper conductor, which is really the objective sought.

TABLE 9.—*Condition of Parkway cable*

(All steel is galvanized)

Soil No.[1]	Years buried	Outer fabric	Inner fabric	Outer steel wrapper	Inner steel wrapper	Lead sheath	Soil No.[1]	Years buried	Outer fabric	Inner fabric	Outer steel wrapper	Inner steel wrapper	Lead sheath
1	7.68	G[2]	G	G	G	G	24	7.93	E	G	G	G	TW
2	5.84	F	G	G	G	W	25	7.62	B	G	G	G	W
3	5.97	F	G	R	SR	TW	26	7.67	B	G	SR	B	TW
4	7.96	F	G	SR	SR	TW	27	6.01	VB	G	SR	SR	TW
5	6.13	F	G	SR	SR	TW	28	5.56	VB	G	BR	R	TW
6	6.13	F	G	R	G	TW	29	7.96	B	G	BR	R	TW
7	7.68	F	G	SR	SR	TW	30	8.17	F	G	G	G	W
8	7.74	F	G	G	G	TW	33	7.63	F	G	G	G	TW
9	7.67	F	F	VSR	G	TW	34	7.96	F	G	SR	G	W
11	7.84	F	G	SR	G	G	35	6.12	G	G	G	G	TW
12	6.12	F	G	SR	VSR	G	36	6.02	F	G	BR	R	TW
13	8.06	VB	VB	P	BR	P	42	6.02	B	G	R	G	G
16	5.98	B	G	R	SR	TW	43	7.98	G	G	G	G	G
18	7.67	F	G	R	G	TW	44	7.58	B	G	BR	G	W
19	7.58	F	G	SR	G	TW	45	7.68	F	G	G	G	G
22	7.59	B	F	BR	R	P	47	7.99	F	G	SR	G	TW

[1] See Table 1 for names and locations of soils.

[2] Ratings:
G, good.
F, fair.
B, bad.
R, rusted.
SR, slightly rusted.
BR, badly rusted.
TW, thin white corrosion product on lead sheath.
W, white corrosion product on lead sheath.
V, very.
P, pitted.

(Ratings by E. R. Shepard and I. A. Denison.)

III. TESTS OF METALLIC COATINGS

1. LEAD COATED PIPE

Since under many conditions lead corrodes less rapidly than iron or steel, lead coating has been suggested as a means of preventing corrosion of steel pipe under ground. In order to secure some data on the effectiveness of lead as a protective coating, specimens of steel pipe 1½ inches in nominal diameter and 6 inches long, and covered by a coating of lead approximately 0.002 inch thick, were buried in 1924. Two specimens of this material were removed from most of the test locations in 1930. Table 10 shows the average rates of loss of weight and penetration of the deepest pits for each pair of specimens removed. All the specimens were exposed to the soils about six years. The times of exposure were the same as those for the galvanized specimens in the same soils and can be found in Table 11. Table 10 shows also similar data for lead-coated steel pipe exposed to the same soils for two years and uncoated steel pipes of the same size exposed to the same soils for approximately six years. The data on specimens removed prior to 1930 are included to facilitate studies of the changes in rates of corrosion with time and the effectiveness of the protective coating.

Comparison of the two and the six year lead-coated specimens with respect to loss of weight and pitting indicates that for most locations the relative performances of the specimens for the two periods were similar; that is, if the soil appeared corrosive with respect to the lead coating at the close of two years, it also appeared corrosive at the close of the 6-year period. This indicates that the rates of loss of weight and pitting are not accidental, but are functions of the character of the test site.

TABLE 10.—*Corrosion of lead-coated steel pipe*

Soil No.[1]	Rates of loss of weight in ounces per square foot per year			Rates of maximum penetration in mils per year			Soil No.[1]	Rates of loss of weight in ounces per square foot per year			Rates of maximum penetration in mils per year		
	Lead coated specimens		Bare steel specimens	Lead coated specimens		Bare steel specimens		Lead coated specimens		Bare steel specimens	Lead coated specimens		Bare steel specimens
	6 years old [2]	2 years old	6 years old	6 years old	2 years old	6 years old		6 years old [2]	2 years old	6 years old	6 years old	2 years old	6 years old
1	0.5475	0.51	1.010	9.7	21	7.0	27	0.1574	0.11	0.690	7.6	13	5.3
3	.0515	.08	.620	3.8	[3]	11.5	28	.4891	.34	1.711	12.8	26	10.7
4	.2109	.16	.725	10.3	15	7.3	29	.3824	.88	1.580	8.1	18	15.3
5	.3263	.15	.735	6.0	12	8.3	30	.1245	.05	.455	10.6	19	4.1
6	.0009	.05	.135	[4]	[3]	[4]	31	.1912	.07	.305	[3]	[3]	4.9
7	.1654	[4]	[4]	9.5	[4]	[4]	32	.0154	.11	.395	4.7	22	5.1
8	.0416	.14	.500	13.2	20	8.8	33	.7494	.24	.805	12.7	15	[3]
9	.0721	[4]	.445	6.1	[4]	5.2	34	.1459	.19	.450	8.1	16	[5] 2.6
10	.0699	.06	.570	5.6	12	6.4	35	.0119	.04	.255	[3]	[3]	[5] 6.6
11	.0641	.08	.235	2.9	[3]	10.1	36	.0190	.11	.290	[3]	[3]	6.2
13	.0077	.05	1.130	2.7	[3]	11.4	37	.5441	[6]	.600	9.0	15	6.4
14	.0170	.05	.420	3.4	8	14.3	38	.0342	.09	.195	[5] 2.0	[4]	3.3
15	.0461	.07	.950	4.1	10	9.0							
16	.0813	[6]	.735	6.7	[3]	15.8	39	.0439	.19	.430	[5] 3.2	13	6.1
							41	.0640	[6]	.750	7.7	19	8.0
17	.3364	.32	.955	5.3	[3]	4.5	42	.1182	.14	1.290	10.1	15	14.0
18	.0179	.07	.560	5.5	9	12.5	43	.4723	.41	1.570	21.8	[7]	10.9
20	.2009	[4]	.445	7.2	[4]	3.9							
22	.1471	.44	.830	7.6	15	10.4	44	.0651	.04	.395	5.1	16	9.0
25	.0355	.08	.325	7.0	19	6.8	45	.1446	.09	.560	14.6	12	6.8
							46	.0405	.09	.510	4.6	9	10.8
26	.0699	.26	.305	8.0	16	12.2	47	.2688	[6]	.255	7.8	13	[3]

[1] See Table 1 for names and locations of soils.
[2] See Table 2 for exact ages of 6-year old lead coated specimens. They are the same as the galvanized specimens in the same soils.
[3] No measurable pits.
[4] Specimen missing.
[5] Depth of pits on one specimen assumed to be 10 mils for purpose of computation.
[6] Specimens cleaned in ammonium citrate. Some of the lead was probably taken off.
[7] Holes.

It will be noticed that in most soils the rate of penetration of the lead-coated specimens for the 6-year period is roughly half, or less than half, the corresponding rate for the 2-year period. Although the rates of penetration of the unprotected steel specimens decreased with time it is somewhat surprising to find that the rate of penetration of the lead-coated specimens also decreases with time. As the thickness of the lead coating is approximately 2 mils, corrosion of the lead in many soils must have exposed the steel beneath the lead, and one might suppose that this exposure of the steel would result in accelerated corrosion, since most tables of electrode potentials [3] indicate that iron is anodic with respect to lead. Although there are six soils in which the rate of penetration appears to increase with time, and although specimens have been found which showed serious corrosion of the steel when the lead coating showed only a pinhole, specimens in 25 soils show no accelerated corrosion. The data in Table 10 suggest the possibility that the potential which exists between lead and iron depends on the soil in which specimens composed of the metals are buried.

The pitted appearance of many of the lead-coated specimens frequently leads the casual observer to conclude that lead coating is

[3] H. S. Rawdon, Protective Metallic Coatings, Chemical Catalog Co., Table 1, p. 18.

ineffective. Although it is evident that the coating fails to furnish complete protection, comparison of the rates of corrosion of the 6-year old lead-coated specimens with those for the uncoated steel specimens exposed to the same soils for the same lengths of time indicates that in half of the soils the lead coating added considerably to the life of the pipe.

In so far as the significance of the data can be determined at this time it appears that the value of lead as a protective coating depends upon the soil to which it is to be exposed. At present not enough is known about the relations of soils to the corrosion of lead to justify a statement as to the soil conditions under which lead will provide satisfactory protection.

2. GALVANIZED PIPE AND SHEET STEEL

Among the specimens buried in 1924 were galvanized pipes and galvanized iron and steel sheet. The pipes were 17 inches long and from 1½ to 3 inches in diameter, the size depending on the kind of material. The galvanized sheets were mostly 16-gage metal 6 inches wide and 12 inches long. Most of the specimens carried 2-ounce coatings of zinc applied by the hot-dip process. It was hoped that the results of the tests would show the influence of the kind of base metal to which the coating was applied and the effect of differences in weights of coating. On this account 16-gage sheet of Bessemer steel, pure open-hearth iron, and open-hearth steel containing approximately 0.2 per cent of copper were buried in 45 soils. In 7 soils there were also buried 16-gage sheets of the last two materials carrying nominally 1.5, 2.5, and 3 ounce coatings, respectively. Eighteen-gage sheets of each material carrying 2-ounce coatings and 18-gage ungalvanized sheets were also buried in 7 soils. Pure open-hearth iron pipes carrying a 2-ounce coating were buried in 46 soils, and in 7 of these soils samples of galvanized wrought iron and steel pipe were also buried. The testing of these specimens is somewhat more fully described in Technologic Paper No. 368. The determination of the conditions of the specimens after their removal in 1930 proved a difficult problem. No method has been found by which all of the corrosion products can be removed from a partially rusted specimen without removing some of the remaining zinc and zinc-iron alloy. It was finally decided to scrub the specimens with a stiff wire brush and then to weigh them. The results of the weighings and pit measurements on the sheets are shown in Table 11. On account of the fact that not all the rust was removed from some of the specimens, the rates of loss of weight are in some cases smaller than they should be.

The appearance of the specimens is indicated in the rating sheet, Table 12, which also shows the average weights of coatings as determined in 1926. The ratings of the specimens were made by R. F. Passano, of the American Rolling Mill Co., and E. S. Taylerson, of the American Sheet & Tin Plate Co., both of whom have had extensive experience in the inspection of galvanized sheet metal. Sheets galvanized by the hot-dip process are subject to some unavoidable variation in the thickness of the coating. Rawdon [4] states that a variation of 17.5 per cent is considered by many manfacturers as good commercial practice and shows a diagram of a repre-

[4] H. S. Rawdon, Protective Metallic Coatings, p. 74, Chemical Catalog Co., New York, N. Y.

sentative sheet with a nominal 2.5-ounce coating which a spot test showed to vary from 1.79 to 2.98 ounces per square foot. When the variations in soil conditions within a few inches are also considered, the agreement in the rates of corrosion of the three specimens in any one soil is in most test locations quite good and too close to indicate that one type of material is superior to the others either on account of the characteristics of the base material or the process of galvanizing.

TABLE 11.—*Corrosion of 16-gage galvanized sheet steel with 2-ounce coatings*

Soil No.[1]	Age (years)	Rates of loss of weight in ounces per square foot per year				Rates of penetration[2] in mils per year			
		A[3] (pipe)	A3	B	Y3	A	A3	B	Y3
1	6.70	(4)	7.993	6.627	6.769	(4)	10.45	9.70	5.60
2	5.84	(4)	.0246	.0256	.0264	(4)	(5)	(5)	(5)
3	5.97	0.0383	.0275	.0292	.0278	(5)	(5)	(5)	(5)
4	6.58	.1733	.2092	.2344	.1841	2.13	2.81	1.98	2.89
5	6.13	.1475	.1704	.1717	.1551	(5)	(5)	(5)	(5)
6	6.13	.0102	.0055	.0078	.0060	(5)	(5)	(5)	(5)
7	6.64	.2379	.1388	.1151	.1296	(5)	(6).83	(5)	(5)
8	6.60	.0733	.0412	.0385	.0449	(5)	(5)	(5)	(5)
9	6.64	.0985	.0555	.0397	.0498	(5)	1.58	1.58	.75
10	6.60	.0344	.0268	.0196	.0247	(5)	(5)	(5)	(5)
11	6.48	.0599	.0373	.0487	.0570	3.70	1.23	4.86	3.16
12	6.12	(4)	(4)	[7].0498	[7].0395	(4)	(4)	(5)	(5)
13	6.13	.1303	.0571	.0532	.1052	(5)	(5)	(5)	(5)
14	6.59	.0350	.0236	.0218	.0243	(5)	(5)	(5)	(5)
15	5.99	.0509	.0242	.0235	.0304	(5)	(5)	(5)	(5)
16	5.98	.0896	.0736	.0839	.0616	1.67	2.26	2.59	1.51
17	6.50	.1390	.2096	.1950	.1609	(5)	(5)	(5)	(5)
18	6.48	.0334	.0168	.0150	.0167	(5)	(5)	(5)	(5)
19	6.46	.0888	.0574	.0678	.0606	(5)	.77	1.86	.54
20	6.71	.1776	.1209	.1208	.1391	(5)	2.76	1.12	2.01
21	(4)	(4)	(4)	(4)	(4)	(4)	(4)	(4)	(4)
22	5.87	.0842	.0837	.1052	.0780	(5)	3.32	2.81	2.39
23	6.12	(4)	2.3947	1.6679	2.6084	(4)	11.44	10.62	12.35
24	6.62	.0160	.0013	.0019	.0011	(5)	(5)	(5)	(5)
25	6.60	.0640	.0451	.0381	.0437	(5)	(5)	(5)	(5)
26	6.63	.0620	.0479	.0417	.0448	(5)	(5)	(5)	(5)
27	6.01	.0718	.0737	.0705	.0654	(5)	1.33	(5)	(5)
28	5.56	.1964	.2297	.2728	.4481	(5)	4.41	4.23	6.56
29	6.01	.2612	.3204	.3309	.3137	1.91	3.83	2.58	2.33
30	7.05	.0912	.1392	.1712	.7469	(5)	(5)	(5)	(5)
31	5.98	.0139	.0087	.0059	.0076	(5)	(5)	(5)	(5)
32	6.71	(4)	.0250	.0298	.0223	(4)	(5)	(5)	(5)
33	6.60	(4)	.1826	.2235	.2198	(4)	(6).83	(6).68	(6).83
34	6.58	.0910	.0876	.0738	.0657	(5)	2.51	1.44	.68
35	6.12	.0632	.0438	.0375	.0387	(5)	(5)	(5)	(5)
36	6.02	.0248	.0126	.0167	.0180	(5)	(5)	(5)	(5)
37	5.98	.2100	.1546	.1633	.1409	(5)	3.18	2.34	.50
38	6.57	.0202	.0037	.0050	.0092	(5)	(5)	(5)	(5)
39	6.56	.0605	.0451	.0398	.0496	(5)	1.14	.23	.84
40	6.01	(4)	.0890	.1101	.0840	(4)	3.24	4.41	3.00
41	6.47	.0533	.0247	.0292	.0280	(5)	(5)	(5)	(5)
42	6.02	.0803	.1455	.0533	.0560	(5)	5.32	2.08	1.00
43	6.70	.1472	.2124	.5604	.0707	(5)	8.36	8.21	(5)
44	6.48	.0532	.0193	.0108	.0206	(5)	(5)	(5)	(5)
45	6.50	.1437	.0614	.1439	.0809	(5)	(5)	3.08	(5)
46	6.50	.0133	.0082	.0085	.0062	(5)	(5)	(5)	(5)
47	6.51	(4)	.0482	.0403	.0492	(4)	(5)	(5)	(5)

[1] See Table 1 for names of soils.
[2] Average of 2 deepest pits, one pit from each side of plate.
[3] See Table 12 for identification of materials.
[4] No specimen.
[5] No pits of measurable depth.
[6] Measurements less than 6 mils assumed to be 3 for calculating purposes.
[7] Average of two specimens.

TABLE 12.—*Condition of galvanized pipe and 16-gage sheet*

Soil No.[1]	A	A3	Y3	B	Soil No.[1]	A	A3	Y3	B
1	------	H	P	H	25	G	F	F	F
2	------	G	G	G	26	E	E	E	R
3	E	G	G	G	27	G	P	R	R
4	P	R	P+	P	28	G	P	P	P
5	G	R	R	R	29	P	P	P	P
6	E	E	E	G	30	------	R	R	R
7	F	P	R	R	31	E	E	E	E
8	G	G	G	G	32	------	E	E	G
9	G	P	P+	P	33	R	P	P	P
10	E	G	G	G	34	E	P	P	P
11	P+	P	P	P	35	E	G	G	G
12	------	------	FG	RG	36	E	E	E	E
13	E	R	R	F	37	F	P	P	P
14	E	G	G	G	38	E	E	E	E
15	G	G	G	G	39	R	P	P	P
16	P	P	P	P	40	------	P	P	P
17	R	P	P	P	41	E	E	E	E
18	E	E	E	E	42	G	P	P+	P
19	E	P	P	P	43	G	P	R	H
20	R	P	P	P	44	E	E	E	G
21	------	------	------	------	45	G	R	R	P
22	E	P	P	P	46	E	E	E	E
23	------	H	H	H	47	G	G	G	G
24	E	E	E	E					

[1] See Table 1 for names and locations of soils.

E, excellent. G, good. F, fair. R, rusted. P, pitted. H, holes. +, better.
A, pure open-hearth iron pipe. Coating=2.82 ounces per square foot.
A3, pure open-hearth iron sheet. Coating=1.98 ounces per square foot.
B, Bessemer steel sheet. Coating=1.62 ounces per square foot.
Y3, open-hearth steel 0.2 per cent copper. Coating=2.15 ounces per square foot.
(Rating by R. F. Passano and E. S. Taylerson.)

It is, of course, possible that when more of the zinc has been removed from the specimens the effects of the base metals will be more apparent. In view of the small number of samples in any one location, the variation in soil condition which may occur within a few inches, and the variation in weight of coating, it is not considered possible from these data to determine such differences in materials as may exist.

Comparison of Tables 1 and 11 indicates that while galvanizing does not permanently protect steel, it adds very considerably to its life in most soils. Because of changes in rates of corrosion of both galvanized and ungalvanized steel with time, it is not possible to determine from the tables the extension of the life of pipes to be expected as the result of galvanizing them. While some soils that are destructive to ferrous materials are not so destructive to galvanized materials, many soils appear to attack both iron and zinc. When a better understanding of soil action has been obtained it may be possible to designate the kinds of soil in which the use of galvanized pipes is advantageous.

If the protection afforded by a zinc coating is the result of the corrosion resisting properties of zinc, it should follow that the thicker the coating the more slowly will the pipe deteriorate. An attempt to determine the influence of the thickness of the zinc coating was made by burying sheets of two materials protected by several weights of coating in seven soils. All of these soils with the exception of soil No. 24 are corrosive with respect to iron and steel.

Table 13 shows the rates of loss of weight and rates of pitting of the materials. The weights of coating are given at the top of the columns. A description of the conditions of these specimens is presented in Table 14. The data on the pipes give no indication that one base material is superior to the others in the soils shown in the table. This is perhaps because all of the pipes with one exception remained in good condition in all of the soils. On the whole, the data on the 16-gage galvanized sheets indicate that the rate of loss of weight is less for the sheets with the thicker coatings of zinc. The data on rates of pitting are less consistent than those for rates of loss of weight. It is probable that the effect of the thickness of the coating will become more evident when specimens buried for a longer period of time are examined. The data on the 18-gage specimens do not differ materially from those of the thicker specimens having approximately the same weights of coating. The data on the ungalvanized specimens show quite clearly that the galvanizing of the sheets afforded them a very considerable amount of protection. The size of the holes in some of the ungalvanized sheets indicates that they failed long before their removal.

TABLE 13.—*Effect of weight of zinc coating on rates of corrosion*

RATES OF LOSS OF WEIGHT IN OUNCES PER SQUARE FOOT PER YEAR

Soil No.	Age (years)	Galvanized pipe				Galvanized sheet										Black sheet		
		A	D	Y	Y	A2	A3	A4	Y2	Y3	Y4	Y5	CA	CB	CY	CA-B	CB-B	CY-B
		[1] 2.82	3.48	3.47	3.47	1.79	1.98	2.65	1.57	2.15	2.76	2.92	1.87	1.66	2.16			
13	6.13	0.1303	0.2719	0.1351	0.1645	0.0606	0.0571	0.0778		0.1052	0.0973	0.0841	0.0500	0.0571	0.0553	0.9304	0.8600	0.9232
24	6.62	.0160	.0147	.0137	.0139	.0017	.0013	[2]	0.0011	.0011	.0031	.0012	.0024	.0034	.0025	.1876	.1811	.1615
28	5.56	.1964	.1522	.1724	.1492	.3135	.2297	.1791	.7424	.4481	.2288	.2961	.2039	.4619	.2142	1.7424	1.5618	1.7420
29	6.01	.2612	.3145	.2740	.2490	.3120	.3204	.2480	.4227	.3137	.2898	.2863	3073	.3084	.2521	1.4136	1.3302	1.3874
42	6.02	.0803	.0965	.0899	.0498	.1498	.1455	.0894	.1560	.0560	.0782	.0990	.0593	.0591	.0667	1.1025	1.3343	1.0821
43	6.70	.1472	.2165	.1871	.1631	.0628	.2124	.1013	.0722	.0707	.0831	.0678	.4505	.3906	.1047	1.3532	1.5266	1.0831
45	6.50	.1437	.3044	.1946	.1395	.0525	.0614	.0743	.4631	.0809	.0719	.0757	.5700	.2830	.1499	1.6540	1.4187	.9396

RATES OF MAXIMUM PENETRATION IN MILS PER YEAR [3]

13	6.13	[4]	[4]	[4]	[4]	3.02	[4]	[4]	[4]	[4]	[4]	[4]	[4]	[4]	[4]	[4]	[4]	[4]
24	6.62	[4]	[4]	[4]	[4]	[4]	[4]	[4]	[4]	[4]	[4]	[4]	[4]	[4]	[4]	3.55	2.49	2.64
28	5.56	[4]	[4]	[4]	[4]	4.68	4.41	4.14	10.70	6.56	5.94	3.78	2.43	3.24	1.89	9.89	9.89	9.89
29	6.01	1.91	[4]	1.67	1.83	3.58	3.83	2.83	3.00	2.33	2.50	2.83	4.16	1.66	1.83	9.15	9.15	9.15
42	6.02	[4]	[4]	[4]	[4]	6.98	5.32	3.99	7.81	1.00	1.83	3.07	3.99	2.91	[4]	9.14	9.14	9.14
43	6.70	[4]	[4]	[4]	[4]	[4]	8.36	[4]	[4]	[4]	[4]	[4]	4.85	7.46	[4]	8.21	8.21	8.21
45	6.50	[4]	[4]	[4]	[4]	[4]	[4]	[4]	5.15	[4]	[4]	[4]	7.92	4.08	2.92	8.46	8.46	8.46

[1] Weight of coating in ounces per square foot.
[2] Weight not available.
[3] In case of sheet, average of two deepest pits, one from each side of specimen.
[4] No pits of measurable depth.

A, pure open-hearth iron.
B, bessemer steel (when separated from another letter by a dash denotes sheets were not galvanized).
C, denotes 18-gage material.
D, wrought-iron pipe.
Y, open-hearth steel containing about 0.2 per cent copper.

Pit measurements by E. R. Shepard and R. B. McDowell.

TABLE 14.—*Condition of specimens with different weights of coatings*

Soil No.	Galvanized pipe			Galvanized 16-gage sheet								Galvanized 18-gage sheet			18-gage black sheet		
	A	D	Y	A2	A3	A4	Y2	Y3	Y4	Y5	B	CA	CB	CY	CA–B	C–B	CY–B
	[1] 2.82	3.48	3.47	1.79	1.98	2.65	1.57	2.15	2.76	2.92	1.62	1.87	1.66	2.16			
13	E, F	E	E, E	P	R	F	F	R	R	R	F	R	R	F	H	H	H
24	E, E	E	E, E	E	E	E	E	E	E	E	E	E	E	E	P	P	P
28	G, G	G	G, G	P	P	P	P	P	P	P	P	P	P	P	H	H	H
29	P, P	F	P, P	P	P	P	P	P	P	P	P	P	P	P	H	H	H
42	G, G	R	R, E	P	P	P	P	P	P	P	P	P	P	F	H	H	H
43	G, G	G	G, G	R	P	G	R	R	R	R	H	P	P	P	H	H	H
45	G, F	F	F, G	R	R	F	P	R	R	R	P	H	P	P	H	H	H

[1] Weight of coating in ounces per square foot.

Rating symbols:
E, excellent.
G, good.
F, fair.
R, rusted.
P, pitted (see Table 13).
H, holes.

Materials:
A, open-hearth iron.
B, Bessemer steel (after a letter signifies no zinc).
Y, open-hearth steel with 0.2 per cent copper.
C, 18-gage sheet.
D, wrought iron.

(Ratings by R. F. Passano and E. S. Taylerson.)

3. LEAD AND ZINC COATED BOLTS

At the request of an advisory committee, specimens of lead coated bolts, sherardized bolts and wrought iron bolts were buried in six soils in 1924. All the bolts were ¾ inch in diameter and 3½ inches long and were provided with nuts of the same materials. Four bolts of each kind were removed in 1930. Table 15 shows the loss of weight of these specimens. Both lead and zinc appear to prolong the life of the bolts in the soils in which they were buried. The maximum corrosion was usually at the threaded end of the bolts.

4. CALORIZED PIPE

Samples of pipe calorized by the wet and by the dry process were buried in six soils in 1924. The data shown in Table 16 indicate that calorizing adds very considerably to the life of pipe in the soils in which the specimens were buried. It is too soon to determine the usefulness of this method of protecting pipes.

IV. TESTS OF COPPER STEEL AND GROUND SPECIMENS

At the suggestion of Dr. F. N. Speller, of the National Tube Co., there were buried in six soils in 1926 two classes of materials, the performances of which are reported here, although they are neither nonferrous materials nor protective coatings. However, they represent suggestions for reduction of corrosion. The first material is steel containing 1.5 per cent of copper. The second group of specimens were intended to indicate whether the type of the pipe surface affected the rate of corrosion. One specimen of steel pipe 2 inches in diameter and 17 inches long and sealed at the ends was ground to a

semipolished surface. This was accompanied by a pipe of similar material with the original mill surface. Similar specimens of wrought iron were furnished by the Reading Iron Co. The surfaces of the ground wrought-iron specimens were, however, much rougher than those of the ground-steel specimens. The data obtained from these specimens are shown in Table 17. There have also been included in this table data on some lead-coated pipe buried with the steel specimensand having the same dimensions.

TABLE 15.—*Rates of loss of weight of nuts and bolts*

[Average of 4 specimens in ounces per square foot per year]

Soil No.	Bolts			Nuts		
	G	D	F	G	D	F
13	0.084	1.344	0.135	0.178	2.206	0.144
24	.022	.100	.056	.025	.086	.083
28	[1].693	[1]1.813	----------	[1].536	[1]1.855	----------
29	.525	1.222	.740	.242	.822	.559
42	.806	1.236	.294	.782	1.188	.225
43	.987	1.542	.621	.687	1.406	.437
45	.231	1.595	1.021	.345	1.734	.669

[1] One specimen only; D, wrought iron; F, lead-coated; G, sherardized.

TABLE 16.—*Corrosion of calorized specimens*

Soil No.	Age (years)	Rates of loss of weight in ounces per square foot per year		Rates of maximum penetration in mils per year		Soil No.	Age (years)	Rates of loss of weight in ounces per square foot per year		Rates of maximum penetration in mils per year	
		Dry cal.	Wet cal.	Dry cal.	Wet cal.			Dry cal.	Wet cal.	Dry cal.	Wet cal.
13	6.13	0.163	0.021	5.38	5.87	42	6.02	3.19	0.122	6.81	8.64
24	6.62	.023	.010	[1]2.42	4.38	43	6.70	1.163	.739	6.57	7.76
28	5.56	.311	----------	6.47	----------	45	6.50	.338	.403	4.92	5.23
29	6.01	.251	.296	6.32	7.65						

[1] Depth of pit on one specimen assumed to be 10 mils for purpose of calculation.

The data do not indicate that the addition of copper to steel improved its resistance to the action of the soils in which the specimens were buried. In four of the six soils the ground wrought iron lost slightly more weight than the unground specimens of the same material, and all of the ground specimens showed deeper pits than the corresponding unground specimens. On the other hand, in four soils out of six the polished steel lost less weight than the unpolished steel. Half of the polished steel specimens were pitted more deeply than the unpolished specimens. The data are not sufficiently consistent to show definitely whether grinding the surface of a pipe improves its resistance to soil action; but if grinding does improve its resistance the improvement is probably not great.

TABLE 17.—*Corrosion of copper steel, ground and unground wrought iron and steel, and of lead-coated pipes*

RATES OF LOSS OF WEIGHT IN OUNCES PER SQUARE FOOT PER YEAR

Soil No.	Age (years)	C	D	K	M	P	L (2 specimens)
13	3.84	1.6158	1.2389	1.7887	1.0417	0.9550	.4833
24	3.92	.3851	.3984	.3560	.3483	.2232	.0615
28	3.92						.9812
29	3.90	4.0924	1.2021	1.5130	1.3762	1.6392	.8527
42	3.94	1.5902	1.7041	1.7787	1.6915	1.4431	.8139
43	3.92	1.2000	.8837	.7096	.8855	.3367	.6911
45	3.91	1.2730	2.4840	3.0243	2.3812	2.7770	.5782

RATES OF MAXIMUM PENETRATION IN MILS PER YEAR

13	3.84	19.27	14.06	19.79	7.81	9.38	[1] 6.50
24	3.92	7.14	5.10	9.18	4.59	8.16	
28	3.92						11.60
29	3.90	29.49	14.87	18.21	14.87	17.18	8.71
42	3.94	20.56	20.56	26.40	23.35	21.07	13.96
43	3.92	15.82	11.99	21.68	27.30	17.86	24.25
45	3.91	16.88	18.41	24.30	27.37	24.55	12.78

[1] Depth of pit on one specimen assumed to be 10 mils for purpose of calculation: C, Steel+1.5 per cent copper; D, wrought iron; K, ground wrought iron; M, bessemer steel; P, ground and semipolished Bessemer steel, L, lead coated pipe.

The lead-coated specimens in this group behaved similarly to the other lead-coated specimens in that they showed less loss of weight than the unprotected specimens although the pits were deeper in one soil.

V. SUMMARY

The information concerning soils which has been obtained as the result of the bureau's soil-corrosion investigations makes it clear th that the rate of corrosion of any metal exposed to soil can not be accurately expressed by a single figure or group of figures. On account of the variations found in all soils the influence of the character of the soil, differences in contact between the soil and the metal, changes in the supply of oxygen and moisture, and the effects of the corrosion products, the best that can be hoped for is an expression representing the average rate of loss of weight or pitting accompanied by a figure for the standard deviation, probable error, or some other expression indicating how much the behavior of any single specimen may be expected to differ from the behavior of the average of a representative group of specimens.

Average values sufficiently accurate to show small differences in the performance of competing materials can only be secured through the testing of a very large number of specimens. Since in any one case any material may prove considerably better or worse than the average, it is doubtful whether the drawing of fine distinctions between materials would be of practical value except for the consumers of very large quantities of materials. Attention should, therefore, be directed chiefly to the unmistakable differences between different kinds of materials rather than to possible small differences between nearly similar materials.

The most general conclusion to be drawn from the data is that for best results the material must be chosen to fit the soil in which it is

to serve, since no one material is best for all soil conditions. Another general conclusion is that small differences in the data should not be considered significant, since it is improbable that a repetition of the test would yield identical results.

In nearly all soils copper and alloys high in copper resist corrosion well. Muntz metal shows at least slight dezincification after six years burial in half of the soils investigated and serious dezincification in a few of them.

In nearly all of the soils considered, lead corroded much less rapidly than iron or steel. The rates of pitting of commercial lead specimens were 3 mils per year or greater in 25 per cent of the soils. The lead containing antimony showed rates of pitting greater than 3 mils per year in nearly 50 per cent of the test locations.

The outer metallic ribbon of the parkway cable showed corrosion in most test locations. The inner ribbon was somewhat less corroded. Serious pitting of the lead sheath occurred only in the soil containing alkali carbonates.

All of the metallic coatings tested appeared to increase the life of the material to which they were applied. Comparison of the effectiveness of the metallic coatings is difficult because they differed in thickness. All coatings showed evidences of deterioration in several soils. In most of the soils, there was no evidence that the rate of penetration by pitting increased after the lead coating had been punctured. The possibility is suggested that the relative positions of lead and iron in the electrochemical series depends upon the soil in which specimens composed of lead and iron are placed. The precision of the data is insufficient to show at this time whether one base material is better than another for galvanized sheets to be used underground, but it appears that any difference which may exist is not great.

In conclusion, the author wishes to recognize and express his appreciation for the work of V. A. Grodsky, R. H. Taylor, E. S. Hammond, and R. B. McDowell, who determined the rates of losses of weight and penetration and prepared the tables for this report.

WASHINGTON, June 20, 1931.

ISOLATION AND DETERMINATION OF THE CYCLOHEXANE IN A MIDCONTINENT PETROLEUM[1]

By Johannes H. Bruun[2] and Mildred M. Hicks-Bruun

ABSTRACT

A midcontinent petroleum was fractionated by distillation into a series of 1° cuts. After removal of the benzene from these cuts (by nitration) and subsequent fractional distillation, the cyclohexane was found to concentrate in the fractions boiling at about 80° C. By systematic equilibrium melting it was then possible to isolate the cyclohexane in a state of high purity, 99.96 mole per cent. The following physical constants were determined for the isolated cyclohexane: Boiling point, freezing point, specific gravity, refractive index, molecular weight, and the critical solution temperature with aniline. Photographs were also taken of the visible and ultra-violet, as well as the infra-red, absorption spectrum of the isolated hydrocarbon.

The petroleum fraction with boiling range of 80° to 80.5° C. was found to consist of about 94 mole per cent of cyclohexane. Based upon the crude petroleum, the percentage of cyclohexane was found to be about 0.33.

CONTENTS

		Page
I.	Introduction	607
II.	Origin and preliminary distillation of the crude petroleum	608
III.	Experimental results	609
IV.	Acknowledgment	615

I. INTRODUCTION

A short time after cyclohexane had been synthesized by Baeyer,[3] Markownikoff[4] was able to show that Caucasian petroleum fractions boiling around 80° C. consisted mainly of this naphthene. Although the presence of cyclohexane has been indicated in many other crude petroleums since that time, it seems that only two investigators have been able to isolate it in a demonstrably pure condition. Chavanne[5] isolated a sample of cyclohexane, the freezing point of which was +3.2° C. (the freezing point of pure synthetic cyclohexane is +6.4° C.) and Fortey[6] obtained a cyclohexane sample with a freezing point of +4.7° C. In addition to physical methods, such as distillation and fractional melting, however, Fortey also subjected the

[1] This paper describes some of the results obtained in an investigation on the separation, identification, and determination of the chemical constituents of commercial petroleum fractions listed as Project No. 6 of the American Petroleum Institute research. Financial assistance in this work has been received from a research fund of the American Petroleum Institute donated by John D. Rockefeller. This fund is being administered by the institute with the cooperation of the Central Petroleum Committee of the National Research Council.

[2] Research associate for the American Petroleum Institute.

[3] A. Baeyer, Ann., **278**, p. 111; 1894.

[4] W. Markownikoff, Ber., **28**, p. 577; 1895; **30**, p. 974; 1897.

[5] G. Chavanne, J. soc. chim. Belg., **31**, p. 361; 1922.

[6] E. C. Fortey, J. Chem. Soc., **73**, p. 932; 1898; **75**, p. 873; 1899.

fractions to the destructive action of chlorosulphonic acid, a procedure which we have avoided since it would render impossible the identification of the other hydrocarbons in these petroleum fractions.

II. ORIGIN AND PRELIMINARY DISTILLATION OF THE CRUDE PETROLEUM

The crude petroleum used for this investigation was obtained from No. 6 well of the South Ponca Field, Kay County, Okla.[7] The preliminary distillation of the crude oil was carried out in a semicommercial batch still[8] capable of handling a charge of 200 gallons. This still was provided with a rectifying column which consisted of 20 bubbling cap plates. Three charges of 200 gallons each were made

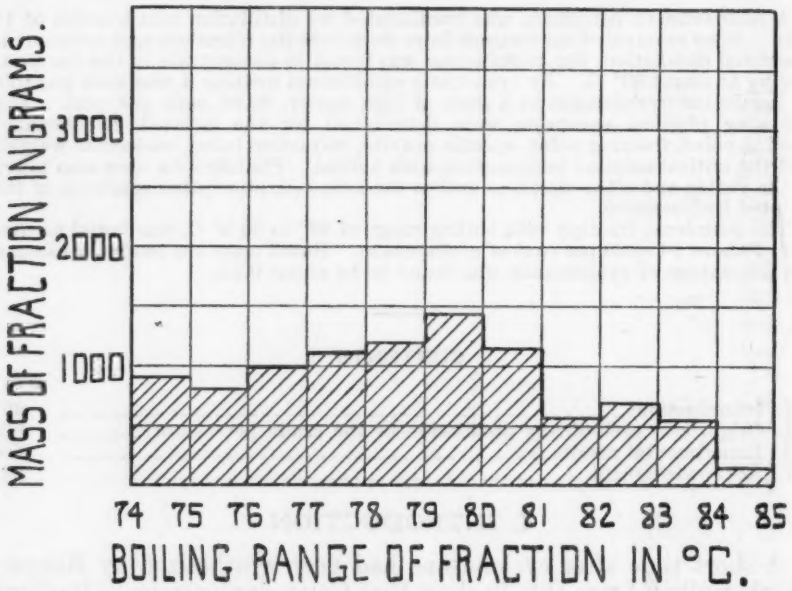

FIGURE 1.—*Distribution of the fractions over their boiling range before removal of the benzene*

in this still, and the corresponding fractions from these distillations were blended into 4-gallon cuts, which were sent to the bureau.

These fractions were redistilled in the stills previously described,[9] with the further assistance of an all-glass still, which has a 35-foot column, packed with chromium plated steel jack chain. In all of the glass stills the rate of distillation was maintained at about 1 ml per minute and a reflux ratio of 10:1 was used. The boiling points of the fractions were determined accurately by means of the continuous boiling point apparatus previously described.[10] Each boiling point was corrected to standard pressure.

As a result of these preliminary distillations the material was fractionated into a series of 1° cuts. The present investigation deals with the fractions between 74° and 85° C.

[7] For properties see E. W. Washburn, J. H. Bruun, and M. M. Hicks, B. S. Jour. Research, **2**, p. 469 Table 1; 1929.

[8] Acknowledgment for this distillation is made to A. E. Pew, Jr., and R. B. Davidson, of the Sun Oil Co

[9] J. H. Bruun and M. M. Hicks-Bruun, B. S. Jour. Research, **6**, p. 870; 1931.

[10] See footnote 9.

III. EXPERIMENTAL RESULTS

The graph in Figure 1 shows the distribution of the petroleum fractions over the boiling range after completion of the preliminary distillations. From this graph it will be noted that 1,200 g of material had a boiling range of 80° to 81° C. (the boiling points of cyclohexane and of benzene are 80.8° and 80.2° C., respectively). For the purpose of removing and determining the benzene, each of the cuts with boiling ranges between 74° and 85° C. was subjected to nitrating treatment according to the method described in previous papers.[11, 12]

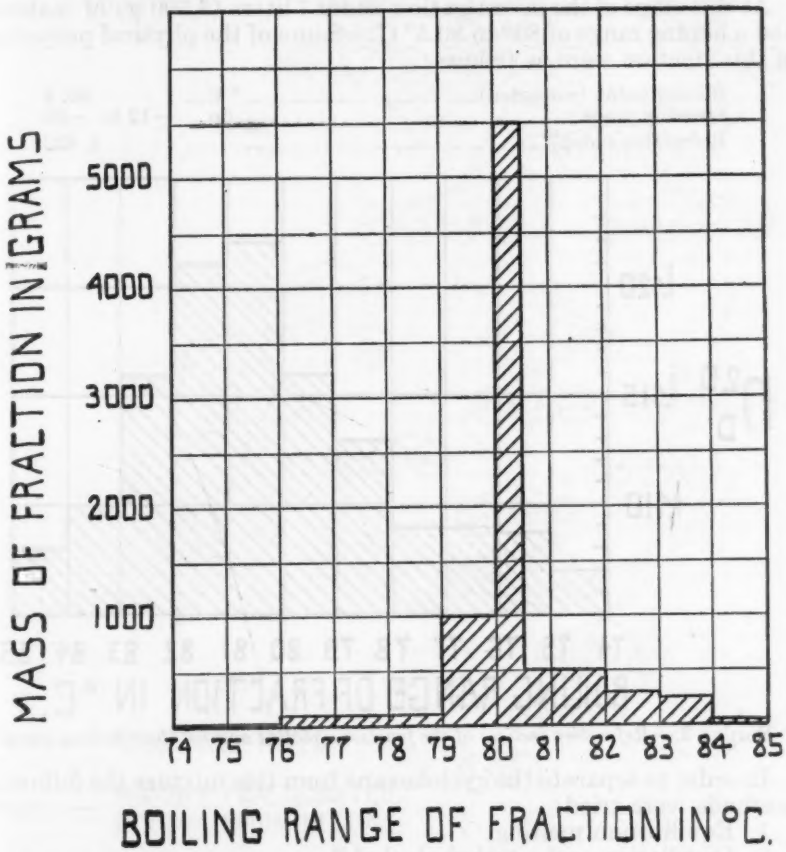

FIGURE 2.—*Distribution of the fractions over their boiling range after removal of the benzene and subsequent fractional distillations*

After the nitration the remaining hydrocarbons were washed with sodium-hydroxide solution and with distilled water, and finally dried over calcium chloride.

When the benzene had been completely removed the aromatic-free fractions were subjected to five more distillations. All of these distillations, as well as the last three of the preliminary distillations, were

[11] J. H. Bruun and M. M. Hicks-Bruun, B. S. Jour. Research, **6**, pp. 869–880; 1931.
[12] J. H. Bruun, R. T. Leslie, and S. T. Shicktanz, B. S. Jour. Research, **6**, pp. 767–768; 1931.

made by S. T. Shicktanz and a staff of still operators. During these distillations most of the material concentrated in the cut boiling between 80° and 80.5° C. The distribution of the fractions over their boiling range at this stage of the investigation is shown in Figure 2.

Figure 3 shows the refractive indices of the different fractions plotted against the boiling range. The maximum on this graph exhibited by the fractions boiling between 80° and 81° C, and the high freezing points of these fractions were taken as indications of the presence of cyclohexane.

At this stage of the investigation about 7 liters (5,500 g) of material had a boiling range of 80° to 80.5° C. Some of the physical properties of this fraction were as follows:

Boiling point (corrected)	° C	80. 4
Freezing range	do	−12 to −36
Refractive index n_D^{20}		1. 422

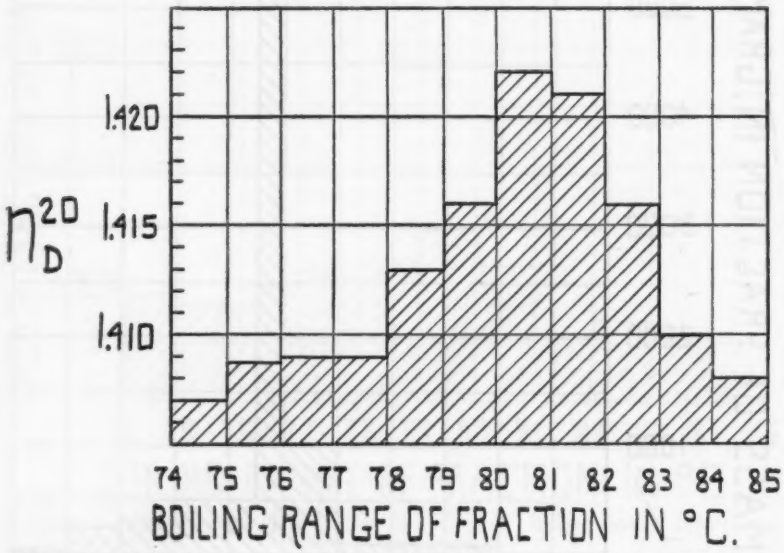

FIGURE 3.—*Refractive indices of the fractions plotted against their boiling range*

In order to separate the cyclohexane from this mixture the following methods were tried:

1. Equilibrium melting.
2. Distillation with methyl alcohol.[13]
3. Distillation with ethyl alcohol.[13]
4. Distillation with aniline.
5. Extraction with aniline.[14]
6. Extraction with benzyl alcohol.[15]

As the first of these six methods gave by far the sharpest separation, a systematic fractionation of the material by means of equilibrium melting was undertaken. The method and technic used depended upon the freezing ranges of the fraction and the quantities of material available. The first fractionations of the comparatively large fractions

[13] For details see J. H. Bruun and M. M. Hicks-Bruun, B. S. Jour. Research, **5**, pp. 933–942; 1930.
[14] For details see footnote 11, p. 609.
[15] For details see H. Steinbrecher, Braunkohlenarchiv, Heft, **31**, p. 1; 1930.

(with freezing ranges of −30 to −10) were made in a closed apparatus.[16] For the resulting smaller fractions with higher melting points it was found more convenient to use a vacuum funnel.[17]

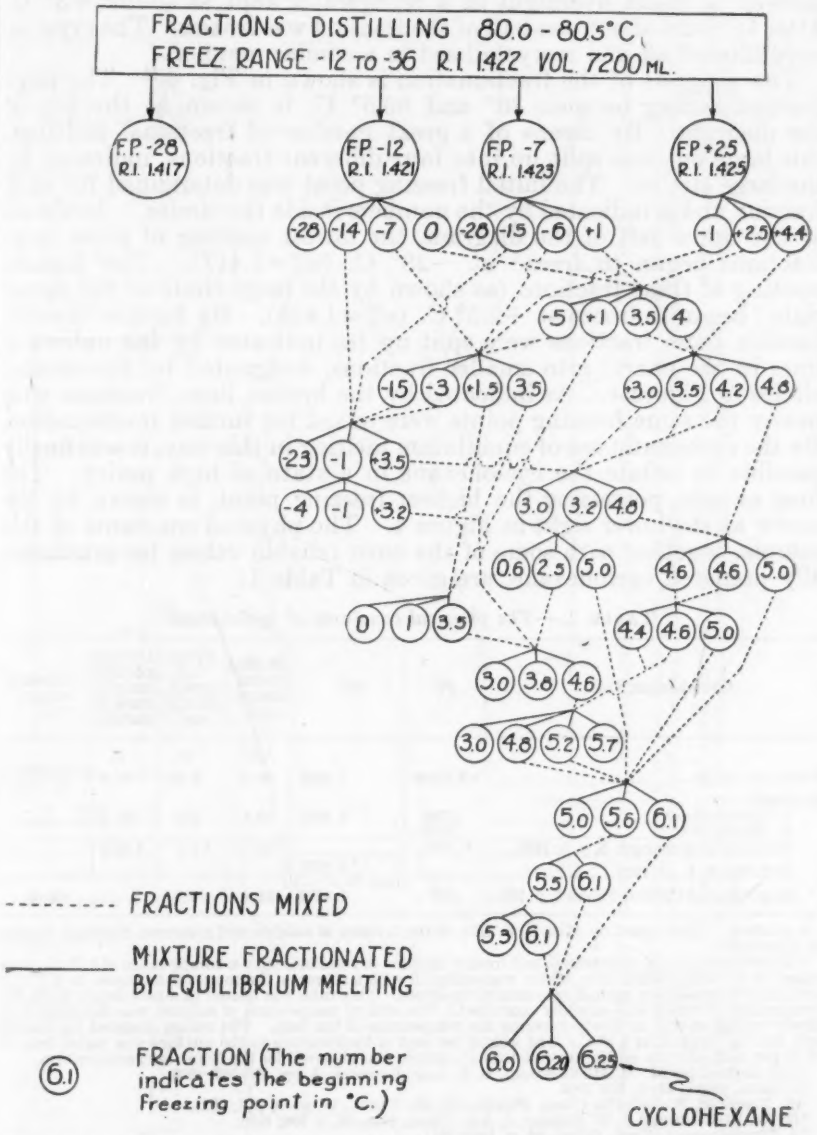
FRACTIONS DISTILLING 80.0 - 80.5° C.
FREEZ. RANGE -12 TO -36 R.I. 1.422 VOL. 7200 ML.
F.P. -28 R.I. 1.417
F.P. -12 R.I. 1.421
F.P. -7 R.I. 1.423
F.P. +2.5 R.I. 1.425
-28 -14 -7 0 -28 -15 -6 +1 -1 +2.5 +4.4
-5 +1 3.5 4
-15 -3 +1.5 3.5 +3.0 3.5 4.2 4.6
-23 -1 +3.5
-4 -1 +3.2
3.0 3.2 4.8
0.6 2.5 5.0 4.6 4.6 5.0
0 1 3.5
4.4 4.6 5.0
3.0 3.8 4.6
3.0 4.8 5.2 5.7
5.0 5.6 6.1
5.5 6.1
5.3 6.1
6.0 6.20 6.25
CYCLOHEXANE
--------- FRACTIONS MIXED
MIXTURE FRACTIONATED BY EQUILIBRIUM MELTING
6.1 FRACTION (The number indicates the beginning freezing point in °C.)

FIGURE 4.—*Chart showing the isolation of the cyclohexane by equilibrium melting*

However, as soon as fractions with freezing ranges above 0° C. were obtained, an ordinary Büchner funnel (covered with a watch glass) was used instead of the vacuum funnels. Suction was applied

[16] R. T. Leslie and S. T. Schicktanz, B. S. Jour. Research, **6**, p. 382; 1931.
[17] For details see M. M. Hicks, B. S. Jour. Research, **2**, p. 484; 1929.

from below, and the unmelted crystals were pressed "dry" by means of a spatula.

For the final crystallization the material was placed in a bottle and allowed to stand overnight in a refrigerator kept at about +3° C. After 18 hours about one-half of the fraction was frozen. The crystals were filtered off and recrystallized in a similar manner.

The progress of the fractionation is shown in Fig. 4.[18] The large fraction boiling between 80° and 80.5° C. is shown at the top of the diagram. By means of a great number of fractional meltings, this large cut was split up into four different fractions, indicated by the large circles. The initial freezing point was determined for each fraction and is indicated by the numbers inside the circles. As shown at the upper left of the diagram, the lowest melting of these large fractions began to freeze at −28° C. ($n_D^{20}=1.417$). The highest melting of these fractions (as shown by the large circle at the upper right) began to freeze at +2.5° C. ($n_D^{20}=1.425$). By further crystallization these fractions were split up (as indicated by the unbroken lines in the chart) into smaller fractions, designated by the smaller circles in Figure 4. As indicated by the broken lines, fractions with nearly the same freezing points were mixed for further fractionation. By the systematic use of equilibrium melting in this way, it was finally possible to isolate the cyclohexane in a state of high purity. The final sample, possessing the highest freezing point, is shown by the arrow at the lower right in Figure 4. The physical constants of this sample, together with some of the most reliable values for synthetically prepared cyclohexane, are given in Table 1:

TABLE 1.—*The physical constants of cyclohexane*

Cyclohexane, C_6H_{12}	d_4^{20}	n_α^{20}	Boiling point corrected	Freezing point (in dry air)	Critical solution temperature in aniline	Molecular weight
			° C.	° C.	° C.	
From petroleum	[1] 0.77849	1.4263	80.8	6.25	[2] 31.0	[2] 83.9±0.2 84.0±0.2
Synthetic:						
J. Timmermans [4]	.7785	1.4263	80.8	6.4	31.0	
F. Eisenlohr [5]	.7783					
Beilstein Ergänzungsl. 5, p. 6; 1930	[6] .7791		[7] 80.75	[6] 6.4	[6] 31.0	
Beilstein 5, p. 21; 1922		[8] 1.4266 (at 19.5 ° C.)				
International Critical Tables 1, p. 202	.779	1.4272	81.4	6.5		84.09

[1] ±0.00001. Determined by Miss E. E. Hill, of the division of weights and measures, National Bureau of Standards.

[2] Known amounts of cyclohexane and freshly distilled dry aniline, with a boiling range of 0.1° C., were placed in a double-walled tube, which was equipped with a stirrer, a thermometer (accurate to 0.1° C.) and suitable protection against atmospheric moisture. This tube was heated in a petrolatum bath, the temperature of which was carefully controlled. The critical temperature of solution was determined by slowly raising as well as slowly lowering the temperature of the bath. The values observed by heating and cooling checked to 0.1° C. The weight per cent of hydrocarbon in the mixture was varied from 50 to 75 per cent, and the critical temperature of solution was observed for the 60 per cent composition.

[3] For method see M. M. Hicks-Bruun, B. S. Jour. Research, 5, pp. 575-583; 1930.

[4] J. chim. phys., 23, p. 760; 1926.

[5] F. Eisenlohr, Fortschritte Chem. Physic, physik. Chem., 18, pt. 9, p. 1; 1925.

[6] T. W. Richards and J. W. Shipley, J. Am. Chem. Soc., 38, p. 996; 1916.

[7] J. Timmermans, Chem. Zentr., 82, p. 1669; 1911.

[8] G. Chavanne and L. J. Simon, Compt. rend., 168, p. 1112; 1919.

[9] N. Zelinsky Ber., 34, p. 2802; 1901.

The visible and ultra-violet absorption spectra of the vapor were determined by M. Davis, of this bureau, at pressures ranging from about 1 to 48 mm. No absorption lines or bands were observed in the region $\lambda=2{,}300$ to 4,878 A.

[18] Acknowledgment is made to F. W. Rose, jr., for drawing the chart in Figure 4.

Figure 5 is the infra-red absorption spectrum of the liquid. This work was done by U. Liddel, of the Fixed Nitrogen Research Laboratory, Department of Agriculture.

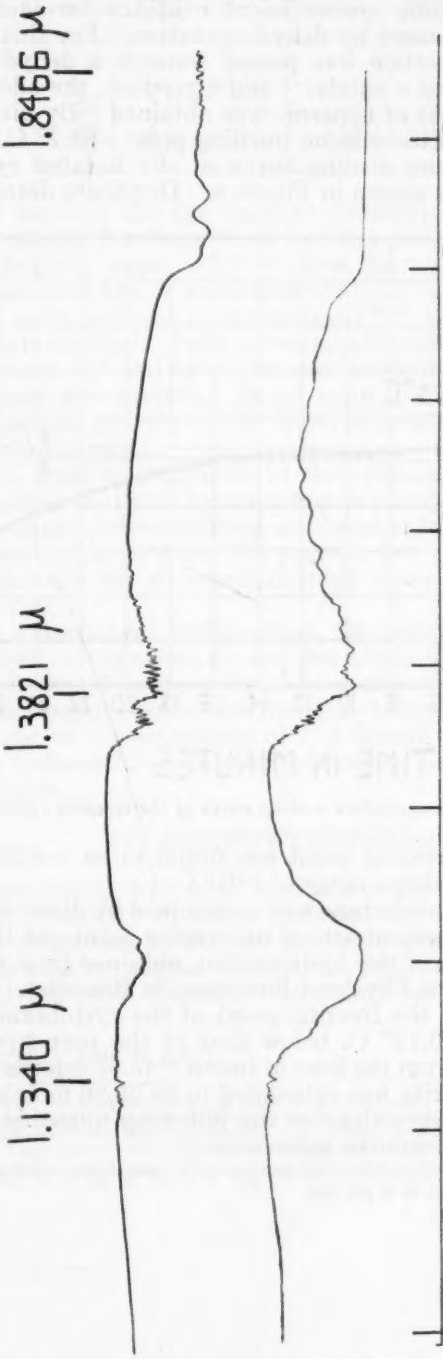

FIG. 5.—*Infra-red absorption spectra of 1 mm and 1 cm cells, respectively, of the isolated cyclohexane. Slit width approximately 10 A*

These are automatically registered energy curves of the emission from a tungsten filament (approximately 2,900° C.) through the cells containing the cyclohexane. Calibration was made on the basis of the Hg lines in this region from the published data on their wave lengths. The wave lengths of the H_2O lines, read from this calibration, curve check the published wave lengths of H_2O within ± 2 A.

The two absorption maxima occurring at 1.725μ and 1.206μ are the first and second overtones, respectively, of the fundamental *H* to *C* vibration occurring at approximately 3.4μ observed in all hydrocarbon compounds. The band at 1.42μ is a combination band of this fundamental with another near 6μ. Measured by U. Liddel, of the Fixed Nitrogen Research Laboratory, Department of Agriculture.

As shown in Table 1, there is excellent agreement between the physical constants of the isolated hydrocarbon and those of the pure cyclohexane, prepared synthetically. Although in this case the physical constants alone are sufficient evidence for identification, further proof was obtained by dehydrogenation. For this purpose a sample of the hydrocarbon was passed through a dehydrogenation furnace (using nickel as a catalyst) and a product, the odor of which strongly resembled that of benzene, was obtained. By nitration this product yielded *m*-dinitrobenzene (melting point = 89.7° C.).

The time-temperature cooling curve of the isolated cyclohexane was determined and is shown in Figure 6. Duplicate determinations

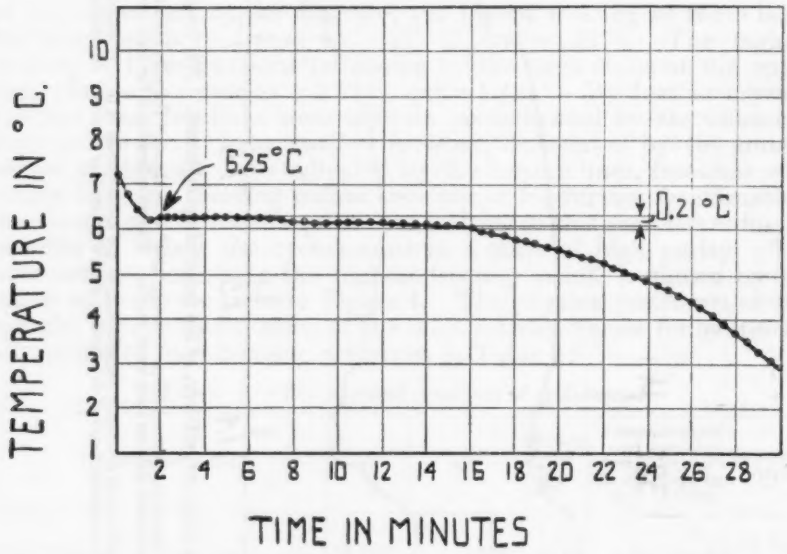

FIGURE 6.—*Time-temperature cooling curve of the isolated cyclohexane*

were made and the freezing point was found to be +6.25° C. The whole sample froze within a range of 0.21° C.

The purity of the cyclohexane was determined by direct comparison (with a Beckmann thermometer) of its freezing point and the freezing point of a pure sample of this hydrocarbon, obtained from the Bureau International d'Etalons Physico-Chimiques (in Brussels). According to this determination the freezing point of the cyclohexane isolated from petroleum was 0.13° C. below that of the pure hydrocarbon. From this value and from the heat of fusion [19] (5.87 calories per gram) of cyclohexane the purity was caluclated to be 99.96 mole per cent.

As a result of this investigation the following quantities of cyclohexane were isolated from the petroleum:

[19] M. Padua, Atti Accad. Lincei, 28, p. 240; 1919.

TABLE 2.—*Quantities of cyclohexane isolated from the petroleum*

Approximate volume	Initial freezing point (in air)	Purity	Approximate volume	Initial freezing point (in air)	Purity
ml	° *C.*	*Mole per cent*	*ml*	° *C.*	*Mole per cent*
200	6.25	99.96	600	5.7	99.77
200	6.2	99.94	700	3.0	98.88
200	6.1	99.91	1,400	+1	98.22
500	6.0	99.88	1,000	−7	95.58

Figure 2 displays the approximate distribution of the cyclohexane in the petroleum fractions used for this investigation. From the beginning freezing point, −12° C. (see the top of fig. 4) of the 80° to 80.5° fraction it can be calculated that this large fraction contained about 93.7 mole per cent of cyclohexane [20] [21] before it was subjected to equilibrium melting. From a conservative estimate of the fractions boiling between 74° and 85° C. we can conclude that at least 6,700 g of cyclohexane was present. Based upon the original 600 gallons of crude oil (specific gravity 0.90), the cyclohexane content is found to be about 0.33 per cent.

As to the possible utilization of the cyclohexane in petroleum, it should be noted that this hydrocarbon is a very desirable solvent for molecular weight determinations in chemical laboratories. Its main advantages over benzene for this purpose are:

1. Cyclohexane has an unusually high cryoscopic constant, 20° C. per mole per kg.

2. Being a naphthene hydrocarbon, its properties are intermediate between those of the aromatic and the aliphatic hydrocarbons. For this reason it should be more generally useful than benzene.

The minor constituents of the fractions boiling between 74° and 85° C. were found to consist mainly of 2, 2-dimethylpentane. The isolation of this hydrocarbon is in progress and the results will be published in a later paper.

IV. ACKNOWLEDGMENT

This investigation was made under the direction of E. W. Washburn, chief, chemistry division, National Bureau of Standards and director of American Petroleum Institute research project No. 6. The authors wish to express their sincere gratitude to him for his kind interest, advice, and valuable suggestions in connection with the problem.

WASHINGTON, July 6, 1931.

[20] Because benzene has a greater antiknock effect than cyclohexane, the value of this fraction, for a motor fuel, could be improved upon by dehydrogenating the cyclohexane to benzene.

[21] This investigation indicates that the separation of cyclohexane from petroleum on an industrial scale is feasible. This fact may prove to be of interest if cyclohexane would be accepted as an upper reference standard for antiknock tests of motor fuels. The advantages of cyclohexane for this purpose have been discussed by J. M. Campbell, W. G. Lowell, and T. A. Boyd, J. Soc. Automotive Eng., **26**, p. 163; 1930.